SOLVENT EXTRACTION AND ELECTROCHEMICAL STUDIES OF LANTHANIDES AND ACTINIDES IN ROOM TEMPERATURE IONIC LIQUID MEDIUM CONTAINING VARIOUS EXTRACTANTS

By

RAMA R
Enrolment No: CHEM02201204007

Indira Gandhi Centre for Atomic Research
Kalpakkam

A thesis submitted to the
Board of Studies in Chemical Sciences
In partial fulfillment of requirements
for the Degree of

DOCTOR OF PHILOSOPHY
of
HOMI BHABHA NATIONAL INSTITUTE

August, 2017

Homi Bhabha National Institute

Recommendations of the Viva Voce Board

As members of the Viva Voce Board, we certify that we have read the dissertation prepared by **Rama. R** entitled "**Solvent extraction and electrochemical studies of lanthanides and actinides in room temperature ionic liquid medium containing various extractants"** and recommend that it may be accepted as fulfilling the dissertation requirement for the Degree of Doctor of Philosophy.

S. Anthonysamy

Chairman- **Dr.S. Anthonysamy** **Date:**

Antony M P

Guide/Convener- **Dr. M.P. Antony** **Date:**

Examiner- **Dr. Tamal Banerjee** **Date:**

N. Sivaraman 4.12.17

Member 1 - **Dr. N. Sivaraman** **Date:**

Member 2 – **Dr. R.V. Subba Rao** **Date:** 4/12/17

K.A. Venkatesan

Technical Adviser – **Dr. K.A. Venkatesan** **Date:** 4/12/17

Final approval and acceptance of this thesis is contingent upon the candidate's submission of the final copies of the dissertation to HBNI.

I hereby certify that I have read this thesis prepared under my direction and recommend that it may be accepted as fulfilling the thesis requirement.

Date: 4.12.2017
Place: Kalpakkam

Antony M P

Dr. M.P. Antony
Guide

STATEMENT BY AUTHOR

This dissertation has been submitted in partial fulfillment of requirements for an advanced degree at Homi Bhabha National Institute (HBNI) and is deposited in the Library to be made available to borrowers under rules of the HBNI.

Brief quotations from this dissertation are allowable without special permission, provided that accurate acknowledgement of source is made. Requests for permission for extended quotation from or reproduction of this manuscript in whole or in part may be granted by the Competent Authority of HBNI when in his or her judgment the proposed use of the material is in the interests of scholarship. In all other instances, however, permission must be obtained from the author.

R. Rama.

Rama. R

DECLARATION

I, hereby declare that the investigation presented in the thesis has been carried out by me. The work is original and has not been submitted earlier as a whole or in part for a degree/diploma at this or any other Institution/University.

R. Rama.

Rama. R

LIST OF PUBLICATIONS ARISING FROM THE THESIS

JOURNAL

a. ***Published***

1. "Insights into the extraction behavior of U(VI) in Aliquat 336 based ionic liquids", **R. Rama**, R. Kumaresan, K.A. Venkatesan, M.P. Antony, P.R. Vasudeva Rao, Radiochimica Acta, **2014**, 102., 1009-1016.

2. "Extraction behavior of americium (III) in benzoylpyrazolone dissolved in pyrrolidinium based ionic liquid", **R. Rama**, Alok Rout, K.A. Venkatesan, M.P. Antony, P.R. Vasudeva Rao, Separation Science and Technology, **2015,** 50., 2164-2169.

3. "Loading behavior of Eu(III) at high aqueous concentrations in diglycolamide /ionic Liquid systems", **R. Rama**, Alok Rout, K.A. Venkatesan, M.P. Antony, P.R. Vasudeva Rao, Journal of Radioanalytical and Nuclear Chemistry, **2016,** 308., 835-842.

4. "Effect of alkyl chain length of tri-*n*-alkyl phosphate extractants on the electrochemical behaviour of U (VI) in ionic liquid medium", **R. Rama**, Alok Rout, K.A. Venkatesan, M.P. Antony, Journal of Electroanalytical Chemistry, **2016**, 771., 87-93.

5. "Comparison in the solvent extraction behavior of Uranium (VI) in some trialkyl phosphates in ionic liquid" **R. Rama**, Alok Rout, K.A. Venkatesan, M.P.Antony, A. Suresh, Radiochimica Acta, **2016**, 104., 865-872.

6. "Voltammetric studies on the complexing behaviour of Eu(III) with acidic extractants in 1-butyl-1-methylpyrrolidinium bis(trifluoromethanesulfonyl)imide", **R. Rama**, Alok Rout, K.A. Venkatesan, M.P. Antony, Journal of The Electrochemical Society, **2016**, 163., H1113-H1121.

7. “A novel phosphoramide task specific ionic liquid for the selective separation of plutonium (IV) from other actinides” **R. Rama**, Alok Rout, K.A. Venkatesan, M.P. Antony, Separation and Purification Technology, **2017**, 172., 7-15.

b. ***Accepted***

1.“Room temperature ionic liquid system for the mutual separation of Pu(IV) from other actinides using 2-hydroxy acetamide extractant”. **R. Rama**, Alok Rout, K.A. Venkatesan, M.P. Antony. Separation and Purification Technology. **2017,** Doi.org/10.1016/j.seppur.2017.08.043. (In Press)

CONFERENCES

National Symposia

1. Extraction behavior of U(VI) in paraffin soluble ionic liquid, In: Recent trends in materials chemistry, **R. Rama**, R. Kumaresan, K.A. Venkatesan, M.P. Antony, P.R. Vasudeva Rao. VIT University, Vellore, India (2013) p-62.

2. Insights into the extraction of U(VI) in Aliquat-336 Ionic Liquids, **R. Rama,** R. Kumaresan, K.A. Venkatesan, M.P. Antony, P.R. Vasudeva Rao. In: Emerging Trends in Separation Science and Technology(SESTEC), BARC, Mumbai. D.K. Singh, P.K. Mohapatra, B.S. Tomar, A. Gowsami, K.L. Ramkumar (eds) (2014) p-56.

3. Third Phase Formation in Solvent Extraction?, In: Nuclear and radiochemistry, **R. Rama**, Alok Rout, K.A. Venkatesan, M.P. Antony. Can Ionic Liquids Avoid BARC, Mumbai. S.B. Deb, K.L. Ramkumar, S. Kannan, S.K. Mukerjee (eds) (2015) p-288-289.

4. Extraction Behavior of Am (III) in Benzoyl Pyrrazolone Dissolved in Pyyrolidnium Ionic Liquid, **R. Rama**, Alok Rout, K.A. Venkatesan, M.P. Antony.

In: Nuclear and radiochemistry BARC, Mumbai. S.B. Deb, K.L. Ramkumar, S. Kannan, S.K. Mukerjee (eds) (2015) p-236-237.

5. A novel phosphoramide task specific ionic liquid for extraction of actinides., **R. Rama**, Alok Rout, K.A. Venkatesan, M.P. Antony. In: Emerging Trends in Separation Science and Technology (SESTEC -2016), IIT, Guwahati. A.C. Deb, S. Sodaye, M.S. Murali, T. Banarjee, P.K. Moharatra, K.L. Ramkumar (eds) (2016) p-84.

6. Feasibility of extraction and electrodeposition of uranium using imidazolium ionic liquid containing trialkyl phosphates, **R. Rama**, Alok Rout, K.A. Venkatesan, M.P. Antony. In: Emerging Trends in Separation Science and Technology, IIT, Guwahati, A.C. Deb, S. Sodaye, M.S. Murali, T. Banarjee, P.K. Moharatra, K.L. Ramkumar (eds) (2016) p-107.

7. Selective separation of Pu(IV) from other actinides using phosphoramide task specific ionic liquid, **R. Rama**, Alok Rout, K.A. Venkatesan, M.P. Antony. Plutonium 75, IGCAR, Kalpakkam (2016).

8. Feasibility of Mutual Separation of U(VI) and Pu(IV) in α –Hydroxyl Acetamide Dissolved in Ionic Liquid Diluent, **R. Rama**, Alok Rout, K.A. Venkatesan, M.P. Antony.. In: Nuclear and radiochemistry, KIIT University, Bhubaneswar, Odisha. M. Mohapatra, S. Dash, P.K. Pujari, S.K. Raskhit, B.S. Tomar (eds) (2017) p-242.

International Conference

1. Mutual separation of Pu(IV) from other actinides using α-hydroxy acetamide in room temperature ionic liquid medium, **R. Rama**, Alok Rout, K.A. Venkatesan, M.P. Antony. In: 3rd International Conference on Ionic Liquids in Separation and Purification Technology (ILSEPT), Kuala Lumpur, Malaysia (2017).

OTHERS

Publication not included in thesis

1.Electrochemical behavior of Eu(III) in imidazolium ionic liquid containing tri-n-butyl phosphate and N,N-dihexyloctanamide ligands. **R. Rama**, Alok Rout, K.A. Venkatesan, M.P. Antony, P.R. Vasudeva Rao. Journal of Electroanalytical Chemistry, 2015, 757., 36-43.

AWARDS

BEST POSTER AWARDS

1. **R. Rama**, Alok Rout, K.A. Venkatesan, M.P. Antony. “A novel phosphoramide task specific ionic liquid for extraction of actinides”, Emerging Trends in Separation Science and Technology (SESTEC -2016), IIT, Guwahati, May 17-20, 2016.
2. **R. Rama**, Alok Rout, K.A. Venkatesan, M.P. Antony. “Selective separation of Pu(IV) from other actinides using phosphoramide task specific ionic liquid”, Plutonium 75, IGCAR, Kalpakkam, May 23 – 25, 2016.

Dedicated to

MY FAMILY

ACKNOWLEDGEMENT

I express my sincere thanks to my Ph.D supervisor **Dr. M.P.Antony,** Head, Irradiated fuel studies Section, MC&MFCG, IGCAR, for his constant encouragement, support and valuable suggestions to improve the quality of work throughout my tenure.

I am extremely grateful to **Dr. U. Kamachi Mudali**, Director, MC&MFCG, IGCAR for his constant support and encouragement. I extend of my sincere thanks to **Dr. M. Joseph,** Associate Director, FCG, MC&MFCG and **Dr.K. Ananthasiavan**, Head, FChD, MC&MFCG for their constant support.

I express my sincere thanks to **Dr.A.K. Bhaduri**, Director**,** IGCAR**, Dr. S.A.V. Satya Murty,** former Director, IGCAR and **Dr.P.R.Vasudeva Rao,** former Director, IGCAR for providing me the opportunity to continue the research work at IGCAR.

I am also extremely indebted to my technology advisor **Dr.K.A. Venkatesan**, for providing necessary infrastructure and resources to accomplish my research work. I am very much thankful to him for his valuable guidance, advice, extensive discussions and his timely help through out my research work.

I am pleased to express my deep sense of gratitude to my doctoral committee chairman, **Dr.S. Anthonysamy**, members **Dr.N. Sivaraman**, **Dr.C. Mallika** a**nd Dr. R.V. Subba Rao** for their fruitful discussions, valuable suggestions, constant support and encouragement.

I am thankful to **Dr. M. Sai Baba** for for his kind advice, support and encouragement.

I express my hearty thanks to **Dr. R. Kumaresan** for his help in learning the experimental procedures during my initial stage of PhD work and also his constant support and encouragement.

I am very much thankful to **Dr. Alok Rout** for his technical support, guidance and timely help through out my research work.

My special thanks to **Mrs. K.V. Syamala** for her kind support and helping me in various ways during the course of this work.

I wish to record my sincere thanks to all my lab members, **Shri. B. Robert Selvan, Shri. A.S. Suneesh. Mrs. T. Prathibha, Mrs. Amutha suba, Shri. P.K. Nayak,** my senior **Dr. Jammu ravi,** my juniors, **Mr. G. Murali Krishna**, **Mr. K. Rama swamy**, **Mr. Ch Venkateswara Rao and Mr. P. Amesh** for their kind support and timely help through out my research work. I express my special thanks to Mrs. Amutha suba for her support and help during my experiments.

I am thankful to all the members of Irradiated Fuel Studies Section, **Dr. G. Panner Selvam, Mrs. Rajeswari, Mr. G.G.S. Subramanian, Mr. Kalayarasu, Mr. Amalraj, Smt. Amrita Sen, Shri. Karunanidhi and Mr.T. Bapuji** for their kind support. I express my special thanks to Mrs. Rajeswari for the viscosity measurements and Mr. T. Bapuji for his help during thesis writing.

The strong co-operation and kind support of all the members of Solution Chemistry and Separation Science section, **Dr.A. Suresh, Shri.C.V.S. Brahmananda Rao, Dr.B. Srinivasulu, Dr. Benadict Rakesh, Mrs. N. Navamani, Mrs. Jayalakshmi, Mrs. Ganga, Ms. Adithi and Mr. Amarendran** is deepely acknowledged.

I would like to extend my sincere thanks to **Dr. M. Joseph**, for his valuable efforts in analyzing the mass of several organic compounds and I also acknowledge **Dr.T. Sairam & Dr. Subramaniam** for the NMR analysis of samples.

I am very much thankful to **Homi Bhabha National Institue, Mumbai**, for providing me the opportunity to carry out my PhD work and also providing fund for attending international conference.

I express my hearty thanks to all the project students worked in my lab, **Swathi, M. Karnan**, **Prakharesh Awasthi, K. Inthumathi, A. Shajila & S. Suganya** and **K. Dasthaiah** (PhD Scholar, IITM) for their sincere help in doing some experiments.

I would like to express my special thanks to my best friends **Ms. G. Ganga Devi**, **Dr. N. Priyadarshini and Dr. Shuvra Singha** for their support and encouragement. I also express my thanks to my batchmates **R. Gopi, P.M. Aishwarya, J.K. Lakshmi** and **all my research scholar friends** for their support.

I would like to express my heartiest gratitude to**,** my parents, **Mr.V. Reghunathan & Mrs.R. Anusuya,** mother in law **Mrs.V. Madhuravalli,** my husband **Mr. V. Balaji,** sister **Mrs. R. Umamaheswari,** brother in law **Mr. R. Balaji** for their love, affection, encouragement and support throughout my life. I thank the **supreme soul** for helping me to reach this level.

Finally, I thank one and all who helped me during the research work.

CONTENTS

CHAPTER 2: EXPERIMENTAL

SYNOPSIS

1.0 Introduction

Electricity is one of the most vital components of infrastructure that determines the economic growth and welfare of nations. The sources of power generation in India ranges from conventional sources like coal, hydro, oil, natural gas and nuclear power to viable non-conventional sources like solar, wind and bio mass. Around 70% of India’s electricity generation is from fossil fuels. Due to the population growth and economic development, India’s rate of energy consumption increases rapidly which in turn results in shortage for fossil fuels. To overcome the future electricity demand, nuclear energy is an inevitable option due to the high energy output and minimal emission of green house gases etc. Currently, India gets 3% of its electricity from the nuclear power plants, however the expected demand from nuclear power plants is approximately 25% in the near future [1].

Nuclear reactors mainly use the natural or enriched uranium as the fuel for electricity production. The nuclear fuel discharged from the nuclear reactor after the power production is known as spent nuclear fuel and it contains significant amount of valuable fissile materials such as unused uranium, plutonium and other useful fission products such as ^{137}Cs and ^{90}Sr. The spent nuclear fuel is therefore reprocessed to recover these fissile elements for further use in reactors as fuels. Two approaches are available for the reprocessing of spent nuclear fuel; (1) Aqueous based industrially well-established, PUREX (Plutonium Uranium Recovery by Extraction) process and a (2) Non-aqueous pyrochemical process. The PUREX process involves the dissolution of spent nuclear fuel in nitric acid medium followed by the liquid-liquid extraction of uranium(VI) and plutonium(IV) from the dissolver solution (3 – 4 M nitric acid medium). The extraction was carried out using a solution of 1.1 M tri-*n*-butyl phosphate (TBP), as an extractant, in *n*-dodecane (*n*-DD) as a diluent [2].

The aqueous waste rejected after the PUREX process is known as “high-level liquid waste”. The HLLW contains several elements such as trivalent actinides called minor actinides (MA), lanthanides fission products, other fission products and corrosion products of structural materials present in 3-4 M nitric acid medium. The long term radioactivity of HLLW is essentially due to the alpha emitting long lived minor actinides such as ^{241}Am ($t_{1/2}$ = 433 y) and ^{244}Cm ($t_{1/2}$ = 18.1 y) Partitioning and Transmutation (P & T) is being considered as a viable strategy for the safe management of HLLW. P&T involves in the separation of minor actinides from HLLW and transmutation of them into stable or innocuous products in advanced fast reactors or accelerator driven system (ADS) [3].

Non-aqueous method for reprocessing of spent nuclear fuel is a high temperature pyrochemical method. The method has several inherent advantages such as the ability to handle high burn-up spent fuel, reduced criticality accident, generation of minimum aqueous waste and feasibility of on-site reprocessing due to compact size. In non-aqueous reprocessing, the methods such as electrowinning, electrorefining and direct oxide reduction are popular for the reprocessing of spent nuclear fuels [4]. This method exploits the differences in the thermodynamic stabilities of various actinides and fission products in high temperature molten salt medium for the dissolution of spent nuclear fuel and the electrochemical recovery of actinides. The molten salt medium is composed of a eutectic of alkali and alkaline earth metal chloride salts. Depending upon the composition of the eutectic, the operating temperature of pyrochemical method ranges from 600-800 K. Requirement of inert atmosphere, high temperature operation and corrosion problems make the pyrochemical method more challenging.

Over the past few decades, Room Temperature Ionin Liquids (RTILs) have been receiving increased attention for possible applications in the area of nuclear fuel reprocessing and waste management [5]. RTILs are composed fully of dissociated ions and their melting points are below 100° C. The distinctive features of ionic liquids include negligible vapor pressure, high thermal stability, wide liquid range, high solubility for organic species, wide electrochemical window and electrical conductivity etc. In addition, the property of ionic liquid can be tuned by suitable combination of cations and anions. A large number of reports are available on the use of ionic liquids as diluents for the extraction of actinides and fission products. Similarly, in the recent years, functionalized ionic liquids (FILs) (or task specific ionic liquids (TSILs)) [6] and the ionic liquids with strongly coordinating anion [7] have been reported as extractants for the metal ion separations. Extraordinary extraction of metal ions has been observed in RTIL medium. Presence of ionic liquid diluents in organic phase facilitates a new mode of recovery of metals by direct electrodeposition from the loaded organic phase after the solvent extraction procedure which is known as Extraction-Electro deposition (Ex-El) approach [8]. In the recent past, electrochemical behavior and electro deposition of some of the actinides and fission products have been reported in RTILs. Similarly, there has been increasing interest to understand the electrochemical behavior of metal ions in room temperature ionic liquid medium in the presence of extractant [9, 10].

2.0 Scope of the present work

The aim of the present work is to study the feasibility of employing the RTILs for the nuclear fuel cycle applications. The present study consists of solvent extraction and electrochemical study of lanthanides and actinides in RTIL medium. In these studies, RTILs were explored for three different roles; i. as diluents, ii. As extractant and iii. As electrolytic medium. For solvent extraction studies, imidazolium and pyrrolidinum cation based ionic liquids were used as diluents and phosphoramide functionalized ionic liquid & dilakyl phosphate anion containing ionic liquid were investigated as extractant. In addition, the present study also focused to understand the electrochemical behavior of lanthanides and actinides in the presence of extractants using RTIL as electrolytic medium.

3.0 Organization of the thesis

This thesis is divided into seven chapters and the brief details of each chapter are given below.

Chapter 1

Chapter 1 describes the importance of nuclear energy programme for the economic growth and welfare of the nation. Spent nuclear fuel reprocessing and its needs are also discussed in detail. This chapter also covers a brief introduction of room temperature ionic liquid and merits of RTILs based extraction system over the conventional extraction system. The roles of RTILs as diluent, extractant and electrolytic medium for the spent nuclear fuel reprocessing have been explained. A short note on scope of the present study and overview of the thesis concludes this chapter.

Chapter 2

Chapter 2 provides a detailed description on the chemicals, reagents, synthetic and purification procedures adopted for the synthesis of various room temperature ionic liquids and extractants used in this present study. Spectroscopic techniques such as NMR, FT-IR and mass spectrometry, transient electrochemical techniques such as cyclic voltammetry, chronopotentiometry and chronoamperometry and also methodologies adopted for the measurement of radioactivity using α-scintillation counting, NaI(Tl) detector are discussed. Experimental set up and procedures adopted for the solvent extraction and electrochemical studies are mentioned in detail.

Chapter 3

In chapter 3, RTILs have been explored as diluents. This chapter deals with solvent extraction studies of some of the actinides namely, Am(III), U(VI) and Pu(IV) using molecular extractants in RTIL medium. This chapter has three parts namely Part A, Part B & Part C and the summary of each part has been described below.

Part A deals with solvent extraction studies of U(VI) using a solution of tri-*n*-alkylphosphates (TalPs) present in 1-octyl-3-methylimidazolium bis(trifluoromethanesulfonyl)imide ([C_8mim][NTf_2]) ionic liquid. The extractants investigated were tri-*n*-propylphosphate (TPP), tri-*n*-butylphosphate (TBP), tri-*n*-amylphosphate (TAP), tri-*n*-octylphosphate (TOP), tri-iso-amylphosphate (TiAP) and tri-iso-butylphosphate (TiBP). The extraction of U(VI) was investigated as a function of various parameters, such as equilibration time, nitric acid concentration, extractant concentration, temperature variation and nature of ionic liquid cation. The distribution ratios of U(VI) increased with an increase in the concentration of nitric acid in all the tri-*n*-alkylphosphates and decreases in the order TOP > TAP $\simeq$ TIAP > TBP $\simeq$ TIBP > TPP. The stoichiometry of metal-solvate complex was found to be 1:2 (U: TAlP) in ionic liquid phase for all the tri-*n*-alkylphosphates. Quantitative stripping of uranium from the loaded ionic liquid phase was achieved using dilute nitric acid

Part B deals with the selective separation of Pu(IV) from the other actinides, U(VI) and Am(III) using *N*,*N*-dioctyl-2-hydroxyacetamide (DOHyA) present in the room temperature ionic liquid namely 1-butyl-3-methylimidazolium bis(trifluoromethanesulfonyl)imide ([C_4mim][NTf_2]). The distribution ratio of plutonium ($D_{Pu(IV)}$) obtained in DOHyA/[C_4mim][NTf_2] was compared with those obtained in DOHyA/*n*-dodecane. Extraordinary extraction of Pu(IV) was achieved when ionic liquid medium acted as diluents. The extraction was studied as a function of various parameters such as concentration of nitric acid, extractant concentration, temperature, alkyl chain length attached to amidic nitrogen of the extractant etc. The separation factor of Pu(IV) over U(VI) ranged from 1833 to 78 and the separation factor of Pu(IV) over Am(III) ranged from 48 to 354 in DOHyA/[C_4mim][NTf_2] at different HNO_3 concentrations. The loaded Pu(IV) in ionic liquid phase was recovered by using complexing agents such as acetohydroxamic acid and oxalic acid.

Part C deals with the studies on the extraction of Am(III) from nitric acid medium by a solution of benzoylpyrazolone (HPMBP) dissolved in 1-butyl-3-methylpyrrolidinium bis(trifluoro-methanesulfonyl)imide ([C_4mpy][NTf_2]) ionic liquid. The distribution ratio of ^{241}Am(III) in ionic liquid phase was investigated as a function of various parameters, such as pH of aqueous phase, duration of equilibration, concentration of ionic liquid and nitrate in aqueous phase etc. Extraordinary extraction was obtained using HPMBP in ionic liquid phase than in *n*-dodecane. The stoichiometry of metal-solvate in ionic liquid phase was determined by the slope analysis of the extraction data and it indicated the formation of 1:3 (Am: HPMBP) complex in ionic liquid phase. Recovery of americium from the loaded ionic liquid phase was achieved using nitric acid.

Chapter 4

Chapter 4 describes the solvent extraction studies of actinides, U(VI), Pu(IV) & Am(III) using RTILs as extractants. In this study, phosphoramide based TSIL & dialkylphosphate anion containing ionic liquid were explored as extractants. The studies involved in this chapter are divided into two parts namely, Part I & part II.

Part I deals with solvent extraction studies of actinides using a task specific ionic liquid. A new task specific ionic liquid, diethyl-3-(-3-butylimidazolium) propylphosphoramide bis(trifluoromethanesulfonyl)imide ([BuImPA][NTf_2]) was synthesized and reported for the solvent extraction studies of Pu(IV),U(VI) and Am(III) from nitric acid medium for the first time. Unlike traditional extractants, the separation factor of Pu(IV) over U(VI) was about 10 and that over Am(III) was of the order 10^3, suggesting the possibility of separating the fissile element plutonium from other actinides. It was found that the –NH- moiety in TSIL was protonated predominantly over >P=O and that seems to facilitate the extraction of Pu(IV) in ionic liquid phase. Quantitative stripping of Pu(IV) from the loaded organic phase was achieved using a complexing agent.

Part II describes the solvent extraction behavior of U(VI) in a PUREX solvent namely 1.1 M tri-*n*-butyl phosphate (TBP) in *n*-dodecane (n-DD) in the presence and absence of the ionic liquid with strongly coordinating anion, tri-*n*-octylmethylammonium di-(2-ethylhexyl)phosphate ($[A336]^+[DEHP]^-$). Remarkable enhancement in the distribution ratio of U(VI) was observed in the presence of ionic liquid. The extraction of U(VI) is accompanied by the extraction of nitric acid leading to the formation of ionic liquid constituents namely $[A336]^+[NO_3]^-$ and HDEHP. Synergic extraction of U(VI) was observed when HDEHP was employed in conjunction with $[A336]^+[NO3]^-$ and TBP. The study revealed that the distribution ratio of U(VI) obtained in presence of ionic liquid was due to the synergic contributions of ionic liquid components and TBP.

Chapter 5

Chapter 5 describes loading behavior of Eu(III) at high aqueous concentration ranging from 1 g/L to 100 g/L in a solution of *N,N,N',N'*-tetra-*n*-octyldiglycolamide (TODGA) dissolved in 1-octyl-3-methylimidazolium bis(trifluormethanesulfonyl)imide ($[C_8mim][NTf_2]$). The extraction of Eu(III) was studied as a function of various parameters such as the concentration of nitric acid, Eu(III) ion concentration in aqueous phase, concentration of TODGA in organic phase, nature of the ionic liquid diluents, nature of extractant, and phase modifier (tri-*n*-butyl phosphate (TBP) and *N,N*-

dihexyloctanamide) etc. The loading of Eu(III) in TODGA/[C_8mim][NTf_2] increased marginally with increase in the amount of Eu(III) present in nitric acid phase. Unlike molecular diluents, the third phase formation was not observed even at 100 g/L Eu(III) present in 3–5 M nitric acid phase. Slope analysis of the extraction data was carried out to determine the stoichiometry of Eu(III) – TODGA complex in ionic liquid phase. Synergic extraction of Eu(III) was observed in the presence of TBP and the dependency of TODGA and TBP in the extraction of Eu(III) was determined. On contrary, the presence of DHOA hardly improved extraction of Eu(III) in TODGA/ionic liquid phase. The results revealed that Eu(III) could be loaded to the extent of 1: 3 stoichiometry in ionic liquid phase without leading to undesirable third phase formation.

Chapter 6

Chapter 6 deals with electrochemical studies where the RTILs are explored as electrolytic medium. This chapter describes the electrochemical behavior of Eu(III) and U(VI) in RTIL medium containing ligands. In this aspect, two different systems have been studied. This chapter is divided into two parts namely Part 1 & Part 2.

Part 1 describes electrochemical behaviour of the actinide representative, U(VI), present in 1-butyl-3-methylimidazolium bis(trifluoromethanesulfonyl)imide (C_4mimNTf_2) containing higher homolog of trialkyl phosphate namely tri-*n*-octyl phosphate (TOP) using cyclic voltammetric technique. The cathodic wave responsible for the reduction of U(VI) to U(V) shifted cathodically and the peak potential lowered in the presence of these ligands. Depending upon the nature of alkyl chain length attached to the phosphoryl group of trialkyl phosphate, the shift was quite different. The diffusion coefficient of U(VI) and the heterogeneous electron transfer rate constant in [C_4mim][NTf_2] decreased in the order U(VI) > U(VI) – TBP > U(VI) –TOP. The stability constant (ln K_f) of U(VI)-ligand complex was determined to be 2.7 and 2.9 for U(VI)-TBP and U(VI)-TOP complexes respectively The results obtained in this study indicated that the electrochemical behaviour of U(VI) in [C_4mim][NTf_2] medium would show a strong dependence on the nature of ligand employed for extraction.

Part 2 describes electrochemical behaviour of Eu(III) in the room temperature ionic liquid, 1-butyl-1-methylpyrrolidinium bis(trifluoromethanesulfonyl)imide ([C_4mpy][NTf_2]) by various transient electrochemical techniques in the presence and absence of ligands such as di(2-ethylhexyl)phosphoric acid (HDEHP) and diglycolamic acids (HDGA) which has been proposed for the mutual separation of lanthanides and actinides at the back end of nuclear fuel. The addition of HDEHP and HDGA to the Eu(III)/[C_4mpy][NTf_2] solution lowered the cathodic peak current and shifted the cathodic peak potential cathodically due to the coordination of Eu(III) with ligands in the ionic liquid medium. The diffusion coefficients and heterogeneous rate constants have been determined. The stability constant (ln Kf) of Eu(III)-ligand complex was determined to be 5 and 5.65 for (Eu(III)-HDEHP) and (Eu(III)- HDGA) complexes respectively, which was in accordance with diffusion coefficients.

Chapter 7

Chapter 7 constitutes the summary of the results, conclusion obtained in the present work and the scope of the future work in this field.

4.0 REFERENCES

1. http://www.world-nuclear.org/information-library/country-profiles/countries-g-n/india.aspx
2. J. L. Swanson, “PUREX Process Flow sheets”, In: Science and Technology of Tributyl phosphate, Eds. W.W. Schulz, L.L. Burger, J.D. Navratil, K.P. Bender, CRC Press Inc. Boca Raton, p 55, 1984.
3. Implications of Partitioning and Transmutation in Radioactive Waste Management. IAEA Technical Reports Series, STI/DOC/010/435, 2004.
4. A.V. Bychkov, O.V. Skiba. Review of Non-Aqueous Nuclear Fuel Reprocessing and Separation Methods. In: Chemical Separation Technologies and Related Methods of Nuclear Waste Management, G.R. Choppin, M.Kh. Khankhasayev, eds., Kluwer Academic Publishers: Netherlands (1999) 71–98.
5. P.R. Vasudeva Rao, K.A. Venkatesan, Alok Rout, T.G. Srinivasan, K. Nagarajan. Potential applications of room temperature ionic liquids for fission products and actinide separation. Sep. Sci. Technol. 47 (2012) 204-222.
6. A.E.Visser, R.P. Swatloski, W.M. Reichert, R. Mayton, S. Sheff, A. Wierzbicki, R.D. Rogers, Task-specific ionic liquids for the extraction of metal ions from aqueous solutions. Chem. Commun. 1 (2001) 135-136.
7. X. Sun, Y. Ji, F. Hu, Bo. He, Ji. Chen, D. Li, The inner synergic effect of bifunctional ionic liquid extractant for solvent extraction. Talanta 81 (2010) 1877–1883.
8. K.A. Venkatesan, T.G. Srinivasan, P.R Vasudeva Rao. A review on the electrochemical applications of room temperature ionic liquids in nuclear fuel cycle. J. Nucl. Radiochem. Sci. 10 (2009) R1-R6.

9. K. Jayachandran, R. Gupta, M. Sundararajan, S.K. Gupta, M. Mohapatra, S.K. Mukerjee. Redox and Photophysical Behaviour of Complexes of NpO^{2+} Ions with Carbomyl methyl phosphine oxide in 1-Hexyl-3-methylimidazolium bis (trifluoromethylsulfonyl) imide Ionic Liquid. Electrochim. Acta. 224 (2017) 269-277.
10. Y. Pan, C.L. Hussey. Electrochemical and Spectroscopic Investigation of Ln^{3+} (Ln= Sm, Eu, and Yb) Solvation in Bis (trifluoromethylsulfonyl) imide-Based Ionic Liquids and Coordination by *N*, *N*, *N′*, *N′*-Tetraoctyl-3-oxa-pentane Diamide (TODGA) and Chloride. Inorg Chem. 52 (2013) 3241-3252.

LIST OF FIGURES

LIST OF TABLES

CHAPTER 1

INTRODUCTION

Electricity is the lifeblood of modern society and it determines the socio-economic growth of a country [1]. The global demand for electricity is increasing rapidly with continued population growth and economic development. The choice of fuel for energy production is essentially dictated by the availability and accessibility of the source, its economic viability, and the convenience it offers. Nearly 75 % of the world energy production is mainly from the fossil fuels such as coal, gas, and oil [2]. However, the use of fossil fuels leads to the generation of green house gases such as carbon dioxide which pollute the environment. In view of this as well as due to the uncertainty in the development of renewable resources such as wind, solar, tidal powers etc., the nuclear energy option for meeting the future energy demand is inevitable since the nuclear energy has several advantages such as carbon-free source of power and enhanced energy production as compared to the fossil fuels. Currently, India gets 3% of its electricity from the nuclear power plants and the expected demand from nuclear power plants is approximately 25% in the near future [3,4].

1.1 Nuclear Fuel Cycle (NFC)

Nuclear power can be generated by technologies based on fission and fusion. Among these two methods, the technology based on fission is industrially well-established. Electricity generation through nuclear fission reactors has several stages which starts from mining of uranium ore and ends with waste management. All these stages are collectively called as nuclear fuel cycle (NFC) [5]. From mining of uranium to fuel loading into nuclear reactor is called as “front end of the fuel cycle” (NFC).

and back end of NFC involves temporary storage and waste management of spent nuclear fuel (SNF) which is discharged from the reactor after the electricity production. There are two options for the SNF ie (i) Long term storage and final disposal without reprocessing (ii) Reprocessing to recover and recycle the usable portion of it. Figure 1.1 illustrates the various stages involved in NFC.

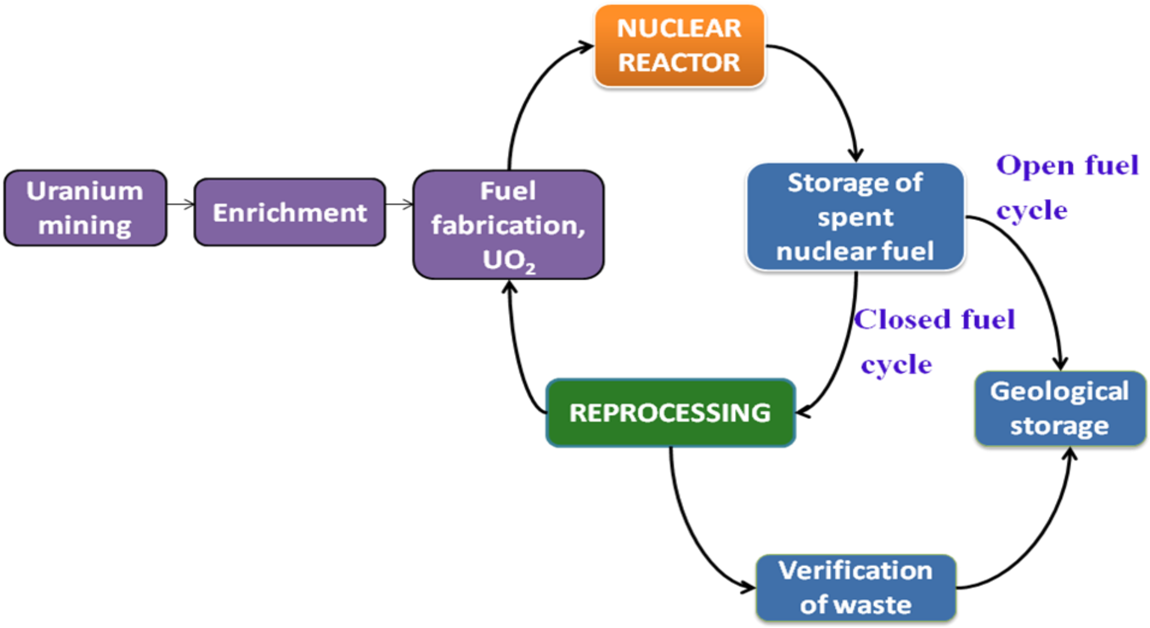

Figure 1.1 Nuclear fuel cycle

1.2 Nuclear power programme in India

In 1954, Dr. Homi Bhabha, the architect of the Indian nuclear programme envisaged a three-stage nuclear programme based on a closed nuclear fuel cycle in order to meet the nation’s energy demand [6]. The ultimate aim of this programme was to judiciously utilize the uranium and thorium resources of the country to the maximum extent. The first stage involves electricity generation using domestic natural uranium fuelled pressurized heavy water reactors (PHWR). Currently, there are eighteen PHWRs, two BWR, and one PWR (VVER) operating with a total capacity of 5780 MWe [7]. The spent fuel from PHWR contains small quantities of fissile ^{239}Pu along with residual uranium (known as depleted uranium, which is predominantly ^{238}U). The spent fuel can be reprocessed chemically to separate plutonium and residual uranium from fission products. The products obtained in the first stage namely plutonium and depleted uranium from the spent fuels of PHWR is used for fueling fast breeder reactors (FBRs) to generate electricity in the second stage. Moreover, in the second stage nuclear power reactors, thorium (^{232}Th) is kept as blanket for converting the fertile ^{232}Th into fissile ^{233}U. A 40 MWt Fast Breeder Test Reactor (FBTR) is in operation at Kalpakkam since 1985 [8] to demonstrate the second stage. India's first commercial fast reactor, the 500 MWe Prototype Fast Breeder Reactor (PFBR) is in the advanced stage of completion. The fissile ^{233}U produced from fertile element thorium (Th) is then utilized in the third stage. Thus, the third stage utilizes the plenteous thorium resources available in India. A 30 kWt reactor, KAlpakkam MINI reactor (KAMINI), kalpakkam, India is the only reactor in the world, which employ ^{233}U as fuel [9].

1.3. Radiotoxicity of spent nuclear fuel (SNF)

The fuel discharged from the nuclear reactor is referred as spent nuclear fuel (SNF) which consists of long-lived alpha emitting actinides such as plutonium, neptunium, americium, curium etc. and fission products (FPs) such as ^{93}Zr, ^{99}Mo, ^{133}Cs, ^{137}Cs, ^{131}I, ^{135}I, ^{103}Ru, ^{106}Ru, Xe, Kr, lanthanides etc. The variation in the relative radiotoxicity of different components of spent nuclear fuel with time is shown in figure 1.2. For the first 100 years after discharge from nuclear reactor, spent fuel radiotoxicity is determined by the FPs [10]. It is then determined by Pu and other minor actinides (MAs) such as Np, Am and Cm.

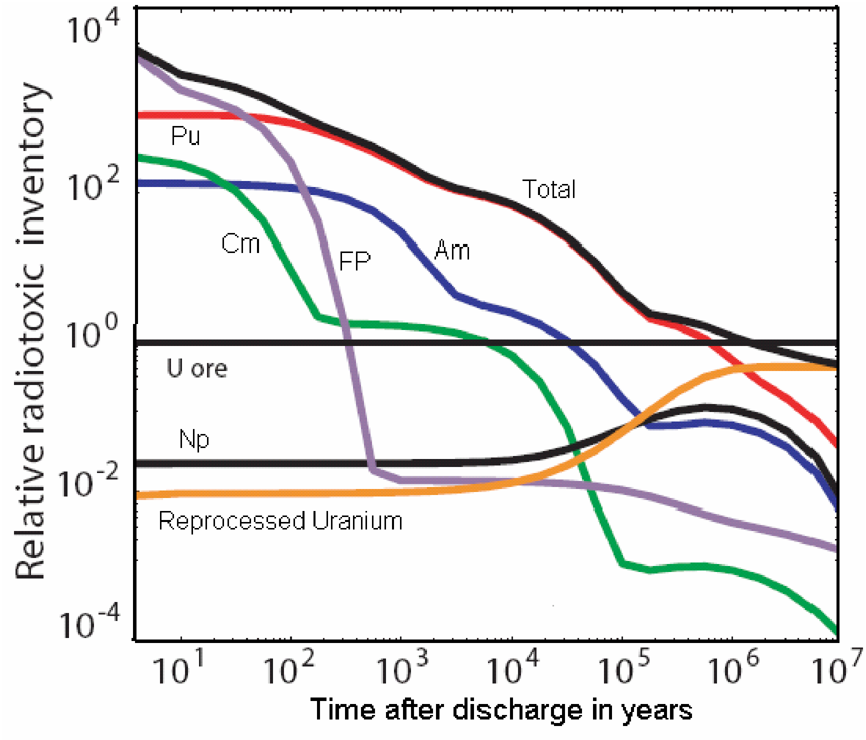

Figure 1.2. Relative radiotoxicity of different components in the spent nuclear fuel from a light water reactor irradiated to 41 M Wd/kg U with respect to the radiotoxicity of the corresponding uranium ore [10].

1.4 Reprocessing of SNF

The spent nuclear fuel discharged from nuclear power reactors contains significant quantities of fissile element, plutonium and un-used uranium which can be reprocessed from the SNF for further use in fast reactors as fuel. Two methods are available for the reprocessing of spent nuclear fuel; (1) Aqueous based industrially well-established, PUREX (Plutonium Uranium Reduction EXtraction) process (2) Non-aqueous pyrochemical process. Among these, the aqueous based process, namely PUREX has been widely employed for reprocessing [11,12].

1.4.1 PUREX Process

PUREX process consists of three major steps namely (i) head end step, which is comprised of decladding, dissolution, and feed preparation, (ii) solvent extraction using TBP (Tri-*n*-butyl Phosphate), which involves co-extraction of uranium and plutonium followed by their partitioning and stripping and (iii) final purification and conversion of uranium and plutonium to their respective oxides. The heart of PUREX process is liquid-liquid extraction of uranium(VI) and plutonium(IV) from the dissolver solution (3 - 4 M nitric acid medium) followed by partitioning of uranium and plutonium. The extraction was carried out using a solution of 1.1 M tri-*n*-butyl phosphate (TBP), as an extractant, in *n*-dodecane (*n*-DD) as a diluent. The metal loaded organic phase is then contacted with an aqueous solution containing uranous nitrate stabilized with hydrazine or ferrous sulfamate, which selectively reduces Pu(IV) present in the organic phase to inextractable Pu(III). The resulting Pu(III) then distributes to aqueous phase and thus enables the separation of uranium and plutonium. The uranium present in the organic phase is recovered by stripping it with dilute nitric acid. The uranium present in the strip is concentrated, precipitated as ammonium diuranate and finally calcined to get uranium oxide. The plutonium product after separation from uranium bulk is once again purified by either solvent extraction or ion exchange method [13] and then it is precipitated as oxalate which is filtered and calcined to obtain plutonium oxide. The aqueous waste rejected after the PUREX process is known as “high-level liquid waste” (HLLW). Figure 1.3 illustrates the schematic diagram PUREX process for an oxide fuel reprocessing.

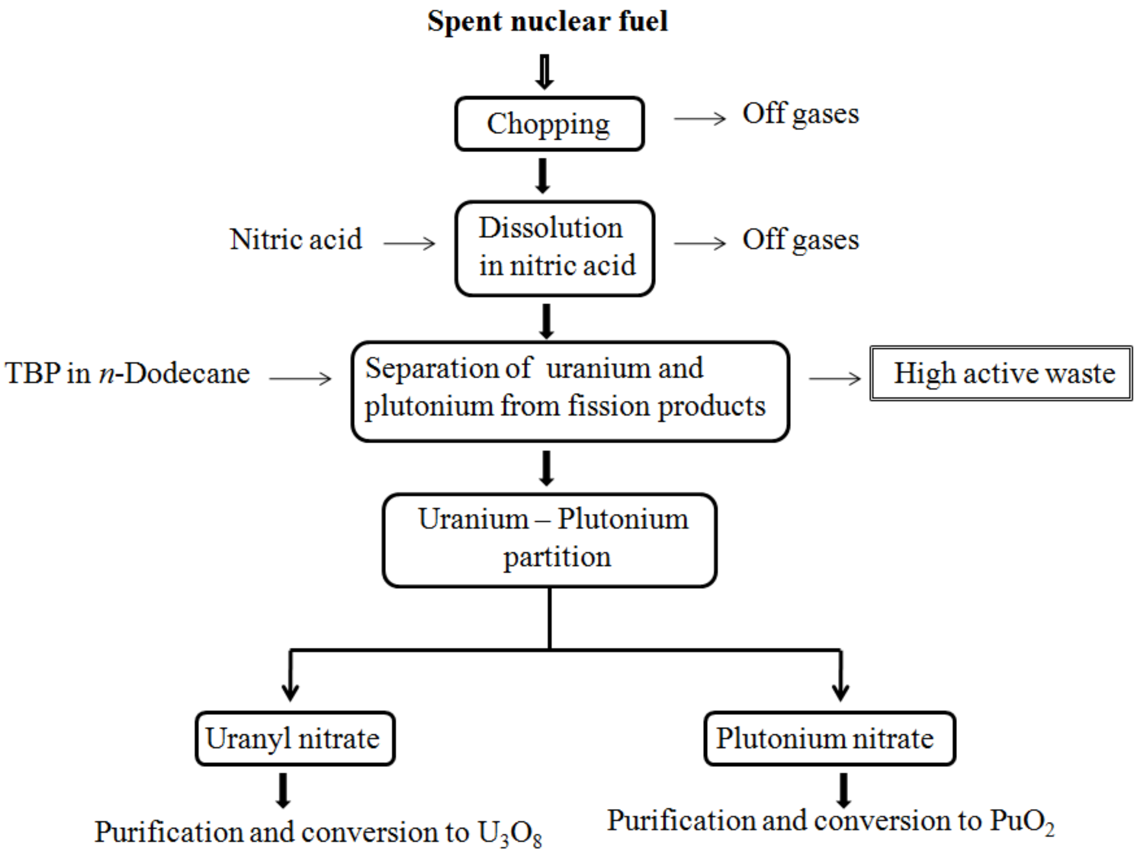

Figure 1.3. Schematic diagram of PUREX process for an oxide fuel reprocessing

1.4.1.1 High level liquid waste management

The HLLW contains several elements such as trivalent actinides called minor actinides (MA), lanthanide fission products, other fission products and corrosion products of structural materials present in 3-4 M nitric acid medium. The long term radioactivity of HLLW is essentially due to the minor actinides such as ^{237}Np, ^{241}Am, ^{243}Am, ^{244}Cm, ^{245}Cm, ^{243}Cm and fission products such as ^{99}Tc, ^{107}Pd, ^{93}Zr, ^{129}I, ^{135}Cs, ^{137}Cs, and ^{90}Sr. Since the half-lives of these isotopes vary from few years to several hundred years, the HLLW poses a long-term risk to the public health and safety of environment. Therefore, the success of nuclear energy programme depends on the safe management of HLLW. Currently, immobilization of HLLW in a suitable non-leachable ceramic or glass matrix, followed by the deposition in deep geological repositories is being practiced [14].

However, it demands the long-term surveillance over thousands of years due to the presence of these minor actinides as their half-lives are very high. Moreover, in case of accidental ground-water invasion into these repositories, the radiotoxic metal ions can be released in to the environment due to their significant solubility and mobility in aqueous medium. Hence the current disposal practice is very expensive option.

Alternatively, partitioning and transmutation (P&T) [15,16] which involves removal of minor actinides from fission products followed by their transmutation in to short lived isotopes in accelerator driven systems (ADS) or fast-reactors is being considered as a viable option for the safe management of HLLW since P&T reduces the radiotoxicity of HLLW enormously and minimises the surveillance period. The success of P&T strategy depends on efficient separation of minor actinides and burning in ADS. The concentration of transplutonium actinides (Am and Cm) in HLLW is ~20 ppm and the concentration of lanthanides fission products is ~3000 ppm. The transplutonium actinides essentially exhibit trivalent oxidation state and chemically behave like trivalent lanthanides (Ln(III)) [8]. Due to high neutron absorption cross-section of Ln(III), the efficient transmutation of An(III) is not possible. Moreover, Ln(III) do not form solid solutions in metal alloys or in mixed oxide transmutation targets, and as a result they segregate in separate phases with the tendency to grow under thermal treatment. In view of these, the complete separation of Ln(III) from An(III) is very important prior to the actinide transmutation [9].

Therefore, the current method for partitioning involves the liquid-liquid extraction of An(III) and Ln(III) together from HLLW in the first extraction cycle, followed by lanthanide-actinide separation in the second cycle. For the co-extraction of An(III) and Ln(III) from HLLW several processes such as TRans Uranium element Extraction (TRUEX) [17-20], TriAlkyl Phosphine Oxides (TRPO)[21-23], Di-IsoDecyl-Phosphoric

Acid (DIDPA)[24,25], DIAMide Extraction (DIAMEX)[26-28], octyl derivatives of diglycolamides (DGAs) [29-35] and in the recent past *N,N,N',N'*-tetraalkyl-3,6-dioxaoctane diamides (DOODA) such as DOODA-C_8 and DOODA-C_{12} were proposed [34]. After co-extraction of An(III) and Ln(III) from 3 - 4 M nitric acid (HLLW acidity), the metal ions are stripped back using dilute nitric acid (0.01 M) or using some complexing agents such as citric acid, lactic acid etc. After the co-extraction, for the mutual separation of Ln(III) and An(III) present in stripped solution, several processes such as TALSPEAK, SETFICS etc have been proposed [35]

1.4.2 Non-aqueous pyrochemical process

Non-aqueous method for reprocessing of spent nuclear fuel is a high temperature pyrochemical method. In non-aqueous reprocessing, the methods such as electrowinning, electrorefining, and direct oxide reduction are popular for the reprocessing of spent nuclear fuels. These methods exploit the differences in the thermodynamic stabilities of various actinides and fission products chlorides in high temperature molten salt medium for the dissolution of spent nuclear fuel. The molten salt medium is composed of an eutectic of alkali and alkaline earth metal chloride salts. Depending upon the composition of the eutectic, the operating temperature of pyrochemical method ranges from 327-527ºC [36-39].

In the electrochemical reduction process (or oxide reduction process) using molten salt, the spent oxide fuel is reduced to supply metal feed to the electro-refining process. Additionally, high heat load fission products are dissolved into the molten salt, thus decreasing the heat load of the spent fuel. In electrorefining process, the SNF is dissolved anodically and then uranium and transuranium elements are deposited at the cathode by electrotransport through a suitable electrolyte with greater purity. In the case of electrowinning process, SNF is dissolved into molten salt eutectic by chlorination and uranium is electrowon while plutonium is precipitated as PuO_2 from the melt. Requirement of inert atmosphere, high temperature operation and corrosion problems make the pyrochemical method more challenging.

1.5. Solvent extraction for aqueous reprocessing and waste management

Liquid- liquid extraction commonly known as solvent extraction is an important separation technology for a wide range of applications in various industries such as nuclear, metallurgical, pharmaceutical, food and beverage, chemical, petrochemical, biochemical, catalysis, polymers, etc,. Solvent extraction is the distribution of a solute (for example, desired metal ion, M) between two immiscible liquids namely aqueous and organic phases in contact with each other. The solute M, dissolved in one liquid distributes into another immiscible liquid until its chemical potential becomes equal in both the phases. This condition is referred as equilibrium. The distribution of solute to the organic phase depends up on the complexing ability of the reagent (known as extractant) present in organic phase. In most of the solvent extraction processes, extractants are dissolved in a non-reactive organic medium in which they are completely miscible, is called as diluents.The distribution ratio of a solute M (D_M) is defined as the ratio of the concentration of the solute in organic phase ($[M]_{org)}$ to that in aqueous phase ($[M]_{aq}$) at equilibrium, as shown in equation 1.1.

$$D_M = [M]_{org} / [M]_{aq} \tag{1.1}$$

D_M is constant for given pair of liquids at constant temperature. In metal recovery operations, the valuable component is a metal ion or metal complex contained in aqueous solution. This aqueous solution is mixed with an immiscible organic phase containing the active extractant. The extractant transfers metal ion from aqueous phase into organic phase by a series of chemical reactions. This process is refered as “extraction”. The metal ion present in the loaded organic phase is recovered by “back extraction” using aqueous reagents. This process is refered as “stripping”. The organic phase after stripping is called lean organic phase and is recycled back for extraction. The aqueous phase containing metal now goes to final metal recovery.

At the front end of nuclear fuel cycle, solvent extraction process is usually employed for the recovery of U and Th in the pure form from various primary and secondary sources. Solvent extraction plays an important role even in the reprocessing of spent nuclear fuel and allied waste management at the backend of nuclear fuel cycle.

1.6 Room temperature ionic liquids (RTILs)

In general, volatile organic compounds (VOCs) such as dichloromethane, chloroform, carbontetrachloride, acetone, chlrofluorocarbon, benzene, toluene, xylene, acetone etc. are widely used as solvents and reaction media in the synthesis of many chemical compounds. The VOCs used in high quantity are harmful to the humankind in nature and they have the main disadvantages such as high-volatility, evolution of harmful gases and less thermal stability. In this context, a new approach has received attention and is being called as Green Chemistry, Clean Chemistry etc. Green chemistry mainly aims at development of safe processes and reducing the waste generated from an industrial chemical process to a minimum acceptable level and hence it requires rethinking and redesign of many existing chemical processes by appropriate use of environmental friendly solvents and chemicals. The technology which includes the design of chemical products and processes to reduce or to eliminate the use and generation of hazardous substances is called the green technology [40].

There are several laws, regulations and protocols in United States for monitoring the use of volatile organic solvents and making use of environment friendly solvents in industries. These include Clean Air Act Amendments, Clean Water Act, Toxic Release Inventory, Toxic Substances Control Act and Montreal protocol [41]. The Montreal protocol suggested green chemistry alternatives for the chemical processes which use aqueous solvents, supercritical or dense phase fluids**,** ionic liquids, immobilized solvents, solvent less conditions, reduced hazard organic solvents and fluorous solvents [42]. Ionic liquids are one of the most promising candidates for green processes due to the distinctive features of ionic liquids which include negligible vapour pressure, high thermal stability, wide liquid range, high solubility for organic species, wide electrochemical window and electrical conductivity etc [42].

Room temperature ionic liquids are composed fully of dissociated ions and their melting points are below 100˚ C [43-47]. They are comprised of bulky, assymmetric, organic cations such as 1-alkyl-3-methylimidazolium, 1-alkylpyridinium, *N*-methyl-*N*-alkylpyrrolidinium and ammonium ions etc. and inorganic or organic anions such as halides, BF_4^-, PF_6^-, triflates, tosylates, bis(trifluoromethanesulfonyl)imide (NTf_2^-) etc. The structure of some of the common cations and anions are given in figure 1.4.

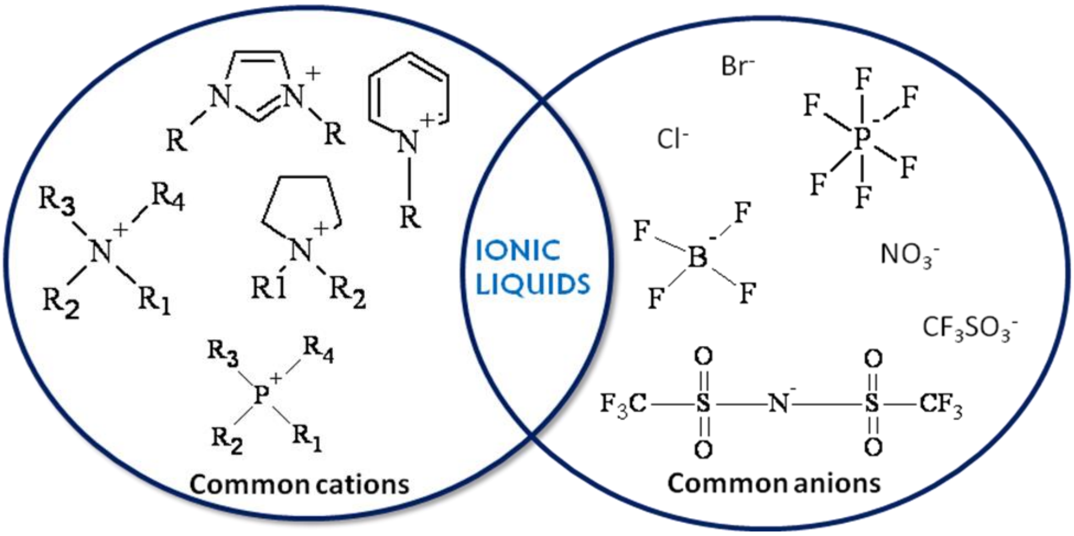

Figure 1.4 Common IL cations and anions

As estimated by Earle and Seddon [40,48], a huge number (10^{12}) of RTILs can be made by various combinations of cations and anions. It is possible to design RTILs as per the required properties for a specific application and so they are called as tailor–made ionic liquids or designer solvents.

1.6.1 Room temperature ionic liquids – A brief history

The history about RTILs has been reviewed in detail by Wilkes and Seddon [46,47]. The chemistry of salts with low melting points was on track in the second half of 19th century. The protic ionic liquid, ethanolammonium nitrate with the melting point of 52-55ºC was discovered by Gabriel [49]. Later in 1914, Paul Walden [50] reported the first stable and useful RTIL, namely, ethyl ammonium nitrate with a melting point of 12.5 ºC. Subsequently, the application of ionic liquids in various areas expanded that led to the synthesis of a variety of ionic liquids with desired physical and chemical properties. Based on the properties of RTILs, it can be classified into three main generations which are given below [51, 52].

(i) First generation ionic liquids

The first generation ionic liquids are a mixture of organic species with $AlCl_3$. These ionic liquids are known as chloroaluminates [53]. The important property of these ionic liquids is their tunable viscosity, melting point and variable acidity of the melt. Major limitation of the first generation ionic liquids is the need of inert atmosphere for handling these types of ionic liquids due to their hygroscopic property. However, these ionic liquids have been used as electrolytes in batteries.

(i) Second generation ionic liquids

The air and water stable ionic liquids comprise the 2nd generation of ionic liquids. In 1992, Wilkis and Zoworoto [54] reported series of ionic liquids with imidazolium/pyridinum cation with anions such as tetrafluoroborate (BF_4^-) and hexafluorophosphate (PF_6^-) which have less reactivity towards water. However, the 2nd generation ILs with anions such as bis(trifluoromethanesulfonyl)imide (NTf_2^-), perfluoroalkylphosphate (FAP^-) are moisture stable and can easily handled without inert atmosphere due to the hydrophobic nature of anions.

(iii) ***Third generation ionic liquids***

Third generation ionic liquids are task specific ionic liquids and chiral ionic liquids. In recent past, task specific ionic liquids (TSILs) have been received much attention and TSILs incorporate a functional group such that it can be applied to a specific task of interest. The cationic or anionic part of the room temperature ionic liquid tethered covalently with organic functionality is known as functionalized ionic liquid (FIL) or task specific ionic liquid (TSIL) [55-66]. These types of ionic liquids exhibit the properties of both ionic liquid and organic functionality and it makes them suitable for a wide range of applications in synthesis, catalysis [57-59] and separation technology [58-66]. A sub class of functionalised ionic liquids known as ionic liquids with strongly coordinating anion wherein the anion of the ionic liquid itself is a functional moiety have been reported in the recent years [67-70]

1.6.2 Synthesis of RTILs

Conventional RTILs

Initially, the general procedure for synthesizing imidazolium based ionic liquids was reported by Huddulson *et al.* and Stark *et al.* [71, 72].The metathesis was generally followed for the preparation of conventional ionic liquids and the general synthetic route of these type of ionic liquids is depicted in figure 1.5

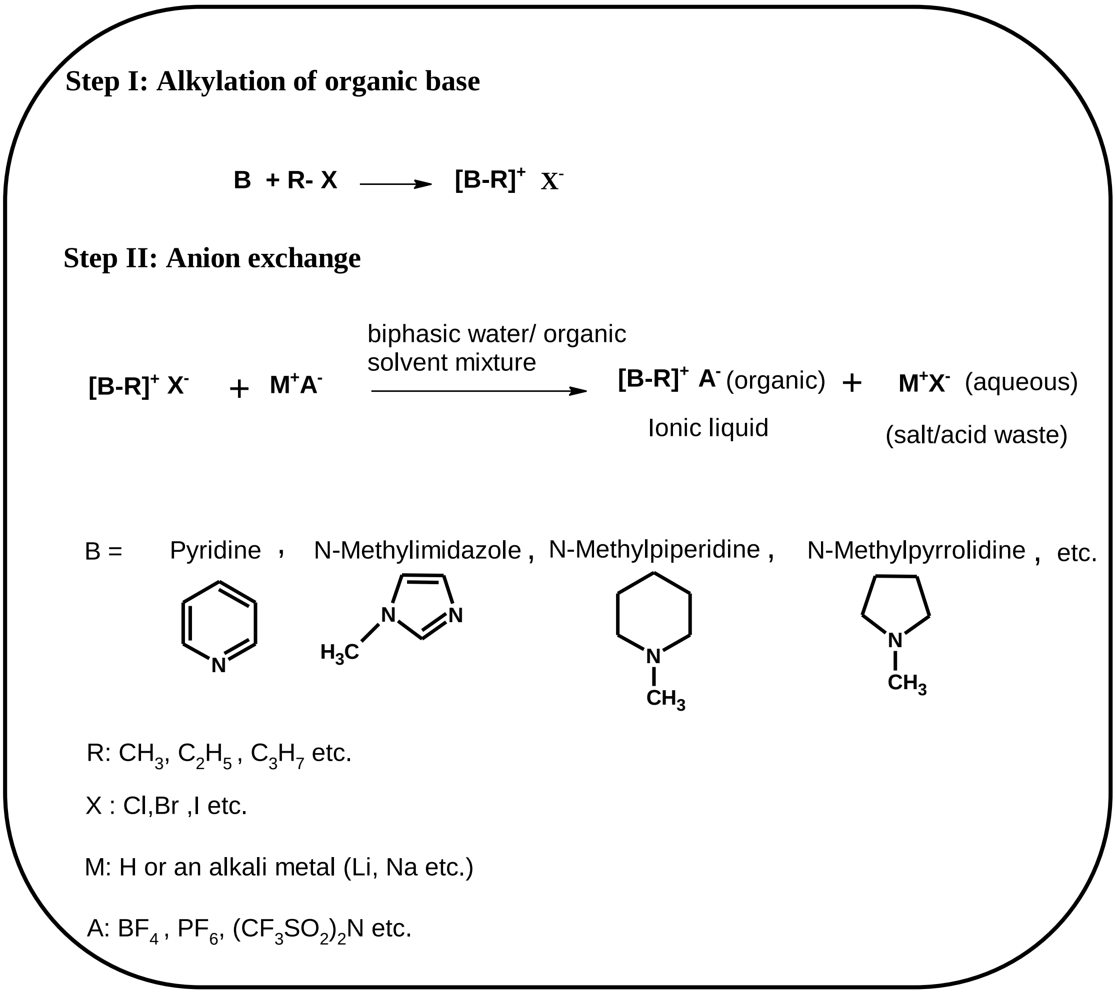

Step I: Alkylation of organic base

$B + R\text{-}X \longrightarrow [B\text{-}R]^+ X^-$

Step II: Anion exchange

$[B\text{-}R]^+ X^- + M^+A^- \xrightarrow{\text{biphasic water/ organic solvent mixture}} [B\text{-}R]^+ A^-$ (organic) $+ M^+X^-$ (aqueous)

Ionic liquid (salt/acid waste)

B = Pyridine , N-Methylimidazole , N-Methylpiperidine , N-Methylpyrrolidine , etc.

R: CH_3, C_2H_5 , C_3H_7 etc.

X : Cl,Br ,I etc.

M: H or an alkali metal (Li, Na etc.)

A: BF_4 , PF_6, $(CF_3SO_2)_2N$ etc.

Figure 1.5 Synthetic route for the preparation of conventional ionic liquids [73]

The first step involves alkylation of an organic base such as *N*-methyl imidazole, *N*-methylpyrrolidine, Pyridine or *N*-methylpiperidine) using a haloalkane to generate an organic halide salt. In the second step, anion exchange was carried out in water medium with appropriate acid or metal salt. The ionic liquid was extracted form the aqueous salt into an organic phase and washed several times with distilled water to remove the halide impurities.The final product was purified by charcoal treatment followed by passing through an alumina column and dried by heating in vaccum. [73].

Task specific ionic liquid (TSIL)

General synthetic scheme for the preparation of a TSIL reported by Davis [55]. The organic halides with the desired functional group have been used and it was reacted with a nucleophile such as imidazolium, pyrrolidinium, ammonium etc. The reaction condition for the synthesis of a TSIL depends on the type of functional group under study. Once the initial product is isolated, ion exchange is usually performed to pair the new cation with an anion of interest for ionic liquid formation. Examples of some task specific (or functionalized) ionic liquids are given in figure 1.7.

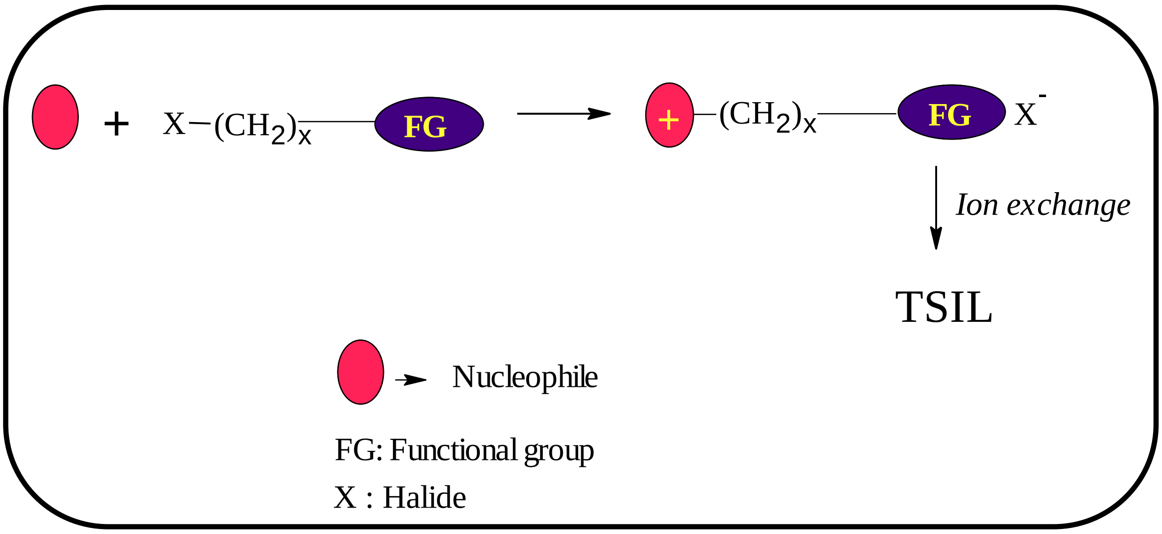

Figure 1.6 Synthetic scheme for TSILs (FILs) [55]

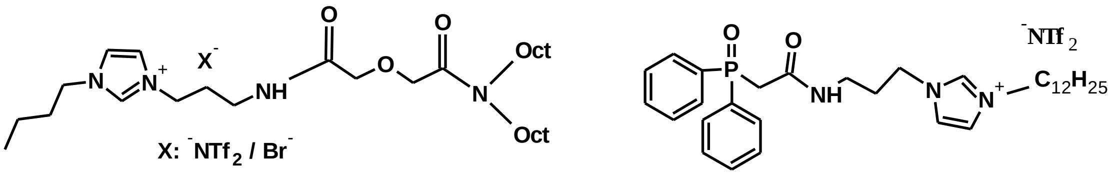

Diglycolamide FIL **CMPO FIL**

Phosphate FIL **Phosphonate FIL**

Figure 1.7. Structures of some TSILs (FILs)

RTILs with strongly coordinating anions

General synthetic procedure of these types of ionic liquids is shown in figure 1.8 [68, 69]. The synthetic procedure of ionic liquids with strongly coordinating anions which is a conjugate base of acids such as phosphate, phosphonate, diketonate etc is quite simple and less time consuming. The reaction involves the addition of IL cation precursor (for example, tri-*n*-octyl methyl ammonium chloride) into the solution of IL anion precursor (for example, Di(2-ethylhexyl)phosphate) in a solvent medium and stirring under reflux condition. Examples of some of RTILs with strongly coordinating anion are shown in figure 1.9.

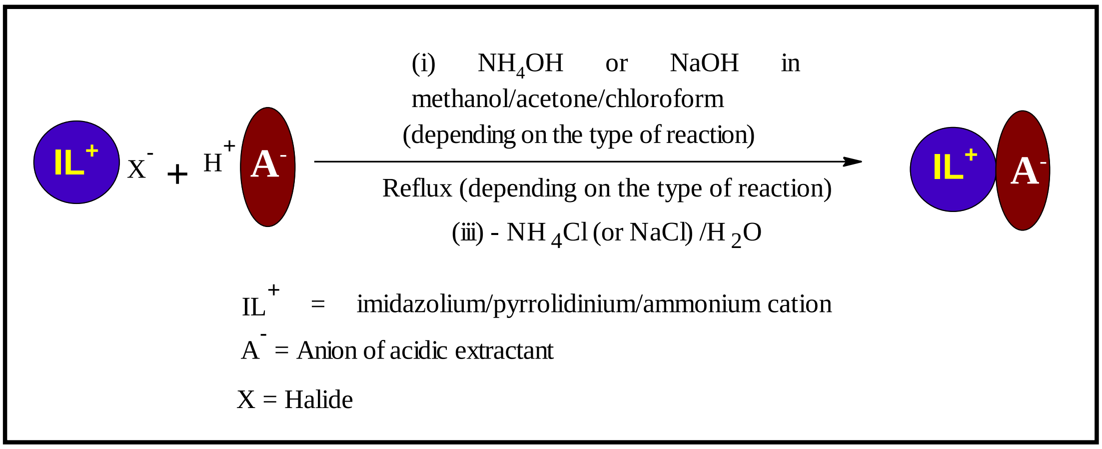

IL^+ = imidazolium/pyrrolidinium/ammonium cation

A^- = Anion of acidic extractant

X = Halide

Figure1.8. Synthetic scheme for RTILs with strongly coordinating anions [68,69]

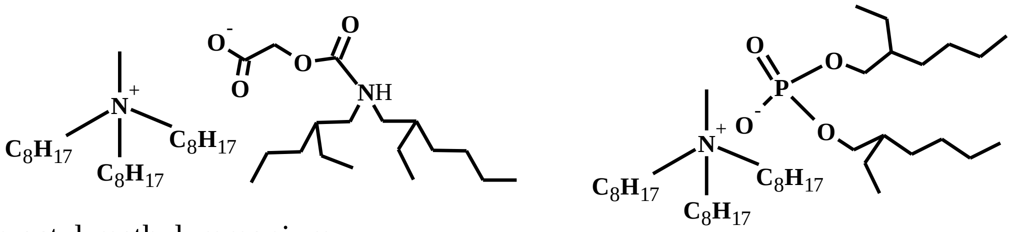

Tri-*n*-octyl-methylammonium bis(2-ethylhexyl)diglycolamate, [A336][DGA]

Tri-*n*-octyl-methylammonium bis(2-ethylhexyl)phosphate, [A336][DEHP]

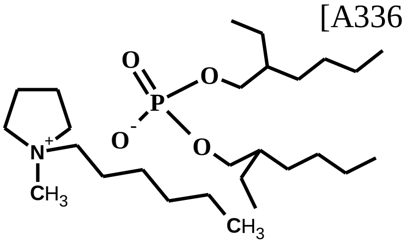

1-Hexyl-1-methylpyrrolidinium bis(2-ethylhexyl)phosphate, [C_6mpyr][NTf_2]

Figure 1.9. Structure of some RTILs with strongly coordinating anions

1.6.3 Properties of RTILs

RTILs have been used for several applications due to their fascinating properties such as negligible vapour pressure, high thermal stability, wide liquid range, high solubility for organic species, wide electrochemical window, tunable properties i.e, the properties of aparticular ionic liquids can be changed by changing cation – anion combination and electrical conductivity etc. A brief detail about some of the properties of ionic liquids is given below.

1.6.3.1 Melting point

Room temperature ionic liquids generally have melting points less than 100°C. Melting point of RTILs depends on the crystal structure, size and symmetry of the ions, charge density of the ions, efficiency of hydrogen bonding and the Vander Waals interactions [74]. When melting points of ILs are compared with that of inorganic salts (for example, 803 °C for NaCl and 60 °C for 1-propyl-3-methylimidazolium chloride) it is clear that the most of the reduction in melting temperature is caused by replacing the small inorganic cations by bulky asymmetric organic cations. The melting point of many ionic liquids is very uncertain due to their supercooling nature [75, 76].

1.6.3.2 Viscosity

Generally, RTILs are viscous liquids and it is generally two to three orders of magnitude greater than the viscosity for conventional organic solvents. However, some ionic liquids show very low viscosities at slightly higher temperatures, for instance, the viscosity of [C_4mim][NTf_2] is 4.2 cP at 114.5ºC and of [C_2mim][NTf_2] is 4.1 cP at 115.2ºC [77]. Bonhote *et al.* [78] reported the influence of the nature of cations and anions on the viscosity of RTILs. Mostly, RTILs with bistriflate imide ion has less viscocity than the other anions such as $[PF_6]^-$ and $[BF_4]^-$. For example, viscosity of [C_4mim][PF_6] is 430 cP [79], [C_4mim][BF_4] is 154 cP [80], and [C_4mim][NTf_2] is 52 cP [78] at 25ºC. MacFarlane *et al.*[81] have reported RTILs based on the dicyanamide anion $N(CN)_2^-$ ([C_4mim][$N(CN)_2$]: Melting point -21°C & viscosity at 25 °C is 21 cP). Seddon *et al.* [82] reported that the viscosity of the l-alkyl-3-methylimidazolium ionic liquids increases with increasing alkyl chain length. Moreover, it was reported that alkylammonium-based IL are more viscous than the imidazolium-based ILs with the same anion [83]

1.6.3.3 Density

Most of the RTILs are denser than water with the values ranging between 1.12 to 2.4 g.cm^{-3}[74] .The densities of a large number of ionic liquids can be found in the book ‘Ionic liquids in Synthesis’ edited by Wasserscheid and Welton [74]. In the case of imidazolium based ionic liquids, the densities are found to be decreasing as the length of alkyl chain increases [82]. The densities of ionic liquids are also influenced by the presence of impurities and water [84] and it increases with increase in the hydrophobicity of the anions. The densities of ionic liquids are less influenced by temperature [74]. The simple halide based ionic liquids have significantly lower densities (density of [C_8mim][Cl] is similar to water and [C_6mim][Cl]) is similar to dioxane [80]. Moreover, quarternary ammonium based ionic liquids such as $[A336]^+[NO_3]^-$, $[A336]^+[Cl]^-$, $[A336]^+[PF_6]^-$ and $[A336]^+[CH_3COO]^-$ have density in the range of 0.8 to 0.90 [84].

1.6.3.4 Electrical conductivity

In general, the electrical conductivities of RTILs range from 0.1 to 18 mS.cm^{-1} [87]. The electrical conductivities of ionic liquids are less than the aqueous electrolytes (30 wt. % aqueous solution of H_2SO_4 is about 730 mS.cm^{-1}) [85]. The specific conductivities of the ionic liquids are adequate to use them as electrolytes for carrying out the electrochemical studies. The conductivities of the ionic liquids are mostly dependent on viscosity and temperature. Galinski et al. [85] has reported the influence of viscosity and temperature on the specific conductivity of ionic liquids.

1.6.3.5 Surface tension

Some measurements are available on the surface tension of ionic liquids which ranges from 33.8 N m^{-1} for [C$_8$mim][Cl] to 54.7 N m^{-1} for [C$_4$mim][I] while [C$_4$mim][PF$_6$] has a value of 49.8 N m^{-1} . The surface tensions of RTILs are lower than that for water (72.7 N m^{-1} at 20 °C) but higher than the values for *n*-alkane (16.0 N m^{-1} for pentane to 25.6 N m^{-1} for dodecane at 20 °C). As the alkyl chain length on the RTIL increases the surface tension value decreases. The surface tension of ionic liquids is less influenced by the presence of water. [72, 86, 87]

1.6.3.6 Electrochemical window

The “electrochemical window” of RTILs is a term commonly used to indicate both potential range and potential difference which is calculated by substracting the reduction potential from the oxidation potential. This is the important property which allows the use of RTILs as the electrolytes. Many ILs has wide electrochemical windows of ~5 -6 V or more [88]. The electrochemical windows for some typical ionic liquids were reviewed by Plechkova and Seddon [89]. Electrochemical stability of various ionic liquids has been reported in literature [90-93].

1.6.3.7 Radiation stability

Generally, RTILs have high radiation stability. The radiation stability of 1,3-dialkylimidazolium nitrate/chloride ionic liquid reported by Allen *et al.* [94]. The ionic liquid of the type [C$_4$mim][NTf$_2$] and [C$_4$mim][PF$_6$] offer high stability to γ-radiation and shows no significant impact on the properties such as density, surface tension and refractive index of such ILs even after the exposure of high gamma dose [95]. Lall-Ramnarine *et al.* [96] investigated pulse radiolysis of bis(oxalato)borate anion based ionic liquids. Efficient scavenging of radiolytically generated electrons was observed in these ionic liquids. Rouzo *et al.* studied the radiochemical stability of [C_4mim][X] (X= NTf_2^-, OTf^-, PF_6^- and BF_4^- up to an absorbed dose of 2 MGy) [97]. The degradation of ionic liquid increased in the order $NTf_2^- < OTf^- < PF_6^- < BF_4^-$. Recently, Ch. Jagadeeswara Rao *et al.* reported radiation stability of some RTILs such as protonated betaine bis(trifluoromethylsulfonyl)imide (HbetNTf_2), aliquat 336 (tri-*n*-octlymethylammonium chloride), 1-butyl-3-methylimidazolium chloride ([C_4mim][Cl]), 1-hexyl-3-methylimidazolium chloride ([C_6mim][Cl]), *N*-butyl-*N*-methylpyrrolidinium bis(trifluoromethylsulfonyl)imide ([C_4mpy][NTf_2]) and *N*-methyl-*N*-propylpiperidinium bis(trifluoromethylsulfonyl)imide ([C_3mpip][NTf_2]) and it was reported that these ionic liquids were stable up to irradiation level of 100 kGy [93].

1.6.3.8 Thermal stability

Generally, RTILs have high thermal stability since they have negligible vapour pressure. The thermal stability of different ionic liquids is nearly independent of cations but it decreases with increase in the anion hydrophilicty [98]. Relative anion stabilities have been suggested as $PF_6^- > NTf_2^- \sim BF_4^- >$ halides. The dependence of the thermal properties on imidazolium and anion structure was investigated by Ngo *et al.* and reported that the thermal stability of the imidazolium salts increases with increased alkyl substitution and halide anions dramatically reduce the thermal stability of ionic liquid [99].The thermochemical properties of [Hbet][NTf_2], [C_4mpy][NTf_2] and [C_3mpip][NTf_2] have been reported by Jagadeeswara Rao *et al.* [93]. Kosmulski *et al.*[100] has reported the thermal stability of some ionic liquids such as 1-alkyl-3-methylimidazolium phosphates and 1-alkyl-3-methylimidazolium triflate and Paulechka *et al.* reported the thermal stability of ionic liquid, [C_4mpy][NTf_2] [101]. Bonhote *et al.*[78] found that

[C_4mim][NTf_2] was stable up to 400 °C and decomposed rapidly between 440 and 480^{0}C whereas [C_2mim][TA] (TA = trifluoroacetate) was only stable up to 150 °C.

1.6.4 Applications of RTILs

Due to the attractive properties of RTILs, they find enormous applications in various research areas. RTILs are explored for applications in electrochemistry, organic synthesis, catalysis, cellulose processing, separation technology and analytical chemistry etc. Figure 1.10 illustrates the several applications of RTILs [102].

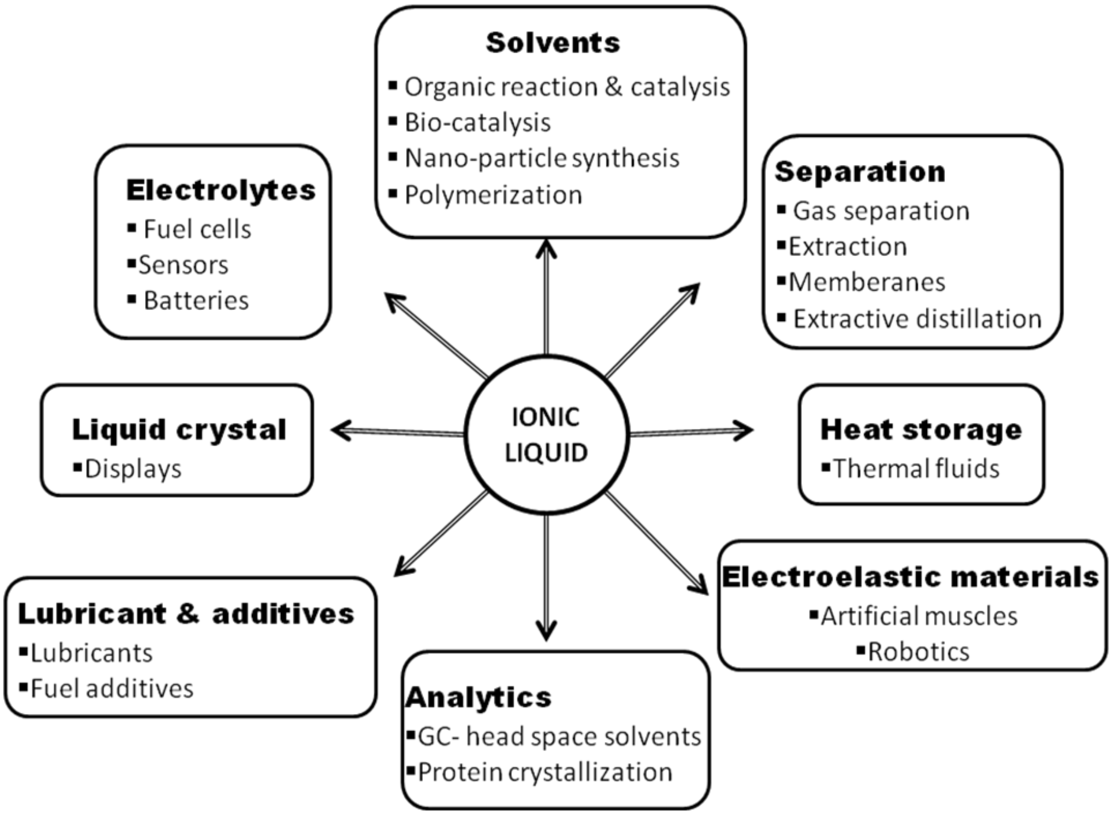

Figure 1.10. Applications of ionic liquids [102]

Initially, the potential application of RTILs as solvents in organic synthesis was proposed by Fry and Pienta [103]. The applications of RTILs in organic synthesis have been described by Sethi *et al.* [104] and also in the book “Ionic liquids in organic synthesis” edited by Malhotra [105]. Reviews on the applications of ionic liquids in chemical analysis i.e., in extraction chromatography, electrochemistry, spectroscopy etc. by Koel [106], electrodeposition of metals from non-aqueous solutions using ionic liquids by Simka *et al.*[107], applications of TSILs as catalyst by Ralf Giernoth [58] and applications of ionic liquids in electrochemical sensors by Wei *et al.*[108] have been reported. Similarly, review on TSILs by Davis *et al.* [55] reported the applications of various TSILs in different areas and D. Han *et al.* reported the applications of RTILs in different areas of separation technology [109].

In addition to the academic research, ionic liquids have been used for several industrial processes. For example, reviews on the applications of RTILs in chemical industry have been reported by Plechkova and seddon [89]. Weyershusen *et al.*[110] reported industrial application of ionic liquids as performance additives. The major industrial ionic liquid application was the BASIL (Biphasic Acid Scavening utilizing Ionic Liquids) process by BASF. Similarly, Eastman operated an IL-based plant for the synthesis of 2,5-dihydrofuran from 1996 to 2004 [89] .

1.6.4.1 Applications of RTILs in SNF reprocessing

Over the past few decades, RTILs have been receiving increased attention for possible applications in the area of nuclear fuel reprocessing and waste management [111-115]. Essentially, RTILs are investigated as possible substitute to the molecular diluent in solvent extraction procedures for the extraction of metal ions [117-131]. In the recent years, functionalized ionic liquids (FILs) (or task specific ionic liquids (TSILs)) and the ionic liquids with strongly coordinating anion have been reported as extractants for the metal ion separations [69, 70, 132-142]. Moreover, the properties of RTILs such as wide electrochemical window, solubility of various extractants and unusual extraction of target metal ions from aqueous medium etc., facilitates the development of novel and environment benign procedures for the treatment of wide variety of aqueous waste using ionic liquid as medium. One such method is the extraction-electrodeposition (EX-EL) approach [115]. Some of the striking features of RTILs that make them promising for nuclear fuel cycle application are (i) Selectivity of target metal ion can be easily manipulated by the change of cation-anion combinations of RTIL diluent, rather than redesigning the structure of the extractant (ii) Presence of ionic diluent in organic phase facilitates a new mode of recovery of metals by direct electrodeposition from the extracted phase (iii) Ionic liquids can be functionalized with organic moieties for task specific applications (iv) RTILs can be designed to be completely incinerable, which would simplify the management of spent organic waste (v) Due to negligible vapor pressure of RTILs, the fire hazard is almost insignificant.

In reprocessing of spent nuclear fuel, RTILs have been explored as diluents, extractants and electrolytic medium and brief detail about these roles of RTILs are described below.

1.6.4.1.1 RTIL as diluent

A large number of reports are available on the use of ionic liquids as diluents for the extraction of actinides and fission products [117-131] and some of studies are given here. Initially, Dai *et al.* (121) and subsequently Visser *et al.* (117) reported to separate group I and II metal ions from aqueous medium using a solution of crown ether in imidazolium based ionic liquid and Visser *et al.* extensively studied the extraction of cesium and strontium from nitric acid medium by using various crown ethers (18C6, DCH18C6, and DtB18C6) in [$C_n$mim][PF_6] (n = 4, 6, 8) ionic liquid. A systematic study of the extraction of actinides (mostly U(VI), Pu(IV) and Am(III)) and lanthanides in ionic liquid medium has been reported elsewhere [118-120,122-131]. The extraction of U(VI) from nitric acid medium by a solution of TBP in [C_4mim][PF_6] or [C_4mim][NTf_2] was reported by Giridhar *et al.* and this study indicates the possibility of varying the distribution ratio of uranium(VI) by changing the cation-anion combinations [130,131]. The mechanism of U(VI) extraction in TBP dissolved in ionic liquid was investigated in detail by Dietz [122]. Similarly, Billard *et al.* investigated the mechanism of U(VI) extraction in TBP/[C_4mim][NTF_2] and the model proposed by the authors involves the extraction of U(VI) through the cation exchange of $[UO_2(TBP)_n]^{2+}$ species with $[C_4mim]^+$ ion and $H^+(TBP)_n$ in ionic liquid phase at low acidities. Anion exchange of $[UO_2\ (NO_3)_3(TBP)m]^-$ species with NTf_2 of ionic liquid was stated to be responsible for uranium extraction at high acidities [123,124].The mutual separation of Eu(III) from Am(III) using acidic extractants in ionic liquid medium was reported by Alok *et al.* (120). Nakashima *et al.* (130) studied, in detail, the extraction of trivalent lanthanides in CMPO/[C_4mim][PF_6] and reported that the extraction efficiency of CMPO for metal ions was higher in ionic liquid medium as compared to the dodecane system. Panja *et al*. reported the extraction behavior of Am(III), Pu(IV) and U(VI) using *N*,*N*,*N′*,*N′*-tetra-*n*-octyl diglycolamide (TODGA) in imidazolium based ionic liquid and reported that the distribution ratio of Am(III), Pu(IV) and U(VI) were found to be higher in ionic liquid system than that obtained in *n*-DD diluents[125].

1.6.4.1.2. RTIL as extractant

In addition to the role of diluent, RTILs are receiving more interest to explore them as an extractant. The cationic or anionic part of the room temperature ionic liquid tethered covalently with organic functionalities, which can perform specific applications are known as functionalized ionic liquids (FILs) or task specific ionic liquids (TSILs) [55].

Due to the presence of the functional group, the resultant FIL is expected to show the properties of both ionic liquid and organic functionality. The use of functionalized ionic liquid could avoid the use of molecular extractants. Since the FILs are usually soluble in ionic liquid diluents, the solvent system is completely devoid of any molecular entities. Therefore, the use of functionalized ionic liquids in nuclear reprocessing applications could offer inherent advantages such as thermal stability and negligible vapour pressure etc. Depending upon the nature of functional group attached, the selectivity of metal ion was found to be different. Extensive studies have been carried out in the recent past for the separation of actinides and fission products from wide variety of feed solutions using functionalized ionic liquid [61-65, 132-142] and some of the studies related to this part is given in this section. For example, 2-hydroxybenzylamine (LH_2) FIL for the extraction of Am(III) and a few TSILs containing phosphoryl moiety attached to the quarternary ammonium ion for the extraction of U(VI) was reported by Ouadi *et al.*[62,63]. In recent years, P.K. Mohapatra *et al.* reported task specific ionic liquids with diglycolamide (DGA) and phosphine oxide (CMPO) moiety anchored on imidazolium cation for the solvent extraction of actinides from nitric acid medium [136,137]. The authors reported the superior extractability of these FILs over conventional DGA and CMPO based extractants. In the recent past, couple of TSILs bearing phosphate and phosphine oxide moiety have been investigated for the extraction of actinides from nitric acid medium, respectively and it was reported that efficient extraction of the target metal ions using TSIL [138,142] was obtained. Similarly, amide ([DOAIm][NTf_2]) and phosphonate ([ImP][NTf_2]) based functionalised ionic liquids [133,134] have been reported by Alok *et al*. and high separation of Pu(IV) from U(VI) and Am(III) was shown by these amide and phosphonate based FILs.

A sub class of functionalized ionic liquid which is known as RTILs with strongly coordinating anions which usually has the conjugate base of the acids such as phosphate, diketonate etc, have also been studied in the recent past. [66-70,132,140]. The advantages of such ionic liquids over functionalized ionic liquids are simple method of preparation, higher loading of metals, miscibility with molecular diluents such as toluene, xylene etc but these ionic liquids were insoluble in paraffins. In the recent past, Sun *et al*. [69] and Ling *et al*. [70] studied the extraction behavior of rare earths from aqueous solution using $[A336]^{+}$ based ionic liquids. Aliquat-336 cation based ionic liquids are strongly hydrophobic, miscible in many of the non-polar solvents. These ionic liquids exhibit a density lower than 0.9 g/mL and negligible solubility in aqueous phase, which are indeed desirable for adapting these ionic liquids for countercurrent solvent extraction applications. In the recent past, Alok *et al* investigated tri-*n*-octylmethylammonium bis-(2-ethylhexyl) phosphate ($[A336]^{+}[DEHP]^{-}$) and tri-*n*-octylmethylammonium bis-(2-ethylhexyl)diglycolamate ($[A336]^{+}[DGA]^{-}$) for the extraction of Eu(III) and Am(III) from aqueous solutions [132] and also reported the extraction behavior of U(VI), Pu(IV), and Am(III) in 1.1 M tri-*n*-butylphosphate (TBP)/ *n*-DD containing small concentration of $[A336]^{+}[DEHP]^{-}$ [140].

1.6.4.1.3. RTIL as electrolytic medium

In the past few decades the concept of using RTILs for non-aqueous reprocessing has evolved and several studies have been reported in this aspect [143-158]. The electrochemistry of actinides and other metal ions in RTILs (chloroaluminate salts) were reported few decades ago. Initially, D'Olieslanger *et al.* reported the studies on electrochemistry of uranium in acidic ($AlCl_3$ + *N*-(*n*-butyl)pyridinium chloride)) and basic ($AlCl_3$ + *N*-(*n*-butylpyridium chloride)) chloroaluminate melt [143]. Similarly, Schoehrechs and Gilbert [144] reported electrochemical studies of neptunium in acidic and basic $AlCl_3$ -1-*n*- butylpyridinium chloride melt at 40ºC. But these 1st generation ILs show inadequacy in electrochemical window and poor cathodic stability. Nikitenko and co-workers [145] investigated the spectroscopic and electrochemical aspects of U(IV)-hexachloro complexes in [C_4mim][[NTf_2] & [$Mebu_3N$][NTf_2] ($Mebu_3N$ = tri-n-butylmethyl ammonium) hydrophobic ionic liquids and due to large electrochemical window of these RTILs, it was possible to study the oxidation and reduction behavior up to the metallic form. Electrochemical behavior of U(VI) in [C_4mim][NTf_2] was reported by Giridhar *et al.* and reported a single step two-electron transfer reduction to uranium oxide (UO_2) deposit at a glassy carbon working electrode [158]. In recent past, several reports are available on the studies dealing with the electrochemical behavior of various metal ions present in ionic liquid medium containing different extractants [148,150-154]. For instance, Gupta *et al.* studied the electrochemical behavior and luminescence of Eu(III) in ionic liquid medium to bring out the dynamics and co-ordination behavior of Eu(III) with dihexyl *N,N*-diethylcarbamoylmethylphosphonate (DHDECMP) extractant [150]. Matsumiya *et al.* studied the electrochemical behavior of rare-earth elements such as Pr, Nd and Dy present in the ionic liquid medium containing tri-*n*-butylphosphate (TBP) ligand [148]. A.Sengupta *et al.* reported the electrochemical characterization of Np(IV) complexes with diglycolamide as well as diphenylcarbamoylmethylphosphine oxide (CMPO) based task-specific ionic liquids in [C_4mim][NTf_2] [153,154].

Moreover, RTILs have been utilized for several other electrochemical applications such as, recovery of valuable by-products of nuclear fission, nuclear waste treatment etc. For example, the separation and recovery of palladium from simulated HLLW using the extraction–electrodeposition (EX–EL) method was reported by Jayakumar *et al.* [149].

This method comprises of solvent extraction of Pd(II) using tri-*n*-octylmethylammonium nitrate (TOMAN) in chloroform and direct electrodeposition of metallic palladium from the organic phase. Moreover, some studies have been reported for nuclear waste treatment using RTILs and in this aspect, Ch. Jagadeeswara Rao *et al.*[157] studied the dissolution of tissue paper waste containing valuable contaminants such as uranium and palladium in 1-butyl-3-methylimidazolium chloride ([C_4mim][Cl]) and they were recovered by electrolysis of the solution by exploiting the wide electrochemical window of [C_4mim][Cl].

1.7 **Motivation for the present study**

Reprocessing of spent nuclear fuel (SNF) is vital for the success of nuclear power programme in India. PUREX process has been adopted for the separation and recovery of uranium and plutonium from the spent nuclear fuel dissolver solution. The raffinate rejected after the extraction of uranium and plutonium is known as HLLW. Eventhough a large number of methods and materials are available for the separation of actinides from dissolver solution and HLLW, processes based on room temperature ionic liquids (RTILs) are being proposed as possible substitute to the traditional methods. RTILs are organic salts molten at temperature below 100ºC. They have several superior properties suitable for industrial exploitation and nuclear fuel cycle application. They are, extraordinary extraction of metal ions from aqueous solutions when RTILs used in conjuction with traditional extractants, possibility of tailoring ionic liquids for task specific applications, feasibility of separating target metals from aqueous wastes and recover by electrodeposition directly from ionic liquid phase etc. Therefore it is envisaged that employment of ionic liquids in the area of nuclear fuel cycle applications would lead to the development of environment benign process that generates minimum waste. In this direction, research work has been taken up with the following objectives.

1.8 Objectives

The objective of present study is threefold. They are,

- To explore the possibility of using RTILs as diluents for the solvent extraction of actinides and lanthanides. In this content, solvent extraction studies were conducted for the separation of Eu(III), U(VI), Pu(IV) and Am(III) from nitric acid medium using a solvent phase composed of molecular extractants dissolved in imidazolium / pyrrolidinium bis(trifluoromethanesulfonyl)imide ionic liquids and the loading behaviour of Eu(III) in ionic liquid medium at higher Eu(III) loading conditions was also investigated .
- To explore the possibility of using task specific ionic liquid (TSIL) and ionic liquid with strongly coordinating anion as extractants for the solvent extraction of actinides. In this content, a new phosphoramide functionalized ionic liquid and a tetraalkyl ammonium phosphate ionic liquid were explored for the separation of actinides from nitric acid medium.
- To explore the technical feasibility of using RTIL as electrolytic medium for the solvent extraction of Eu(III) and U(VI) in ionic liquid medium followed by electrodeposition of extracted metals. In this direction the electrochemical behavior of U(VI) and Eu(III) in the presence of molecular extractants dissolved imidazolium and pyrrolidinium bis(trifluoromethanesulfonyl)imide ionic liquids was studied and the results are discussed in thesis.

CHAPTER 2

EXPERIMENTAL

This chapter describes about experimental procedures involved in liquid –liquid extraction and electrochemical studies of some actinides and lanthanides. The synthesis and characterization of various room temperature ionic liquids (RTILs), task specific ionic liquid and various extractants used in the present study have been described in this chapter. The spectroscopic techniques such as FT-IR, ^{1}H, ^{13}C *&* ^{31}P*-NMR and mass spectrometry used for characterization of various ionic liquids and organic compounds synthesized are presented. Methods and materials employed for the analysis of radioactive and non-radioactive samples along with instruments such as NaI(Tl) detector, alpha scintillation counter and electrochemical system have been described here. Moreover, Voltammetry techinques such as cyclic voltammetry, chronopotentiometry and chronoamperometry, have been also explained.*

2.1. Chemicals and reagents

All the chemicals and reagents used in this study were of analytical grade and used as received unless otherwise mentioned.

Tributylphosphate (TBP)

TBP (Purity: $\geq$ 99%) was obtained from M/s. Sigma Aldrich / M/s. Merck. It was washed with dilute sodium carbonate solution (~0.2 M) followed by distilled water and then dried under vacuum before use.

1-Methylimidazole

1-Methylimidazole (Purity: 99%) was procured from M/s. Fluka / M/s. ACROS Organics and used after purification by distillation.

Chloroalkane (Alkyl = butyl, hexyl and octyl)

Chloroalkanes (Purity: $\geq$ 99%) were procured from M/s. Acros and purified by distillation mehod prior to use.

Bis(trifluoromethanesulfonyl)imide lithium salt ($LiNTf_2$)

$LiNTf_2$ was procured from M/s Sigma Aldrich (> 99%) / M/s. Alfa Aesar (>98%).

Iodomethane

Iodomethane (Purity: $\geq$ 99%) was procured from M/s. Sigma Aldrich.

N-methylpyrrolidine

N-Methylpyrrolidine (Purity: $\geq$ 97%) was procured from M/s. S.D Fine Chemicals and used after purifying by distillation method.

1–Bromoalkane

1-Bromobutane & 1-bromopropane (Purity: 99%) were procured from M/s. Merck / M/s S D. Fine Chemical Limited.

Tri-n-octylmethylammonium chloride (Aliquat-336) & Triisobutylphosphate (TiBP)

Aliquat 336 (Purity $\geq$ 99%) and TiBP (Purity: $\geq$ 97%) were procured from M/s. Sigma Aldrich.

3-Methyl -1-phenyl-2- pyrazolin-5-one (MPP)

3-Methyl -1-phenyl-2- pyrazolin-5-one (MPP) (Purity > 98%) was purchased from M/s. Alfa Aesar.

Benzoyl chloride

Benzoyl chloride (Purity > 99%) was obtained from M/s. Rankem chemicals and used as received.

N, N-dihexyloctanamide (DHOA)

DHOA was obtained from heavy water board, Tuticorin, India.

Diethyl chlorophosphate and 1–(3-aminopropyl)imidazole

Diethyl chlorophosphate (Purity > 97%) and 1–(3-aminopropyl)imidazole (Purity > 97%) were obtained from M/s. Sigma Aldrich.

N, N-dialkyamines (alkyl = hexyl/ octyl/ decyl) & Bis (2-ethylhexyl)amine

N,N-dihexylamine (Purity: 97%), *N,N*-dioctylamine (Purity: 97%), *N,N,*-didecylamine (Purity: 98%) and bis(2-ethylhexyl)amine (Purity: 98%) were procured from M/s. Sigma Aldrich.

Choloroacetyl chloride

Choloroacetyl chloride (Purity: > 98%) was obtained from M/s. Sigma Aldrich.

Bis(trifuoromethanesulfonyl)imide (80% aqueous solution)

Bis(trifuoromethanesulfonyl)imide (80% aqueous solution) was procured from M/s.Iolitec.

Triethylamine (TEA) & methanol

TEA and methanol were procured from M/s. Ranbaxy. TEA was purified by distillation method.

Sodium nitrate

Sodium nitrate (Purity: 99%) was obtained from M/s. Alfa Aesar

Ttoluene

Toluene was procured from M/s. S D Fine Chemicals.

Acetonitrile

Acetonitrile (Purity: $\geq$ 99%) was procured from M/s. Merck.

Europium oxide (Eu_2O_3)

Eu_2O_3 was obtained from M/s. S D Fine Chemicals.

Palladium wires and Glassy Carbon

Palladium wires and Glassy Carbon were obtained from M/s.Johnson Matthey.

Calcium chloride

$CaCl_2$ (Purity: ≥ 99.9%) was proscured from M/s.Sigma Aldrich.

n-Dodecane (n-DD)

n-Dodecane (Purity: 99%) was obtained from M/s.Spectrochem private Limited, Mumbai, India.

Dichloromethane (DCM), Ethylacetate & Chloroform

These solvents were obtained from M/s.Fischer Inorganics and Aromatics Limited, Chennai and used as such.

1-(2-theonoyl)-3,3,3-trifluoroacetone (HTTA) &* Tetrahydrofuran (*THF)

HTTA (Purity: 98%) & THF (Purity: $\geq$ 99%) was procured from M/s.Sigma Aldrich. THF was distilled before use.

Acid solutions

The acid solutions (HNO_3, HCl, GR grade, M/s.Merck Specialities Private Limited, Mumbai, India) were prepared by the dilution of concentrated acids, and were standardized by standard acid-base titration method using standardized NaOH and phenolphthalein indicator.

Sodium hydroxide

Sodium hydroxide (AR grade) was obtained from M/s.S.D Fine Chemicals / M/s Sigma Aldrich.

Phenolpthalein

Phenolpthalein (Merck Specialities Private Limited, Mumbai, India) solution was prepared by dissolving ~ 500 mg of solid in 100 mL of 1:1 mixture of distilled water and ethanol.

Sodium nitrite

Sodium nitrite was obtained from M/s. S.D. fine Chemicals, Mumbai, India.

Ethylenediaminetetraacetic acid (EDTA) & Hexamethylenetetramine (HMTA), Acetohydroxamic Acid(AHA) & Oxalic acid (OA)

EDTA, HMTA (Purity: $\geq$ 99%), AHA (Purity: $\geq$ 98%) and OA (Purity: $\geq$ 99%) were procured from M/s. Sigma Aldrich.

Methyl Thymol Blue

Methyl thymol blue was obtained from M/s.S D Fine Chemicals. The solution of methyl blue was prepared by dissolving ~20 – 25 mg of it in 10 mL of distilled water for using as indicator for the standardization of neodymium solution.

Naphthalene

Scintillation grade naphthalene was procured from M/s. Loba Chemie Pvt. Ltd.

1, 4-Dioxane

1,4-Dioxane was procured from M/s. Merck Specialities Private Limited, Mumbai and purified prior to use to remove the peroxides that are normally present as quenching impurities. About 2 litres of 1,4-Dioxane was refluxed with ~ 80 g of NaOH pellets for four hours. The dioxane was then distilled and the fraction that distilled between 373 – 375 K was collected after discarding the initial 100 mL fraction. This purified 1, 4 - Dioxane was used for the preparation of cocktail for liquid scintillation counting.

2,5- Diphenyl Oxazole (PPO)

Scintillation grade 2,5-diphenyl oxazole (PPO) was obtained from M/s. Loba Chemie Pvt. Ltd.

1,4-Bis(5-phenyloxazol-2-yl)benzene (POPOP)

Scintillation grade 1,4-Bis(5-phenyloxazol-2-yl)benzene (POPOP) was obtained from M/s. Koch-Light Laboratories Ltd. Colnbrook Buch, England.

Tri-n-octyl phosphinoxide (TOPO)

Tri-*n*-octyl-phospinoxide (TOPO) obtained from M/s.Sigma Aldrich.

2.2.Radioactive tracers

$^{(152+154)}$*Eu*

$^{(152+154)}$Eu dissolved in dilute nitric acid was procured from Board of Radiation and Isotope Technology, Mumbai, India and the purity of $^{152+154}$Eu was ascertained by γ-counting technique.

^{241}*Am*

^{241}Am was procured as Am_2O_3 from Oak Ridge National Laboratory and it was dissolved in nitric acid and purity of ^{241}Am was ascertained by α-counting technique.

$^{239}Pu(NO_3)_4$ *and* $^{233}UO_2(NO_3)_2$

$^{239}Pu(NO_3)_4$ and $^{233}UO_2(NO_3)_2$ in nitric acid solution (~ 0.5 M) was obtained from Reprocessing Group, Indira Gandhi Centre for Atomic Research, India. Uranium was purified by solvent extraction with 5 % TBP/*n*-DD from 4M HNO_3. The loaded organic phase was subjected to scrubbing with 4 M HNO_3 in order to remove the co-extracted impurities. Then ^{233}U was stripped from the organic phase by 0.01 M HNO_3 and used as tracer.

Plutonium was purified by anion exchange method. The isotopic composition of plutonium was as follows (values in atom %) ^{238}Pu:0.017; ^{239}Pu: 93.60; ^{240}Pu: 6.24; ^{241}Pu: 0.12; ^{242}Pu: 0.023. The specific activity of this plutonium tracer was 1.665 x 10^5 dpm/μg. The plutonium (IV) tracer was prepared by the following procedure. The acidity of the plutonium solution was adjusted to 1 M HNO_3 and about 0.2 – 0.4 mL of 2.5 M $NaNO_2$ solution was added drop-wise with constant shaking. The resulting Pu(IV) was extracted with 0.5 M thenoyltrifluoroacetone (TTA)/xylene solution. The organic phase was scrubbed with 1 M HNO_3 solution to remove the impurities. The loaded plutonium was stripped by 8 M HNO_3 and used as a stock solution. For the Pu(III) extraction studies, the oxidation state of plutonium was adjusted to Pu(III) by adding freshly prepared ferrous sulfamate, and hydroxylamine hydrochloride [159].

Tracer solution

A tracer solution of all the actinides (^{233}U (VI), ^{239}Pu(IV) & ^{241}Am(III) and lanthanide ($^{152+154}$ Eu(III)) were diluted with double distilled water (~10^{-4} M) and used for all extraction studies.

2.3 Instrumentation

2.3.1. Gamma counter

The activity of gamma emitting radioisotopes such as ^{241}Am and $^{(152+154)}$Eu was measured using a gamma counter with single channel analyzer and well type NaI(Tl) detector. The NaI(Tl)-PMT integral assembly was procured from M/S Harshaw, U.S.A and other electronic modules were obtained from ECIL (Electronic Corporation of India Limited), Hyderabad, India.

2.3.2. Liquid scintillation counter

Alpha activity of samples containing U^{233} or Pu^{239} was measured using an in-house fabricated a liquid scintillation counter. In liquid scintillation counting, the energy of alpha particles is absorbed by the cocktail (solvent containing organic scintillators) and converted into photons in the visible region which in turn are converted into photoelectrons by photomultiplier tube and subsequently measured as an electronic pulse. 1,4-dioxane was used as the primary solvent, 2,5-diphenyloxazole (PPO) was used as the primary scintillator. 1,4-di-2-(5-phenyloxazolyl)benzene (POPOP) was used as a wavelength shifter and tri-*n* octylphosphine oxide (TOPO) as the complexing agent. The liquid scintillation counter consists of a machined perspex vial holder, coupled to a single low noise photo multiplier tube. The discriminator was set with ^{241}Am source and the efficiency was verified with a plutonium source.

In addition, the α-radioactivity of various radioisotopes was also estimated by using α-β discriminating liquid scintillation counter (300SL TDCR liquid scintillation analyzer, Hidex, Finland). The known amount of sample from both organic and aqueous phase was taken in ultima gold AB cocktail (Perkin Elmer) for liquid scintillation counting.

2.3.3. Rotary evaporator

A rotary evaporator with model R-3000 from M/s. Buchi Laboratories Technique AG, Switzerland, was used for distilling off volatile solvents and drying ionic liquids in order to remove water content.

2.3.4. pH meter

All pH measurements were made with Cyberscan 500 pH, Metrohm. The meter was calibrated at 298 K with standard buffers of pH 4, 7 and 10.

2.3.5. Vaccum oven

Vaccum oven (Model-VT-AP-11.) with digital temperature control from M/s. Technico was utilized for drying ionic liquids prior to use. The oven was connected to a vaccum pump with pressure gauge and pressure control.

2.3.6 Viscometer

The viscosity of ionic liquid phase was measured using Brook- field viscometer (model D-II +) with a small sample adapter. The temperature of adapter was maintained at a particular temperature using a constant temperature water bath-circulator.

2.3.7. Mass spectrometer

A home built reflectron time of flight mass spectrometer and ESI mass spectrometer were used for the mass analysis. In TOF-MS, nicotinic acid was used as matrix and fourth harmonic of Nd-YAG laser (266 nm) was used for the desorption/ionization.

2.3.8 NMR spectrometer

A Brucker Avance III 500 MHz (AV 500) multi nuclei solution NMR spectrometer was used the structure analysis of synthesized ionic liquids and extractants. MeOD, $CDCl_3$ and CD_3COCD_3 were used as solvents.

2.3.9 FT-IR spectrometer

The infrared spectrum of the sample was recorded using BRUKER TENSOR II FT-IR spectrometer equipped with an ATR (attenuated total reflectance) diamond crystal.

2.3.10 CHNS analyzer

Microelemental CHNS analysis of the samples were carried out by using Elementer Vario-EL.

2.3.11 Electronic single pan balance

A calibrated electronic single pan balance with a sensitivity of 0.01 mg was used to weigh chemicals and solutions

2.3.12 Thermostatted rotary water bath shaker

A refrigerated water bath (PolyScience, Model-9100, USA) with a temperature controlling accuracy of ± 0.010 K was used for the solvent extraction experiments. A JULABO (F33-HE) refrigerated circulator with a temperature controlling accuracy of ± 0.010 K and a heating immersion circulator with a temperature controlling accuracy of ± 0.010 K were also used for the experiments.

2.3.13 Karl- Fischer Titrator

A Karl- Fischer Titrator (Spectralab-AT 36) was used for the determination of water content. Samples with known weight were taken for the determination of water content. Calibration was carried out using known quantity of water. The method is based on the reaction between iodine and sulfur dioxide in aqueous medium. Water and iodine are consumed quantitatively in a 1:1 mole ratio in the reaction. Once all the water present in the sample is consumed, excess iodine is detected voltametrically. Pyridine free KarlFischer reagent was used for the determination of water content in the samples.

2.3.14 Electrochemical system

All the electrochemical studies in this work were carried out using an Autolab electrochemical system (model: PGSTAT – 302N by Eco Chemie B.V, Netherlands) equipped with an IF 030 interface. It uses computer based software, namely, General Purpose Electrochemical System (GPES) version 4.9.

2.3.15 Electrochemical cell

The electrochemical cell had a single leak-tight compartment where the test solution for the electrochemical study was kept in a glass beaker. All the electrodes were placed in the same compartment (Photograph 1) and kept under argon atmosphere during entire study. The total setup was kept in silicone oil bath and heated for attaining the required temperatures.

Photograph 1

2.4 Analytical Procedures

2.4.1 Standard EDTA solution

The solution of EDTA was prepared by dissolving required quantity of EDTA salt by weight in distilled water to get the desired concentration solution. This solution was then standardized by using standard neodymium solution (5.135 mg/g) at pH 6 (adjusted using saturated solution of HMTA) using methyl thymol blue as indicator.

2.4.2 Preapration of europium nitrate solution

Europium nitrate solution was prepared by dissolving Eu_2O_3 in the concentrated nitric acid followed by drying under an IR lamp. The nitric acid was evaporated to dryness and the europium nitrate was redissolved in 0.01 M HNO_3. The free acidity of $Eu(NO_3)_3$ solution was measured by acid base titration along with potassium oxalate solution as a holding agent for Eu(III). The solution was then quantitatively transferred to a pre weighed volumetric flask and filled up to the level by 0.01M HNO_3.

2.4.3 Standardisation of europium nitrate solution

A known volume of europium nitrate solution was taken in a beaker, diluted with distilled water and pH was adjusted to 6 by adding saturated solution of HMTA. Then it was titrated using standard EDTA solution with methyl thymol blue as indicator. The end point was blue to yellow. From this standard stock solution of $Eu(NO_3)_3$, different concentrations of Eu(III) solution were prepared as per the requirement.

2.4.4 Preparation of the solutions of aqueous complexing agents

Appropriate weight of various aqueous complexing agents such as acetohydroxamic acid and oxalic acid were dissolved in distilled water and made up to the required volume to get the solutions on molar basis. The acidity of the corresponding solutions was adjusted to the required concentration by adding calculated amount of concentrated nitric acid.

2.4.5 Preparation of solutions with various concentrations of NO_3^- ion or C_4mpy^+ ion or NTf_2^- ion

Various concentrations of nitrate ion or C_4mpy^+ or NTf_2^- solution were prepared by taking appropriate amounts of sodium nitrate crystal or $[C_4mpy][Br]$ or $LiNTf_2$ and required quantity of nitric acid with higher concentration in distilled water made up to the required volume to get the solutions on molar basis.

2.4.6 Preparation of europium tris[bis(trifluoromethanesulfonyl)imide ($Eu(NTf_2)_3$)

$Eu(NTf_2)_3$ was prepared as per the procedure given in literature [160]. 0.5 mol of Eu_2O_3 was added to an aqueous solution of 3 mol of $HNTf_2$ and the mixture was stirred at 343 K for several hours. $Eu(NTf_2)_3$ (1 mol) formed was dried in a rotary evaporator at 353 K.

2.4.7 Preparation of uranyl bis(trifluoromethanesulfonyl)imide, $UO_2(NTf_2)_2$

The uranyl bis(trifluoromethanesulfonyl)imide, $UO_2(NTf_2)_2$, was prepared by the procedure described elsewhere [161]. Initially, uranium trioxide (UO_3) was prepared by heating uranyl nitrate hexahydrate powder (UO_2 $(NO_3)_2.6H_2O$) [162]. UO_3 (1.0 g) was allowed to dissolve in an 80% solution of bis(trifluoromethanesulfonyl)imide (10 mL) by vigorous stirring at 323 K for 3 d. Then the temperature was raised to 353 K and refluxed overnight. Water was removed by distillation under vacuum. The acidic impurity ($HNTf_2$) present in the system was extracted with dichloromethane (3×20 mL) and then the crude product redissolved in ethanol and filtered through a crucible to remove any unreacted UO_3. Finally,the product, $UO_2(NTf_2)_2$, was dried under vacuum prior to use.

2.5 Liquid – liquid extraction studies

All the extraction experiments were conducted in duplicate at 298 K with 1:1 aqueous: ionic liquid (or organic) phase ratio and all the results were reported with an accuracy of ±5% unless otherwise mentioned. The ionic liquid phase was the solution of desired concentration molecular extractant or functionalized ionic liquid in RTIL diluent. Organic phase was desired concentration of molecular extractant or functionalized ionic liquid in *n*-dodecane (*n*-DD) and ionic liquid (or organic) phase was pre-equilibrated with desired concentration of nitric acid prior to metal ion extraction. The aqueous phase was desired concentration of nitric acid spiked with a radioisotope. (In the case of loading experiments, aqueous phase was desired concentration of nitric acid containing high concentration of metal ion and spiked with corresponding radioisotope).The extraction experiments involved equilibration of equal volumes (1 mL) of ionic liquid/organic phase and aqueous phase in a 10 mL capacity test tube immersed in a constant temperature water bath and rotated in up-side-down manner for about an hour unless otherwise mentioned. After equilibration the radioactivity present in both organic or ionic liquid and aqueous phases was measured. The γ-radioactivity for ^{241}Am(III), and $^{(152+154)}$Eu(III) isotopes was measured using a well-type NaI(Tl) scintillation detector and for α, β – emitting radionuclides, ^{233}U & ^{239}Pu, radioactivity was measured by liquid scintillation counter. The distribution ratio (D_{M}) of the metal ion was determined using the equation 2.1.

$$D_{\mathrm{M}} = \frac{[\mathrm{M}]_{\mathrm{IL(or)org}}}{[\mathrm{M}]_{\mathrm{aq}}} \tag{2.1}$$

where $\mathrm{M}_{\mathrm{IL\ or\ org}}$ and M_{aq} are the radioactivity of radionuclide in ionic liquid/organic phase and aqueous phase respectively. M = ^{239}Pu(IV) or ^{233}U(VI) or ^{241}Am(III) or $^{152+154}$Eu (III).

In the loading experiments, the amount of metal ion loaded into the ionic liquid phase was calculated using the distribution ratio (D_{M}) and the initial concentration of metal ion in aqueous phase as shown in equation 2.2.

$$C_{IL} = D_M . C_{aq}^{\ initial} \Big/ (D_M + 1) \tag{2.2}$$

where C_{IL} is the concentration of metal ion loaded in ionic liquid phase and $C_{\mathrm{aq}}^{\mathrm{initial}}$ is the initial concentration of metal ion in aqueous phase.

The separation factors between two metal ions were calculated from the equation 2.3.

$$SeparationFactor(SF) = \frac{D_{Pu(IV)}}{D_{U(VI)}} \, or \, \frac{D_{Pu(IV)}}{D_{Am(III)}} \, or \, \frac{D_{U(VI)}}{D_{Am(III)}} \tag{2.3}$$

The enthalpy change (ΔH_{tot}) accompanied by the extraction of metal ion from the desired concentration of nitric acid phase was determined by studying the uptake of these metal ions as function of temperature using Van’t Hoff equation of the form shown in equation 2.4.

$$\frac{\partial \ln D}{\partial (1/T)} = \frac{-\Delta H_{tot}}{R} \tag{2.4}$$

where T is temperature and R is gas constant. Plot of ln $D_{Pu(IV)}$ against 1/T was drawn and the enthalpy of extraction was calculated from the slope of straight line obtained by the linear regression of extraction data.

2.6 Electroanalytical techniques

The techniques which are used to evaluate the momentary behavior of the analyte at the electrode-electrolyte interface in an electrochemical system after a small perturbation from its equilibrium position are called as the electrochemical transient techniques [163]. These include polarography, voltammetry (galvanostatic and potentiostatic) etc. The techniques used in this work have been described below.

2.6.1 Voltammetry

Voltammetric techniques are among the mostly used electrochemical transient techniques to study the behaviour of the analyte at an electrode-electrolyte interface. Mostly a three electrode cell consisting of a working electrode, a counter electrode and a reference electrode is used in voltammetric techniques [164, 165]. The electrolyte could be a liquid containing ions or solid. The electrode may be made of metal or non-metal which conducts electrons. The electrolyte is an ionic conductor and the electrodes are electronic conductors.

The electrode at which the redox process of interest occurs is called as the working electrode. Commonly used working electrodes are glassy carbon rod, Pt, W wires, graphite rod etc. The potential and the current of the system are monitored across this electrode. The current carrying electrode in the cell is the counter/auxiliary electrode at which the counter reaction (counter reaction to the reaction occurring at working electrode) takes place. The third electrode is called the reference electrode, which carries no current, and the potential of the working electrode is monitored against this reference electrode. The reference electrode should have a constant potential over a time and it should be reversible. In general, a standard hydrogen electrode, calomel electrode, Ag/Ag^+ and quasi-reference electrodes such as Pd or Ag wire are used as reference electrodes in both aqueous and non-aqueous electrolyte solutions. These voltammetric techniques are in general classified broadly as potentiostatic and galvanostatic techniques [164,165].

In potentiostatic technique, the potential of the system is controlled and the response in the form of current is measured and in the case of galvanostatic technique, the current of the system is controlled and the potential response is measured. Electroanalytical techniques are further categorized into step (for both and current) and sweep (potential) techniques according to the mode of imposition of potential/current. Sweep techniques involve continuous scanning of the potential applied at the working electrode from one potential to another. Voltammetric methods such as cyclic voltammetry and linear sweep voltammetry are sweep techniques. In step techniques, the potential or current is varied in a predetermined manner with time. It can have single or several steps and chronomethods are step techniques.

2.6.1.1 Cyclic voltammetry

Cyclic voltammetry (CV) is very frequently used because it offers a wealth of experimental information and insight into both the kinetic and thermodynamic details of many chemical systems [166]. It is the most versatile electroanalytical technique for the study of electroactive species [167]. In this technique, the potential of the working electrode with respect to the standard reference electrode is monitored by potentiostat and the current of the system is measured through working and counter electrodes. The potential of the working electrode is scanned from an initial point where there is no faradaic process to a specified final point and then switched back to other side of potential and then swept to the initial point. The potential of the working electrode is changed with time at some particular rate called the sweep rate or scan rate and denoted by ν. It has the units of volts per second, $V.s^{-1}$.

The response of the system is obtained in the form of a plot of current (Y-axis) versus applied potential (X-axis) called cyclic voltammogram (figure 2.1). In the convention used in this thesis, cathodic currents are taken as negative and positive potentials are plotted to the right. In a typical CV experiment, the potential of the working electrode is continuously scanned from initial value to final value at a specified scan rate. The scan is commenced at a potential where no electrochemical reaction takes place (no current) and scanned to a region where electrochemical oxidation or reduction takes place.

It can be well viewed from the figure 2.1 that no current flows at initial or start potential (E_i) where no faradaic electrochemical process occurs. If the potential is scanned in the cathodic direction (negative direction), reduction takes place at the electrode since according to the Nernst equation (equation 2.5) product (R) formed towards negative potentials.

$$E = E^{0'} + \frac{RT}{nF} \ln \frac{C_O}{C_R} \qquad (2.5)$$

where C_R is concentration of reduced form and C_O is concentration of oxidized form.When the potential is scanned further, at E_{Onset}, the current starts rising where the faradaic process (reduction) starts occurring and the ‘O’ (electroactive species) start to diffuse from bulk of the solution to the electrode to compensate for the concentration drop at the electrode. Further scanning of the potential to more negative potentials leads to the maximum current, i_p (peak), where the concentration of ‘O’ at electrode surface falls to zero and the current decays further as controlled by diffusion of ‘O’. Similarly, if the potential is scanned in the anodic direction (positive direction) from the switching potential (E_λ), oxidation reaction occurs at the electrode.

The unique parameters associated with cyclic voltammogram

A typical cyclic voltammogram for a redox process is shown in figure 2.1. The important characteristics of the voltammogram, which will be used in the analysis of the redox process, are given below [164,165].

$\mathbf{E_p^c}$ = Cathodic peak potential (reduction); $\mathbf{E_p^a}$ = Anodic peak potential (oxidation)

$\mathbf{i_p^c}$ = Cathodic peak current; $\mathbf{i_p^c}$ = Anodic peak current

$\mathbf{E_{p/2}}$ = Half peak potential (the potential where the i_p is $i_{p/2}$)

$\mathbf{E_\lambda}$= Switching potential; $\mathbf{E_{1/2}}$ = half wave potential; $\mathbf{E_p} - \mathbf{E_{p/2}}$ is width of the peak

$$\mathbf{E_{1/2}} = \text{half wave potential} = \frac{E_P^{Red} + E_P^{Ox}}{2} = E^{0'}$$

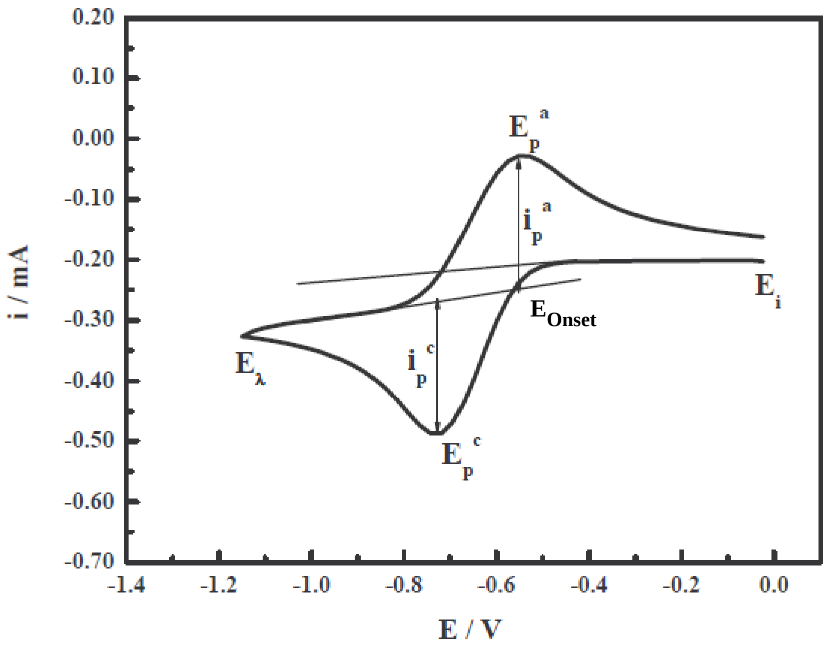

Figure 2.1. A typical cyclic voltammogram of a redox couple

Based on the comprehensive analysis of the cyclic voltammetry, the reversibility of the electrochemical processes can be judged as discussed below [164,165,168,169].

Reversible process

In reversible process, the rate of electrochemical process is controlled by diffusion (mass transfer) but not by charge transfer kinetics and the charge transfer is rapid and the mass transfer is slow (rate determining step). The key criterion for a reversible charge transfer process is that E_p is independent of scan rate (ν) and the peak separation is given by equation 2.6.

$$E_p^c - E_p^a = 2.29\,\frac{RT}{nF} \tag{2.6}$$

The peak current is given by Randles-Sevcik [164].

$$i_p = 0.4463\,nFC_O A\nu^{1/2} D_O{}^{1/2}\left(\frac{nF}{RT}\right)^{1/2} \tag{2.7}$$

where n is the number of electrons involved in the charge transfer reaction, F is the Faraday constant, A is area of the electrode (cm^2), C_O is the bulk concentration of electro-active substance ($mol.cm^{-3}$), R is the gas constant, T is the absolute temperature (K), ν is the scan rate ($V.s^{-1}$) and D_O is the diffusion coefficient ($cm^2.s^{-1}$) of ‘O’.

Irreversible process

In this process, the rate of the redox process is controlled mostly by charge transfer kinetics and the main criterion of the irreversible charge transfer kinetics is the shift in the peak potential with scan rate. The peak separation (E_p^c - E_p^a) is very large and sometimes the reverse peak (oxidation peak) can not be seen in the scan reversal of the cyclic voltammogram. The wave shape is determined by charge transfer coefficient (α) which is a measure of the symmetry of the energy barrier and is independent of scan rate. For the irreversible process the following equations can be used to deduce the important parameters using cyclic voltammetry

$$\left|E_p^c - E_{p/2}^c\right| = \frac{1.857\ RT}{\alpha\, n_\alpha F} \qquad (2.8)$$

Charge transfer coefficient value is in the range of - 0.1 ≥ α ≤ 0.9. Equation 2.9 shows the current equation used in irreversible processes [164].

$$i_p = 0.496\, nFC_O AD_O^{1/2}\left(\frac{(\alpha\, n_\alpha)F\nu}{RT}\right)^{1/2} \qquad (2.9)$$

Quasi-reversible process

The process in which the rate of the electrochemical reaction is a mixed control of both diffusion and charge transfer kinetics is known as quasi-reversible process where the peak potential shifts with scan rate and the peak shape visually broadens as scan rate is increased. Similarly, the difference between the cathodic and anodic peak potentials (ΔE_P) increases with scan rate and the average of the peak potentials (($E_P^a + E_P^c$) / 2) is constant at different scan rates.

Heterogeneous charge transfer coefficient, k_s, can be obtained by using the following equation which was proposed by Klingler and Kochi [165, 170].

$$k_s = 2.18\left[D_0(\alpha n_\alpha)\frac{\nu F}{RT}\right]^{1/2} \exp\left[\frac{\alpha^2 nF}{RT}\left(E_P^c - E_P^a\right)\right] \qquad (2.10)$$

Depending upon the magnitude of k_s the electrode reaction can be classified [164] as, reversible when $k_s \geq 0.3\nu^{1/2}$ cm.s^{-1}, quasi-reversible when $0.3\nu^{1/2} \geq k_s \geq 2 \times 10^{-5}\nu^{1/2}$ cm.s^{-1} and irreversible when $k_s \leq 2 \times 10^{-5}\nu^{1/2}$ cm.s^{-1}.

2.6.1.2 Chronopotentiometry (controlled current technique)

In this technique, the controlled current is applied between the working and counter electrodes and the potential of the working electrode versus reference electrode is monitored/measured simultaneously. A plot of the resulting potential against time is called as chronopotentiogram. When the constant current is applied between the working and counter electrodes, the concentration of the analyte ion decreases and the potential of the working electrode changes. This process continues until the concentration of the analyte ion at the electrode becomes zero. Since the concentration of the analyte ion changes with time, obviously, the potential of the electrode also changes. The duration of this potential change or the concentration change of the analyte ion is called as the transition time and is denoted by τ [171]. The relation between the applied current and transition time is given by Sand's relation [164,165] shown in equation 6. The experimentally determined value of τ at a particular i, can be used to determine the diffusion coefficient (D_o) using the above Sand's equation (equation 2.11).

$$i\tau^{1/2} = nFAD_o^{1/2}\pi^{1/2}C \big/ 2 \qquad (2.11)$$

2.6.1.3 Chronoamperometry (Controlled potential technique)

Chronoamperometry is one of the potential step techniques and in this method, constant potential step is applied to the working electrode and current is measured as a function of time [164, 172]. The instantaneous current obtained is given by the Cottrell eqation (equation 2.12) [164,165]. The Cottrell plot of i vs $t^{-1/2}$ is linear with zero-intercept and it allows the conclusion of the simple diffusion controlled process and from the slope of the plot, diffusion coefficient, D_o can be calculated.

$$i = \frac{nFAD_o^{1/2}C}{(\pi t)^{1/2}} \qquad (2.12)$$

2.7 Electrochemical studies

Cyclic voltammograms of metal ion (Eu(III)/ U(VI)) in ionic liquid medium in the presence and absence of extractants were recorded at various scan rates and at various temperatures. To determine the diffusion coefficient, the value of αn_α was determined from equation 2.8. Diffusion coefficient values were calculated using the equation 2.9. The charge transfer rate constant, k_s (cm/s) was determined using equation 2.10. Moreover, the Diffusion coefficient values for Eu(III) in [C_4mpy][NTf_2] in the presence and absence of extractants were determined using chronopotentiometry and chronoamperometry techniques also. The chronopotentiogram was recorded at various applied current densities at 373 K. Transient time (τ) was obtained by the linear extrapolation of the sections on the chronopotentiometry transients before and after the inflection. Using the equation 2.11, the diffusion coefficient was calculated. Similarly, chronoamperograms for the cathodic reduction of Eu(III) to Eu(II) in [C_4mPy][NTf_2] at 373 K was recorded in the presence and absence of ligands and the diffusion coefficient of Eu(III) was determined using the equation 2.12. From the cyclic voltammograms recorded at 373 K at the scan rate of 0.1 V.s^{-1} for U(VI)/U(V) or Eu(III)/Eu(II) couple in RTIL medium containing various concentrations of extractants, the stability constant (ln K_f) and the co-ordination number (m) of metal-complex were determined using the equation 2.13 [173,174].

$$\Delta E_{1/2} = (E_{1/2})_C - (E_{1/2})_M = -(RT/\alpha nF)(\ln K_f + m \ln[L]) \qquad (2.13)$$

where $(E_{1/2})_C$ and $(E_{1/2})_M$ are the half wave potential of complexed and free metal ion, respectively, [L] is the ligand concentration in M, n is the number of electrons transferred, m is the stoichiometry of the complex and α is the charge transfer coefficient. From the magnitude of the intercept and slope obtained from the plot of -$\Delta E_{1/2}/(RT/\alpha nF)$ against the logarithmic value of extractant concentration , ln K_f and m were determined.

2.8 Experimental procedures

2.8.1 Extraction behavior of U(VI) using some tri *n*-alkyl phosphates (TAlPs) present in imidazolium based room temperature ionic liquid

2.8.1.1 Effect of HNO_3 concentration

A 1.1 M TAlP in $[C_8mim][NTf_2]$ was prepared and it was pre-equilibrated with desired concentration of nitric acid in order to fix the equilibrium acidity. Extraction of U(VI) as a function of nitric acid concentration was studied by equilibrating 1 mL of pre-equilibrated ionic liquid phase with 1mL of desired concentration of nitric acid solution containing ^{233}U(VI) tracer.

2.8.1.2 Effect of TAlP concentration

The extraction of U(VI) as a function of TAlP concentration in the ionic liquid phase was studied by equilibrating 1 mL of 3 M nitric acid solution spiked with ^{233}U tracer with 1 mL of TAlP/$[C_8mim][NTf_2]$ (which was pre-equilibrated with 3M HNO_3) for one hour. The concentration of TAlP present in IL was varied from 0.2 M to 1.2 M.

2.8.1.3 Effect of temperature

Enthalpy change accompanied by the extraction of U(VI) in 1.1 M TAlP/ $[C_8mim][NTf_2]$ was determined by measuring the distribution ratio of U(VI) in 3 M HNO_3 spiked with ^{233}U tracer at various temperatures (298 K to 333 K).

2.8.1.4 Stripping of U(VI)

Stripping of U(VI) from the loaded ionic liquid phase was carried out using 0.01 M HNO_3. The loading of U(VI) from nitric acid phase into the ionic liquid phase was performed by equilibrating equal volume of 1.1 M TAlP/ [C_8mim][NTf_2] (which was pre-equilibrated with 3M HNO_3) with 3 M nitric acid spiked with ^{233}U tracer for about 1 hour. After equilibration, ionic liquid phase was separated and it was taken into two tubes such that each tube containing 1 ml of ionic liquid phase. Then the ionic liquid phase was equilibrated, for 1 hour, with the equal volume (1 mL) of 0.01 M HNO_3. After equilibration, an aliquat was taken from the aqueous phase . The aqueous phase from the equilibrated sample was removed and the ionic liquid phase (1 mL) was contacted again with fresh 0.01 M HNO_3 (1 mL) for 1 hour. Again an aliquat was taken from the aqueous phase and the procedure was repeated until the uranium loaded in organic phase was recovered completely.

2.8.2 **Mutual separation of Pu(IV) from other actinides using 2-hydroxy acetamide extractant in room temperature ionic liquid**

2.8.2.1 Effect of nitric acid concentration

0.02 M solutions of DAlkHyA/[C_4mim][NTf_2], DOMeOA/[C_4mim][NTf_2] and DHOA/[C_4mim][NTf_2] were prepared and they were pre-equilibrated with desired concentration of nitric acid. Extraction of Pu(IV) (or U(VI) or Am(III)) as a function of nitric acid was studied by equilibrating 1 mL of pre-equilibrated ionic liquid phase with 1 mL of desired concentration of nitric acid solution containing tracer ^{239}Pu(IV) or ^{233}U(VI) or ^{241}Am(III).

2.8.2.2 Effect of concentration of DOHyA

The extraction of Pu(IV) as a function of DOHyA concentration in the ionic liquid phase was studied by equilibrating 1 mL of DOHyA/ [C_4mim][NTf_2] (which was pre-equilibrated with 3M HNO_3 **)** with 1 mL of 3 M nitric acid solution spiked with ^{239}Pu tracer, for one hour. The concentration of DOHyA was varied from 0.005 M to 0.05 M.

2.8.2.3 Effect of temperature

Enthalpy change accompanied by the extraction of Pu(IV) in 0.02 M DOHyA/ [C_4mim][NTf_2] was determined by measuring the distribution ratio of Pu(IV) with 3 M HNO_3 spiked with ^{239}Pu tracer at various temperatures (298 K to 333 K).

2.8.2.4 Stripping study

0.05 M Oxalic acid and 0.5 M acetohydroxamic acid diluted in 0.35 M HNO_3 was used for stripping of Pu(IV) from the loaded ionic liquid phase. The loading of plutonium (IV) from nitric acid phase into the ionic liquid phase was performed by equilibrating equal volume of 0.02 M [DOHyA]/[C_4mim][NTf_2] (which was pre-equilibrated with 3M HNO_3) with 3 M nitric acid spiked with ^{239}Pu tracer for about 1 hour. After equilibration, ionic liquid phase was separated and it was taken into two tubes such that each tube containing 1 ml of ionic liquid phase. Then the ionic liquids phase was equilibrated, for 1 hour, with the equal volume (1 mL) of stripping formulations (0.35 M nitric acid containing 0.05 M oxalic acid or 0.35 M nitric acid containing 0.5 M acetohydroxamic acid). An aliquat was taken from the aqueous phase. The aqueous phase from the equilibrated sample was removed and the ionic liquid phase (1 mL) was contacted again with fresh stripping solution (1 mL) for 1 hour. Again an aliquat was taken from the aqueous phase and the procedure was repeated until the plutonium loaded in organic phase was recovered completely.

2.8.3 Solvent extraction study of americium(III) using benzoylpyrazolone extractant dissolved in pyrrolidinium based room temperature ionic liquid

2.8.3.1 Effect of nitric acid concentration

0.01 M solutions of HPMBP/[C_4mpy][NTf_2], MPP/[C_4mpy][NTf_2] and HPMBP/*n*-DD were prepared and it was pre-equilibrated with desired pH solutions. Extraction of

Am(III) as a function of pH was studied by equilibrating 1 mL of pre-equilibrated ionic liquid phase or *n*-dodecane phase with 1 mL of desired pH solution containing ^{241}Am(III) tracer.

2.8.3.2 Effect of HPMBP concentration

The extraction of Am(III) as a function of HPMBP in [C_4mpy][NTf_2] was studied by equilibrating 1 mL of HPMBP / [C_4mim][NTf_2] (which was pre-equilibrated with pH2 solution) with 1 mL of pH 2 solution spiked with ^{241}Am tracer, for one hour. The concentration of HPMBP was varied from 0.005 M to 0.03 M.

2.8.3.3 Effect of C_4mpy^+ and NO_3^- concentration

The effect of C_4mpy^+ and NO_3^- concentration on the distribution ratio of Am(III) was studied by equilibrating 0.01 M solution of HPMBP/[C_4mpy][NTf_2] (pre-equilibrated with pH 2 solution) with pH 2 solution containing various concentrations of [C_4mpy][Br] (0.01 to 0.06 M) or $NaNO_3$ (0.1 – 0.7 M) spiked with ^{241}Am(III) tracer. The concentration of additives C_4mpy^+ or NO_3^- was varied by adding the required quantity of [C_4mpy][Br] or $NaNO_3$ in aqueous phase.

2.8.3.4 Stripping study

Stripping of Am(III) from the loaded ionic liquid phase was carried out using different different concentrations of nitric acid (0.1 M to 3 M HNO_3). The loading of Am(III) from nitric acid phase into the ionic liquid phase was performed by equilibrating equal volume of 0.01 M HPMBP/ [C_4mpy][NTf_2] with pH2 solution spiked with ^{241}Am tracer for about 1 hour. After equilibration, ionic liquid phase was separated and it was taken into two tubes such that each tube contained 1 ml of ionic liquid phase. Then the ionic liquid phase was equilibrated, for 1 hour, with the equal volume (1 mL) of HNO_3 (0.1 M to 3 M). An aliquat was taken from the aqueous phase and Am(III) stripped into the aqueous phase was determined.

2.8.4 Mutual separation of Pu(IV) from other actinides using TSIL

2.8.4.1 Effect of nitric acid concentration

A 0.3 M solution of TSIL/[C_4mim][NTf_2] and [C_4mim][NTf_2] were pre-equilibrated with desired concentration of nitric acid (1-8 M HNO_3) in order to fix the equilibrium acidity. Extraction of plutonium(IV) (or U(VI) or Am(III)) as a function of nitric acid was studied by equilibrating 1 mL of pre- equilibrated ionic liquid phase with 1 mL of desired concentration of nitric acid solution containing tracer ^{239}Pu(IV) or ^{233}U(VI) or ^{241}Am(III).

2.8.4.2 Effect of [BuImPA][NTf_2] concentration

The extraction of Pu(IV) as a function of [BuImPA][NTf_2] concentration in [C_4mim][NTf_2] was studied by equilibrating equal volume of [BuImPA][NTf_2] / [C_4mim][NTf_2] (pre-equilibrated with 3 M HNO_3) with 3 M nitric acid solution spiked with ^{239}Pu tracer, for one hour. The concentration of [BuImPA][NTf_2] was varied from 0.05 M – 0.5 M.

2.8.4.3 Effect of NTf_2^- concentration

The effect of NTf_2^- concentration on the distribution ratio of Pu(IV) was studied by equilibrating 0.3 M [BuImPA][NTf_2] / [C_4mim][NTf_2] (pre-equilibrated with 5M HNO_3) with 5M HNO_3 containing various concentrations of $LiNTf_2$ (0.1 to 0.9M) spiked with ^{239}Pu(IV) tracer.

2.8.4.4 Stripping study

The stripping study was carried out by using 0.1 M oxalic acid in 0.35 M nitric acid medium as the stripping formulation. Loading of Pu(IV) in ionic liqulid phase was carried out by equilibrating equal volume of 0.3 M [BuImPA][NTf_2]/[C_4mim][NTf_2] (pre-equilibrated with 3 M HNO_3) with 3 M nitric acid spiked with ^{239}Pu tracer for about 1 hour. After the extraction, the ionic liquid phase was separated and was equilibrated with the equal volume of 0.35 M nitric acid containing 0.1 M oxalic acid solution for 1 hour. After equilibration, an aliquat was taken from the aqueous phase. The aqueous phase from the equilibrated sample was removed and the ionic liquid phase (1mL) contacted with fresh stripping solution (1mL) for 1 hour. An aliquat was taken again form the aqueous phase and the procedure was repeated until the plutonium loaded in organic phase was recovered completely.

2.8.5 Insights into the solvent extraction behavior of U(VI) in PUREX solvent containing RTIL with strongly coordinating anion

2.8.5.1 Effect of nitric acid concentration

The organic phase was composed of 1.1 M TBP/*n*-DD or (1.1 M TBP + ionic liquid)/ *n*-DD or (1.1 M TBP + Aliquat NO_3)/*n*-DD or (1.1 M TBP + HDEHP)/*n*-DD or ionic liquid/ *n*-DD or (Aliquat NO_3 + HDEHP + TBP) /*n*-DD. The organic phase was pre-equilibrated with desired concentration of nitric acid (0.1 M to 5 M). The extraction behaviour of U(VI) as a function of nitric acid concentration was studied by equilibrating the pre-equilibrated organic phase (1 mL) with fresh aqueous phase (1 mL) containing desired concentration of nitric acid (0.1 M to 5 M) spiked with ^{233}U(VI) tracer.

2.8.6 Loading behavior of Eu(III) in diglycolamide/room temperature ionic liquid system

2.8.6.1 Effect of nitric acid concentration

A solution of 0.01 M TODGA/[C_8mim][NTf_2], [C_8mim][NTf_2] , 0.1 M TODGA/*n*-DD, various solutions of TODGA with or without TBP/DHOA in ionic liquid and 1M DHOA or 1M TBP in *n*-DD were pre-equilibrated with desired concentration of nitric acid (0.1 to 6 M HNO_3). Extraction of europium(III) as a function of nitric acid was studied by equilibrating 1 mL of pre- equilibrated ionic liquid phase with 1 mL of desired concentration of nitric acid solution containing tracer $^{152+154}$Eu.

2.8.6.2 Loading studies

The amount of Eu (III) in the nitric acid phase was varied from 1 g/L to 95 g/L. This solution was spiked with $^{(152+154)}$Eu(III) tracer (~10^{-4} M). Then the aqueous solution was mixed with equal volume (1 mL) of ionic liquid phase (DGA in ionic liquid / DGA+ (TBP or DHOA) in ionic liquid) for equilibration. Using the distribution ratio obtained from the radioactive measurements, the amount of Eu(III) loaded in the ionic liquid phase was determined.

2.8.6.3 Effect of TODGA concentration

The extraction of Eu(III) as a function of [TODGA] in [C_8mim][NTf_2] was studied by equilibrating 1 mL of TODGA/[C_8mim][NTf_2] (pre-equilibrated with 3 M HNO_3) with 1 mL of fresh 3 M nitric acid solution spiked with $^{152+154}$Eu tracer, for one hour. The concentration of TODGA was varied from 0.005 M – 0.03 M.

2.8.7 Electrochemical study of U(VI) in the presence of higher homologue of TBP dissolved in RTIL medium

2.8.7.1 Preparation of U(VI) solutions in [C_4mim][NTf_2]

A solution of U(VI) in [C_4mim][NTf_2] was prepared by dissolving the required quantity of UO_2 $(NTf_2)_2$ complex in [C_4mim][NTf_2] and heating the resulting mixture at 373 K for few hours under flowing argon gas to ensure the complete removal water before carrying out the electrochemical studies. A similar procedure was also adopted when TBP and TOP were added to the solution. The water content in the solution was determined to be ~100 ppm.

2.8.7.2 Voltametric studies

A solution of U(VI) in [C_4mim][NTf_2] was prepared and in some cases TBP or TOP was added. The concentration of U(VI) in [C_4mim][NTf_2] was 0.1 M, concentration of TBP was varied from 0.02 M to 0.120 M and concentration of TOP was varied from

0.01 M to 0.08 M in the solution. Voltammetric studies were carried out in a temperature range 353 K to 383 K. A glassy carbon rod (cylindrical SA = 0.52 cm^2) was used as working electrode. A glassy carbon rod and Pd wire acted as counter and quasi-reference electrodes respectively. The internal standard, ferrocene was added to [C_4mim][NTf_2] and all the redox potentials were referred against the Fc/Fc^+ redox couple.

2.8.8 Electrochemical study of Eu(III) in the presence of acidic extractants dissolved in RTIL medium

2.8.8.1 Preparation of Eu (III) solutions in [C_4mpy][NTf_2]

A solution of Eu (III) in [C_4mpy][NTf_2] was prepared by dissolving the required quantity of $Eu(NTf_2)_3$ in [C_4mpy][NTf_2] and heating the resulting mixture at 373 K for few hours under flowing argon atmosphere to remove the residual water, if any, prior to the electrochemical studies. A similar procedure was also adopted when HDEHP and HDGA were added to ionic liquid medium. The water content in the solution was determined to be ~120 ppm.

2.8.8.2 Voltammetric studies

A solution of Eu(III) in [C_4mpy][NTf_2] was prepared and in some cases HDEHP or HDGA was added. The solution of Eu(III) in the ionic liquid ([C_4mpy][NTf_2]) phase containing various concentration of HDEHP and HDGA were prepared. The concentration of Eu(III) in [C_4mpy][NTf_2] was 100 mM and the concentration of HDEHP (or HDGA) was varied from 0.02 M to 0.08 M. A glassy carbon rod (cylindrical SA =0.196 cm^2) was used as working electrode. A glassy carbon rod and Pd wire acted as counter and quasi-reference electrodes respectively. The internal standard, ferrocene was added to [C_4mpy][NTf_2] and all the redox potentials were referred against the Fc/Fc^+ redox couple.

2.9 Synthesis and characterisation of RTILs and extractants

2.9.1. 1-Alkyl-3-methylimidazolium bis(trifluoromethanesulfonyl)imide ([$C_n$mim][NTf_2]) [n = 4, 6 and 8]

1-Alkyl-3-methylimidazolium bis(trifluoromethanesulfonyl)imide was prepared as described elsewhere [72] and the synthetic procedure is depicted in figure 2.2. First step is preparation of 1-alkyl-3-methylimidazolium chloride ([$C_n$mim][Cl]) and it involves refluxing a mixture of 1-methylimidazole with 1-chloroalkane in the mole ratio of 1:1.2 at 343 K for 72 hours. The resulting product ([$C_n$mim][Cl]) was washed a few times with ethyl acetate and acetonitrile .Then the solvent was removed by rotary evaporation and product was dried under vacuum at 343 K for more than 24 hours. A quantitative yield was obtained.

The second step involves in the metathesis reaction between [$C_n$mim][Cl]) and Lithium bis(trifluoromethanesulfonyl)imide ($Li^+ \ {}^-N(CF_3SO_2)_2$) in the mole ratio of 1:1. This reaction mixture was stirred for overnight at 298 K in water medium. After stirring, the bottom layer of ionic liquid was removed and washed several times with distilled water in order to remove unreacted precursors and LiCl salt. The final product product was purified by charcoal treatment and dried at 343 K under vacuum in order to remove the moisture [78]. Around 85% yield was obtained for each ionic liquid.

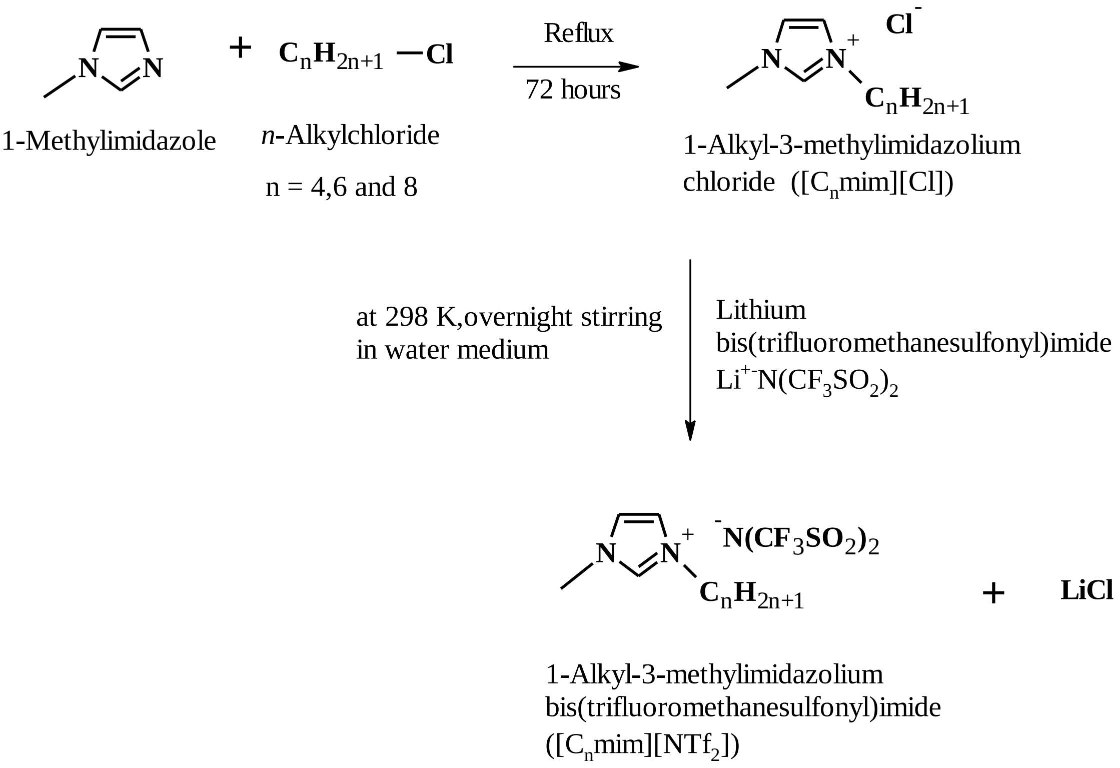

Figure 2.2. Synthesis of 1-alkyl-3-methylimidazolium bis(trifluoromethanesulfonyl)imide ([$C_n$mim][NTf_2] [n = 4, 6 and 8][72]

Characterization:

[$C_n$mim][NTf_2] (n=4, 6, 8)

FT-IR (ν/cm^{-1}): 3157, 3113(CH stretch of imidazole ring), 2964, 2932, 2879 (aliphatic C-H stretch), 1568, 1462 (C-C stretch bands of imidazole ring), 1425, 1340 (C-H) symmetric stretch of CH_3), 1129 (SO_2 symmetric strech), 1182 (C-F) asymmetric stretch), 1050 (S-N-S asymmetric stretch).

[C_4mim][NTf_2]

^{1}H NMR (500 MHz; MeOD; Me_4Si): 8.76 (1H, s), 7.63 (1H, t), 7.58 (1H,t), 4.28 (2H,t), 3.98 (3H,s), 1.89 (2H,q), 1.36 (2H, m), 0.93 (3H,t). ***^{13}C NMR (125 MHz; MeOD; Me_4Si)***: 136 (CH), 123.5 (CH), 122.2 (CH), 115 (CF_3 x 2), 50 (N-CH_2), 36.2 (CH_3), 31 (CH_2), 19 (CH_2), 13 (CH_3).

[C_6mim][NTf_2]

***^{1}H NMR* (500 MHz, MeOD, Me_4Si)**: 8.69(1H, s), 7.63 (1H, t), 7.58 (1H,t), 4.15 (2H,t), 3.93 (3H,s), 1.85 (2H,q), 1.3 (6H, m), 0.88(3H,t). ***^{13}C NMR* (125 MHz, MeOD, Me_4Si)**: 135.9 (CH), 123.7(CH), 122.3 (CH), 118.2 (CF_3 x 2), 50.15 (N-$\underline{C}H_2$), 36.2 (N-$\underline{C}H_3$), 30.8 (CH_2), 29.9 (CH_2), 25.6 (CH_2), 22.2(CH_2), 13.7 (CH_3).

[C_8mim][NTf_2]

^{1}H NMR* (500 MHz; MeOD; Me_4Si)*: 8.76 (1H, s), 7.3 (1H, t), 7.58 (1H,t), 4.15 (2H,t), 3.93 (3H,s), 1.83 (2H,m), 1.3 (10H, m), 0.88 (3H,t). ***^{13}C NMR* (125 MHz; MeOD; Me_4Si)*:***135.9 (CH), 123.7 (CH), 122.2 (CH), 118 (CF_3 x2), 53 (N-CH_2), 50.18 (N-$\underline{C}H_3$), 36.2(CH_2), 31.5(CH_2), 29.9 (CH_2), 28.7(CH_2), 26 (CH_2), 22.5 (CH_2), 13.9 (CH_3).

2.9.2. *N*-butyl *N*-methylpyrrolidinium bis (trifluoromethanesulfonylimide) ([C_4mpy][NTf_2])

The synthesis of [C_4mpy][NTf_2] was carried out by two steps as described in the literature [175] and synthetic scheme is shown in figure 2.3. First step is the synthesis of *N*-butyl *N*-methylpyrrolidinium bromide ([C_4mpy][Br]) and it involves drop-wise addition of *N*-butyl bromide (0.5 mole, 54 ml) to a solution of *N*-methylpyrrolidine medium at 273 K. The reaction mixture was stirred for 4 hours and left overnight. The resulting product [C_4mpy][Br] was dried again using rotary evaporator at 343 K and purified by recrystallization from acetonitrile. Yield of [C_4mpy][Br] is 98%.

The second step involves in the metathesis reaction between ([C_4mpy][Br]) and Lithium bis(trifluoromethanesulfonyl)imide (Li^+ $^-N(CF_3SO_2)_2$) in the mole ratio of 1:1. This reaction mixture was stirred for 4 hours at 298 K in water medium. After stirring, the bottom layer of ionic liquid was washed several times with distilled water and the product was purified by charcoal treatment. Then it was dried at 343 K under vacuum in order to remove the moisture. Around 90% yield was obtained for [C_4mpy][NTf_2].

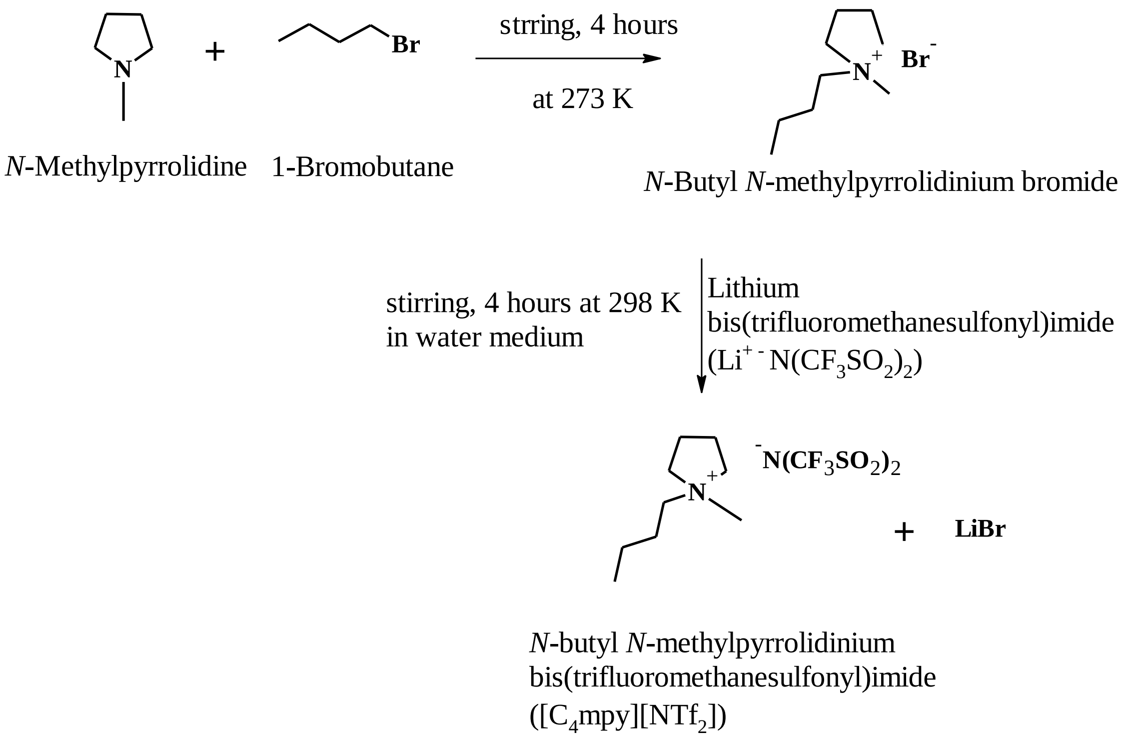

Figure 2.3. Synthesis of N-butyl-N-methylpyrrolidinium bis(trifluoromethanesulfonyl)imide ($[C_4mpy][NTf_2]$) [175]

Characterization:

$[C_4mPy][NTf_2]$

Elemental analysis: (% theoretical value in parenthesis) C: 31.24 (31.27), H: 4.71 (4.73), N :6.64 (6.63), S: 15.2 (15.16). **FT-IR (ν/cm^{-1}):**1180 (C-H asymmetric stretch), 1130 (SO_2 symmetric stretch), 1054 (S-N-S asymmetric stretch), 2876 (C-H stretch), 2970, 2944 (ring C-H stretch), 2179 (ring methylene C-N stretch), 1462, 1345 (methylene and methyl(C-Nstretch). ***^{1}H NMR* (500 MHz; $CDCl_3$; Me_4Si):** 0.95(t,3H),1.41(m,2H),1.73(m,2H),2.21(m,4H), 2.98(s,2H), 3.06(s,2H), 3.06(s,1H), 3.32(m,2H), 3.51(m,4H), 2.98(s, 3H), 3.06(s,1H), 3.32(m,2H), 3.51(m,4H), ***^{13}C NMR* (125 MHz; $CDCl_3$; Me_4Si):** 121.1 (CF_3), 118.55 (CF_3) ,64.62 (N-CH_2 ring), 64.42 (N-

CH_2), 48.53 (ring CH_2), 48.24 (ring CH_2), 25.74(CH_2), 21.56 (CH_2), 19.54(CH_2), 13.37(CH_3), 13.13 (CH_3).

2.9.3.Diethyl-3-(-3-alkylimidazolium)propylphosphoramide bis(trifluoromethanesulfonyl)imide ([BuImPA][NTf$_2$])

The TSIL, [BuImPA][NTf$_2$], have been synthesized for the first time. The reaction scheme for the synthesis of [BuImPA][NTf$_2$] is shown in figure 2.4. A solution of diethylchlorophosphate (28 g, 0.162 mol) in dichloromethane (50 ml) was added dropwise to a solution of 1-(3-aminopropyl)imidazole (20.3 g, 0.162 mol) and triethylamine (32.8 g, 0.324 mol) in dichloromethane (100 ml) at 5^0C. The reaction mixture was stirred over night at 5°C, and the triethylamine hydrochloride formed was removed by filtration. The filtrate was dried in a rotary evaporation to obtain a yellowish viscous liquid, diethyl-3-imidazoliumpropylphosphoramide (I) with the yield of 60%. The product I was dissolved in acetonitrile and added to a solution of butyl bromide in acetonitrile (1: 1.1 mol ratio) at 0°C under vigorous stirring. The reaction mixture was stirred at room temperature for 72 hours. Acetonitrile was then evaporated and product was dried in a rotary evaporator and to obtain a brownish red liquid, diethyl-3-(3-butylimidazolium)propylphosphoramide bromide (yield~ 88 %) (II). The product II was dissolved in deionised water and added slowly to the aqueous solution of bis(trifluoromethanesulfonyl) imide lithium salt (1: 1.2) at room temperature. The mixture was stirred over night. The top aqueous layer was removed, and the bottom ionic liquid phase was washed with deionised water several times. The product was dried at 80°C in a rotary evaporator yielding a thick viscous brownish oil (yield ~ 63 %) of phosphoramide –functionalised ionic liquid (III). Similar procedure was adopted for the synthesis of methyl derivative ([MeImPA][NTf$_2$]) and propyl derivative ([PrImPA][NTf$_2$]) of the phosphoramide –functionalised TSIL.

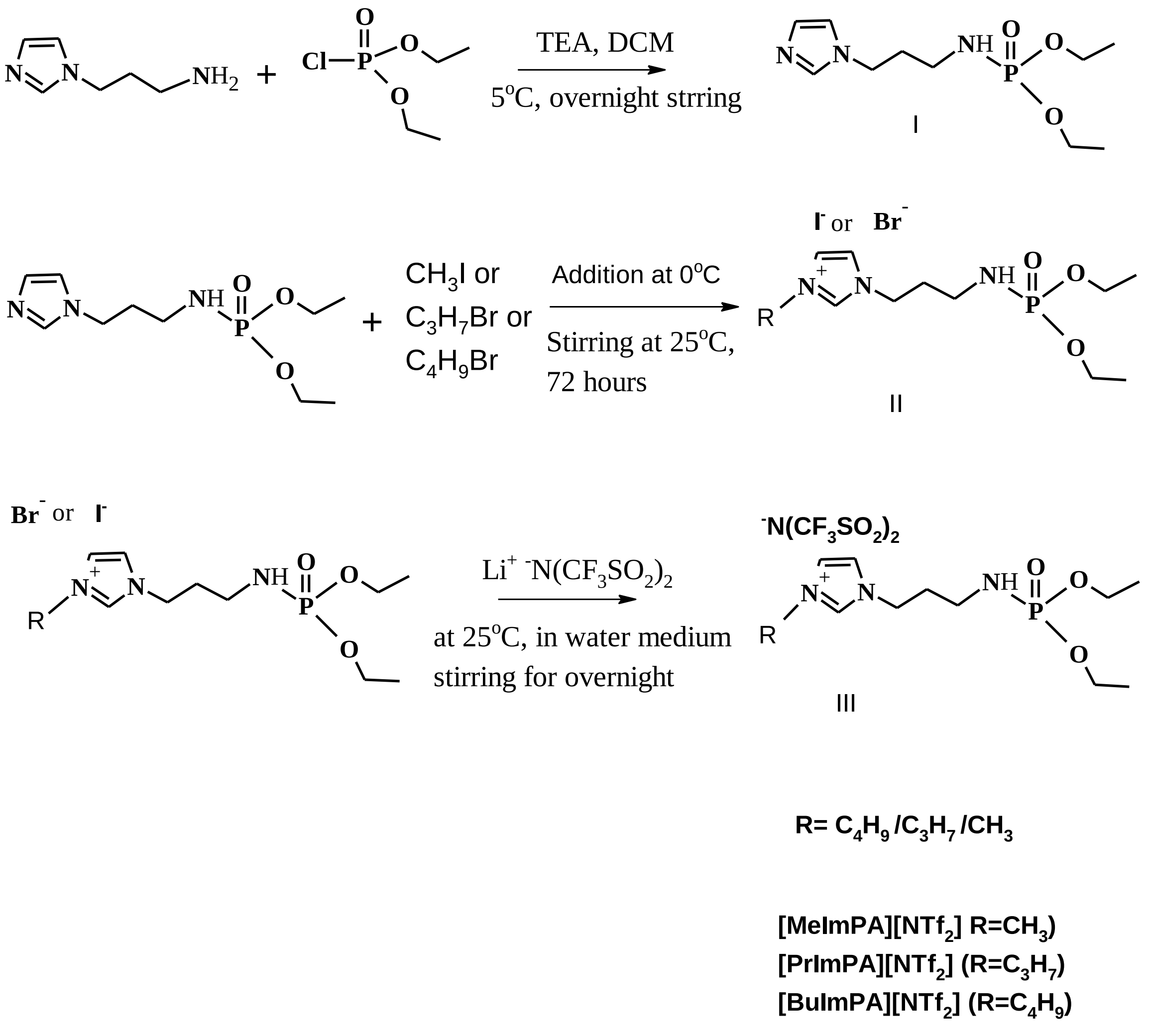

Figure 2.4. Synthesis of diethyl-3-(-3-alkylimidazolium)propylphosphoramide bis(trifluoromethanesulfonyl)imide ([BuImPA][NTf$_2$]/ [PrImPA][NTf$_2$]/ [MeImPA][NTf$_2$])

Characterization:

[BuImPA][NTf$_2$]: **FTIR (ν/cm^{-1}):** 3356 (NH stetching), 2967-2879 (CH streching), 1180 (P=O stretching), 1350 (C-N stretching), 1468, 1570 (C-C symmetric stretch in imidazole ring), 1049 (C-F stretching). ***^{1}H NMR*** **(400 MHz, D$_3$CCOCD$_3$, Me$_4$Si)**: 0.9(t, 3H), 1.78(t,2H), 4.15(t,2H), 2.5(m,2H), 1.9(m,2H), 3.38(m,2H), 3.88 (q,4H), 1.25(t,6H), 7.2(t,1H), 7.4(t,1H), 7.85(t,1H), 9.2(s,1H). ***^{13}C NMR* (125 MHz, D_3CCOCD_3, Me_4Si):** 136 (N-$\underline{C}$H-N), 121(-$\underline{C}$H=CH-), 122(-CH=$\underline{C}$H-), 118($\underline{C}F_3$), 61.8(O-$\underline{C}H_2$), 49.17(N$\underline{C}H_2CH_2CH_2CH_3$), 32(O-$CH_2$-$\underline{C}H_3$), (51(N$\underline{C}H_2$-), 19, 15, 13.8 (various CH_2 group). **Mass (ESI)**: m/z of cation $[BuImPA]^+$ = 318, anion ($[NTf_2]^-$) = 280.

<u>[PrImPA][NTf$_2$]</u>: FTIR (ν/cm^{-1}): 3356 (NH stretching), 2967-2879 (CH streching), 1180 (P=O stretching), 1350(C-N stretching), 1468, 1570(C-C symmetric stretch in imidazole ring), 1049 (C-F stretching). **^{1}H NMR (400 MHz, D_3CCOCD_3, Me_4Si):** 0.9(t,3H), 1.55(m,2H), 4.3(t,2H), 2.5(m,2H), 2(m,2H), 3.38(m,2H), 4(q,4H), 1.25(t,6H), 7.2(t,1H), 7.4 (t,1H), 7.85(t,1H), 9.2(s,1H). **^{13}C NMR (125 MHz, D_3CCOCD_3, Me_4Si):** 137($\underline{C}$H=N) 123(-$\underline{C}$H=CH-), 124(-CH=$\underline{C}$H-), 118($\underline{C}F_3$), 62(O-$\underline{C}H_2$), 52(CH=N$\underline{C}H_2$), 49.17(N$\underline{C}H_2CH_2CH_3$), 22, 17(various CH_2 group). **Mass (ESI)**: m/z of $[PrImPA]^+$ = 304, $[NTf_2]^-$ = 280.

<u>[MeImPA][NTf$_2$]:</u> FTIR (ν/cm^{-1}): 3356(NH stretching), 2967-2879 (CH streching), 1180 (P=O stretching), 1355(C-N stretching), 1468, 1570 (C-C symmetric stretch in imidazole ring), 1049 (C-F stretching). **^{1}H NMR (400 MHz; D_3CCOCD_3; Me_4Si):** 3.2(s,3H), 2.5(m,2H), 2(m,2H), 3.5(m,2H), 4(q,4H), 1.25(t,6H), 7.4(t,1H), 7.7(t,1H), 7.85(t,1H), 9.2(s,1H). **^{13}C NMR (125 MHz; D_3CCOCD_3; Me_4Si):** 137($\underline{C}$H=N), 123(-$\underline{C}$H=CH-), 124(-CH=$\underline{C}$H-), 118($\underline{C}F_3$), 62(O-$\underline{C}H_2$), 57(CH=N$\underline{C}H_3$), 22, 17(various CH_2 group). **Mass (ESI):** m/z of $[MeImPA]^+$ = 276, $[NTf_2]^-$ = 280.

2.9.4. <u>1-Phenyl -3-methyl- 4-benzoyl pyrazalone-5 (HPMBP)</u>

HPMBP have been synthesized as per the procedure described in the literature [176]. And recystallized from slightly acidified methanol-water and characterized by NMR, IR and mass spectrometry.Synthetic procedure of HPMBP is shown in figure 2.5.

Characterization:

HPMBP

Melting point: 120°C,

FTIR (υ/cm^{-1}): 1654 (C=O in ring), 1600 (C=O in side chain stretch), 2567 (N-H stretch - intramolecular hydrogen bonding), 1561(C-C phenyl stretch), 1514 (C=C=C stretch), 950 (C-C_6H_5 stretch), 1401, 1335 (pyrazole ring stretch), 1169 (C-H plane deformation), 3300 (sp C-H stretching). **^{1}H NMR (500 MHz, CD_3COCD_3, Me_4Si)**: 2.1 (s, 3H , CH_3), 7.28 (s, 1H, pyrazole ring), 7.33 – 7.9 (phenyl protons, m). **Mass – TOF**: m/z**:** 278

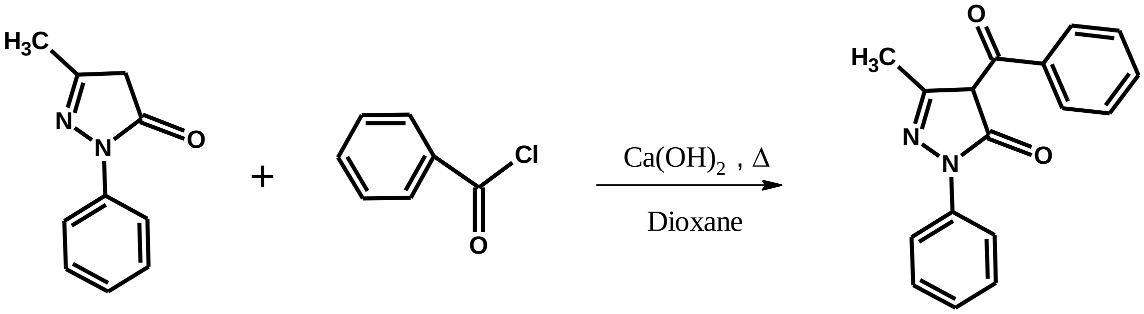

Figure 2.5. Synthesis of 1-phenyl -3-methyl- 4-benzoyl pyrazalone-5 (HPMBP) [176]

2.9.5. Tri-*n*-octylmethylammonium (2-ethyl)hexylphophate ([A336]$^+$[DEHP]$^-$)

Synthesis of [A336]$^+$[DEHP]$^-$ was carried out as per the procedure given elsewhere [177]. A thick viscous liquid, which turned to semi solid upon cooling, was obtained. The synthetic procedure of [A336]$^+$[DEHP]$^-$ is depicted in figure 2.6. The purity of the product was ascertained by IR and NMR techniques.

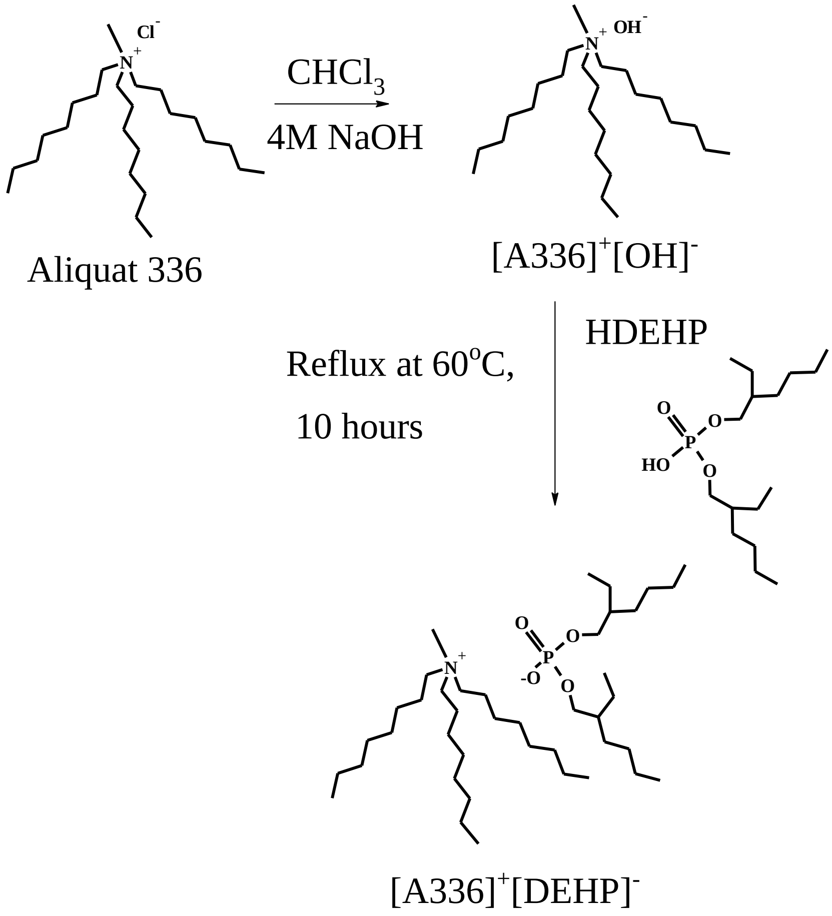

(Tri-*n*-octylmethylammonium
bis-(2-ethylhexyl)phosphate)

Figure 2.6. Synthesis of Tri-n-octylmethylammonium (2-ethyl)hexylphophate ($[A336]^+[DEHP]^-$) [177]

Characterization

$[A336]^+[DEHP]^-$-: **FTIR (ν/cm^{-1}):** 2855, 2925, 2958 (C-H str), 1050 (P-O-C), 1239(P=O), 1463(CH_3-N^+) 1378 (C-H symmetric deformation). **^{1}H NMR (500 MHz, CD_3COCD_3, Me_4Si):** 0.86-0.88 (9H, m), 1.27 (30H,m), 1.3(12H,m), 3.25 (3H,s), 3.4-3.45(6H, m), 1.28 (m, 6H), 1.36 (m,4H), 1.4 (m, 1H), 1.66 (m, 6H), 3.9-3.93(m,4H).

^{13}C NMR (125 MHz, CD_3COCD_3, Me_4Si) : 61.56 (3 x $\underline{C}H_2N$), 48.98 ($\underline{C}H_3N$), 31.75, 30, 29.3, 29.1, 29, 23.69, 23, 22.56, 22.69 (various $\underline{C}H_2$), 14.1 (3 x CH_3), 26.48 (CH_2), 40 (CH), 48.98 (CH_2), 10.9 (CH_3).

2.9.6. *Trialkyl phosphates (TAlPs)*

Trialkyl phosphates were prepared as per the procedure described elsewhere [178]. The synthetic scheme is shown in figure 2.7. Products were characterized by NMR.

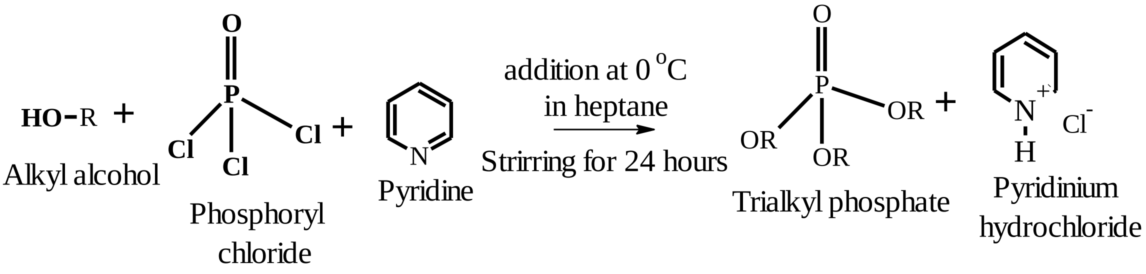

Figure 2.7 Synthesis of trialkyl phosphate (TAlP) [178]

Charecterization:

TPP: **^{1}H NMR (400 MHz; CDCl$_3$; Me$_4$Si):** 4(t, 2H, O-CH_2), 1.72(m, 2H, CH_2), 0.98(t, 3H, CH$_3$). **^{13}C NMR (125 MHz; CDCl$_3$; Me$_4$Si):** 69(O-$\underline{C}$H$_2$), 23.6(O-CH$_2$-$\underline{C}$H$_2$-CH$_3$), 10($\underline{C}$H$_3$).

TAP: **^{1}H NMR (400 MHz; CDCl$_3$; Me$_4$Si):** 4(t, 2H, O-CH_2), 1.3 -1.6 (m, 6H, various CH_2 group), 0.9(t, 3H, CH_3). **^{13}C NMR (125 MHz; CDCl$_3$; Me$_4$Si):** 67.6(O-$\underline{C}$H$_2$), 30(O-CH$_2$-$\underline{C}$H$_2$-_CH$_2$), 27(O-CH$_2$- CH$_2$- $\underline{C}$H$_2$), 22(O-CH$_2$- CH$_2$-CH$_2$-$\underline{C}$H$_2$-CH$_3$), 13($\underline{C}$H$_3$).

TiAP: **^{1}H NMR (400 MHz; CDCl$_3$; Me$_4$Si):** 4(t, 2H, O-CH_2), 1.3 (m, 4H 2xCH_2), 1.5 (m, H, CH-(CH_3)), 0.9(t, 3H, CH_3). **^{13}C NMR (125 MHz; CDCl$_3$; Me$_4$Si):** 66(O-$\underline{C}$H$_2$), 39(O-CH$_2$- $\underline{C}$H$_2$- CH-(CH$_3$)$_2$), 24.5(O-CH$_2$- CH$_2$- $\underline{C}$H-(CH$_3$)$_2$), 14($\underline{C}$H$_3$).

TOP: **^{1}H NMR (400 MHz; CDCl$_3$; Me$_4$Si):** 3.95(t, 2H, O-CH_2), 1.28 - 1.63(m, various - CH$_2$- protons), 0.93(t, 3H, CH_3). **^{13}C NMR (125 MHz; CDCl$_3$; Me$_4$Si)**: 69(O-$\underline{C}$H$_2$), 40(O-CH$_2$-$\underline{C}$H$_2$-_CH$_2$-), 29(O-CH$_2$- CH$_2$- $\underline{C}$H$_2$-),23(-$\underline{C}$H$_2$-CH$_3$),14($\underline{C}$H$_3$).

2.9.7. *N, N-dioctyl-2-methoxyacetamide (DOMeOA)*

N,*N*-dioctyl-2-methoxyacetamide was synthesized as per the procedure given in elsewhere [179] and it is shown in figure 2.8. The product was characterized using NMR and IR techniques.

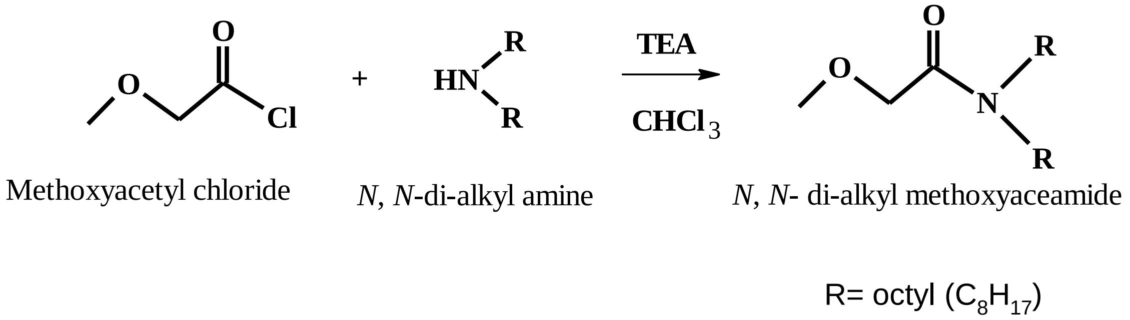

Figure 2.8. Synthesis of N, N-di-alkyl-2-methoxyacetamides (DOMeOA) [179]

Characterization

DOMeOA:FT-IR (ν /cm^{-1}): 2922, 2858 (C–H stretch), 1651(C = O stretch), 1458 (–CH_2–scissoring), 1378 (C–N stretch), 1122 (C–O–C stretch). **^{1}H NMR (500 MHz; $CDCl_3$; Me_4Si):** 4.076 (s, 2H), 3.423(s, 3H), 3.307 (t, 2H), 3.194 (t,2H), 1.553 (m, 4H), 1.285 (m, 20H), 0.887 (m, 6H). **^{13}C NMR (125 MHz; $CDCl_3$; Me_4Si)** 168.25 (CO), 71.28 (O$\underline{C}H_3$) , 58.74 (MeO-$\underline{C}H_2$-CO-), 46.73 (-N-$\underline{C}H_2$-), 45.46 (-N-$\underline{C}H_2$-), 31.59, 29.91, 29.34, 29.14, 27.35, 27.22, 26.73, 22.64 (various CH_2 groups), 14.06 (CH_3).

2.9.8. *N, N-dialkyl-2-hydroxy acetamide (DAlkHyA)*

DOHyA was synthesized as per the procedure described in literature [180]. The synthetic scheme of DOHyA has been shown in figure 2.9. The product was characterized using NMR and IR techniques.

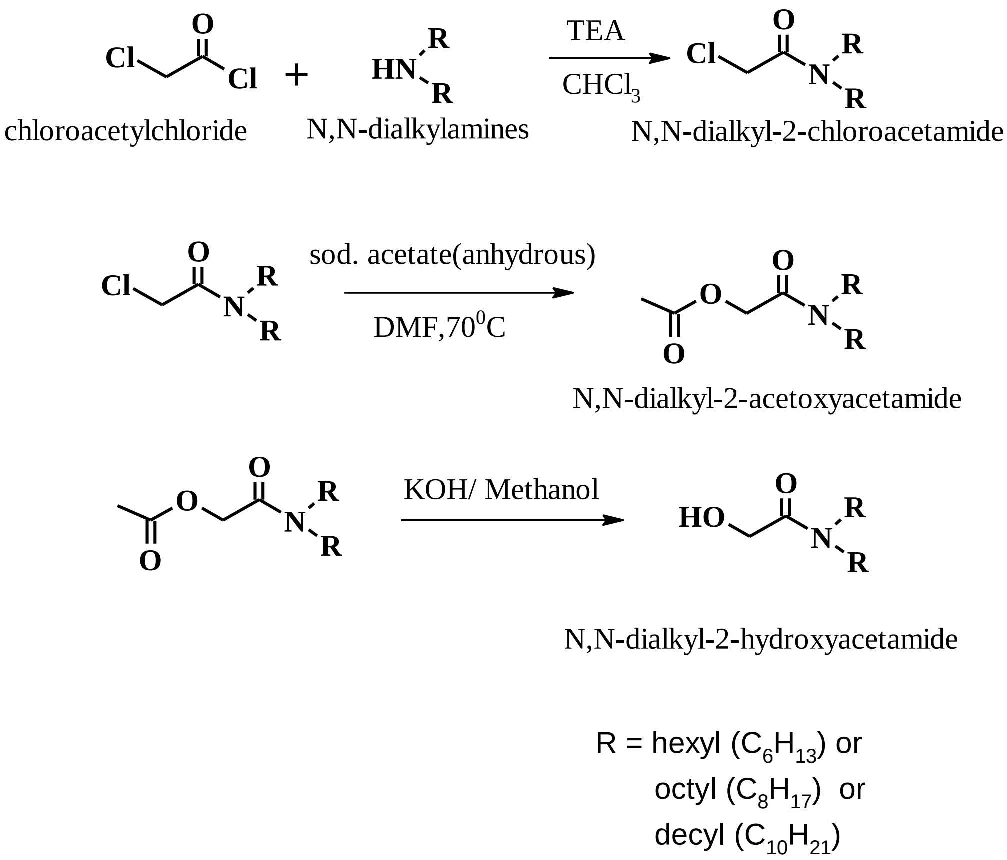

Figure 2.9 Synthesis of N,N-dialkyl-2-hydroxy acetamide (DAlkHyA) **[180]**

Characterization:

<u>DHHyA:</u> FTIR (ν/cm^{-1}): 3410 (broad, O-H stretch), 2926, 2858 (C-H stretch), 1646 (C=O stretch), 1462 (-CH_2-scissoring), 1402 (C-N stretch), 1278 (-CH_2-wagging), 1083 (C-O stretch of hydroxyl). **^{1}H NMR (500 MHz; $CDCl_3$; Me_4Si):** 4.142 (d, 2H), 3.727 (t, 1H), 3.365 (t, 2H), 3.055 (t, 2H), 1.542 (m,4H), 1.255 (m,12H), 0.892 (m, 6H). **^{13}C NMR (125 MHz; $CDCl_3$; Me_4Si)**: 170.98 (CO), 59.68 (HO-$\underline{C}H_2$-CO-), 46.07 (-N-$\underline{C}H_2$-), 45.79 (-N-$\underline{C}H_2$-), 31.58, 31.47, 28.52, 27.53, 26.65, 26.51, 22.58 (various $\underline{C}H_2$ groups),14.02 ($\underline{C}H_3$).

<u>DOHyA:</u> FTIR (ν/cm^{-1}): 3410 (broad, O-H stretch), 2926, 2858 (C-H stretch), 1646 (C=O stretch), 1462 (-CH_2-scissoring), 1402 (C-N stretch), 1278 (-CH_2-wagging), 1083 (strong, C-O stretch of hydroxyl). **^{1}H NMR (500 MHz; $CDCl_3$; Me_4Si):** 4.138 (d, 2H), 3.706 (t, 1H), 3.361 (t, 2H), 3.047 (t, 2H), 1.538 (m, 4H), 1.286 (m, 20H), 0.883 (m, 6H). **^{13}C NMR (125 MHz; CDCl$_3$; Me$_4$Si):** 171.01 (CO), 59.71 (HO-$\underline{C}$H$_2$-CO-), 46.11 (-N-$\underline{C}$H$_2$-), 45.82 (-N-$\underline{C}$H$_2$-), 31.77, 29.31, 29.22, 29.12, 28.52, 27.54, 26.96, 26.81, 22.60 (various CH$_2$ groups), 14.03 (CH$_3$).

DDHyA*:* FTIR (ν /cm^{-1}): 3410 (broad, O-H stretch), 2926, 2858 (C-H stretch), 1646 (C=O stretch), 1462 (-CH$_2$-scissoring), 1402 (C-N stretch), 1278 (-CH$_2$-wagging), 1083 (C-O stretch of hydroxyl). **^{1}H NMR (500 MHz; CDCl$_3$; Me$_4$Si):** 4.138(d, 2H), 3.716 (t, 1H), 3.359 (t, 2H), 3.046 (t, 2H,), 1.537 (m, 4H), 1.262 (m, 28H), 0.880 (m, 6H). **^{13}C NMR (125 MHz; CDCl$_3$; Me$_4$Si)** 171.0 (CO), 59.71 (HO-$\underline{C}$H$_2$-CO-), 46.11 (-N-$\underline{C}$H$_2$-), 45.83 (-N-$\underline{C}$H$_2$-), 31.86, 29.53, 29.46, 29.35, 29.26, 28.51, 27.54, 26.96, 26.81, 22.64 (various CH$_2$ groups), 14.06 (CH$_3$).

2.9.9. *Tetraalkyldiglycolamide*

Synthesis of tetraalkyldiglycolamide was carried out as per the procedure described in litearture [181] and synthetic procedure is shown in figure 2.10.

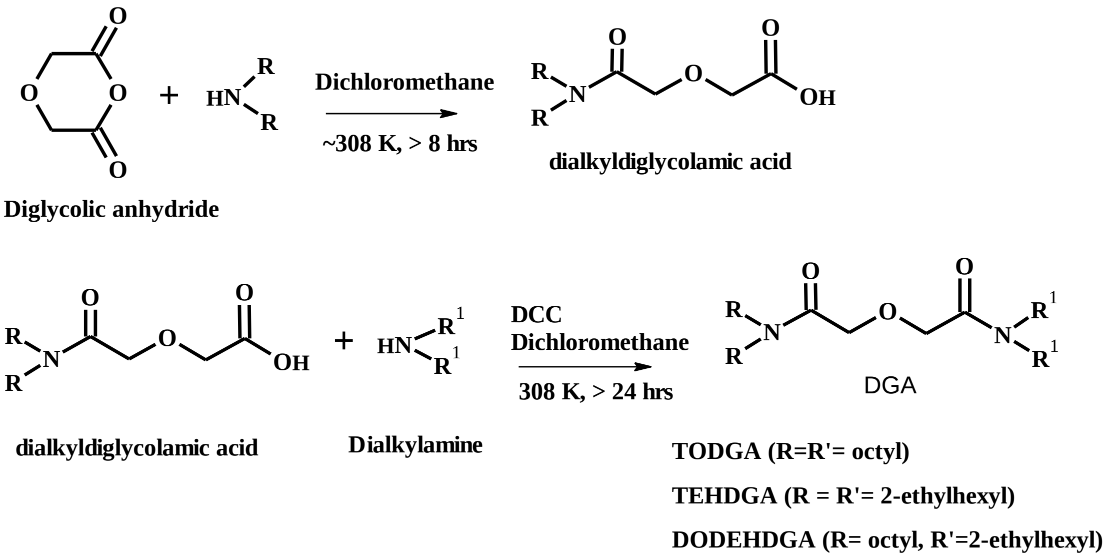

Figure 2.10. Synthesis of tetraalkyldiglycolamide [181]

Characterization:

TODGA: ^{1}H NMR (500 MHz; $CDCl_3$; Me_4Si): 4.307 (s, 4H), 3.291 (t, 4H), 3.177 (t, 4H), 1.519 (m, 8H), 1.272 (m, 40H), 0.885 (t, 6H), 0.876(t, 6H). **^{13}C NMR (125 MHz; $CDCl_3$; Me_4Si):** 168.32 ($\underline{C}O$), 68.97($\underline{C}H_2$-O), 46.92($\underline{C}H_2$-N), 45.68 ($\underline{C}H_2$-N), 31.80, 29.38, 29.29, 29.20, 28.89, 27.56, 27.02, 26.87, 22.64, 22.63 (various CH_2 groups), 13.93($\underline{C}H_3$).

TEHDGA: **^{1}H NMR (500 MHz; $CDCl_3$; Me_4Si)**: 4.3 (s, 4 H); 3.37 (m, 4 H); 3.04 (d, 4 H), 1.66 (m, 3 H); 1.56 (m, 3 H); 1.25 (m, 30 H); 0.88 (m, 24 H). **^{13}C NMR (125 MHz; $CDCl_3$; Me_4Si**: 169.52 ($\underline{C}O$), 68.72 ($\underline{C}H_2$-O), 49.94($\underline{C}H_2$-N), 47.89($\underline{C}H_2$-N), 37.91, 36.63, 30.52, 28.81, 28.79, 23.81, 23.06, 14.07, 14.03, 10.90, 10.61.

DEHDODGA: **^{1}H NMR (500 MHz; $CDCl_3$; Me_4Si):** 4.30 (S, 2H), 4.27 (S, 2H), 3.32-3.20 (m, 4H), 3.17- 3.14 (m, 2H), 3.06 (d, 2H), 1.77-1.65 (m, 2H), 1.50-1.49(m, 6H), 1.25 (m, 34H), 0.86-0.85 (m, 18H). **^{13}C NMR (125 MHz; $CDCl_3$; Me_4Si):** 169.53($\underline{C}O$), 168.49($\underline{C}O$), 69.15($\underline{C}H_2$-O), 69.07($\underline{C}H_2$-O), 50.06, 47.98, 47.96, 46.94, 45.78, 37.95, 36.69, 31.78, 31.72, 30.56, 30.49, 29.34, 29.29, 29.20, 29.17, 28.95, 28.81, 28.70, 28.69, 27.58, 27.01, 26.82, 23.80, 23.78, 23.05, 22.98, 22.59, 22.58, 14.02, 13.98, 10.91, 10.59, 10.58.

2.9.10. *Di-2-ethylhexyldiglycolamic acid (HDGA)*

Di-2-ethylhexyldiglycolamic acid (HDGA) was synthesized by the reaction of diglycolic anhydride with di-(2-ethyl)hexylamine in dichloromethane as described elsewhere [120].

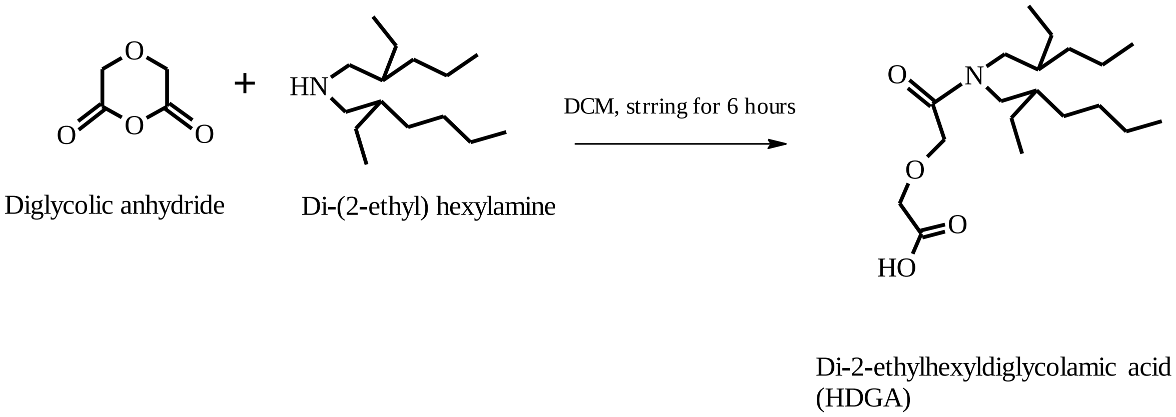

Figure 2.11. Synthesis of di-2-ethylhexyldiglycolamic acid (HDGA)[120]

Characterization:

<u>HDGA</u>: FTIR(ν/cm^{-1}): 3454 (COOH), 1739 (-CO in COOH), 1622(-CO in –CON), 1226**.** **^{1}H NMR (500 MHz; $CDCl_3$; Me_4Si):** 10.67 (s, 1H), 4.32 (s, 2H), 4.11 (s, 2H), 3.17-3.31 (m, 4H), 2.96-2.98 (m, 2H), 1.15-1.24 (m, 16H), 0.77-0.84 (m, 12H). **^{13}C NMR (125 MHz; $CDCl_3$; Me_4Si):** 172.22 ($\underline{C}O$), 172.14 ($\underline{C}O$), 77.21($-O\underline{C}H_2$), 71.1($-\underline{C}H_2O-$), 49.34 ($-\underline{C}H_2-N$), 37.16 ($\underline{C}H$), 30.35, 28.47, 23.58, 22.86, 13.9 (various $\underline{C}H_2$ groups), 10.47 ($\underline{C}H_3$). MS (EI+, m/z): 356.5.

2.10 Some typical spectra of synthesized ionic liquids and extractants

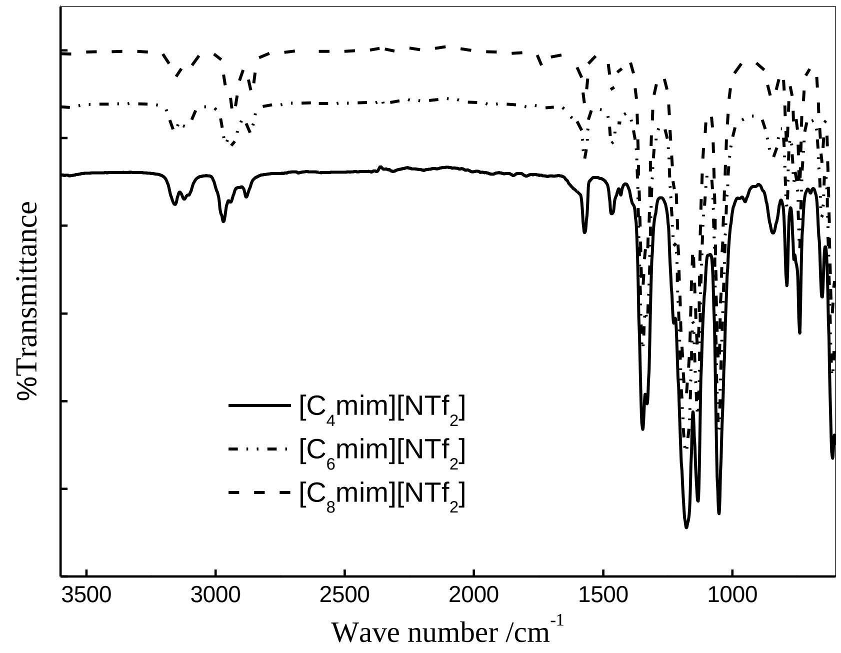

Figure 2.12 FTIR spectra of [$C_n$mim][NTf_2] (n= 4,6,8)

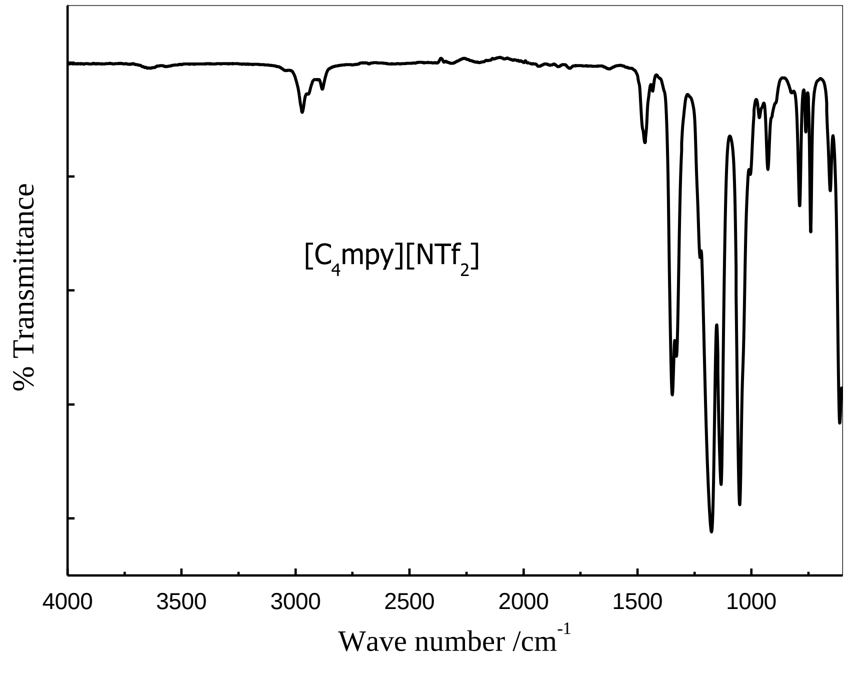

Figure 2.13 FTIR spectra of [C_4mpy][NTf_2]

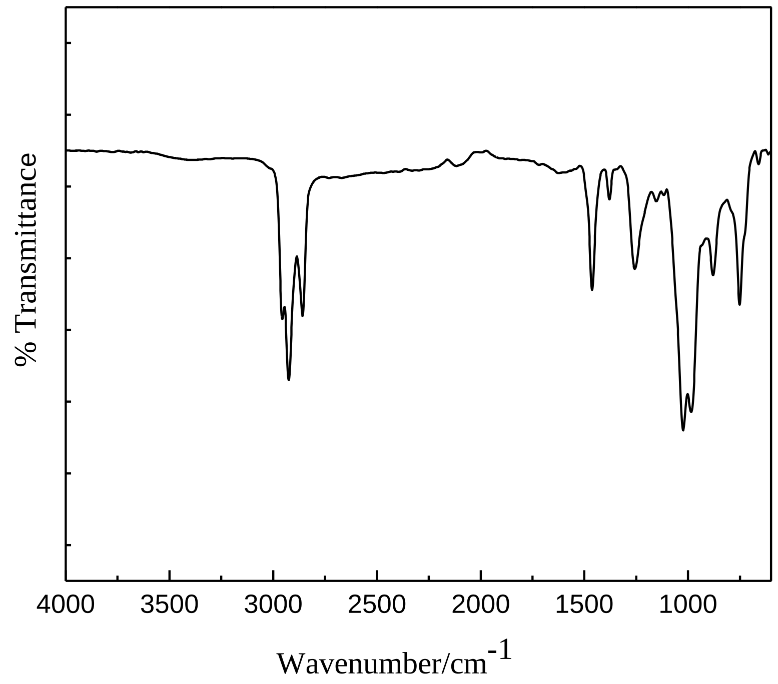

Figure 2.14 FTIR spectrum of [A336]$^{+}$DEHP]$^{-}$

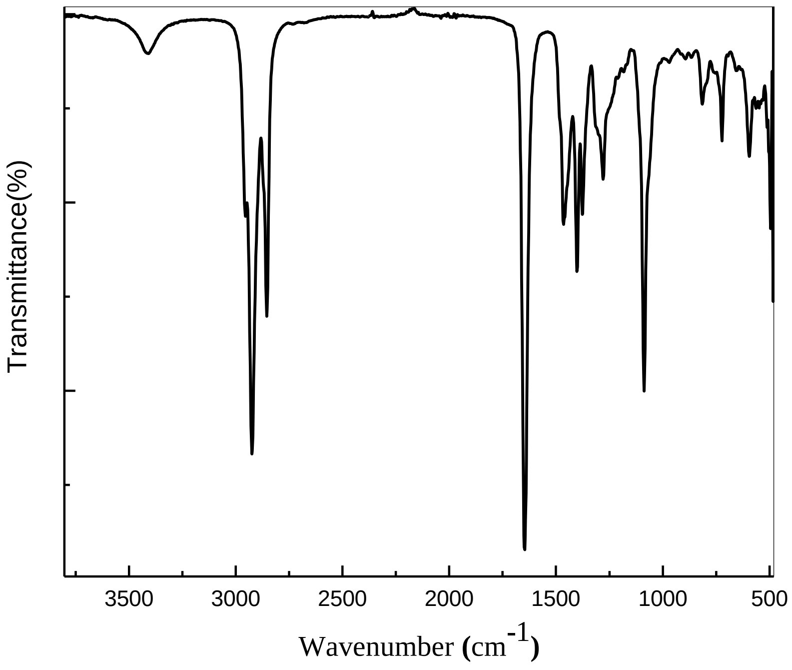

Figure 2.15 FTIR spectrum of DOHyA

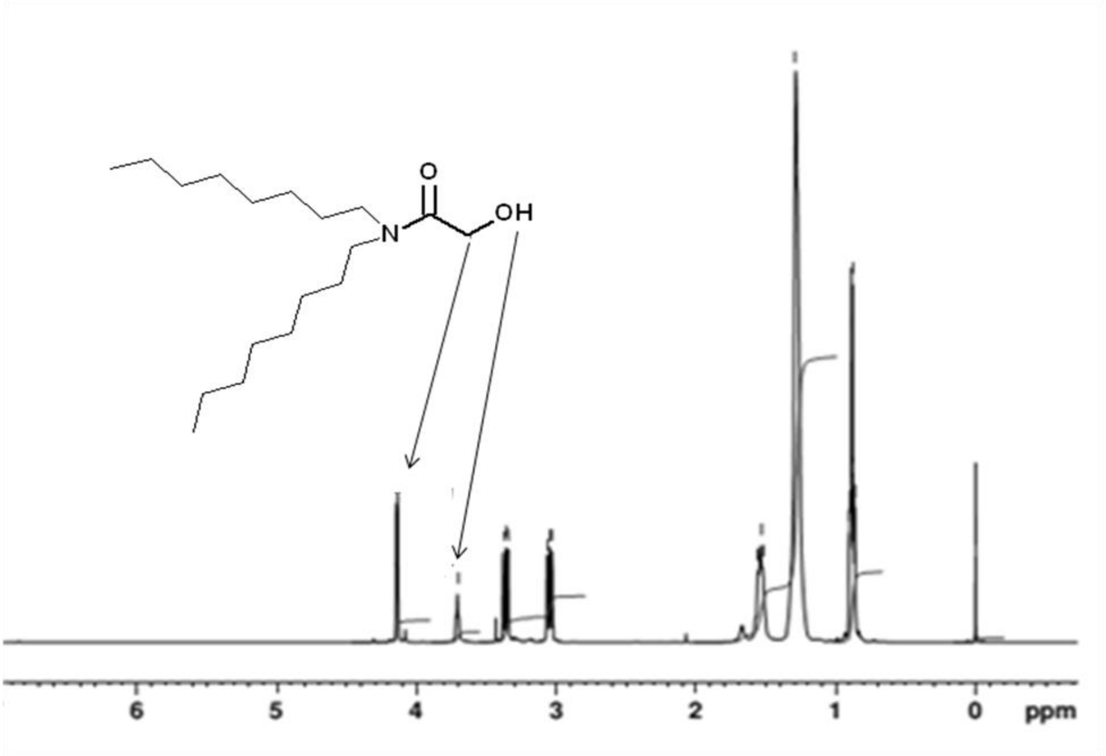

Figure 2.16 ^{1}H NMR spectrum of DOHyA

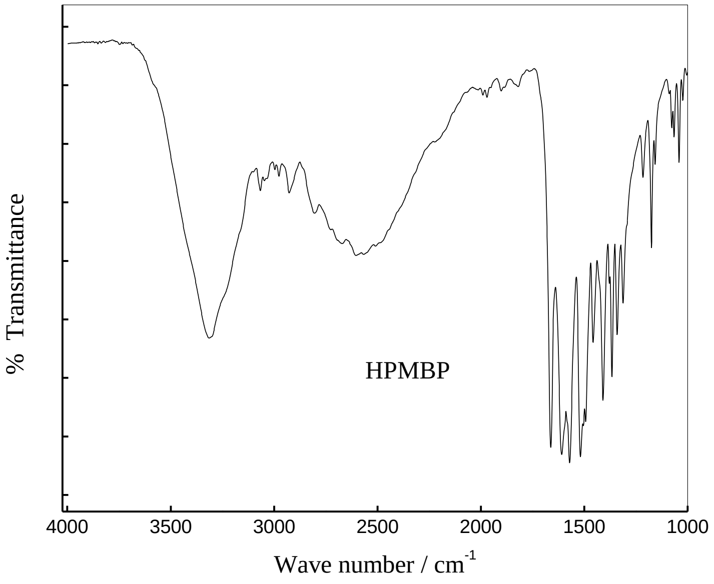

Figure 2.17 FTIR spectrum of HPMBP

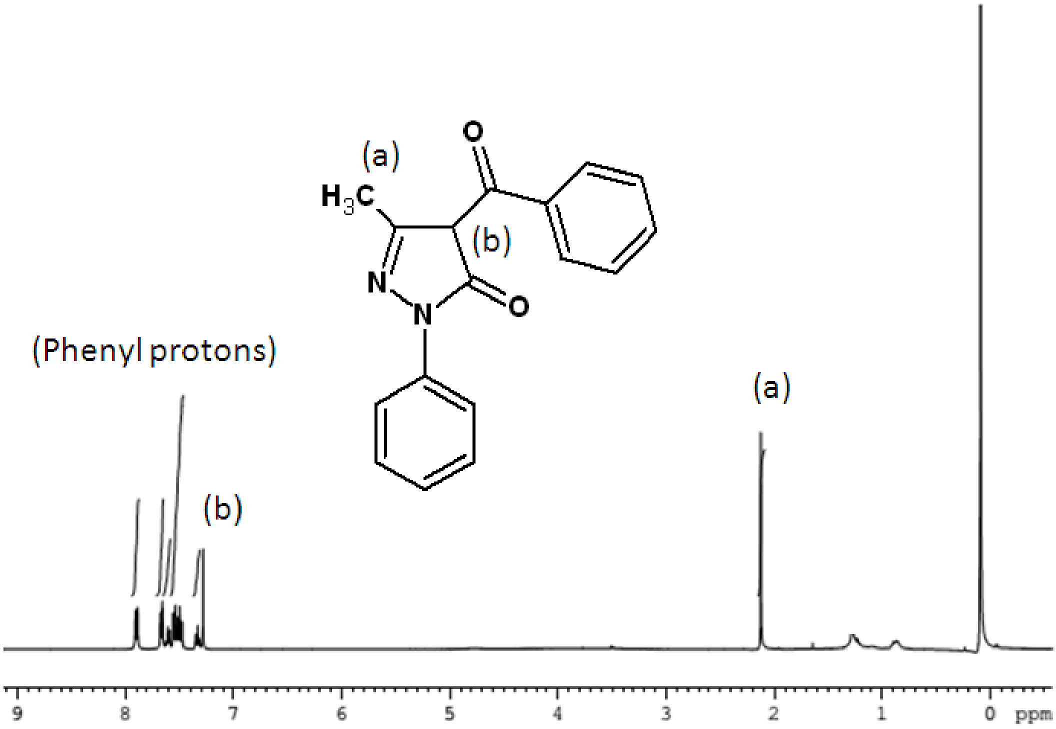

Figure 2.18 ^{1}H NMR spectrum of HPMBP

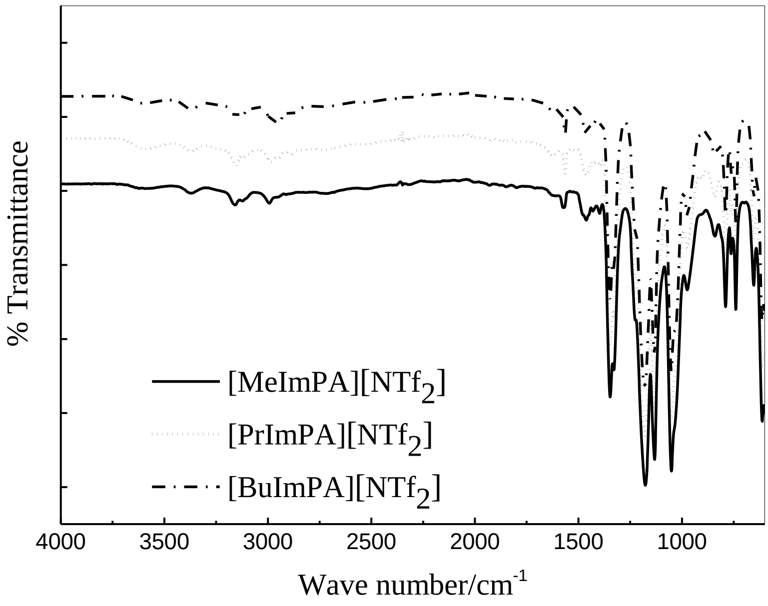

Figure 2.19. IR spectrum of TSILs -

[BuImPA][NTf$_2$],[PrImPA][NTf$_2$]&[MeImPA][NTf$_2$]

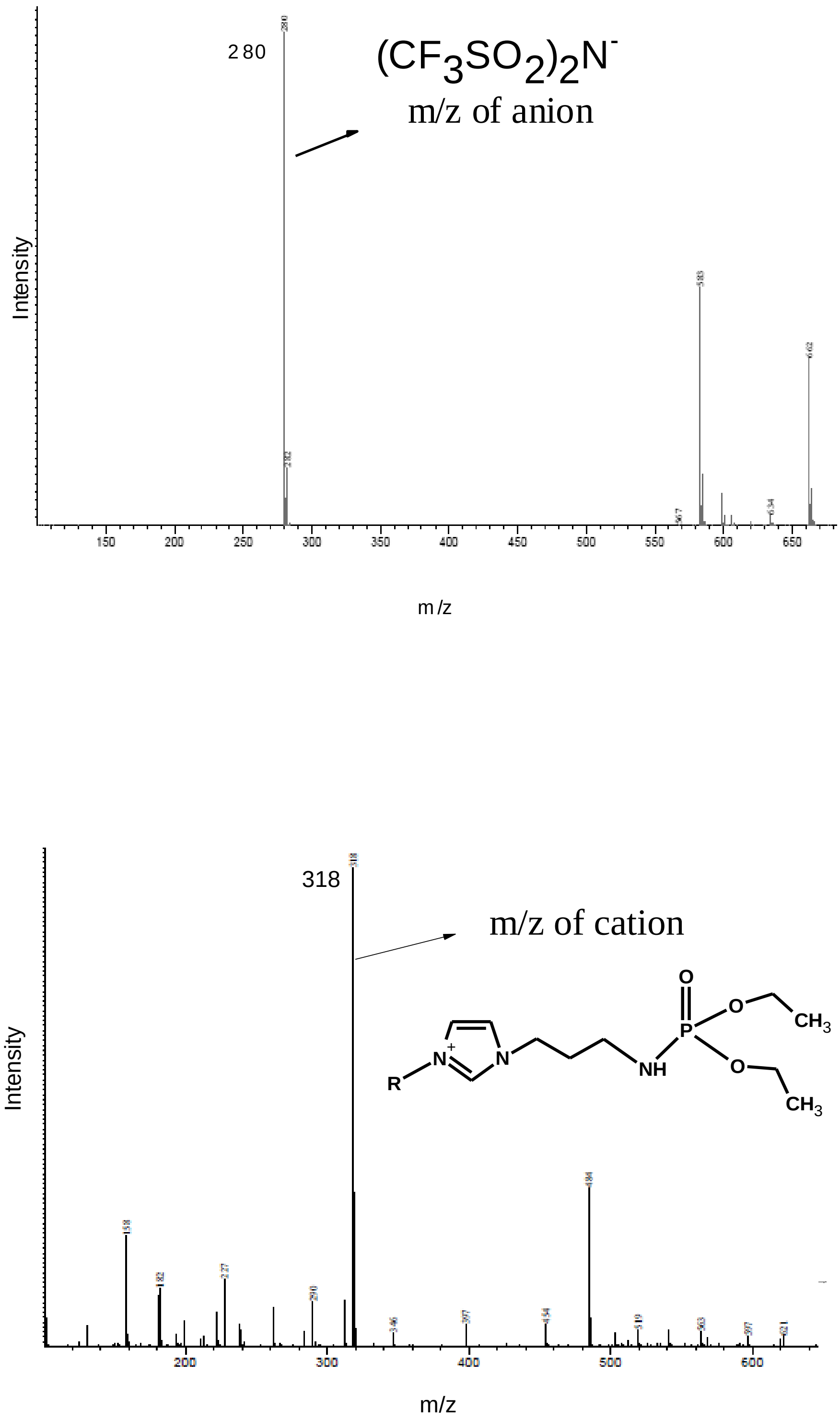

Figure 2.20 ESI-Mass spectrum of TSIL - [BuImPA][NTf$_2$]

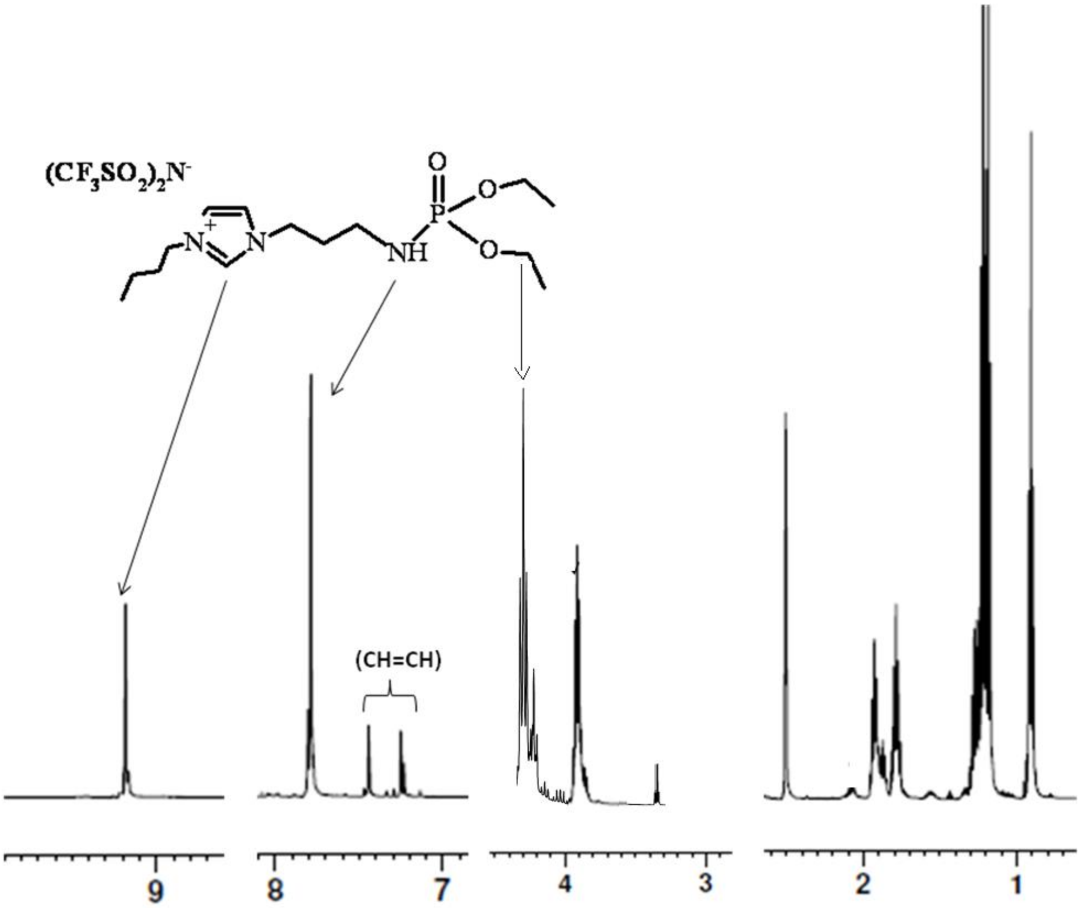

Figure 2.21 ^{1}*H NMR spectrum of TSIL - [BuImPA][NTf*$_2$*]*

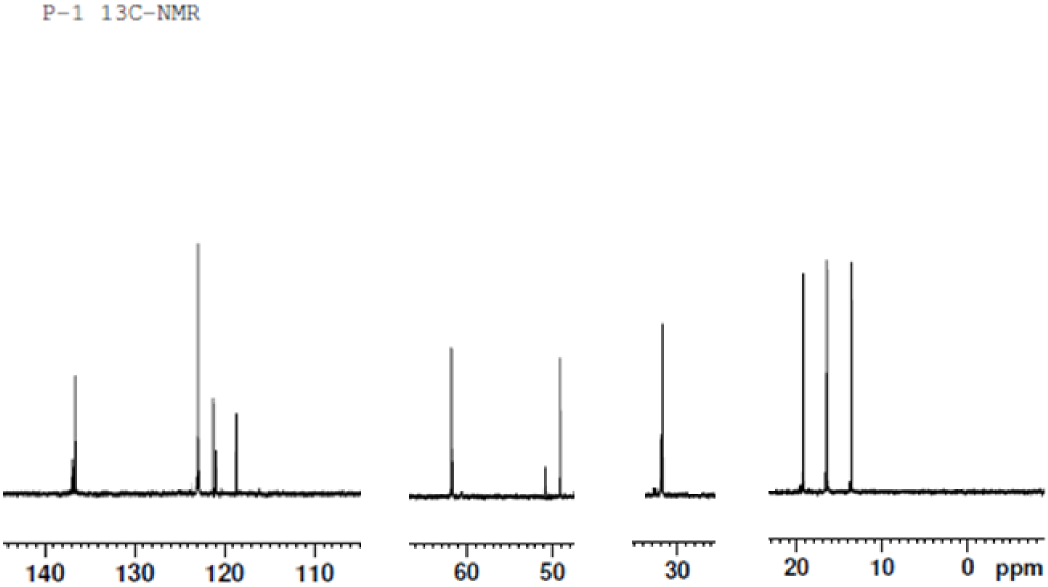

Figure 2.22 ^{13}*C NMR spectrum of TSIL - [BuImPA][NTf*$_2$*]*

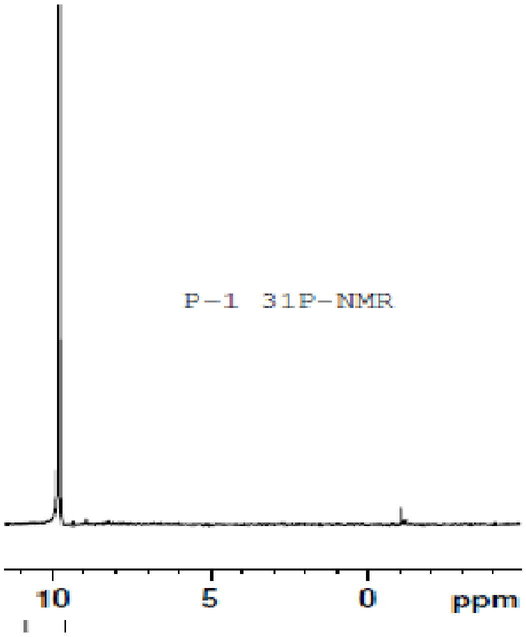

Figure 2.23 ^{31}P NMR spectrum of TSIL - [BuImPA][NTf$_2$]

CHAPTER 3

ROOM TEMPERATURE IONIC LIQUID AS A DILUENT FOR SOLVENT EXTRACTION OF ACTINIDES

3.1 Introduction

Over the past few decades, RTILs have been receiving increased attention for possible applications in the area of nuclear fuel reprocessing and waste management [111-115]. Essentially, they are being explored as possible substitute to molecular diluent (*n*-dodecane) in solvent extraction procedures due to the distinctive features of ionic liquids such as negligible vapour pressure, wide liquid range, and high solubility for organic species. Initially, Dai *et al*. [121] and Visser *et al*. [117] studied the extraction of group I and II metal ions by crown ethers present in ionic liquid. Those investigations revealed that ionic liquid diluents provide superior extraction of target metal ion than the conventional molecular diluents. The main reasons for high distribution ratio obtained in the RTIL system could be the ionic nature and solvating capability of the ionic liquid by virtue of which the metal-solvate species gets stabilized in the extracted phase. There has been growing interest to study the solvent extraction behaviour of several metal ions of nuclear interest in RTIL diluents.

In the present chapter, RTIL was explored as diluent and results on solvent extraction of actinides namely, U(VI), Am(III) and Pu(IV) using molecular extractants present in RTIL diluents have been reported. This chapter has three parts (Part A, B &C). Part A discusses the solvent extraction behaviour of U(VI) in some tri-*n*-alkylphosphates (TAlPs) dissolved in imidazolium bis(trifluoromethanesulfonyl)imide. In part II, the studies on solvent extraction of U(VI), Am(III) and Pu(IV) using hydroxy acetamide

(DOHyA) dissolved in imidazolium bis(trifluoromethanesulfonyl)imide ionic liquid have been reported. Part III describes the solvent extraction behaviour of Am(III) in benzoylpyrazolone (HPMBP) dissolved in pyrrolidinium bis(trifluoromethanesulfonyl)imide ionic liquid.

Experimental parts of the present chapter have been discussed in the section 2.5, 2.8.1, 2.8.2 and 2.8.3 of the chapter 2.

PART A

Extraction behavior of U(VI) in some tri *n*-alkyl phosphates (TAlPs) present in imidazolium based room temperature ionic liquid

PUREX process has been in vogue, worldwide, for the recovery of uranium and plutonium from the spent nuclear fuel [11,12]. This process uses a solution of 1.1 M tri-*n*-butylphosphate (TBP) in *n*-dodecane (*n*-DD) for the separation of U(VI) and Pu(IV) from the spent nuclear fuel dissolver solution (3–4 M nitric acid). Since TBP exhibited excellent selectivity for U(VI) and Pu(IV), high loading capacity and excellent stripping behavior, it is indispensable since its introduction for reprocessing of spent nuclear fuels from thermal reactors. The dissolver solution of thermal reactor fuel is essentially composed of U(VI) in nitric acid medium, as the fuel for thermal reactor is uranium oxide. It also contains small amounts of transuranium elements, fission products and corrosion products [182]. However, the situation is quite different when dealing with fast reactor dissolver solution. In this case, plutonium is the major constituent of dissolver solution as the fuel for fast reactor is $Pu_xU_{1-x}C$ or $Pu_xU_{1-x}O_2$ (x= 55 or 70). Since the burn-ups achieved in fast reactors are significantly high [183,184], the fission products content in the dissolver solution is also quite significant.

Plutonium in the dissolver solution exists in tetravalent oxidation state. The third phase formation tendency of Pu(IV) and Zr(IV) (fission product) in TBP/*n*-DD, hydrolytic and radiolytic degradation of solvent pose interesting challenges to separations [185]. One option to resolve the issue of third phase formation is to develop alternate extractants exhibiting lesser tendency for third phase formation, at the same time exhibiting the same extraction and stripping behavior as that of TBP. In this context, several trialkyl phosphates (TAlPs) such as tri-*n*-propyl phosphate (TPP), tri-*n*-amyl phosphate (TAP), tri-*n*-octyl phosphate (TOP), tri-*n*-iso-amyl phosphate (TiAP), tri-2-

methyl butyl phosphate (T2MBP) etc. have been synthesized and studied in molecular diluent for fast reactor fuel reprocessing applications [178,186,187]. The physicochemical properties, batch extraction and third phase formation behavior of these phosphates have been evaluated and compared with TBP in a comprehensive manner. The results revealed that the higher homologs of TAlP exhibited high capacity to load Pu(IV) and Th(IV) without any third phase formation. In addition their extraction behavior was comparable to that of TBP [178,187]. When trialkyl phosphates are proposed for fast reactor fuel reprocessing, it is necessary to study the extraction behavior of these trialkyl phosphates in ionic liquids also.

The literature studies showed that a large number of studies have been carried out on the extraction of U(VI) using TBP in ionic liquid [122,123,129,129]. For example, a systematic study on the extraction of U(VI) from nitric acid medium by a solution of TBP in [C_4mim][PF_6] or [C_4mim][NTf_2] was reported by Giridhar *et al*. [128,129]. The mechanism of U(VI) extraction in TBP dissolved in ionic liquid was investigated in detail by Dietz *et al*. and Billard *et al*. [122-124]. However, no studies have been reported so far on the extraction of U(VI) in homologs of trialkyl phosphate dissolved in ionic liquid diluent.

Therefore, the objective of the part A in chapter 3 is to report the results on the extraction and stripping behavior of U(VI) in some trialkyl phosphates (TAlP) present in 1-octyl-3-methylimidazolium bis(trifluoromethanesulfonyl)imide ([C_8mim][NTf_2]). The extraction of U(VI) was studied as a function of various parameters such as nitric acid concentration, temperature, extractant concentration and equilibration time etc.

Table 3.1. Structures of molecular extractants and RTILs used in part A of chapter 3

Name	Structure
Extractant	
Tri-*n*-alkyl phosphates 1.Tri-*n*-propyl phosphate (TPP) (R: C_3H_7) 2.Tri-*n*-butyl phosphate (TBP) (R: C_4H_9) 3.Tri-*n*-amyl phosphate (TAP) (R: C_5H_{11}) 4.Tri-*n*-octyl phosphate (TOP) (R: C_8H_{17})	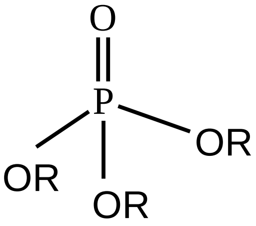
Tri-*n*-isobutyl phosphate (TiBP)	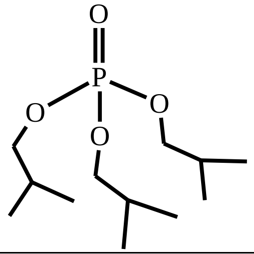
Tri-*n*-isoamyl phosphate (TiAP)	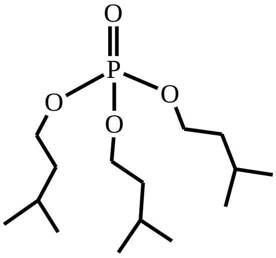
Ionic liquid	
1-Alkyl-3-methylimidazolium bis(trifluoromethanesulfonyl)imide ([$C_n$mim][NTf_2] Butyl derivative: [C_4mim][NTf_2] (R: C_4H_9) Hexyl derivative: [C_6mim][NTf_2] (R: C_6H_{13}) Octyl derivative: [C_8mim][NTf_2] (R: C_8H_{17})	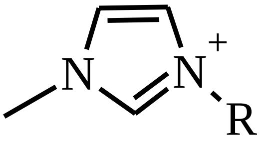 $(CF_3SO_2)_2N^-$

Synthesis of the ionic liquid and extractants used in part A have been discussed in section 2.9.1 & 2.9.6 of chapter 2 respectively.

3.2 Results and discussions

3.2.1 Effect of nitric acid concentration

The solvent extraction behavior of U(VI) in 1.1 M solution of various TAlPs present in [C_8mim][NTf_2] is shown in Figure 3.1 and it shows the extraction of U(VI) in 1.1 M TBP/*n*-DD for comparison [187]. The alkyl group present in the tri-*n*-alkyl phosphates was varied from *n*-propyl to *n*-octyl group. It can be seen that the distribution ratio of U(VI) ($D_{U(VI)}$) increases gradually in all these TAlPs with increase in the concentration of nitric acid. Above 5 M nitric acid, the variation in the $D_{U(VI)}$ is insignificant. It is noted that using different tri-*n*-alkyl phosphates, the distribution ratio of U(VI) marginally increases in the order of TPP < TBP < TAP < TOP, which is the increasing order of chain length of alkyl group attached to the phosphoryl moiety of tri-*n*-alkyl phosphates. As the phosphoryl moiety of tri-*n*-alkyl phosphates is involved in the coordination of uranium during extraction, the increase in the extraction trend observed in these tri-*n*-alkyl phosphates could be attributed to the increase in the basicity of phosphoryl moiety upon increasing in the chain length of alkyl group. In addition, it was reported that the solubility of the extracted uranium- TAlP complex in *n*-DD increases with increase in the chain length of alkyl group attached to phorphoryl moiety [187]. This leads to higher stability of the extracted complex and hence the distribution ratio increases with increase in the alkyl chain length of trialkyphosphate. The extraction trend and the magnitude of distribution ratios observed in the present study is quite comparable with the U(VI) extraction trend reported in these tri-*n*-alkyl phosphates present in *n*-dodecane diluent, perhaps, this similarity could be due to the employment of octyl-derivative of the imidazolium ionic liquid, [C_8mim][NTf_2]. [122].

It was reported by Dietz and Stepinski [122] that the octyl and decyl derivatives of imidazolium ionic liquid behave similar to *n*-dodecane during the extraction of U(VI) from nitric acid medium, unlike hexyl and butyl derivatives of imidazolium ionic liquids. It should be noted that the concentration of nitric acid in the present study was varied from 1 M to 8 M which is in contrast to the Dietz *et al.* work, wherein the concentration of nitric acid was varied from 0.1 M to 8 M [122]. At low nitric acid concentration (< 0.5 M), the authors reported the possibility of cation exchange mechanism for U(VI) extraction. However, at higher nitric acid concentrations, Dietz *et al.* reported solvation type mechanism. The similarity in the U(VI) extraction trend observed in the present study with those obtained by Dietz *et al.* at higher nitric acid concentration (1 M–8 M) indicates the possibility of solvation type mechanism operating for U(VI) extraction in the present case also.

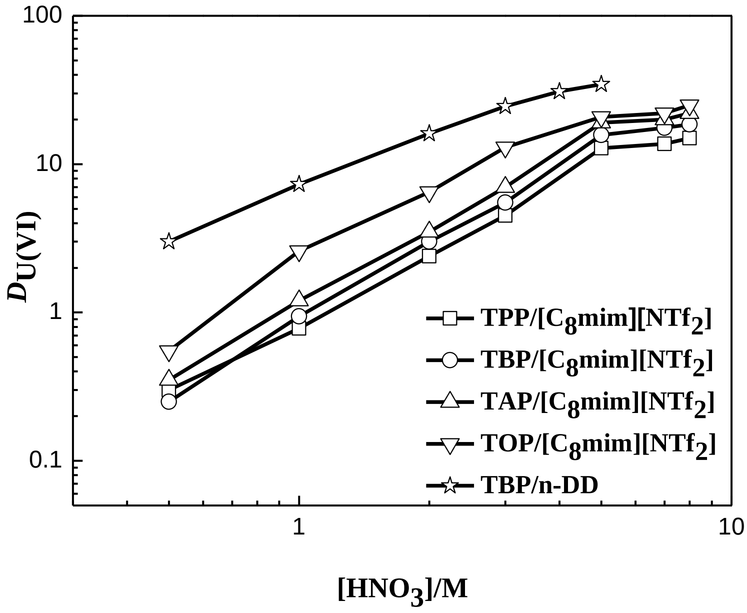

Figure 3.1 Variation in the distribution ratio of U(VI) as a function of nitric acid concentration in aqueous phase. Ionic liquid phase: 1.1 M TAlP (TAlP = TPP, TBP, TAP, TOP)/ [C$_8$mim][NTf$_2$], Organic phase: 1.1 M TBP/ n-DD. Aqueous phase: 0.5 M – 8 M HNO$_3$ spiked with ^{233}U(VI) tracer.

Fgure 3.2 compares the distribution ratio of U(VI) ion in isomeric TAlPs dissolved in ionic liquid medium. The *n*-alkyl group in tri-*n*-alkyl phosphates was compared with its iso-alkyl phosphate. It can be seen that the distribution ratio of U(VI) increases with increase in the concentration of nitric acid in all these tri-*n*-alkyl phosphates as expected. It is also noted that the $D_{U(VI)}$ achieved in the isomeric TAlPs are comparable. A similar behavior was also reported for the extraction of U(VI) in *n*-DD medium for these isomeric TAlPs [187].

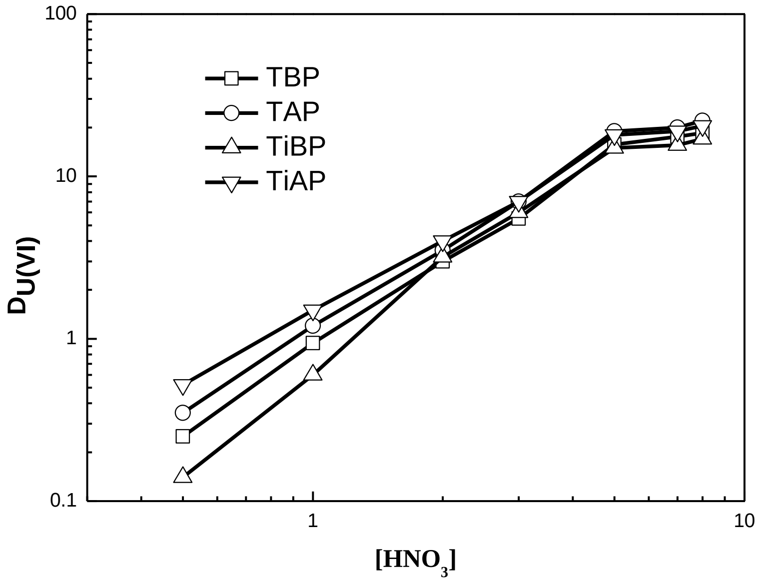

Figure 3.2. Variation in the distribution ratio of U(VI) as a function of nitric acid concentration in aqueous phase. Ionic liquid phase: 1.1 M TAlP (TAlP = TBP, TiBP, TAP, TiAP/ [C_8mim] [NTf_2], Aqueous phase: 0.5 M – 8 M HNO_3 spiked with ^{233}U(VI) tracer.

3.2.2 Extraction kinetics

The variation in the distribution ratio of U(VI) as a function of equilibration time is shown in Figure 3.3. It can be seen that the distribution ratio of U(VI) increases with increase in the duration of equilibration. The variation in the distribution ratio was insignificant after 20 min of equilibration. Therefore, for all extraction studies, the equilibration was carried out for 1 h to ensure the equilibrium was established.

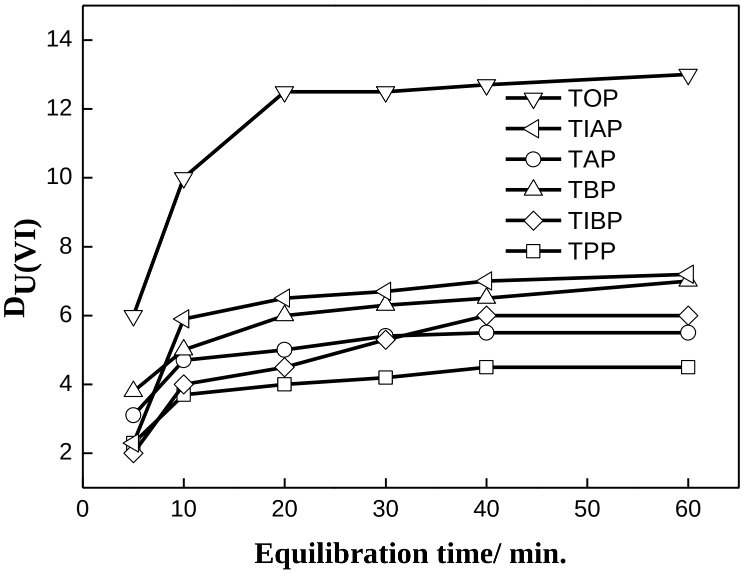

Figure 3.3. Variation in the distribution ratio of U(VI) as a function of equilibration time. Ionic liquid phase: 1.1M TAlP (TAlP = TPP, TBP, TAP, TOP,TiBP, TiAP)/[C$_8$mim][NTf$_2$]. Aqueous phase: 3 M HNO$_3$ spiked with ^{233}U(VI) tracer. Equilibration time = 5 min – 60 min.

3.2.3 Extraction stoichiometry

As the extraction trend of U(VI) observed in ionic liquid (Figures 3.1 and 3.2) was similar to that observed in *n*-DD [122], the mechanism of U(VI) extraction in these TAlP could be similar to those observed in *n*-DD. Therefore, the extraction of uranium in TAlP can be represented by equation 3.1.

$$UO_2^{2+}{}_{aq} + 2NO_3^-{}_{aq} + xTAlP_{IL} \Leftrightarrow UO_2(NO_3)_2\,(TAlP)_{x\ IL} \qquad (3.1)$$

The subscripts “aq” and “IL” denote the aqueous and ionic liquid phases, respectively, and “x” is the number of TAlP molecules involved in the extraction of uranium. The equilibrium constant for the above reaction can be represented by equation 3.2.

$$K_{ex} = \frac{[UO_2(NO_3)_2(TAlP)x]_{IL}}{[UO_2^{2+}]_{aq}[NO_3]_{aq}^2[TAlP]_{IL}^x} \quad (3.2)$$

Upon rearranging equation 3.2 results in equation 3.3

$$\log D_{U(VI)} = \log K_{ex} + 2\log[NO_3]_{aq} + x\ \log[TAlP]_{IL} \quad (3.3)$$

To determine the number of molecules of TAlP coordinated to U(VI) in the ionic liquid phase, the effect of TAlP concentration on the extraction of uranium (VI) in the ionic liquid phase was studied. The slope obtained from the plot of log $D_{U(VI)}$ against log [TAlP] gives the number of molecules of TAlP coordinated to uranium in the ionic liquid phase. The plot of Figure 3.4 displays the variation in the distribution ratio of U(VI) as a function of TAlP concentration in the ionic liquid phase at constant nitrate ion concentration (3 M HNO_3) in the aqueous phase.

It can be seen that the distribution ratio of U(VI) increases with increase in the concentration of TAlP in the ionic liquid phase. Linear regression analysis of the extraction data results in a slope value ranging from 1.8 to 2.1 in all TAlPs. This shows that about two molecules of TAlP are involved in the extraction of U(VI) in the ionic liquid phase. The U(VI) – $(TAlP)_2$ stoichiometry obtained in the present study is in good agreement with the stoichiometry reported for these trialkylphosphates in *n*-DD medium [122,129].

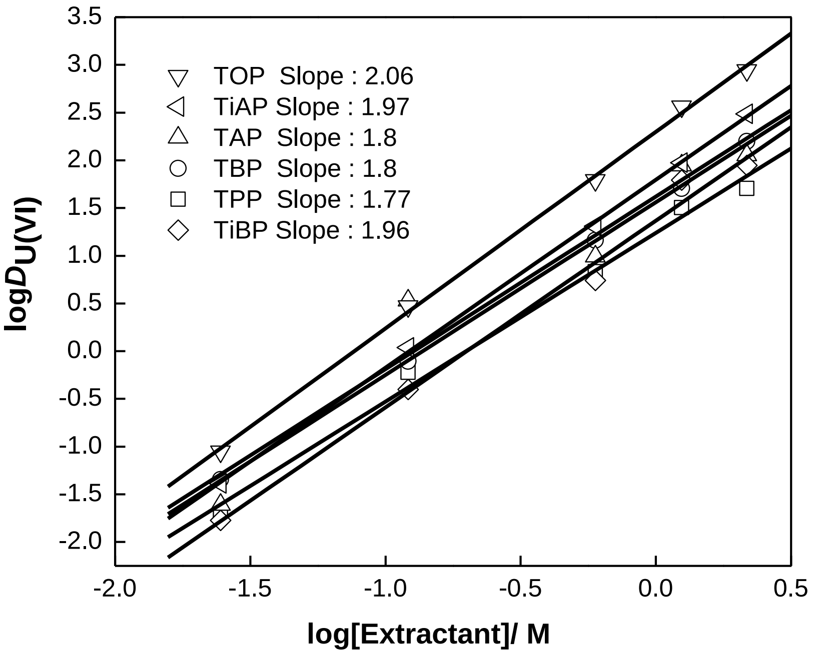

Figure 3.4. Variation in the distribution ratio of U(VI) as a function of concentration of TAlP. Ionic liquid phase: 0.2 M – 1.2 M TAlP (TAlP = TPP, TBP, TAP, TOP, TiBP, TiAP) in [C_8mim][NTf_2]. Aqueous phase: 3 M HNO_3 spiked with ^{233}U(VI) tracer.

3.2.4 Thermodynamic parameters

The extraction of U(VI) from 3 M nitric acid medium was carried out in a solution of 1.1 M TAlP in [C_8mim][NTf_2] at various temperatures ranging from 298 K to 333 K, to understand the influence of the temperature on extraction of uranium in the ionic liquid phase. The variation of log $D_{U(VI)}$ as a function of reciprocal temperature is shown in Figure 3.5.

It can be seen that the distribution ratio of U(VI) decreases with increase of temperature. This indicates that the extraction of U(VI) in TAlP/ionic liquid is exothermic. The total enthalpy change (ΔH_{tot}) involved in the extraction of U(VI) in trialkylphosphate – ionic liquid medium can be calculated from the slope of the plot shown in Figure 3.5 and using Van't Hoff relation of the form shown in equation 3.4. The ΔH_{tot} values obtained are shown in Table 3.2

$$\frac{\partial \log D}{\partial (1/T)} = \frac{-\Delta H_{tot}}{2.303\ R} \tag{3.4}$$

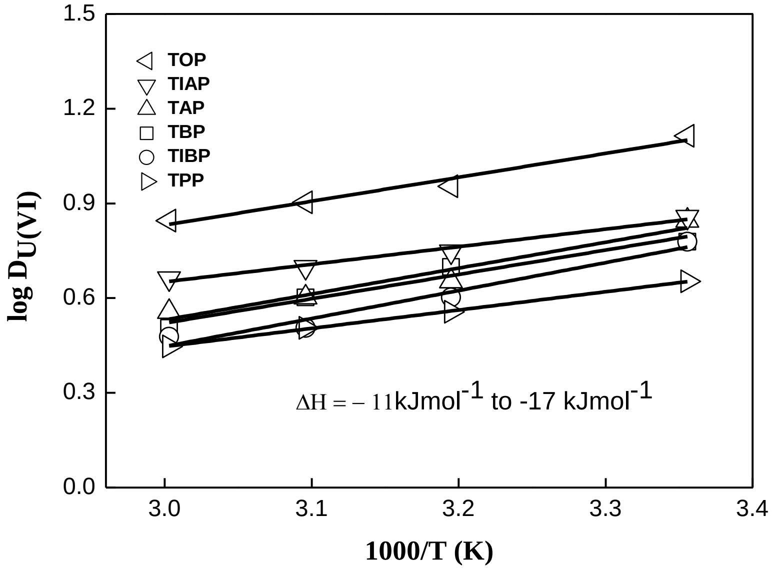

Figure 3.5. Variation in the distribution ratio of U(VI) as a function of temperature. Ionic liquid phase: 1.1M TAlP (TAlP = TPP, TBP, TAP, TOP, TiBP, TiAP)/[C_8mim][NTf_2]. Aqueous phase: 3 M HNO_3 spiked with ^{233}U(VI) tracer.

It is noted that there is no trend in the ΔH_{tot} values obtained for various TAlP and it varies marginally from –11 kJmol^{-1} to –17 kJmol^{-1} depending upon the nature of TAlP. The correct reason for the similarity in the ΔH_{tot} values is not clear at present, however, this could be attributed to the marginal difference in the complexing abilities of these TAlP towards U(VI) as shown in Figures 3.1 and 3.2.

Table 3.2 ΔH for extraction of U(VI) using 1.1 M TAlP/[C_8mim][NTf_2]. Aqueous phase: 3 M HNO_3 spiked with ^{233}U(VI) tracer. Organic phase: 1.1M TAlP/[C_8mim][NTf_2].

1.1M TAlP/ [C_8mim][NTf_2]	**ΔH (kJmol^{-1})**
TPP	**-11**
TBP*	**-15**
TAP	**-16**
TOP	**-15**
TiBP	**-17**
TiAP	**-11**

∗ ΔH in 1.1MTBP/C_8mim][PF_6] is -22 kJ.mol and 1.1M TBP/*n*-DD is -13 kJ/mol [128, 129]

3.2.5 Effect of ionic liquid cation

Figure 3.6 presents the distribution ratio of U(VI) in TAlP/ ionic liquid at 3 M nitric acid. The alkyl substituent in the ionic liquid [$C_n$mim][NTf_2] (n = 4 to 8) was varied from butyl to octyl moiety. It can be seen that the $D_{U(VI)}$ values are almost constant irrespective of the nature of the ionic liquid and the distribution ratio of U(VI) increases with increase in the chain length of alkyl group in TAlP, as expected. The constancy in the distribution ratios of U(VI) in three different ionic liquid indicates that U(VI)–TAlP complex seems to be stabilized in the ionic liquid phase to equal extent. However, it should be noted that this is applicable only at 3 M nitric acid.

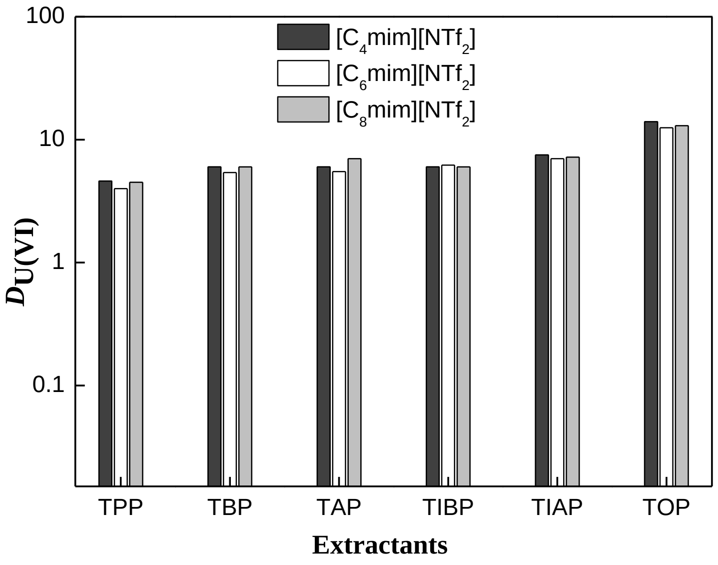

Figure 3.6. Variation in the distribution ratio of U(VI) in TAlP as a function of alkyl chain length of the ionic liquid. Aqueous phase: 3M HNO_3 spiked with ^{233}U(VI) tracer. Ionic liquid phase: 1.1M TAlP /[$C_n$mim][NTf_2] (n = 4, 6 and 8).

3.2.6 Stripping study

In conventional TAlP/*n*-dodecane systems, the back extraction of U(VI) from the extracted phase is usually carried out by contacting the loaded organic phase with dilute nitric acid (~0.01–0.1 M). The stripping behavior of U(VI) from the loaded ionic liquid phase in the present system is shown in Figure 3.7. Initially, U(VI) extraction using 1.1 M TAlP/[C_8mim][NTf_2] from 3 M HNO_3 was carried out. It can be seen that the recovery of U(VI) is ~60% in a single contact with 0.01 M nitric acid for all trialkylphosphates and the recovery of uranium (VI) is quantitative in three contacts. Therefore, the study shows that the loaded uranium can be quantitatively recovered with dilute nitric acid.

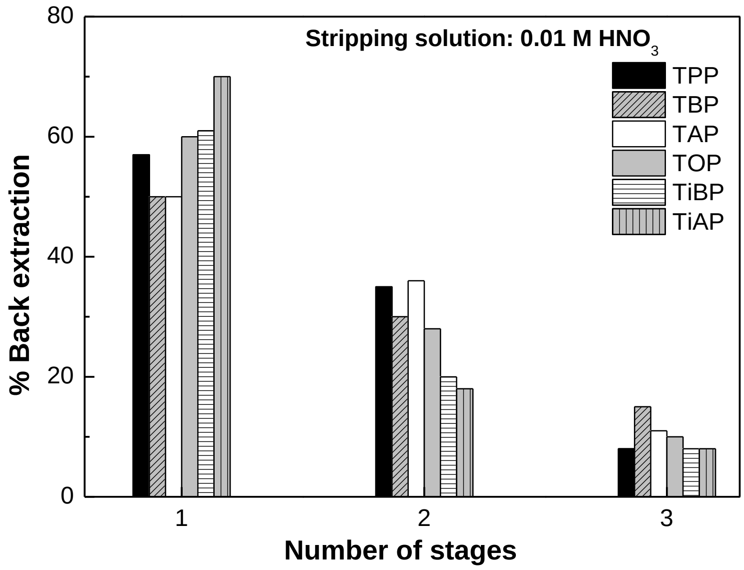

Figure 3.7. Stripping of U(VI) from ionic liquid phase as a function of number of stages. Ionic liquid phase: 1.1M TAlP (TAlP = TPP, TBP, TAP, TOP, TiBP, TiAP) /[C_8mim][NTf_2] containing U(VI) extracted from 3 M HNO_3. Aqueous phase: 0.01 M HNO_3.

3.3 Conclusion

Extraction of U(VI) from nitric acid medium was studied in different types of tri alkyl phosphates dissolved in 1-octyl-3-methylimidazolium bis(trifluoromethanesulfonyl)imide ([C_8mim][NTf_2]) ionic liquid. The distribution ratio of U(VI) increased with increase in the concentration of nitric acid, reaches maximum at 6 M nitric acid followed by a plateau with further increase in the nitric acid concentration. The extraction of U(VI) in TAlP present in [C_8mim][NTf_2] was very similar to those observed in a molecular diluent, *n*-dodecane. The distribution ratio of U(VI) increased in the order TPP < TBP < TAP < TOP, which was attributed to the increase in the basicity of TAlP upon increasing in the chain length of alkyl group attached to the phosphoryl moiety. Slope analysis of the extraction data indicated that two molecules of TAlP were coordinated to U(VI) in the ionic liquid phase. Change in the nature of ionic liquid hardly altered the distribution ratio of U(VI) at 3 M nitric acid. The extraction of U(VI) in all the extractants was found to be exothermic. Complete stripping of loaded U(VI) was achieved in 2–3 contacts with dilute nitric acid. The results indicate that TAlP present in ionic liquid medium is a promising candidate for fast reactor fuel reprocessing applications.

PART B

Mutual separation of Pu(IV) from other actinides using 2-hydroxy acetamide extractant in room temperature ionic liquid

In the recent past, CHNO based extractants are considered as promising candidates for the separation of trivalent acinides from HLLW due to their completely incinerable property [30,188]. DGA contains three oxygen donor atoms for complexation with the metal ions and hence it acts as tridentate ligand. Among the DGAs, *N,N,N′,N′*-tetraoctyldiglycolamide (TODGA) and *N,N,N′,N′*-tetra-2-ethylhexyldiglycolamide (TEHDGA) are studied extensively [32,189-192]. Recently, *N*,*N*-dialkyl-2-hydroxy acetamide, which is a radiation degradation product and synthetic precursor of DGA was identified for the extraction of actinides and lanthanides. Kannan *et al.* investigated the extraction behavior of lanthanides and actinides using *N*,*N*-dioctyl-2-hydroxyacetamide (DOHyA) in molecular diluent (*n*-dodecane) [193]. Prathibha *et al.* studied the modifier free separation of Am (III) using *N,N*-dialkyl-2-hydroxyacetamide in *n*-dodecane medium [180] and also reported [194] the radiolytic stability of various *N*,*N*-di-alkyl-2-hydroxyacetamides and observed that radiation stability was comparable with those for parent DGA molecules.However, no work has been reported for the extraction of actinides using *N,N*-dialkyl-2-hydroxyacetamide dissolved in ionic liquid diluent.

The aim of the part B in chapter 3 is to investigate the extraction and stripping behavior of Pu(IV) in a solution of *N*,*N*-dioctyl-2-hydroxyacetamide/1-butyl-3-methylimidazolium bis(trifluoromethanesulfonyl)imide ([C_4mim][NTf_2]). The extraction was studied as a function of various parameters such as nitric acid concentration, temperature, extractant concentration etc. Separation factor of Pu(IV) over U(VI) and Am(III) have been reported.

Table 3.3. Structures of molecular extractants and RTILs used in part B of chapter 3

Name	Structure
Extractants	
N, N'- Dialkyl 2-hydroxy acetamide (DAlkHyA) i. Hexyl derivative (DHHyA) (R: C_6H_{13}) ii. Octyl derivative (DOHyA) (R: C_8H_{17}) iii. Decyl derivative (DDHyA) (R: $C_{10}H_{21}$)	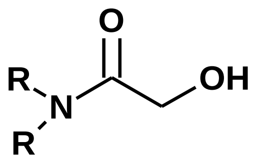
N,N-Dioctylmethoxyacetamide (DOMeOA)	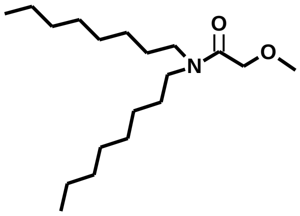
N,N-Dihexyloctanamide (DHOA)	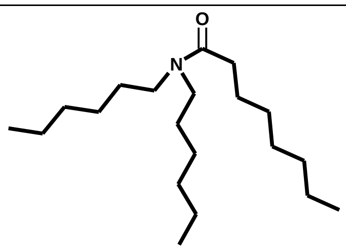
Ionic liquid	
1-Butyl-3-methylimidazolium bis(trifluoromethanesulfonyl)imide ($[C_4mim][NTf_2]$)	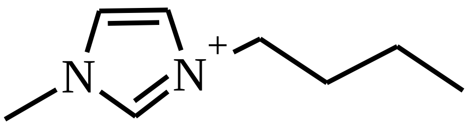 $(CF_3SO_2)_2N^-$

Synthesis of the ionic liquid and extractants used in part B have been discussed in section 2.9.1, 2.9.7 & 2.9.8 of chapter 2.

3.4 Results and Discussions

3.4.1 Effect of nitric acid concentration

The extraction of Pu(IV) was carried out in various solvent systems comprising of [C_4mim][NTf_2], 0.02 M DOHyA in [C_4mim][NTf_2] and 0.02 M DOHyA in *n*-DD. The extraction of Pu(IV) was studied as a function of nitric acid concentration and the results are shown in figure 3.8. It can be seen that the distribution ratio of Pu(IV) obtained in [C_4mim][NTf_2] alone is negligible at nitric acid concentrations lower than 3 M but it starts increasing above 3 M HNO_3. From the literature reported results [133] it was ascertained that the predominant mode of Pu(IV) transfer in to ionic liquid phase at higher nitric acid concentration (>2 M) is through anion exchange of $[Pu(NO_3)_5(H_2O)]^-$ and $[Pu(NO_3)_6]^{2-}$ with $NTf_2{}^-$ ion of ionic liquid (equation 3.7). The $D_{Pu(IV)}$ obtained in 0.02 M DOHyA in *n*-DD is quite similar to that obtained for [C_4mim][NTf_2] alone. In contrast to both these, the distribution ratio of Pu(IV) obtained in 0.02 M DOHyA/[C_4mim][NTf_2] is much higher than those obtained in DOHyA/*n*-DD as well as in [C_4mim][NTf_2] alone . This observation indicates that Pu(IV) is extracted to an appreciate value only when DOHyA is dissolved in ionic liquid medium. It can be seen that the distribution ratio of Pu(IV) decreases with increase in the concentration of nitric acid up to 3 M HNO_3 and thereafter the $D_{Pu(IV)}$ remains constant.

The initial decrease can be due to the cation exchange mechanism [122] i.e. the exchange of cationic part (C_4mim^+) of IL with the metal ion and it is shown in equation 3.8. At high nitric acid concentrations (> 3M HNO_3), the distribution ratios remain almost same indicating the occurrence of both coordination and anion exchange mechanism. Following equations explains probable extraction mechanisms where the value of x can be 1 or 2.

$$[Pu(NO_3)_5]^-_{aq} + \{[C_4mim][NTf_2]\}_{IL} \Leftrightarrow \{[C_4mim][Pu(NO_3)]_5\}_{IL} + [NTf_2^-]_{aq} \qquad (3.7)$$

$$\mathrm{Pu}^{4+}{}_{aq} + xDOHyA_{IL} + 4[\mathrm{C_4mim}][\mathrm{NTf_2}]_{IL} \Leftrightarrow (Pu(DOHyA)_x([NTf_2])_4)_{IL} + 4[\mathrm{C_4mim}]^{+}{}_{aq} \tag{3.8}$$

$$Pu^{4+}{}_{aq} + xDOHyA_{IL} + 4NO_3^{-}{}_{aq} \Leftrightarrow \{Pu(DOHyA)_x(NO_3)_4\}_{IL} \tag{3.9}$$

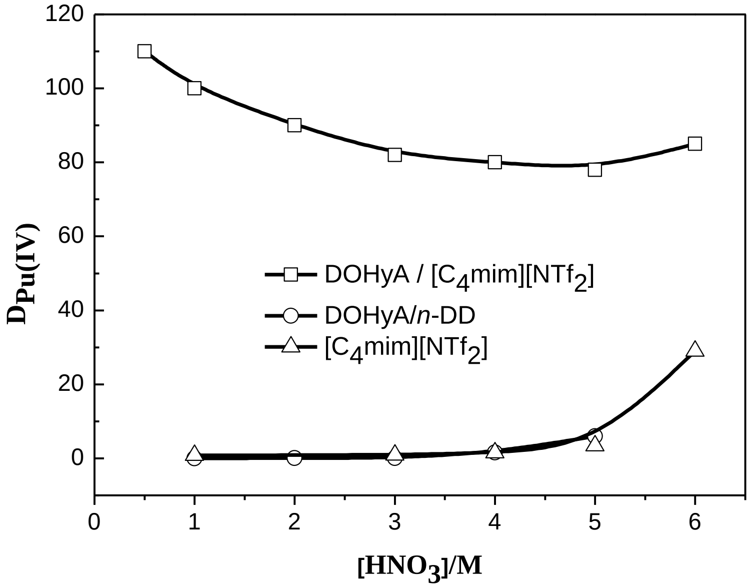

Figure 3.8. Variation in the distribution ratio of Pu(IV) as a function of the nitric acid concentration in aqueous phase. Ionic liquid phase: 0.02 M DOHyA/[C_4mim][NTf_2] or [C_4mim][NTf_2] alone. Organic phase: 0.02 M DOHyA/n-DD, aqueous phase: [HNO_3] = 0.5 M - 6 M spiked with ^{239}Pu(IV) tracer.

3.4.2 Variation of [DOHyA]

Figure 3.9 shows the effect of DOHyA concentration in a solution of DOHyA/[C_4mim][NTf_2] on the distribution ratio of Pu(IV) at 3 M HNO_3. It can be seen that the $D_{Pu(IV)}$ increases with increase in the concentration of DOHyA. The slope obtained from the log $D_{Pu(IV)}$ against log [DOHyA] gives the number of DOHyA molecules coordinated to Pu(IV) in ionic liquid phase. A slope of 1.6 was obtained from linear regression analysis of the extraction data indicates that 1 or 2 molecules of DOHyA might be involved in the extraction process in the ionic liquid phase.

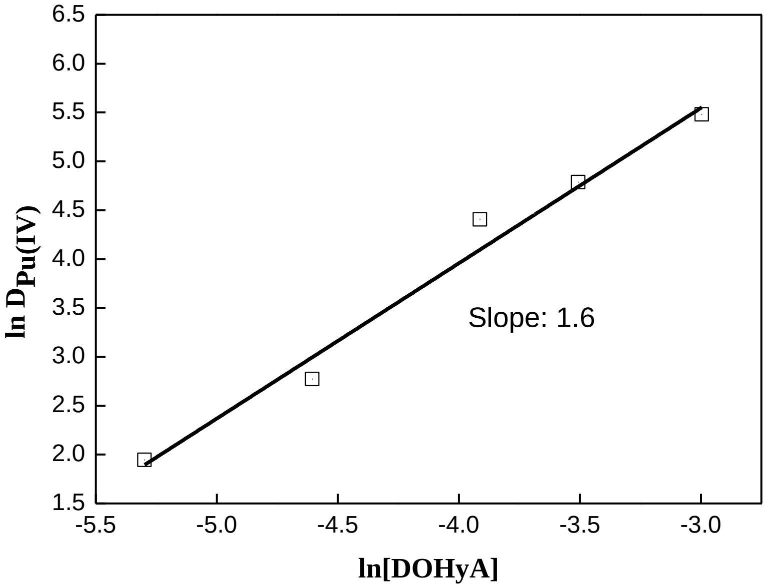

Figure 3.9: Variation in ln $D_{Pu(IV)}$ as a function of ln [DOHyA]. Ionic liquid phase : 0.005 M – 0.05 M DOHyA/[C_4mim][NTf_2], aqueous phase: [HNO_3] = 3 M spiked with ^{239}Pu(IV) tracer.

3.4.3 Role of OH group in DOHyA

It is interesting to compare the distribution ratio of Pu(IV) achieved in DOHyA with substituted amides. The amides chosen for comparison were *N*,*N*-dioctylmethoxy acetamide (DOMeOA) and *N*,*N*-dihexyloctanamide (DHOA). Substitution of –OH group in DOHyA by –OMe group results in DOMeOA and substitution of heptyl group in place of –OH, and *N*,*N*-dihexyl in place of *N*,*N*-dioctyl in DOHyA, results in DHOA (table 3.3). The distribution ratio of Pu(IV) in 0.02 M solution of these extractants in [C_4mim][NTf_2] is shown in figure 3.10. It can be seen that distribution ratio of Pu(IV) in DHOA/[C_4mim][NTf_2] and DOMeOA/[C_4mim][NTf_2] increases with increase in the concentration of nitric acid. It was observed that at all the nitric acid concentrations, the $D_{Pu(IV)}$ values in DOHyA/[C_4mim][NTf_2] were much higher than that obtained for DHOA or DOMeOA dissolved in [C_4mim][NTf_2]. Higher $D_{Pu(IV)}$ obtained in DOHyA could be due to the bidendate coordination of DOHyA and intramolecular hydrogen bonding as discussed elsewhere [180,194]. Since DHOA is a monodentate ligand and hydrogen bonding is not possible in DOMeOA, these extractants show poor extraction of Pu(IV) as compared to DOHyA. However, more studies are needed to confirm this behavior.

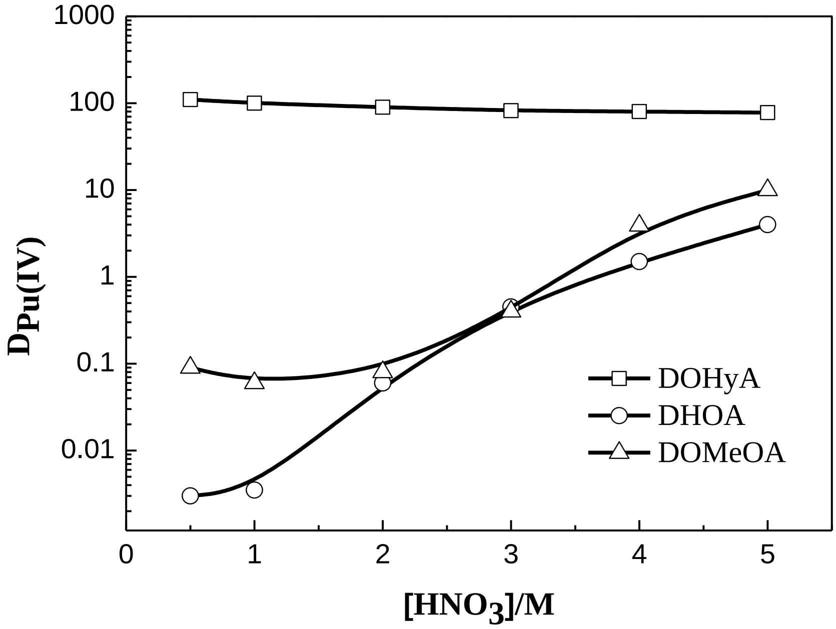

Figure 3.10. Variation in the distribution ratio of Pu(IV) as a function of the nitric acid concentration in aqueous phase. Ionic liquid phase : 0.02 M DOHyA/[C_4mim][NTf_2] or 0.02 M DHOA/[C_4mim][NTf_2] or 0.02 M DOMeOA/[C_4mim][NTf_2], aqueous phase: [HNO_3] = 0.5 M - 5 M spiked with ^{239}Pu(IV) tracer.

Comparing the chemical structure of DOHyA and DHOA, the present study showed that the oxygen atom at the 2-position of the amidic carbonyl group in DOHyA was necessary for the extraction of Pu(IV). Similarly, comparing the methoxy- and hydroxy acetamides, the distribution ratio of Pu(IV) indicates that the –OH group at the 2-position was mandatory in acetamide derivatives for the extraction of Pu(IV) from nitric acid medium.

3.4.4 Extraction of U(VI) & Am(III)

In order to understand the selectivity for Pu(IV) in DOHyA over other actinides, extraction of U(VI) and Am(III) was carried out in 0.02 M DOHyA/[C_4mim][NTf_2] and compared with the extraction behavior of Pu(IV) at various concentrations of nitric acid in figure 3.11. It can be seen that $D_{Am(III)}$ decreases from 2.3 to 0.2 and $D_{U(VI)}$ increases from 0.06 to 1 with increase of nitric acid concentration from 0.5 M to 5M. The distribution ratio of U(VI) and Am(III) are about two order lower than those achieved for Pu(IV) under similar conditions. The separation factor of U(VI) over Am(III), Pu(IV) over Am(III) & U(VI) have been compared from distribution ratios and they are tabulated in table 3.4. The separation factor of Pu(IV) over U(VI) decreases from 1833 to 78 and the separation factor of Pu(IV) over Am(III) increases from 48 to 354, with increase of HNO_3 concentration from 0.5 M to 5 M. Therefore the study shows the possibility of mutual separation of Pu(IV) from U(VI) and Am(III) using 0.02 M DOHyA/[C_4mim][NTf_2]. In addition the study also shows the separation factor of Am(III) over U(VI) varies from 38 to 0.2 with increase of HNO_3 concentration from 0.5 M to 5 M. This result indicates that there is an option for individual separation of Pu(IV), U(VI) and Am(III) from nitric acid medium using 0.02 M DOHyA in [C_4mim][NTf_2].

Moreover, in table 3.5, the separation factor of Pu(IV) over U(VI) obtained in 0.02 M DOHyA/ [C_4mim][NTf_2] was compared with that obtained in 0.2 M DOHyA/*n*-DD (literature reported value) [193]. It can be seen that the concentration of DOHyA required in *n*-DD is an order higher than that used in ionic liquid. In spite of this low concentration, the separation factor of Pu(IV) over U(VI) achieved in ionic liquid medium is reasonably higher than those observed in *n*-DD.

Similarly, table 3.6 compares the distribution ratio and the separation factor of Pu(IV) over U(VI) obtained in the present study with that obtained in

TODGA/[C$_8$mim][NTf$_2$] and DOBA (*N*,*N*-dioctylbutyramide)/ [C$_4$mim][NTf$_2$] systems which were reported in literature [125,133]. The results obtained in the present study clearly indicates that DOHyA has advantages over TODGA and DOBA systems to obtain high separation factor of Pu(IV) over U(VI) at all nitric acid concentrations.

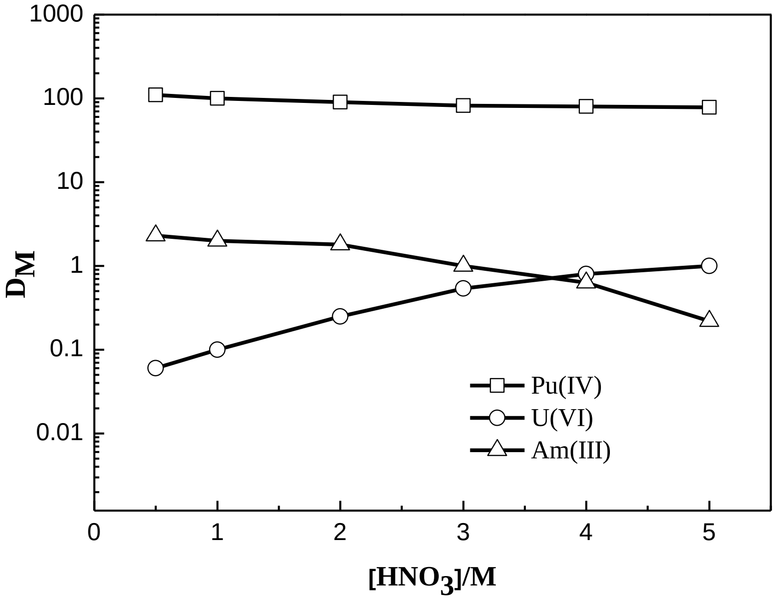

Figure 3.11. Variation in the distribution ratio of actinides as a function of nitric acid concentration in aqueous phase. Ionic liquid phase : 0.02 M DOHyA/[C$_4$mim][NTf$_2$], aqueous phase: [HNO$_3$] = 0.5 M - 5.0 M spiked with An tracer (An = ^{239}Pu(IV), ^{233}U(VI) and ^{241}Am(III)).

Table 3.4. Separation factor of Pu(IV) over U(VI) and Am(III) achieved using 0.02 M DOHyA/[C$_4$mim][NTf$_2$]. Aqueous phase = 0.5 M - 5 M nitric acid.

[HNO$_3$]$_{eq.}$/M	**Separation factor of actinides in 0.02 M DOHyA/[C$_4$mim][NTf$_2$]**		
	SF$_{Am(III)/U(VI)}$	SF$_{Pu(IV)/Am(III)}$	SF$_{Pu(IV)/U(VI)}$
0.5	38	48	1833
1	20	50	1000
2	7.2	50	360
3	1.9	82	152
4	0.79	127	100
5	0.22	354	78

Table 3.5. Comparision of separation factor of Pu(IV) over U(VI) obtained in 0.02 M DOHyA/ [C$_4$mim][NTf$_2$] with 0.2 M DOHyA/n-DD (literature reported value [193])

[HNO$_3$]/M	**Separation factor of Pu(IV) over U(VI)**	
	0.2 M DOHyA/*n*-DD [193]	**0.02 M DOHyA/ [C$_4$mim][NTf$_2$]**
0.5	41	1833
1	51	100
2	258	360
3	423	152
4	100	100
5	59	78

Table 3.6. Comparison of distribution ratios of Pu(IV) and U(VI) and their separation factors in DOHyA/[C$_4$mim][NTf$_2$] with that of TODGA/[C$_8$mim][NTf$_2$] and DOBA/[C$_4$mim][NTf$_2$]. Aqueous phase: 0.5 M – 6 M + ^{239}Pu(IV) (or ^{233}U(VI)) tracer.

[HNO$_3$] /M	**0.02M DOHyA in [C$_4$mim][NTf$_2$]**			**0.01 M TODGA in [C$_8$mim][NTf$_2$] [125]**			**0.5 M DOBA in [C$_4$mim][NTf$_2$] [133]**		
	$D_{Pu(IV)}$	**$D_{U(VI)}$**	**SF**	**$D_{Pu(IV)}$**	**$D_{U(VI)}$**	**SF**	**$D_{Pu(IV)}$**	**$D_{U(VI)}$**	**SF**
0.5	110	0.06	1833	~1000	~7	~143	0.03	0.23	0.13
1	100	0.1	1000	~500	~5	~100	0.05	0.15	0.33
2	90	0.25	360	-	-	-	-	-	-
3	82	0.54	152	258	3.32	77.5	1	0.13	7.7
4	80	0.8	100	-	-	-	3	0.15	20
5	78	1	78	-	-	-	5	0.4	12.5
6	-	-	-	~10	~2	~5	-	-	-

3.4.5 Effect of alkyl chain length of the extractant

Figure 3.12 shows the comparison in the distribution ratio of Pu(IV) obtained by varying the chain length of the alkyl group attached to the amidic nitrogen atom in hydroxy acetamide. The alkyl group was varied from C$_6$ to C$_{10}$. The extraction of Pu(IV) was carried out in 0.02 M solution of *N*,*N*-dihexyl-2-hydroxyacetamide(DHHyA), *N*,*N*-dioctyl-2-hydroxyacetamide (DOHyA) and *N*,*N*-didecyl-2-hydroxyacetamide(DDHyA) in [C$_4$mim][NTf$_2$]. It was observed that $D_{Pu(IV)}$ remains nearly constant at 1 M HNO$_3$ and decreases marginally at nitric acid concentration of >1M with increase in alky chain length from octyl to decyl. The decrease in $D_{Pu(IV)}$ from hexyl to decyl derivative of hydroxyl acetamide could be due to the steric factors, increase in hydrophobicity, and extent of solubility of the extracted complex in the IL phase. However, more studies are needed to understand this observation.

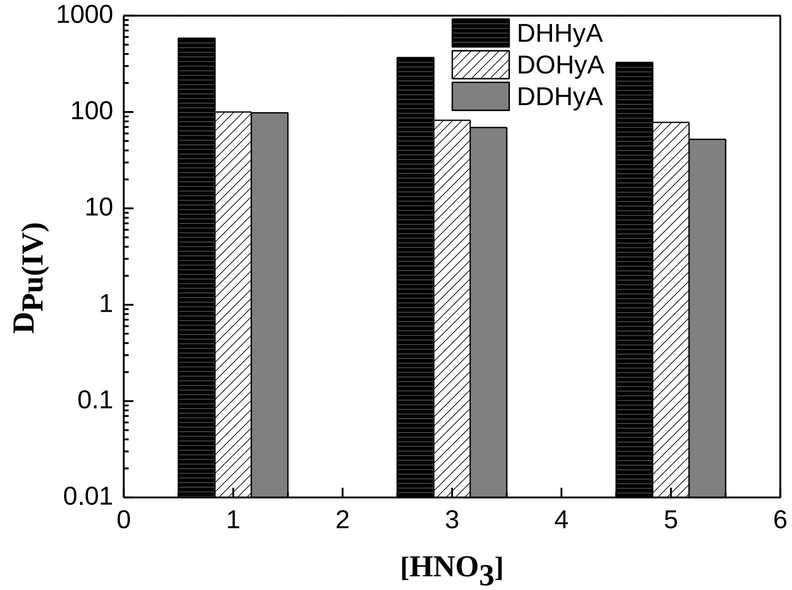

Figure 3.12. Effect of alkyl chain length attached to amidic nitrogen atom on the distribution ratio of Pu(IV) at various nitric acid concentrations. Ionic liquid phase: DHHyA or DOHyA or DDHyA /[C_4mim][NTf_2], aqueous phase: [HNO_3] = 1 M - 5 M spiked with ^{239}Pu(IV) tracer.

3.4.6 Temperature Variation

In order to study the effect of temperature on the distribution ratio of Pu(IV), the extraction studies were conducted at various temperatures ranging from 298 K to 333 K using 0.02 M DOHyA/[C_4mim][NTf_2]. It can be seen that $D_{Pu(IV)}$ increases with increase of temperature. The plot of ln $D_{Pu(IV)}$ against 1/T is shown in figure 3.13. This shows that the extraction of Pu(IV) in [DOHyA]/[C_4mim][NTf_2] is endothermic. The enthalpy change involved in the extraction of Pu(IV) can be determined using Vant Hoff's equation which is shown in equation 3.4. From the slope of the straight line, the ΔH_{tot} was determined to be 10.6 kJ/mol.

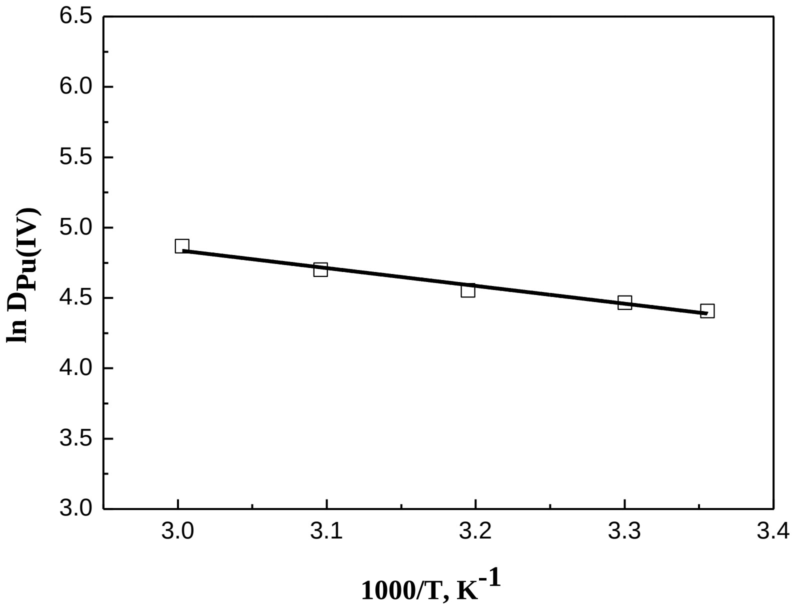

Figure 3.13. Variation in the distribution ratio of Pu(IV) as a function of reciprocal temperature. Ionic liquid phase : 0.02 M DOHyA/[C_4mim][NTf_2], aqueous phase: [HNO_3] = 3 M spiked with ^{239}Pu(IV) tracer., temperature = 298K – 333K.

3.4.7 Stripping

Since high distribution ratio of Pu(IV) was obtained in DOHyA/[C_4mim][NTf_2] at all nitric acid concentrations investigated in the present study, stripping of Pu(IV) from the loaded ionic liquid phase could not be performed with HNO_3, which was usually employed in conventional molecular diluents. In view of this, aqueous soluble complexing agents such as oxalic acid and acetohydroxamic acid have been tried for back extraction of Pu(IV) from the loaded ionic liquid phase. Prior to stripping, the extraction of Pu(IV) was carried out using 0.02 M DOHyA/[C_4mim][NTf_2] at 3 M HNO_3. Stripping was performed by contacting the loaded ionic liquid phase with 0.05 M oxalic acid/0.35 M HNO_3 as well as with 0.5 M acetohydroxamic acid/0.35 M HNO_3. The results of stripping are shown in figure 3.14. It can be seen that quantitative stripping of plutonium (IV) is achieved in 2 - 3 contacts of loaded ionic liquid phase with oxalic acid and in 3- 4 contacts with acetohydroxamic acid.

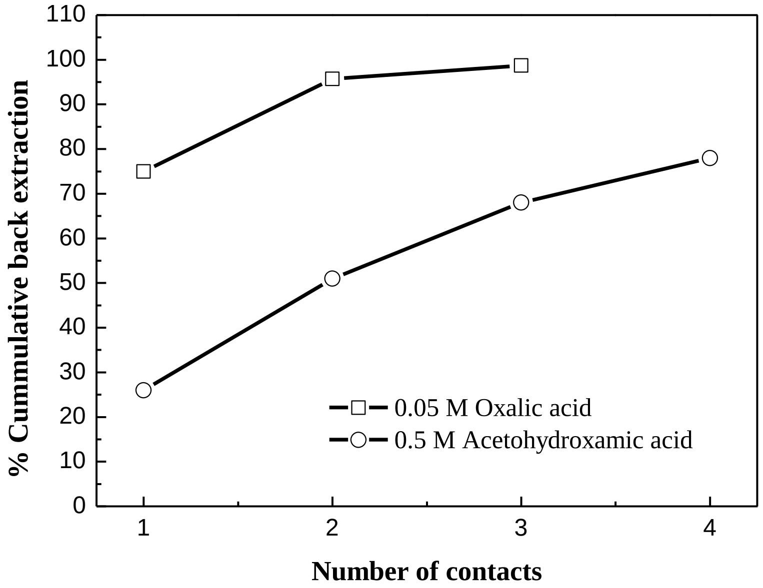

Figure 3.14. Stripping of Pu(IV) from ionic liquid phase as a function of number of contacts. Ionic liquid phase : 0.02 M DOHyA/ [C$_4$mim][NTf$_2$] containing Pu(IV) extracted from 3 M HNO$_3$. Aqueous phase: 0.5 M acetohydroxamic acid (AHA) or 0.05 M oxalic acid (OA) in 0.35 M HNO$_3$.

3.5 Conclusion

N, *N*-dioctyl-2-hydroxyacetamide in [C$_4$mim][NTf$_2$] was evaluated for the extraction of Pu(IV) from nitric acid medium, for the first time. The distribution ratio of Pu(IV) obtained in 0.02 M DOHyA/[C$_4$mim][NTf$_2$] was much higher than those obtained for DOHyA /*n*-DD and [C$_4$mim][NTf$_2$]. The Distribution ratio of Pu(IV) decreased marginally with increase in the concentration of nitric acid up to 3 M and thereafter it attained a plateau. The distribution ratio of uranium(VI) and amrecium(III) were much lower than that obtained for Pu(IV) in DOHyA/[C$_4$mim][NTf$_2$]. Unlike the traditional molecular extractant, the separation factor of Pu(IV) over U(VI) was in the order of 10^3 and Pu(IV) over Am(III) was of the order of 10^2. This observations indicated the possibility of separating Pu(IV) from other actinides using DOHyA/[C$_4$mim][NTf$_2$]. The

$D_{Pu(IV)}$ obtained by DOHyA/[C_4mim][NTf_2] was compared with that obtained for DOMeOA and DHOA in [C_4mim][NTf_2]. Extraordinary extraction of Pu(IV) in DOHyA/[C_4mim][NTf_2] compared to DOMeOA/[C_4mim][NTf_2] and DHOA/[C_4mim][NTf_2] revealed that –OH group at the 2-position is mandatory for the extraction of Pu(IV) in acetamide. The effect of temperature on the extraction of Pu(IV) was studied and it was found to be endothermic. Quantitative stripping of Pu(IV) from the loaded organic phase was achieved using complexing agents.

PART C

Solvent extraction study of americium(III) using benzoylpyrazolone extractant dissolved in pyrrolidinium based room temperature ionic liquid

In the past few decades, pyrazalone based extractants have been investigated for the extraction of metal ions from aqueous solutions [195-204]. Among the various pyrazalone derivatives, the 1-phenyl-3-methyl-4-benzoylpyrazol-5-one (HPMBP) is having relatively low pKa value (4.05) as compared to other well known diketone based extractant like thenoyltrifluoroacetone (HTTA) (pKa = 6.25). As a result, HPMBP is more acidic and it could facilitate the extraction of metal ions at lower pHs. Therefore, they can be employed easily in moderate pH conditions for the separation of metal ions. Pan *et al.* [203] reported the extraction behaviour of rare earth metals using HPMBP dissolved in [C_4mim][PF_6] and very recently, Gujar *et al.* [204] studied the extraction behaviour of trivalent actinides and lanthanides using HPMBP in [C_8mim][NTf_2]. However, the studies on solvent extraction of lanthanides and actinides using HPMBP in room temperature ionic liquids is very limited. Moreover, literature [117- 131] shows that imidazolium based ionic liquids have been employed extensively as diluent for the solvent extraction studies of metal ions but the use of pyrrolidinium ionic liquids as diluents for solvent extraction applications is very scant though the role of pyrrolidinium ionic liquids has extensively studied as electrolytes in electrochemical study of metal ions. There is only one literature wherein Rout *et al*. employed pyrrolidinium based ionic liquids as diluent for rare earth separation [205]. Hence it is appealing to investigate the pyrrolidinium ionic liquid as diluent for the solvent extraction studies of actinides.

The part C deals with the extraction and stripping behavior of americium (III) in 1-butyl-3-methylpyrrolidinium bis(trifluoromethanesulfonyl)imide ([C_4mpy][NTf_2]) containing the extractant, 1-phenyl-3-methyl-4-benzoylpyrazol-5-one (HPMBP). The ionic liquid [C_4mpy][NTf_2] has been employed for the first time with pyrazolone derivative. The dependence of Am(III) extraction on the aqueous phase pH, concentrations of extractant, ionic liquid cation and nitrate ion in the feed phase was studied to understand the extraction mechanism in ionic liquid medium.

Table 3.7. Structures of molecular extractants and RTIL used in part C chapter 3

Name	**Structure**
Extractants	
1-Phenyl-3-methyl-4-benzoylpyrazol-5-one (HPMBP)	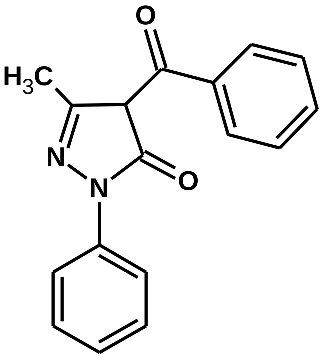
3-Methyl -1-Phenyl-2- pyrazolin-5-one (MPP)	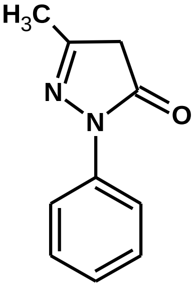
Ionic liquid	
1-Butyl-1-methylpyrrolidinium bis(trifluoromethanesulfonyl)imide ([C_4mpy][NTf_2])	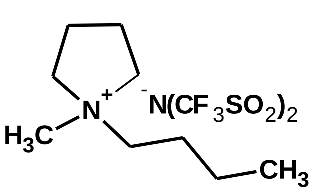

Synthesis of the ionic liquid and extractant used in part C have been discussed in section 2.9.2, 2.9.4 of chapter 2.

3.6 Results and Discussions

3.6.1 Effect of aqueous pH

The extraction behavior of Am(III) from nitric acid medium in 0.01M HPMBP/[C_4mpy][NTf_2] is shown in the figure 3.15. The distribution ratio of Am (III) increases with increase of pH, which is the characteristics of 1, 3-diketone based extractants. This indicates that the acidic proton from the HPMBP is exchanged with Am (III) for extraction. The extraction of Am (III) in the ionic liquid [C_4mpy][NTf_2] alone is also given in the figure 3.15. Negligible extraction of Am (III) at all pH indicates that the ionic liquid do not extract Am (III) under the given conditions. This shows that the extraction of Am (III) occurs only in the presence of HPMBP in ionic liquid phase and ionic liquid alone do not extract americium.

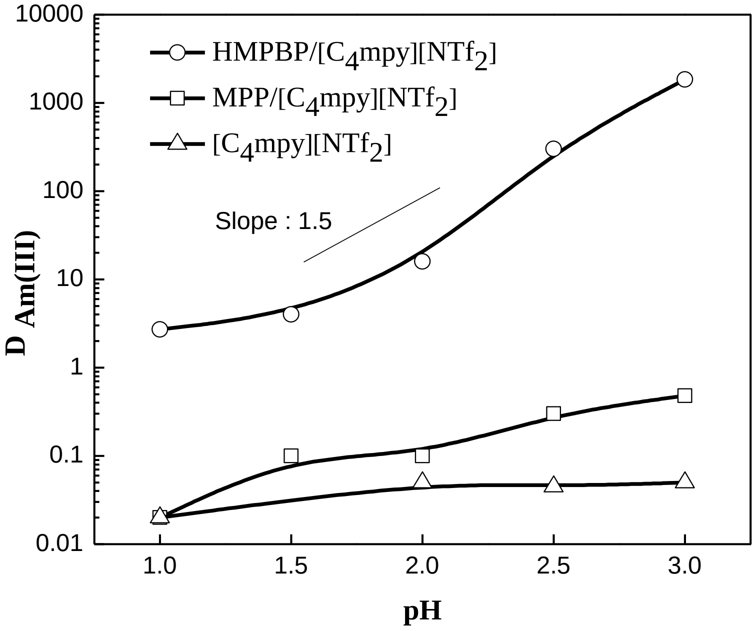

Figure 3.15. Variation in the distribution ratio of Am(III) as a function of pH. Ionic liquid phase: 0.01M HPMBP (or 0.01 M MPP)/ [C_4mpy][NTf_2] or [C_4mpy][NTf_2]. Aqueous phase: pH 1 to 3 spiked with ^{241}Am tracer.

Figure 3.15 also represents the comparison of the distribution ratio of Am (III) using 3-methyl -1-phenyl-2- pyrazolin-5-one (MPP) and its benzoyl derivative, HPMBP (0.01M each) in [C_4mpy][NTf_2] medium. It can be seen that the extraction of Am (III) in HPMBP is much higher than MPP. The result shows that the distribution ratio of Am (III) increases remarkably upon substitution of benzoyl moiety in MPP. This is obviously due to the formation of 1, 3-diketone in pyrazolone, which is a strongly acidic chelating ligand. Moreover, the study also shows that the presence of only one carbonyl group in the pyrazolone moiety is inadequate for the extraction of Am (III).

3.6.2 Extraction Kinetics

Figure 3.16 shows the variation in the distribution ratio of Am(III) in HPMBP/[C_4mpy][NTf_2] as a function of time. The extraction of Am(III) was carried out from pH 2 solution. The distribution ratio of Am(III) increases with increase in the duration of equilibration. The equilibrium is quickly established in ~60 minutes of equilibration; thereafter the variation in the distribution ratio is insignificant. In order to ensure establishment of equilibrium, the ionic liquid and aqueous phases were mixed for 1 hour in all subsequent experiments.

3.6.3 Extraction stoichiometry

The distribution ratio of Am (III) was measured as a function of extractant concentration in ionic liquid phase and the results are plotted in figure 3.17. The distribution ratio of Am (III) increases with an increase in the concentration of HPMBP in ionic liquid phase. Linear regression analysis of the extraction data results in a straight line with a slope of ~3. This suggests that three molecules of HPMBP could be involved in the extraction of Am (III) from aqueous phase. Based on this result, it is quite likely that three protons are released to the aqueous phase for the extraction of Am (III) in ionic liquid phase.

A slope of 1.5 obtained from the figure 3.15 indicates the release of 1 or 2 H^+ ions during extraction of Am (III). The dependence of Am (III) distribution ratio on nitrate ion concentration in aqueous phase was studied and the results are shown in figure 3.18. It can be seen that there is hardly any change in the distribution ratio with increase in the nitrate ion concentration in the aqueous phase. This observation confirms that nitrate ions do not participate in extraction of Am (III) and some other mechanism could be responsible for extraction. Since NO^{3-} ion is not participating, it is quite likely that the NTf_2^- ion present in organic phase itself could compensate the charge of Am (III) ion for maintaining the charge neutrality. Therefore, most plausible mechanism for the extraction of Am (III) in ionic liquid medium can be given by the equation 3.10.

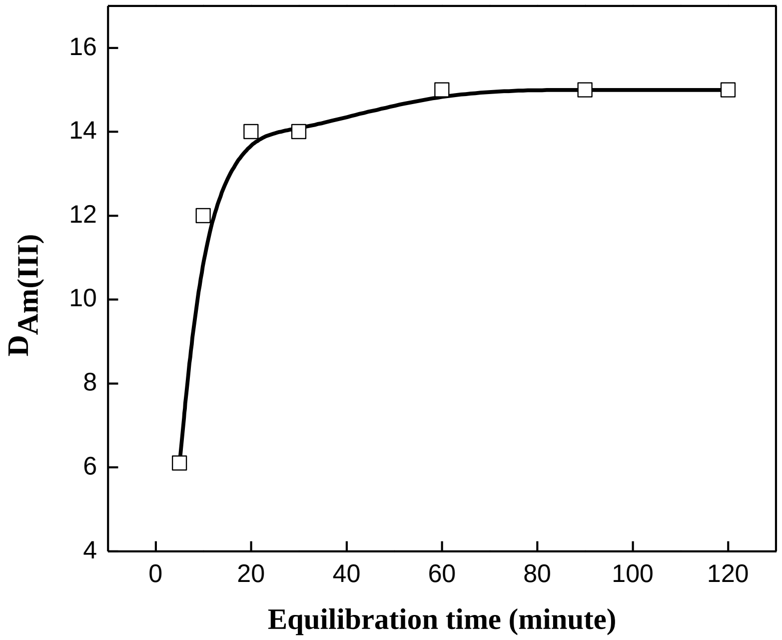

Figure 3.16. Variation in the distribution ratio of Am(III) as a function of equilibration time. Ionic liquid phase: 0.01M HPMBP /[C$_4$mpy][NTf$_2$]. Aqueous phase: pH 2 spiked with ^{241}Am tracer. Equilibration time = 5 - 120 minutes.

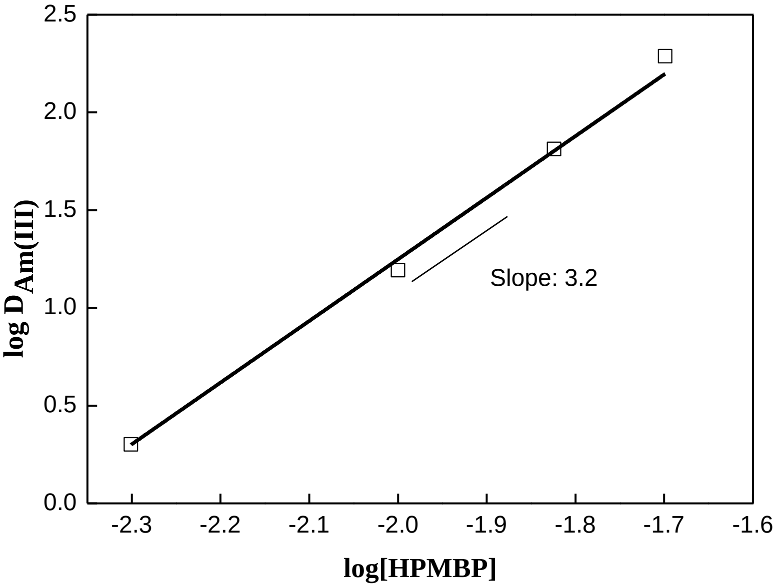

Figure 3.17. Variation of logD$_{Am(III)}$ with log[extractant]. Ionic liquid phase : 0.005 M – 0.02 M HPMBP/[C$_4$mpy][NTf$_2$]. Aqueous phase: pH 2 spiked with ^{241}Am tracer.

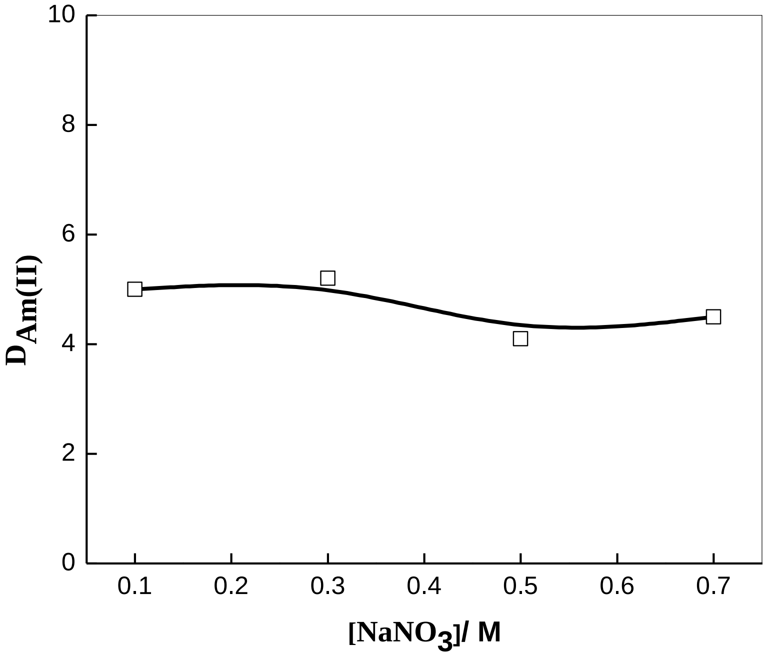

Figure 3.18. Variation in the distribution ratio of Am (III) as a function of nitrate ion concentration in the aqueous phase. Ionic liquid phase : 0.01M HPMBP / [C$_4$mpy][NTf$_2$]. Aqueous phase: pH 2 and 1M – 0.7M NO$_3^-$ ion (in the form of NaNO$_3$) spiked with ^{241}Am tracer.

$$\mathrm{Am}^{3+}{}_{aq} + 3\mathrm{HPMBP}_{IL} + \mathrm{x}\,[\mathrm{C_4mpy}][\mathrm{NTf_2}]_{IL}$$
$$\Leftrightarrow [\mathrm{Am(PMBP)_{3\text{-}x}(HPMBP)_x}].[\mathrm{NTf_2}]_{3\text{-}x}]_{IL} + (3-x)\,\mathrm{H}^{+}{}_{aq} + (3-x)\,[\mathrm{C_4mpy}]^{+}{}_{aq} \tag{3.10}$$

To verify the mechanism proposed in equation 3.10, the effect of $[C_4mpy]^+$ ion in aqueous phase on the extraction behavior of Am (III) at pH 2 was studied and the results are shown in figure 3.19. The concentration of $[C_4mpy]^+$ present in aqueous phase was varied from 0.02 M to 0.06 M by adding aqueous soluble $[C_4mpy][Br]$. The distribution ratio of Am (III) decreases with increase in the concentration of ionic liquid cation in aqueous phase. This indicates that Am (III) is extracted in ionic liquid phase at the expense of ionic liquid cation by common ion effect. From all these observations, the most plaucible mechanism repoponsible for the extraction of Am (III) in pyrazolone/ionic liquid phase can be represented by equation 3.10.

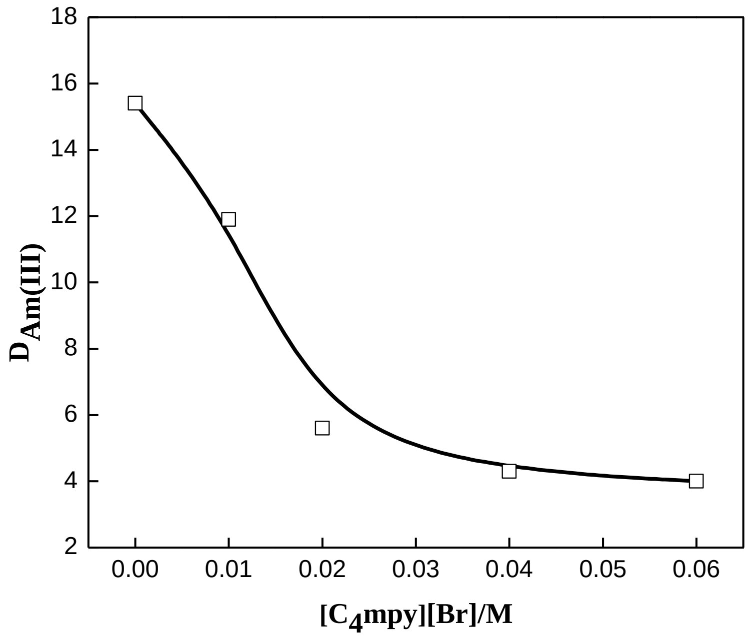

Figure 3.19. Variation in the distribution ratio of Am (III) as a function of $[C_4mpy][Br]$ concentration in the aqueous phase. Ionic liquid phase: 0.01M HPMBP / $[C_4mpy][NTf_2]$. Aqueous phase: pH 2 and 0.01M – 0.06 M $[C_4mpy][Br]$

spiked with ^{241}Am tracer.

3.6.4 Comparison of extraction with n-DD

The extraction of Am (III) in 0.01 M HPMBP in [C$_4$mpy][NTf$_2$] was compared with that of *n*-dodecane (*n*-DD) and the results are shown in the figure 3.20. It is noted that quite high extraction of Am (III) is observed when ionic liquid acted as diluents, as compared to *n*-dodecane. The D$_{Am(III)}$ increases from ~3 to >300 with increase of pH from 1 to 3 in case of ionic liquid while very insignificant distribution ratio is observed for *n*-DD (0.002 to 4 under same experimental conditions). Moreover it is quite likely that the mechanism of extraction in both cases is different. It is likely that the dissociation of HPMBP is poor in *n*-dodecane than in ionic liquid phase resulting the lower distribution ratio of Am (III) in *n*-DD phase.

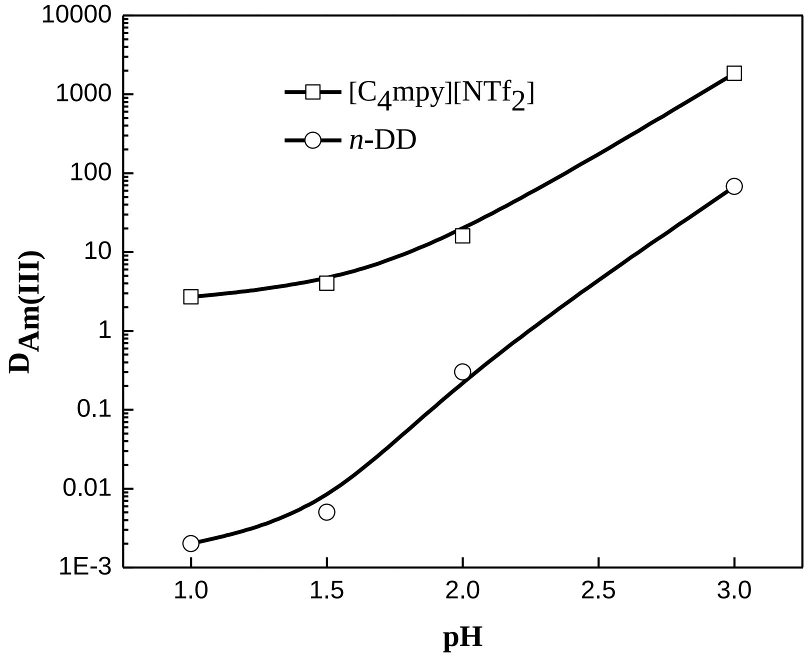

Figure 3.20. Comparison of the distribution ratio of Am (III) in ionic liquid and n-DD. Ionic liquid phase: 0.01M HPMBP/ [C$_4$mpy][NTf$_2$] (or n-DD). Aqueous phase: pH 1 to 3 spiked with ^{241}Am tracer.

3.6.5 Stripping study

Figure 3.21 shows the variation of percentage stripping as a function of concentration of stripping acid. It is noticed that the percentage of stripping increases with increase in aqueous phase acidity. Nearly 50% of Am (III) is recovered in one contact from the loaded ionic liquid phase by using 0.5M HNO_3 as the stripping solution. About 80% of Am (III) is back extracted within one contact using 3 M nitric acid and therefore it can be expected that rest of Am (III) would be back extracted in the next couple of stages using nitric acid itself.

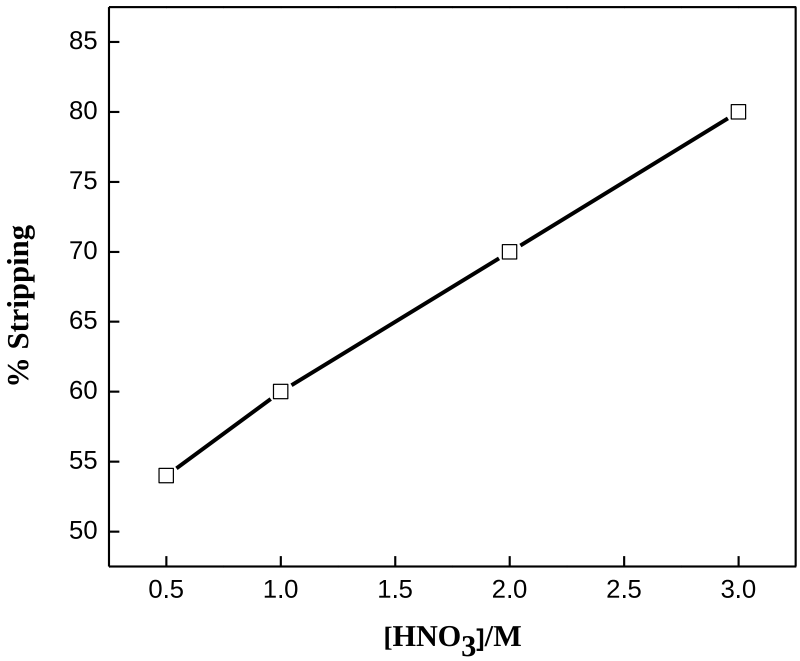

Figure 3.21. Percentage stripping as a function of nitric acid concentration. Ionic liquid phase : 0.01M HPMBP/ [C_4mpy][NTf_2] containing Am(III). Aqueous (or stripping phase: 0.5 M – 3M nitric acid.

3.7 Conclusion

The extraction behavior of americium (III) from the nitric acid medium was studied in a solution of HPMBP present in 1-butyl-1-methylpyrrolidinium bis(trifluoromethane-sulfonyl)imide ([C_4mpy][NTf_2]). The ionic liquid [C_4mpy][NTf_2] was explored as diluent for the first time in the extraction of Am(III). The distribution ratio of Am (III) increased with increase of aqueous phase pH. The slope analysis of the extraction data indicates the involvement of three molecules of HPMBP for the extraction of Am (III). Cation exchange mechanism seems to be most plausible mode for the extraction of Am (III) in ionic liquid phase. The extraction in ionic liquid was remarkably higher than that observed in conventional solvent (*n*-DD). Quantitative recovery of Am (III) can be achieved in few contacts with dilute nitric acid.

CHAPTER 4

ROOM TEMPERATURE IONIC LIQUID AS AN EXTRACTANT FOR SOLVENT EXTRACTION OF ACTINIDES

4.1 Introduction

In addition to the role of diluent, RTILs are being explored as an extractant. In this aspect several functionalized ionic liquids (FILs) or task specific ionic liquids (TSILs) in which cationic or anionic part tethered covalently with organic functionalities have been reported in the recent past [61-65, 133-139,141,142]. These types of ionic liquids exhibit the properties of both ionic liquid and organic functionality [55]. The use of functionalized ionic liquid could avoid the use of molecular extractants. Since the FILs are usually soluble in ionic liquid diluents, the solvent system is completely devoid of any molecular entities. Therefore, functionalized ionic liquids in nuclear reprocessing applications could offer inherent advantages such as thermal stability and negligible vapour pressure etc. Depending upon the nature of functional group attached, the selectivity of metal ion was found to be different. Moreover, a sub class of functionalised ionic liquids known as ionic liquids with strongly coordinating anion wherein the anion of the ionic liquid itself is a functional moiety have also been studied for the metal ion extraction[66-70,132,140]. The advantages of such ionic liquids are simple method of preparation, higher loading of metals, excellent miscibility with non-polar diluents such as toluene, dodecane etc. However, the research in this class of ionic liquids is very preliminary and requires further study to establish their various applications in desired fields.

In this chapter, a novel task specific ionic liquid (TSIL) and a RTIL with strongly coordinating anion have been explored as extractants for the extraction of actinides from nitric acid medium. This chapter consists of two parts namely part I and part II. Part I describes the synthesis of a novel phosphoramide based TSIL and solvent extraction studies of Pu(IV), U(VI) and Am(III) using TSIL as an extractant in imidazolium based ionic liquid diluent. In part B, insights into the extraction behavior of U(VI) in PUREX solvent containing ionic liquid namely, tri-*n*-octylmethylammonium bis-(2-ethylhexyl)phosphate ($[A336]^+[DEHP]^-$), has been reported.

Experimental parts of the present chapter have been discussed in the section 2.5, 2.8.4, and 2.8.5 of the chapter 2.

PART I

Mutual separation of Pu(IV) from other actinides using TSIL

Several studies have been reported in literature for the separation of actinides from wide variety of feed solutions using functionalized ionic liquids [61-65,133-139, 141,142,206-209]. For instance, task specific ionic liquids with diglycolamide (DGA) and phosphine oxide (CMPO) moiety anchored on imidazolium cation have been reported in literature for the solvent extraction of actinides from nitric acid medium [137,209]. The authors reported the superior extractability of these FILs over conventional DGA and CMPO based extractants. Similarly, Alok *et al.* studied the separation of actinides and fission products using amide ([DOAIm][NTf_2]) and phosphonate ([ImP][NTf_2]) based functionalised ionic liquids [133,134]. These FILs showed remarkably high separation of Pu(IV) from U(VI) and Am(III). In the very recent years, couple of TSILs bearing phosphate and phosphine oxide moiety have been reported in literature for the extraction of U(VI) and Nd(III) from nitric acid medium, respectively [141,142]. However, the phosphoramide functionalized ionic liquids have not been studied in detail except one literature wherein the authors reported some preliminary extraction results of U(VI) in phosphoramide functionalized on ammonium based ionic liquid [63]. Hence it is appealing to synthesize a novel phosphoramide based TSIL and study for the solvent extraction of actinides.

The objective of the part I in chapter 4 is to report the synthesis of a novel task specific ionic liquid, Diethyl-3-(3-butylimidazolium)propylphosphoramide bis(trifluoromethanesulfonyl)imide ([BuImPA][NTf_2]) and explore it as an extractant for the solvent extraction of Pu(IV), U(VI) and Am(III) from nitric acid medium.

Table 4.1. Structure of TSIL and diluent used in Part I of chapter 4

Name	**Structure**
TSIL	
Diethyl-3-(3-alkylimidazolium)propyl phosphoramide bis(trifluoromethanesulfonyl)imide. [BuImPA][NTf$_2$] (R=C$_4$H$_9$) [PrImPA][NTf$_2$] (R=C$_3$H$_7$) [MeImPA][NTf$_2$] (R=CH$_3$)	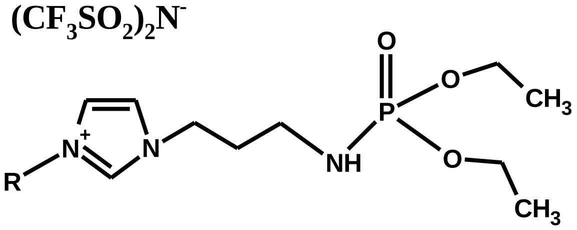 **(Present study)**
diethyl-2-(3-methylimidazolium)ethyl phosphonate bis(trifluoromethanesulfonyl)imide, (ImPNTf$_2$)	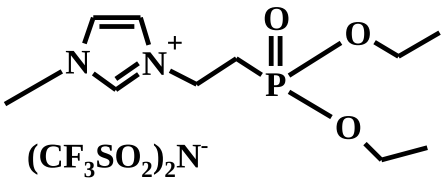 [134]
N,N-dioctyl-2-(3-methylimidazolium)acetamide bis(trifluoromethanesulfonyl)imide (DOAImNTf$_2$)	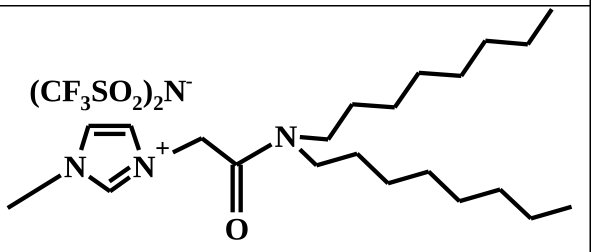 [133]
Diluent	
1-Alkyl-3-methylimidazolium bis(trifluoromethanesulfonyl)imide ([C$_n$mim][NTf$_2$] [C$_4$mim][NTf$_2$] (R: C$_4$H$_9$) [C$_6$mim][NTf$_2$] (R: C$_6$H$_{13}$) [C$_8$mim][NTf$_2$] (R: C$_8$H$_{17}$)	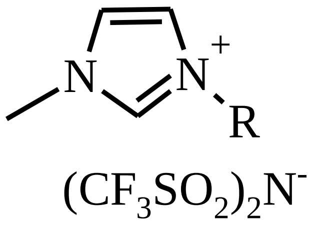

Synthesis of the ionic liquids used in part I have been discussed in section 2.9.1 & 2.9.3 of chapter 2.

4.2 Results and Discussions

4.2.1 Extraction of Pu(IV) in [BuImPA][NTf$_2$] /[C$_4$mim][NTf$_2$]

Solvent extraction of Pu(IV) was carried out as a function of nitric acid concentration using the diluent ([C$_4$mim][NTf$_2$]) alone and also using phosphoramide TSIL ([BuImPA][NTf$_2$]) dissolved in [C$_4$mim][NTf$_2$] and the results are shown in figure 4.1.

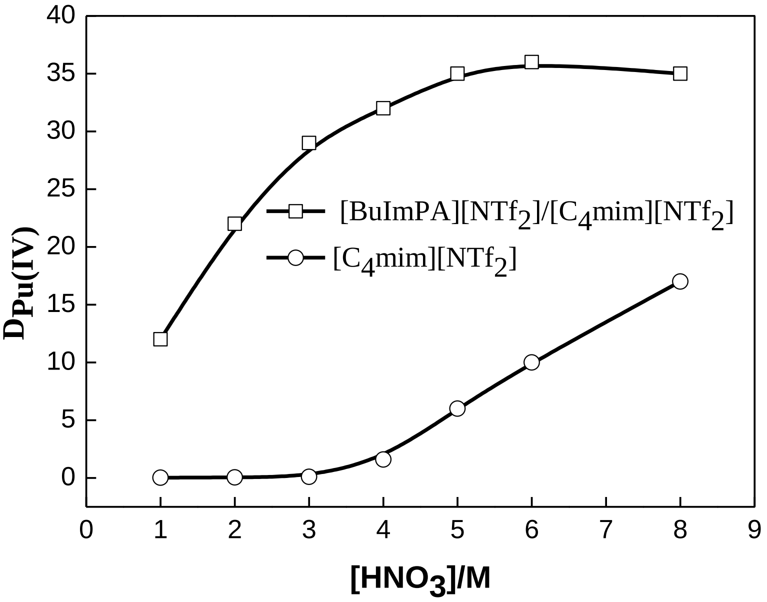

Figure 4.1. Variation in the distribution ratio of Pu(IV) as a function of the nitric acid concentration in aqueous phase. Ionic liquid phase: 0.3 M [BuImPA][NTf$_2$]/[C$_4$mim][NTf$_2$] or [C$_4$mim][NTf$_2$] alone, aqueous phase: [HNO$_3$] = 1 M – 8 M spiked with ^{239}Pu(IV) tracer.

The extraction of Pu(IV) in [C$_4$mim][NTf$_2$] is negligible at nitric acid concentrations lower than 3 M. A marginal increase in extraction is observed at nitric acid concentration above 3 M. This was attributed to the anion exchange of [Pu(NO$_3$)$_5$(H$_2$O)]$^-$ or [Pu(NO$_3$)$_6$]$^{2-}$ species present in aqueous phase with the NTf$_2$$^-$ ion of ionic liquid phase, as reported elsewhere [133,134]. However, the distribution ratio of Pu(IV) in 0.3 M [BuImPA][NTf$_2$]/[C$_4$mim][NTf$_2$] is much higher than those observed in

$[C_4mim][NTf_2]$ at all nitric acid concentration and it increases with increase in the concentration of nitric acid, reaches a maximum value at 5 M nitric acid, followed by the attainment of plateau with further increase in nitric acid concentration.

4.2.2 Comparison of $D_{Pu(IV)}$ in phosphramide TSIL with that in amide & phosphonate TSIL

It is worthwhile to compare the Pu(IV) extraction results obtained in phosphoramide-ionic liquid with those obtained in phosphonate [134] and amide [133] functionalised ionic liquids reported in literature. The distribution ratios of Pu (IV) obtained in these systems are compared in table 4.2.

Table 4.2. Comparison of the distribution ratio of Pu(IV) in phosphoramide-FIL with that of amide and phosphonate-FIL. Ionic liquid phase: 0.3 M FIL/ $[C_4mim][NTf_2]$, aqueous phase: 1 M - 8 M nitric acid.

$[HNO_3]_{eq.}$/M	**0.3 M TSIL/$[C_4mim][NTf_2]$**		
	$[BuImPA][NTf_2]$ (present work)	**$[DOAIm][NTf_2]$ [133]**	**$[ImP][NTf_2]$ [134]**
1	12	44	120
2	22	37	20
3	29	30	7
4	32	21	4
5	35	20	4
6	36	21	NA*
8	35	28	NA*

In amide functionalized ionic liquid ($[DOAIm][NTf_2]$), the extraction of Pu(IV) decreased with increase in the concentration of nitric acid, reached a minimum value of distribution ratio at 4 - 5 M in nitric acid followed by increase in distribution ratios. In phosphonate-ionic liquid ($[ImP][NTf_2]$) the distribution ratio of Pu(IV) decreased with increase in the concentration of nitric acid. The decrease in the distribution ratio of

Pu(IV) in amide- and phosphonate -ionic liquids was attributed to competition between H^+ ion and Pu(IV) ion for coordination with FIL in ionic liquid phase [133,134]. The increase in $D_{\mathrm{Pu(IV)}}$ observed in amide ionic liquids at nitric acid concentrations above 5 M was attributed to the anion exchange of $[Pu(NO_3)_5(H_2O)]^-$ complex with NTf_2^- ion of ionic liquid phase as reported elsewhere [133].

This observation indicates that the mode of Pu(IV) extraction in phosphoramide-FIL could be similar to those observed in molecular diluents, wherein the Pu(IV) is extracted as neutral $Pu(NO_3)_4$ species in ionic liquid phase as shown in equation 4.1. This mechanism demands the participation of four molecules of nitrate ion for the formation of neutral species. Figure.4.2 shows the extraction of nitric acid (nitrate ion) in 0.3 M $[BuImPA][NTf_2]/[C_4mim][NTf_2]$. It can be seen that the amount of nitric acid extracted in ionic liquid phase increases from 0.086 M to 1.12 M with increase in aqueous phase nitric acid concentration from 1 M to 8 M. This indicates that significant amount of nitric acid is extracted into ionic liquid phase and the nitrate ion is readily available for aiding the formation of neutral $Pu(NO_3)_4$ species in ionic liquid phase.

In phosphoramide-FIL, the extraction of Pu(IV) increased with increase in the concentration of nitric acid, as discussed above. However, in phosphonate-FIL the extraction of Pu(IV) decreased with increase in concentration of nitric acid from 1 M to 5 M (table 4.2). The decrease in extraction observed in phosphonate-FIL was attributed to the extraction of nitric acid that competes with Pu(IV) ion for coordination in FIL phase. However, the studies on the extraction of nitric acid showed that, the amount of nitric acid extracted in phosphoramide-FIL and phosphonate-FIL [134] are similar. But the distribution trend of Pu(IV) observed in them is quite different. These results indicate that the extracted nitric acid in phosphoramide-TSIL does not seem to compete with Pu(IV) for extraction in ionic liquid phase. This could be possible only when the extracted acid predominantly protonates the amidic (-NH-) moiety in phosphoramide-FIL instead of >P=O which is required for extracting Pu(IV). Upon protonation, the anionic plutonium(IV) nitrate complex is co-extracted in to the ionic liquid phase to preserve the charge balance in phosphoramide FIL. Since the phosphonate-FIL does not contain –NH- moiety in ionic liquid, the extracted acid predominantly protonates the >P=O moiety, thus making >P=O unavailable for Pu(IV) extraction. Therefore the Pu(IV) distribution ratio decreased in phosphonate FIL and increased in case of phosphoramide-FIL with increase in the concentration of nitric acid.

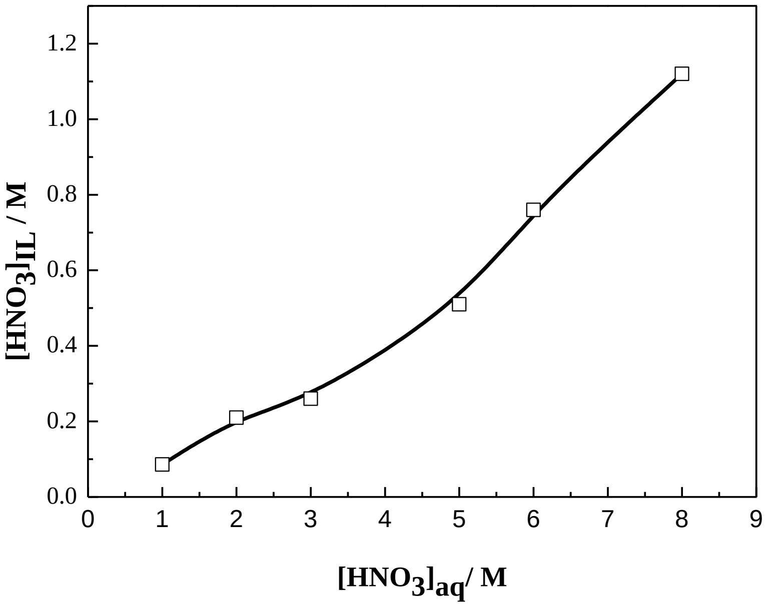

Figure 4.2. Nitric acid extraction isotherm of [BuImPA][NTf$_2$]/[C$_4$mim][NTf$_2$]at 298 K. Ionic liquid phase: 0.3 M [BuImPA][NTf$_2$]/[C$_4$mim][NTf$_2$], aqueous phase: [HNO$_3$] = 1 M - 8 M spiked with ^{239}Pu(IV) tracer

IR spectrum of acid equilibrated 0.3 M [BuImPA][NTf$_2$]/[C$_4$mim][NTf$_2$] was compared with that obtained without acid equilibration in order to confirm the protonation of H$^+$ with –NH- group of phosphormide-FIL. A strong band occurring at

3356 cm^{-1} in [BuImPA][NTf$_2$] is due to N-H stretching. This band disappears upon acid equilibration. Perhaps, the band could have shifted and merged with other strong bands appearing at 3000 cm^{-1}. This indicates that the –NH- present in phosphoramide FIL is protonated upon acid equilibration. The FTIR spectra are shown in figure 4.3.

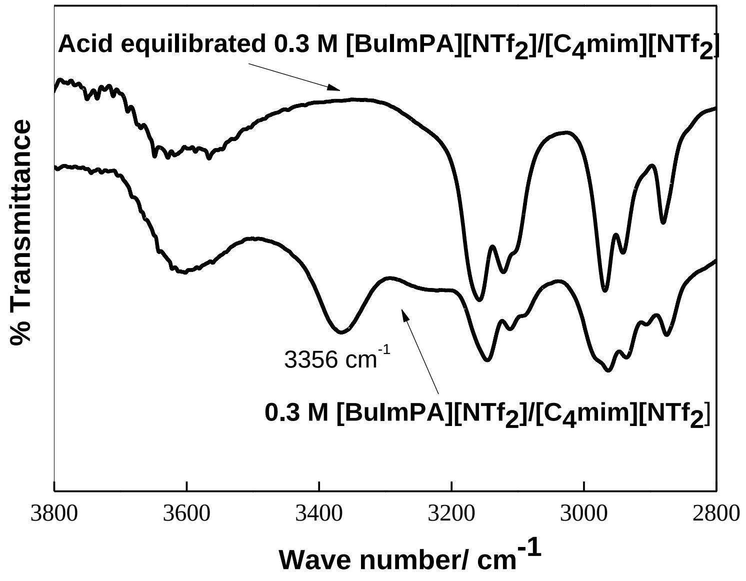

Figure 4.3 FTIR spectra of ionic liquid phase and acid equilibrated ionic liquid phase

4.2.3 Extraction stoichiometry

Since the extraction trend of Pu(IV) in phosphoramide-TSIL is similar to that observed in conventional systems such as TBP in *n*-DD etc. [178,211,212], the plausible mechanism of Pu(IV) extraction in [BuImPA][NTf$_2$]/[C$_4$mim][NTf$_2$] at lower nitric acid concentration (1 M - 4 M) can be represented by equation 4.1.

$$Pu^{4+}{}_{aq} + 4NO_3^-{}_{aq} + y\{[Bu\mathrm{Im}PA][NTf_2]\}_{IL} \Leftrightarrow Pu(NO_3)_4\{[Bu\mathrm{Im}PA][NTf_2]\}_{y_{IL}} \quad (4.1)$$

Subscripts "aq." and "IL" denote the aqueous and ionic liquid phases respectively and "x and y" are the number of nitrate ions and phosphoramide ionic liquid involved in the extraction of plutonium respectively.

The equilibrium constant for the above reaction can be represented by equation 4.2.

$$K_{ex} = \frac{[\mathrm{Pu(NO_3)_4}\{[Bu\mathrm{Im}PA][NTf_2]\}_y]_{IL}}{[Pu^{4+}]_{aq}[\mathrm{NO_3^-}]_{aq}^4\{[Bu\mathrm{Im}PA][NTf_2]\}_{IL}^y}$$

(4.2)

Upon rearrangement, equation 4.2 results in equation 4.3.

$$\log D_{Pu(IV)} = \log K_{ex} + 4\log[NO_3^-]_{aq} + y\log\{[Bu\mathrm{Im}PA][NTf_2]\}_{IL} \qquad (4.3)$$

The effect of [BuImPA][NTf2] concentration on the extraction of plutonium (IV) in ionic liquid phase was studied. The slope obtained from the plot of log $D_{\mathrm{Pu(IV)}}$ against log [BuImPA][NTf2] gives the number of [BuImPA][NTf2] coordinated to Pu(IV) in ionic liquid phase. Figure 4.4 displays the variation in the distribution ratio of Pu(IV) as a function of [BuImPA][NTf2] concentration in ionic liquid phase at constant nitric acid concentration (3 M HNO_3) in aqueous phase.

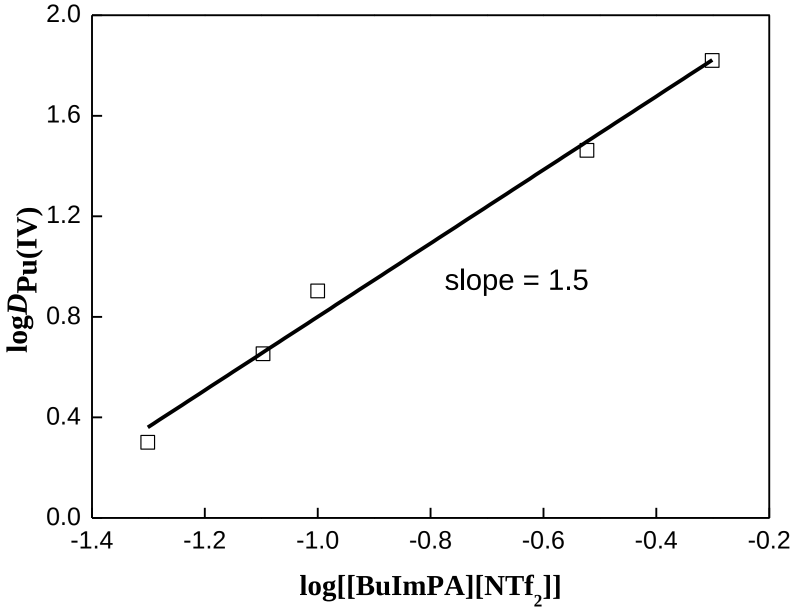

Figure 4.4. Variation in log $D_{Pu(IV)}$ as a function of log [[BuImPA][NTf2]]. Ionic liquid phase: 0.05 M – 0.5 M [BuImPA][NTf2]/[C4mim][NTf2], aqueous phase: [HNO_3] = 3 M spiked with ^{239}Pu(IV) tracer.

It can be seen that the distribution ratio of Pu(IV) increases with increase in the concentration of [BuImPA][NTf_2] in ionic liquid phase. Linear regression analysis of the extraction data results in a slope value of 1.5. This shows that about 1-2 molecules of [BuImPA][NTf_2] are involved in the extraction of Pu(IV) in ionic liquid phase. In addition to this, the extraction of Pu(IV) can also occur by anion exchange mode with [BuImPA][NTf_2] upon protonation on –NH- moiety as discussed above. Therefore the observed slope may be due to both coordination and association of Pu(IV)-complex with protonated FIL.

4.2.4 Anion exchange mechanism

Above 4 M (figure 4.1), the extraction of Pu(IV) could be due to participation of both neutral solvate extraction (as discussed above) and also due to other type of mechanism since the diluent, [C_4mim][NTf_2], also starts extracting Pu(IV) at nitric acid concentrations above 4 M due to the exchange of anionic complex of Pu(IV) with NTf_2^-. To confirm the involvement of anion exchange mechanism in the present case at higher acidity, the variation in the distribution ratio of Pu(IV) in 0.3M [BuImPA][NTf_2]/[C_4mim][NTf_2] was studied as a function of [NTf_2^-] at 5 M nitric acid. The results are shown in the figure 4.5. It is observed that the distribution ratio of plutonium (IV) decreases with increase in the concentration of NTf_2^- ion in aqueous phase, as expected. A similar observation was also reported by Alok *et al.* [134,134]. These results confirm the participation of anion exchange mechanism, shown in equation 4.4, for the extraction of plutonium (IV) in 0.3 M [BuImPA][NTf_2]/[C_4mim][NTf_2] at higher nitric acid concentrations.

$$[Pu(NO_3)_5]^- + \{[C_4mim][NTf_2]\}_{IL} \Leftrightarrow \{[C_4mim][Pu(NO_3)_5]\}_{IL} + [NTf_2^-]_{aq} \qquad (4.4)$$

From the above mentioned studies, the equations 4.1 and 4.4 have been proposed for the extraction of plutonium from phosphoramide-FIL medium. However, it should be noted that NTf_2^-, water and nitrate ions present in the medium can also co-ordinate with Pu(IV) and form other anionic complex and undergo similar kind of extraction. At present it is not possible to point out the presence of such species in the system with the present data. Therefore, further studies are needed to understand the co-ordination chemistry of Pu(IV) in the present ionic liquid system and other possible mechanisms.

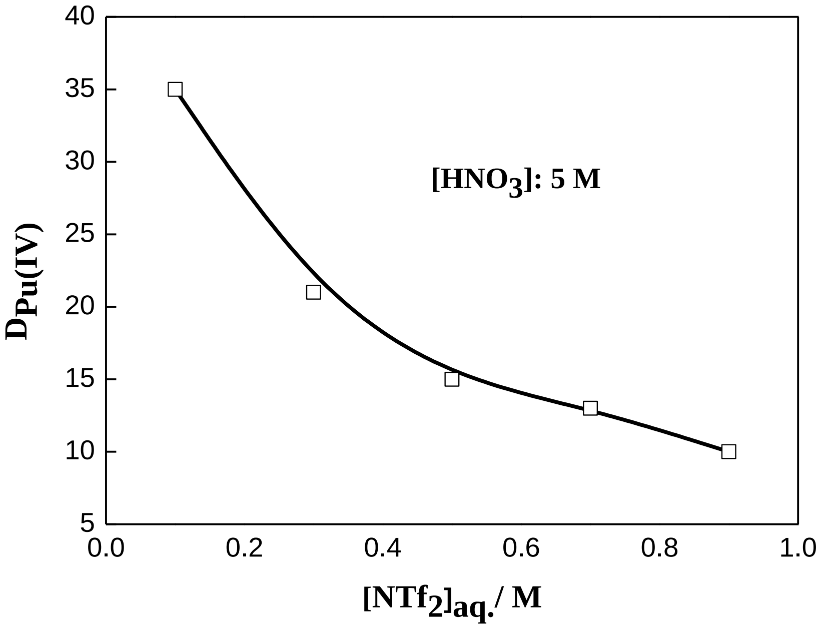

Figure 4.5. Variation in the distribution ratio of Pu(IV) as a function of NTf_2^- concentration in aqueous phase. Ionic liquid phase: 0.3 M [BuImPA][NTf_2]/[C_4mim][NTf_2], aqueous phase: 5 M HNO_3 + varied concentration of [NTf_2^-] ion spiked with ^{239}Pu(IV) tracer.

4.2.5 The separation factor of Pu(IV) over U(VI) and Am(III)

The extraction behavior of Pu(IV) was compared with that of U(VI) and Am(III) in [BuImPA][NTf_2]/[C_4mim][NTf_2] as a function of nitric acid concentration and it is shown in figure 4.6. It is observed that the distribution ratio of U(VI) decreases marginally from 5.4 to 2.4 with increase in nitric acid concentration from 1 M to 8 M unlike Pu(IV). In contrast to both U(VI) and Pu(IV) , the distribution ratio of Am(III) is insignificant (10^{-2}) at all acidities. Table 4.3 shows the separation factor of Pu(IV) over U(VI), Pu(IV) over Am(III) and U(VI) over Am(III) at all nitric acid concentrations.

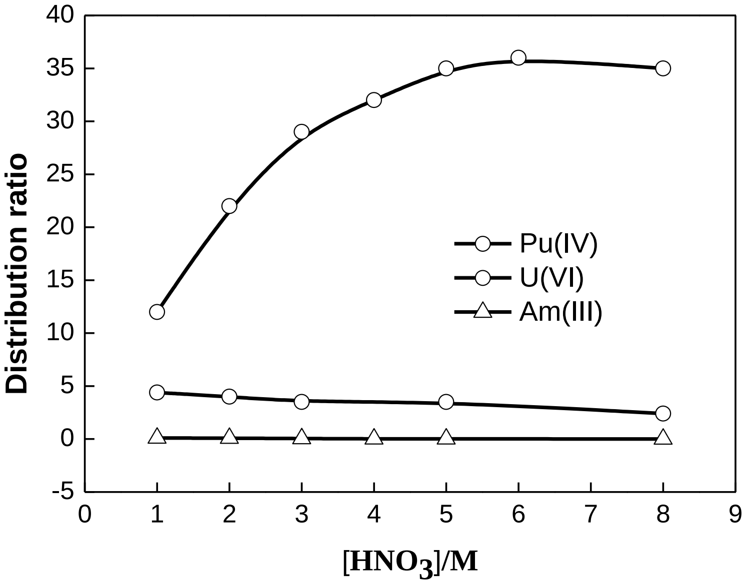

Figure 4.6. Variation in the distribution ratio of actinides as a function of nitric acid concentration in aqueous phase. Ionic liquid phase: 0.3M [BuImPA][NTf$_2$]/[C$_4$mim][NTf$_2$], aqueous phase: [HNO$_3$] = 0.1 M - 8.0 M + spiked with An tracer (An = ^{239}Pu(IV), ^{233}U(VI) and ^{241}Am(III)).

Table 4.3. Separation factor of Pu(IV) over U(VI) and Am(III) achieved using 0.3 M [BuImPA][NTf$_2$]/[C$_4$mim][NTf$_2$]. Aqueous phase = 1 M - 8 M nitric acid. (Separation factor = quotient of distribution ratios).

[HNO$_3$]$_{eq.}$/M	**Separation factor of actinides in 0.3 M [BuImPA][NTf$_2$]/[C$_4$mim][NTf$_2$]**		
	$SF_{Pu(IV)/U(VI)}$	$SF_{Pu(IV)/Am(III)}$	$SF_{U(VI)/Am(III)}$
1	3	120	44
2	5.5	275	50
3	8.3	580	70
5	10	1750	175
8	15	3500	240

It can be seen that the separation factor of Pu(IV) over U(VI) varies from 3 to 15 with the increase in the nitric acid concentration from 1 M to 8 M. However, a separation factor of < 2 was reported in molecular extractants present in *n*-DD [178,211,212]. In the present study, the separation factor of Pu(IV) over Am(III) varies from 120 to 3500 with increase in nitric acid concentration from 1M to 8M. This result indicate that the fissile element plutonium can be easily separated from other actinides U(VI) and Am(III) by using phosphoramide-FIL. Higher extraction of Pu(IV) over other actinides in [BuImPA][NTf_2] /[C_4mim][NTf_2] could be attributed to the extraordinary and specific solvating ability of plutonium complexes in ionic liquid phase. Table 4.3 also shows the separation factor of U(VI) over Am(III) and it varies from 44 to 240 with the increase in nitric acid concentration from 1M to 8M. This observations indicates the possibility of individual separation of Pu(IV), U(VI) and Am(III) from a mixture using phosphoramide-FIL.

4.2.6 Effect of alkyl group attached to imidazolium moiety of TSIL

The effect of alkyl group attached to imidazolium moiety of phosphoramide-FIL on the extraction of Pu(IV) as a function of nitric acid concentration have been studied and it is shown in figure 4.7. The distribution ratio of Pu(IV) increases with increase in the chain length of the alkyl group attached to phosphoramide-FIL at all acidities. This could be attributed to the increase in hydrophobicity of phosphoramide-FIL that seems to facilitate the extraction of neutral $Pu(NO_3)_4$ species in ionic liquid phase.

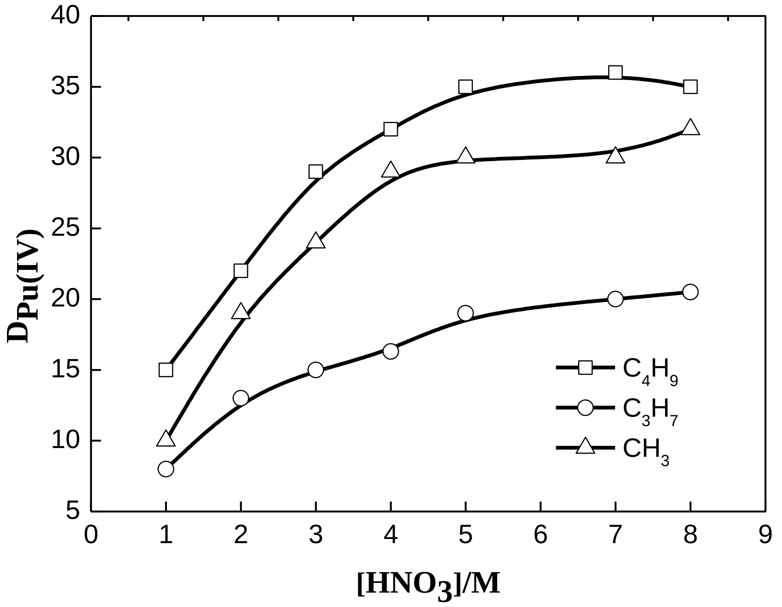

Figure 4.7. Effect of alkyl chain length of imidazolium moiety on the distribution ratio of Pu(IV) at various nitric acid concentrations. Ionic liquid phase: 0.3 M [C_nH_{2n+1}ImPA][NTf_2] (n= 1, 3 and 4) /[C_4mim][NTf_2], aqueous phase [HNO_3] = 1 M – 8 M spiked with ^{239}Pu(IV) tracer.

4.2.7 Effect of alkyl group attached to imidazolium moiety of diluent

The effect of alkyl chain length of [$C_n$mim][NTf_2] ionic liquid on the extraction behavior of Pu(IV) in 0.3 M [BuImPA][NTf_2]/[$C_n$mim][NTf_2] (n = 4,6 and 8) was studied. Figure 4.8 displays the variation in the distribution ratio of Pu(IV) as a function of alkyl chain length attached to imidazolium moiety of ionic liquid diluent. It is interesting to note that the distribution ratio of Pu(IV) decreases with increase in the chain length of the diluent ionic liquid at low acidity (1M – 3M) and increases at high acidity (> 3M). The increasing trend observed at higher acidities, could be attributed to the increase in the hydrophobicity of the [$C_n$mim][NTf_2] ionic liquid [213]. A similar behavior was also reported by us in other ionic liquid system [133]. The reason for the decrease in the distribution ratio of Pu(IV) observed at lower acidities is not clear at present and more studies are needed to understand this behavior.

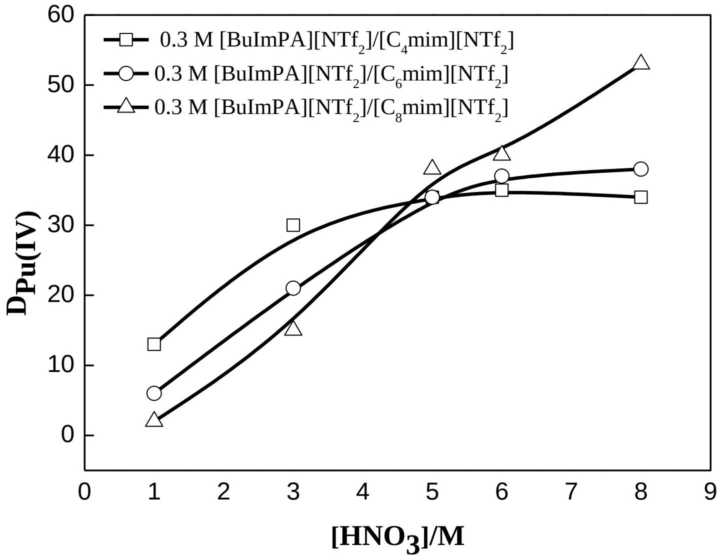

Figure 4.8. Effect of alkyl chain length of imidazolium moiety present in ionic liquid diluent on distribution ratio of Pu(IV) at various nitric acid concentrations. Ionic liquid phase: 0.3 M [BuImPA][NTf$_2$] /[C$_n$mim][NTf$_2$] (n = 4,6 and 8), aqueous phase: [HNO$_3$] = 1 M - 8 M spiked with ^{239}Pu(IV) tracer.

4.2.8 Effect of temperature

To understand the influence of the temperature on the extraction of plutonium (IV) in [BuImPA][NTf$_2$]/[C$_4$mim][NTf$_2$] , the extraction studies were carried out at various temperatures ranging from 298 K to 333 K, to understand the influence of the temperature on the extraction of plutonium (IV) in ionic liquid phase. The variation of log $D_{\mathrm{Pu(IV)}}$ as a function of reciprocal temperature is shown in figure 4.9. It can be seen that the distribution ratio of Pu(IV) at 3 M nitric acid decreases with increase of temperature. This shows that the extraction of Pu(IV) in [BuImPA][NTf$_2$]/[C$_4$mim][NTf$_2$] is exothermic.

The total enthalpy change (ΔH_{tot}) involved in the extraction of Pu(IV) in ionic liquid medium was calculated using Van't Hoff relation of the form shown in equation 4.5. From the slope of the plot shown in figure 4.9, the ΔH_{tot} was found to be -22 kJmol^{-1}.

$$\frac{\partial \log D}{\partial (1/T)} = \frac{-\Delta H_{tot}}{2.303\ R} \qquad (4.5)$$

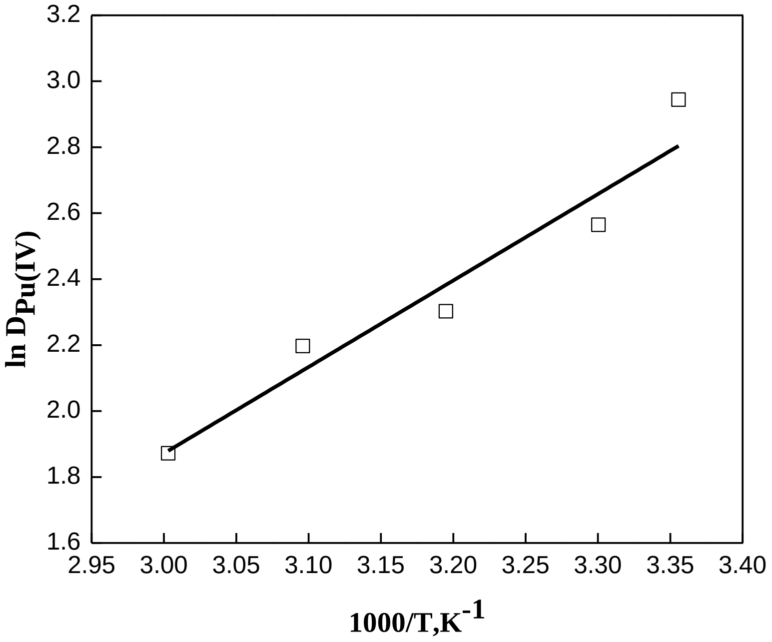

Figure 4.9. Variation in the distribution ratio of Pu(IV) as a function of reciprocal temperature. Ionic liquid phase: 0.3 M [BuImPA][NTf$_2$]/[C$_4$mim][NTf$_2$], aqueous phase: [HNO$_3$] = 3 M spiked with ^{239}Pu(IV) tracer.

4.2.9 Stripping of plutonium

In traditional molecular extraction systems, the back extraction of actinides from the loaded organic phase was usually carried out by using dilute nitric acid. However, stripping of plutonium (IV) from 0.3 M [BuImPA][NTf$_2$] /[C$_4$mim][NTf$_2$] using dilute nitric acid is difficult due to high distribution ratio of Pu(IV) observed at all nitric acid concentration (figure 4.1). Therefore, the complexing agent such as oxalic acid was used for stripping of Pu(IV) from the loaded ionic liquid phase. Prior to stripping, the extraction of Pu(IV) was carried out from 3 M nitric acid in 0.3 M [BuImP][NTf_2]/[C_4mim][NTf_2]. Back extraction was carried out using 0.1M oxalic acid. It was observed that quantitative stripping of plutonium (IV) was achieved in 3 - 4 contacts (1st contact: 69%; 2nd contact: 15% and 3rd contact: 5.7%) with 0.1 M oxalic acid.

4.3 Conclusions

A novel phosphoramide functionalized ionic liquid, [BuImPA][NTf_2], was prepared and studied for the extraction of Pu(IV), U(VI) and Am(III) from nitric acid medium. The extraction of Pu(IV) increased with increase in the concentration of nitric acid reached a plateau at nitric acid concentration more than 4 M. In contrast to this, the extraction of U(VI) and Am(III) showed a decreasing trend and the $D_{U(VI)}$ and $D_{Am(III)}$ were much lower than that obtained for Pu(IV). Unlike traditional extractants, the separation factor of Pu(IV) over U(VI) was about 10 and that over Am(III) was of the order 10^3, suggesting the possibility of separating the fissile element plutonium from other actinides. Below 4 M nitric acid, the primary mode of Pu(IV) extraction in ionic liquid phase seems to be through the ($Pu(NO_3)_4$–([BuImPA][NTf_2])$_2$) neutral species extraction. However, above 4 M nitric acid, anion exchange mode also participates in the extraction of Pu(IV). The -NH- moiety in phosphormide-TSIL was protonated predominantly over >P=O and that seems to facilitate the extraction of Pu(IV) in ionic liquid phase**.**

PART II

Insights into the solvent extraction behavior of U(VI) in PUREX solvent containing RTIL with strongly coordinating anion

In the recent past, the quaternary ammonium salt (Aliquat-336) based ionic liquids are becoming popular in the area of solvent extraction, owing to their unique and favorable properties [69-70,132,140,210]. Aliquat-336 (trioctylmethylammonium chloride, $[A336]]^+[Cl]^-$) is regarded as a versatile and affordable cation source for the synthesis of new family of hydrophobic ionic liquids. Aliquat-336 based ionic liquids are strongly hydrophobic and miscible in many of the non-polar solvents. These ionic liquids exhibit a density lower than 0.9 g/mL and negligible solubility in aqueous phase, which are indeed desirable for adapting these ionic liquids for counter-current solvent extraction applications. In addition, ionic liquids namely trioctylmethylammonium chloride ($[A336]]^+[Cl]^-$) and trioctylmethylammonium nitrate $[A336]]^+[NO_3]^-$) are available commercially and affordable for making a new family of hydrophobic ionic liquids.

Sun *et al.* [69] and Ling *et al.* [70] studied the extraction behavior of rare earths from aqueous solution using $[A336]^+$ based ionic liquids. The authors reported that the solubility of these ionic liquids in aqueous phase were negligible and did not undergo any ion exchange during extraction. Alok *et al.* synthesized a couple of Aliquat-336 based ionic liquids namely tri-*n*-octylmethylammonium bis-(2-ethylhexyl) phosphate ($[A336]^+[DEHP]^-$) and tri-*n*-octylmethylammonium bis-(2-ethylhexyl)diglycolamate ($[A336]^+[DGA]^-$) and studied for extraction of Eu(III) and Am(III) from aqueous solutions [132] and also studied the extraction behavior of U(VI), Pu(IV) and Am(III) from nitric acid medium in using $[A336]^+[DEHP]^-$[140]. The miscibility of $[A336]^+[DEHP]^-$ ionic liquid in *n*-DD was exploited to modify the extractive properties of the PUREX solvent, 1.1 M TBP/n-DD, to exhibit selectivity towards Pu(IV). However, the mechanistic aspects of extraction of actinides using $[A336]^+[DEHP]^-$ were not studied.

The aim of part II in chapter 4 is to report the results on the extraction of U(VI) in $[A336]^+[DEHP]^-$ ionic liquid as well as in 1.1 M TBP/*n*-DD solution containing small concentrations of $[A336]^+[DEHP]^-$. The extraction of U(VI) was also studied in the constituents of $[A336]^+[DEHP]^-$ ionic liquid, namely $[A336]^+[NO_3]^-$ and bis-(2-ethylhexyl)phosphoric acid (HDEHP), to bring out the insights of extraction.

Table 4.4 Structures of RTILs and molecular extractants used in part II of chapter 4

Name of RTIL	Structure
Tri-*n*-octylmethylammonium bis-(2-ethylhexyl)phosphate ($[A336]^+[DEHP]^-$)	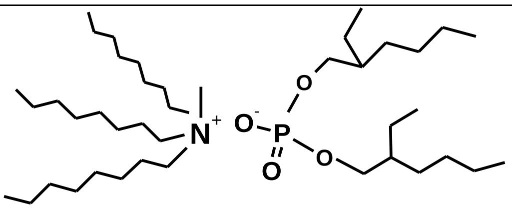
Tri-*n*-octylmethylammonium nitrate ($[A336]^+[NO_3]^-$)	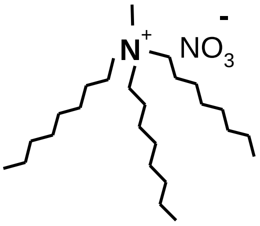
Di(2-ethylhexyl)phosphoric acid (HDEHP)	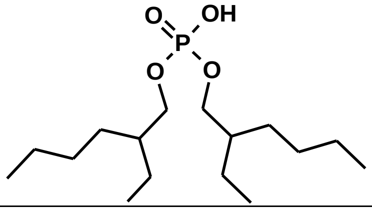
Tri-*n*-butylphosphate (TBP)	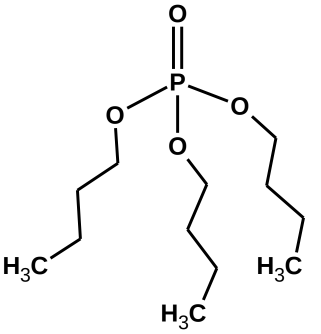

Synthesis of the ionic liquid used in part II has been discussed in section 2.9.5 of chapter 2.

4.4 Results and Discussion

4.4.1 Extraction of U(VI) in TBP in presence of ionic liquid

The extraction behavior of U(VI) in PUREX solvent (1.1 M TBP/*n*-DD) was studied in the presence and absence of $[A336]^+[DEHP]^-$ as a function of nitric acid concentration and it is depicted in figure 4.10.

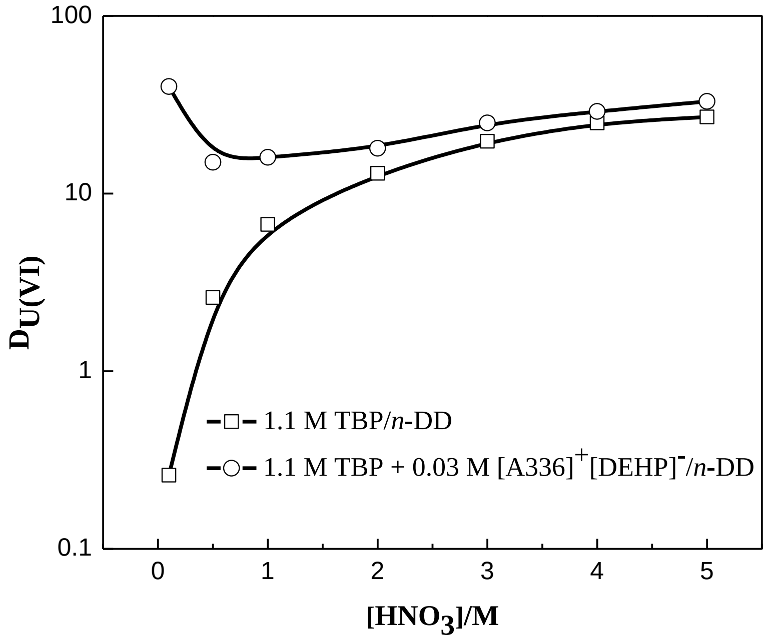

Figure 4.10. Effect of adding of $[A336]^+[DEHP]^-$ ionic liquid in 1.1 M TBP/n-DD on the extraction of U(VI) from nitric acid medium. Organic phase: 1.1 M TBP/n-DD or 1.1 M TBP + 0.03 M $[A336]^+[DEHP]$ /n-DD. Aqueous phase: Nitric acid concentrations ranging from 0.1 to 5 M spiked with $^{233}U(VI)$ tracer.

The distribution ratio of U(VI) in 1.1 M TBP/*n*-DD increases with increase in concentration of nitric acid as described elsewhere [158]. The extraction behavior observed in the presence of 0.03 M $[A336]^+[DEHP]$ is remarkably different from the other. A two fold increase in the distribution ratio of U(VI) was observed in the presence of ionic liquid at low nitric acid concentrations (~ 0.1 M). The distribution ratio of U(VI) initially decreases with increase in concentration of nitric acid, reaches a minimum at

0.5 M nitric acid, followed by gradual increase in distribution values. The distribution ratios in presence of ionic liquid are similar to that observed in TBP/*n*-DD at acidities more than 2 M.

This extraction trend is quite similar to the trend observed for the extraction of U(VI) in 1.1 M TBP in $[C_4mim][NTf_2]$ medium reported by Giridhar *et al.* [158] as well as by Dietz *et al.* [122]. In addition, Dietz *et al*. [122] also studied the mechanism of U(VI) extraction in TBP/$[C_nmim][NTf_2]$ solution. The decrease in extraction trend observed at low acidities was attributed to the cation exchange mechanism, and the mechanism was reported to change from ion exchange to solvation type with the increase of alkyl chain length attached to the imidazolium moiety from butyl to decyl group. Therefore, the initial decrease in the distribution ratios observed in the present study suggests the possibility of cation exchange at low acidities. However, it is necessary to probe the possibility of such ion exchange in systems containing $A336^+$ cation, which is regarded as strongly hydrophobic.

4.4.2 Extraction of U(VI) in Ionic liquid ($[A336]^+[DEHP]^-$)

The extraction of U(VI) by ionic liquid alone was studied as a function of nitric acid concentration to understand the role of ionic liquid when it was dissolved in PUREX solvent. Since the ionic liquid, $[A336]^+[DEHP]^-$ contains strongly coordinating anion, bis(2-ethylhexyl) phosphate (DEHP), it is quite likely that U(VI) is extracted by ionic liquid itself. Figure 4.11 shows the variation in the distribution ratio of U(VI) in 0.03 M $[A336]^+[DEHP]^-$/*n*-DD. It is observed that the distribution ratio of U(VI) decreases with increase in the concentration of nitric acid. The decreasing trend suggests the possibility of cation exchange. The cation exchange could occur by the exchange of $A336^+$ cation with UO_2^{2+} or $\{UO_2(NO_3)^+\}$ ion as shown in the equation 4.8 and 4.9.

$$UO_{2\,aq.}^{2+} + 2\,[A336]^{+}[DEHP]^{-}_{IL} \Leftrightarrow UO_2(DEHP)_{2IL} + 2\,A336^{+}_{aq.} \quad . \quad (4.8)$$

$$UO_2(NO_3)^{+}_{aq.} + [A336]^{+}[DEHP]^{-}_{IL} \Leftrightarrow UO_2(NO_3)(DEHP)_{IL} + A336^{+}_{aq.} \quad (4.9)$$

However, such possibility is quite unlikely as the A336$^+$ cation is strongly hydrophobic. Another possibility for the extraction of U(VI) by $[A336]^+[DEHP]^-$ could be through the ion exchange of H$^+$ from HDEHP with UO_2^{2+} or $UO_2(NO_3)^+$ ion by the reactions shown in equations 4.10 and 4.11. However, such a possibility requires conversion of $[DEHP]^-$ ion present in organic phase to HDEHP during equilibration with nitric acid.

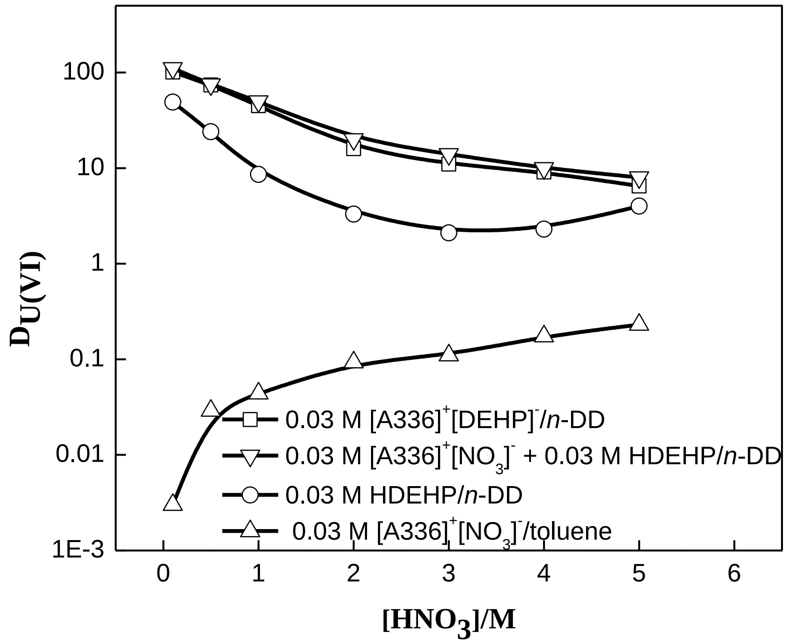

Figure 4.11. Extraction of U(VI) in ionic liquid and constituents of ionic liquid. Organic phase: Ionic liquid or constituents of ionic liquid in n-DD. Aqueous phase: Nitric acid concentrations ranging from 0.1 to 5 M spiked with ^{233}U(VI) tracer.

$$UO_{2\,aq.}^{2+} + 2\,(HDEHP)_{2IL} \Leftrightarrow UO_2\,(HDEHP)_2(DEHP)_{2IL} + 2\,H^{+}_{aq} \quad (4.10)$$

$$UO_2(NO_3)^{+}_{aq.} + HDEHP_{IL} \Leftrightarrow UO_2(NO_3)(DEHP)_{IL} + H^{+}_{aq.} \quad (4.11)$$

$$[A336]^{+}[DEHP]^{-}_{IL} + HNO_{3aq.} \Leftrightarrow [A336]^{+}[NO_3]^{-}_{IL} + HDEHP_{IL} \quad (4.12)$$

Figure 4.12 shows the extraction of nitric acid in 0.03 M $[A336]^+[DEHP]^-$/*n*-DD. It can be seen that the extraction of nitric acid increases with increase in the concentration of nitric acid in aqueous phase. Nearly 0.02 M of nitric acid is extracted into 0.03 M $[A336]^+[DEHP]^-$ even at the aqueous phase concentration of 1 M. This indicates that the ionic liquid $[A336]^+[DEHP]^-$ present in organic phase is converted to its constituents $[A336]^+[NO_3]^-$ and HDEHP by the reaction shown in equation 4.12. Therefore it is quite likely that U(VI) is extracted by HDEHP as well as $[A336]^+[NO_3]^-$ under this condition. In view of this, the extraction of U(VI) in $[A336]^+[DEHP]^-$ can be visualized to consist of extractions contributed by $[A336]^+[NO_3]^-$ and HDEHP. Therefore, it is necessary to study the extraction of U(VI) in $[A336]^+[NO_3]^-$/*n*-DD as well as HDEHP/*n*-DD and compare with $[A336]^+[DEHP]^-$.

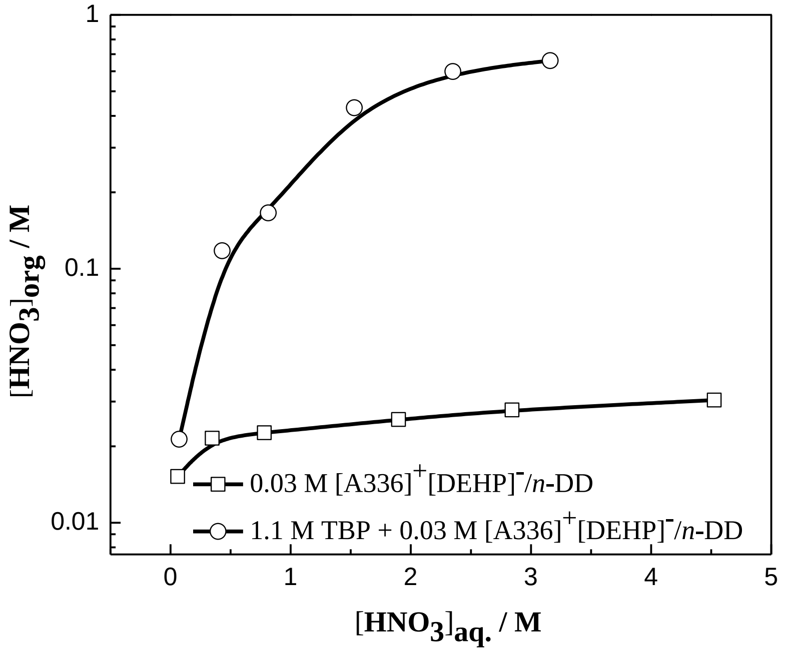

Figure 4.12. Extraction of nitric acid in ionic liquid and TBP + ionic liquid. Organic phase: 0.03 M $[A336]^+[DEHP]$ /n-DD or 1.1 M TBP + 0.03 M $[A336]^+[DEHP]$ /n-DD. Aqueous phase: Nitric acid concentrations ranging from 0.1 to 5 M.

4.4.3 Extraction of U(VI) in HDEHP and $[A336]^+[NO_3]^-$

The extraction behavior of U(VI) in 0.03 M HDEHP/*n*-DD is shown in figure 4.11 The results are compared with 0.03 M $[A336]^+[DEHP]^-$ in *n*-DD. The distribution ratio of U(VI) in 0.03 M HDEHP/*n*-DD decreases with increase in the concentration of nitric acid as expected for the ion exchange mechanism [122] shown in equations 4.10 & 4.11 at low acidities (< 2 M). Above 2 M nitric acid, the distribution ratio of U(VI) in 0.03 M HDEHP/*n*-DD increases marginally due to the solvation type of mechanism operating for extraction, as described elsewhere [214]. It is important to note that the distribution ratios observed in HDEHP are lower than those observed in $[A336]^+[DEHP]^-$. This could perhaps be due to the participation of $[A336]^+[NO_3]^-$ in facilitating the extraction of U(VI) in $[A336]^+[DEHP]^-$. To confirm this, it is necessary to study the extraction of U(VI) in $[A336]^+[NO_3]^-$. Since $[A336]^+[NO_3]^-$ was not soluble in *n*-DD, the distribution ratio of U(VI) in 0.03 M $[A336]^+[NO_3]^-$/*n*-DD could not be measured. Instead, the distribution ratio of U(VI) was measured in a solution of 0.03 M $[A336]^+[NO_3]^-$ present in an aromatic diluent, toluene, and results are plotted in figure 4.11. It is observed that the distribution ratios vary from 10^{-3} to 0.23 with increase in nitric acid concentration from 0.1 M to 5 M, indicating that U(VI) is inextracable by $[A336]^+[NO_3]^-$. However, higher distribution ratios observed in $[A336]^+[DEHP]^-$ shows that the presence of $[A336]^+$ ion facilitates the extraction of U(VI). This could be possible only when $[A336]^+[NO_3]^-$ in conjunction with HDEHP, synergically extracts U(VI) from nitric acid medium.

To verify this hypothesis, the distribution ratio of U(VI) was measured in a solution of 0.03 M $[A336]^+[NO_3]^-$ + 0.03 M HDEHP/*n*-DD and compared with 0.03 M $[A336]^+[DEHP]^-$/*n*-DD. The results are also shown in figure 4.11. It should be noted that $[A336]^+[NO_3]^-$ is soluble in *n*-DD in the presence of HDEHP and TBP. It is interesting to note that the distribution ratio of U(VI) in both the systems are comparable, even though the $[A336]^+[NO_3]^-$ and HDEHP are added independently in *n*-DD. This shows that the presence of $[A336]^+[NO_3]^-$ in conjunction with HDEHP/n-DD facilitates the extraction of U(VI). The result also confirm that $[A336]^+[DEHP]^-$ reacts with nitric acid by the reaction shown in equation 4.12, leading to the formation of $[A336]^+[NO_3]^-$ and HDEHP. The synergic combination of these constituents in organic phase seems to govern the extraction of U(VI).

4.4.4 Extraction of U(VI) in TBP/*n*-DD containing IL constituents

Based on the above studies, the difference in the extraction of U(VI) observed in the presence of ionic liquid in case of 1.1 M TBP/*n*-DD shown in figure 4.13 ,could be attributed to the extraction governed by the constituents of ionic liquid. It is evident from figure 4.12 that significant amount of nitric acid is extracted into 1.1 M TBP + 0.03 M $[A336]^+[DEHP]^-$/*n*-DD, leading to the formation of ionic liquid constituents in organic phase. Therefore, it is necessary to study the extraction behavior of U(VI) in 1.1 M TBP/*n*-DD in the presence of ionic liquid constituents $[A336]^+[NO_3]^-$ and HDEHP. The extraction behavior of U(VI) in 1.1 M TBP + 0.03 M $[A336]^+[NO_3]^-$/*n*-DD is shown in figure 4.13. The distribution ratio of U(VI) obtained in this case is comparable to that obtained in 1.1 M TBP/*n*-DD.

This shows that the presence of $[A336]^+[NO_3]^-$ in TBP/*n*-DD does not play any role. Similarly, the variation in the distribution ratio of U(VI) in 1.1 M TBP + 0.03 M HDEHP/*n*-DD is also shown in figure 4.13. It is interesting to note that the distribution ratios observed in this case are comparable with those observed in 1.1 M TBP + 0.03 M $[A336]^+[DEHP]^-$. This indicates that the extraction of U(VI) in TBP + $[A336]^+[DEHP]^-$ is governed essentially by the extraction in TBP and HDEHP. A twofold increase in the distribution ratio observed at low acidities and a comparable distribution ratios observed at higher acidities can be thus attributed to the synergic extraction of U(VI) by a solution of TBP and HDEHP present in *n*-DD [215].

The extraction of U(VI) in a combined solution of 1.1 M TBP + 0.03 M $[A336]^+[NO_3]^-$ + 0.03 M HDEHP/*n*-DD is also shown in figure 4.13

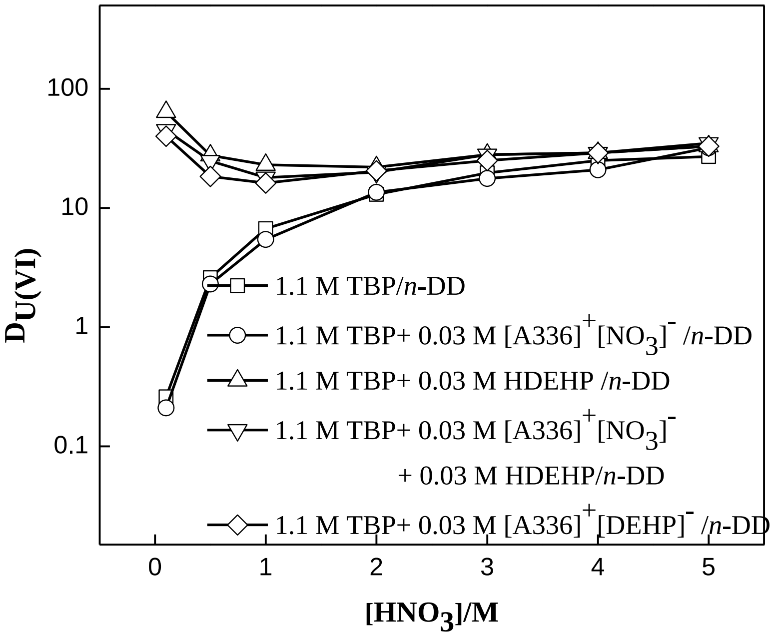

Figure 4.13 Comparison in the extraction behavior of U(VI) in 1.1 M TBP/n-DD in presence of $[A336]^+[DEHP]^-$, $[A336]^+[NO3]^-$ and HDEHP at various concentrations of nitric acid. Organic phase: 1.1 M TBP or 1.1 M TBP + ionic liquid or 1.1 M TBP + ionic liquid constituents in n-DD. Aqueous phase: Nitric acid concentrations ranging from 0.1 to 5 M spiked with ^{233}U(VI) tracer.

The extractants $[A336]^+[NO_3]^-$ and HDEHP were added independently in 1.1 M TBP/*n*-DD to obtain this solution. The distribution ratios obtained in this case are comparable with those obtained in 1.1 M TBP + 0.03 M HDEHP/*n*-DD as well as 1.1 M TBP + 0.03 M $[A336]^+[DEHP]^-$/*n*-DD. These results indicate that $[A336]^+[NO_3]^-$ present in the organic phase does not play any role in the present solution, which is in contrast to that observed in the extraction of U(VI) by $[A336]^+[DEHP]^-$ alone. It appears that the presence of TBP in organic phase nullifies the role of $[A336]^+[NO_3]^-$. This fact can be evident by comparing the distribution ratios of U(VI) observed in 0.03 M $[A336]^+[DEHP]^-$/*n*-DD in the presence and absence of TBP as shown is figure 4.14.

It can be seen that the presence of TBP in 0.03 M $[A336]^+[DEHP]^-$/*n*-DD lowers the distribution ratio of U(VI) at nitric acid concentration lower than 2 M. This could be perhaps due to the protonation of $DEHP^-$ ion by nitric acid, which is extracted by the organic phase to a larger extent in the presence of TBP. (figure 4.12). As the nitric acid concentration in aqueous phase is increased the availability of $DEHP^-$ seems to decrease remarkably by protonation and above 2 M nitric acid, TBP and HDEHP (perhaps the mixed species) controls the extraction of U(VI) as discussed above. The result thus confirms that the presence of TBP at low nitric acid concentration (< 2 M) nullifies the participation of $[A336]^+[NO_3]^-$ for extraction. Moreover, the study also indicates that the extraction of U(VI), in TBP+$[A336]^+[DEHP]^-$/*n*-DD from nitric acid medium is accompanied by the extraction of nitric acid leading to the formation of ionic liquid constituents, namely $[A336]^+[NO_3]^-$ and HDEHP. The constituents present in conjunction with TBP/*n*-DD seems to control the extraction of U(VI) from nitric acid medium. Based on the above observations, the following equations 4.12 & 4.13 could be proposed for the extraction of U(VI) in TBP+$[A336]^+[DEHP]^-$/*n*-DD.

$$[A336]^+[DEHP]^-_{IL} + HNO_{3aq.} \Leftrightarrow [A336]^+[NO_3]^-_{IL} + HDEHP_{IL} \qquad (4.12)$$

$$UO_{2\,aq}^{2+} + (2-x)NO_{3\,aq}^{-} + x\,HDEHP_{org} + (2-y)TBP_{org} \Leftrightarrow UO_2(NO_3)_{(2-x)}(DEHP)_x(TBP)_{(2-y)org} + xH^+_{aq}$$

$$\text{where} \quad 0 > x < 2 \; and \; 0 > y < 2 \qquad (4.13)$$

In this equation the two molecules of TBP is considered for extraction, which is well established [11]. Both HDEHP and TBP are proposed to participate in the extraction of uranium (VI) at all acidities [215]. However, the contribution of HDEHP is predominant at lower acidity and that of TBP at higher acidity.

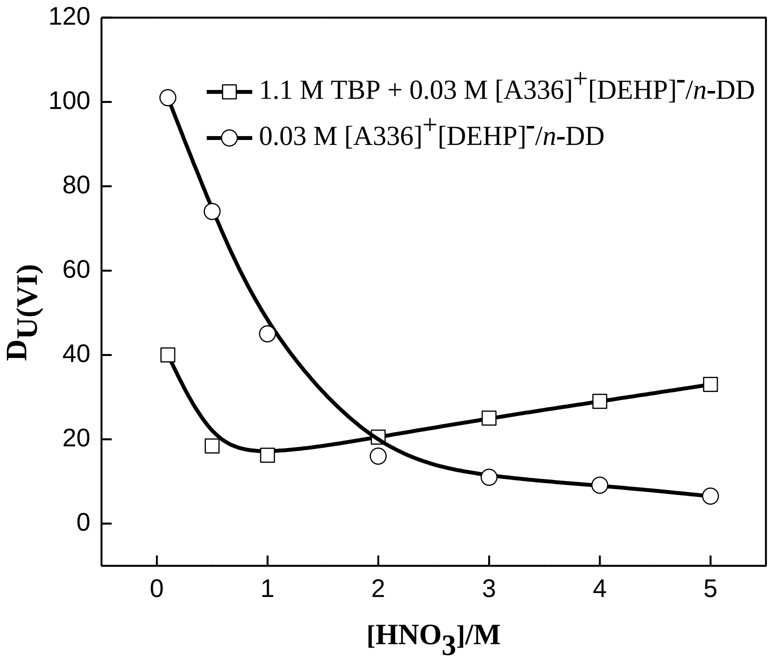

Figure 4.14. Comparison in the extraction behavior of U(VI) in $[A336]^+[DEHP]^-$/n-DD and TBP + $[A336]^+[DEHP]^-$/n- DD at various concentrations of nitric acid. Organic phase: 0.03 M $[A336]^+[DEHP]^-$/n-DD or 1.1 M TBP + 0.03 M $[A336]^+[DEHP]^-$/n-DD. Aqueous phase: Nitric acid concentrations ranging from 0.1 to 5 M spiked with ^{233}U(VI) tracer.

4.5 Conclusion

The extraction behavior of U(VI) in the PUREX solvent, 1.1 M TBP/*n*-DD, was studied in the presence of a paraffin soluble ionic liquid, $[A336]^+[DEHP]^-$. Remarkable enhancement in the distribution ratio of U(VI) was observed in the presence of ionic liquid. The extraction of U(VI) in $[A336]^+[DEHP]^-$/*n*-DD alone was studied to understand the role of ionic liquid in the PUREX solvent during extraction. The distribution ratio of U(VI) in $[A336]^+[DEHP]^-$/*n*-DD decreased with increase in the concentration of nitric acid. The extraction of U(VI) in $[A336]^+[DEHP]^-$ medium was accompanied by the extraction of nitric acid leading to the formation of ionic liquid components namely $[A336]+[NO_3]^-$ and HDEHP in organic phase. The presence of these constituents facilitated the extraction of U(VI) in organic phase. Synergic extraction of U(VI) was observed when HDEHP was employed in conjunction with $[A336]^+[NO_3]^-$ and TBP. The study revealed that the distribution ratio of U(VI) obtained in presence of ionic liquid was due to the synergic contributions of ionic liquid components and TBP.

CHAPTER 5

LOADING BEHAVIOUR OF Eu(III) IN DIGLYCOLAMIDE/ROOM TEMPERATURE IONIC LIQUID SYSTEM

5.1 Introduction

The third phase formation is an undesirable event in solvent extraction procedures and usually it occurs due to the incompatibility of polar metal-solvate (or acid-solvate) with non-polar hydrocarbon diluents at metal loadings beyond a particular value referred as limiting organic concentration (LOC) and the corresponding aqueous phase concentration of metal ion is called as critical aqueous concentration (CAC) [185]. The organic phase splits into two phases during the course of solvent extraction with the heavier one, rich in metal—solvate, and the lighter phase rich in diluent. The heavy phase is known as “Third Phase”. The formation of third phase creates an inhomogeneous density and changes in the viscosity of organic phase leading to complication in the hydrodynamics of solvent extraction process. The third phase formation is one of the major problems in the extraction of actinides due to the accumulation of fissile elements at third phase, causing criticality problems. Therefore, elimination of third phase formation is essential for the successful operation of solvent extraction procedures, especially during the extraction of actinides. The third phase formation is dependent on several parameters such as temperature, equilibrium aqueous phase acidity, structure of the extractant and nature of diluent etc. [216].

Several studies have been reported to avoid the third phase formation by adding phase modifiers to the organic phase, in significant concentration [192,217,218]. The phase modifiers in such cases are usually another extractant or long chain aliphatic alcohol. However, the addition of phase modifier to the solvent phase increased the extraction of unwanted metal ion, and decreased the selectivity of target metal ions. Therefore, it is envisaged that the solvent phase without any phase modifier would be desirable for the extraction of target metal ions from aqueous medium.

The use of room temperature ionic liquids as diluent in solvent extraction would be expected to change the physical and chemical properties of organic phase [122] due to the ionic nature of RTILs. It is expected that ionic liquids could stabilize the polar metal-solvate complex in organic phase and could prevent the undesirable third phase formation, if ionic liquids are used as diluent in place of conventional diluent, *n*-dodecane. Recently, the loading behavior of europium(III) from nitric acid medium in a solution of *n*-octyl(phenyl)-*N,N*-isobutylcarbamoylmethylphosphine oxide (CMPO) and tri-*n*-butylphosphate (TBP) dissolved in 1-butyl-3-methylimidazolium bis(trifluoromethanesulfonyl) imide ([C_4mim][NTf_2]) was reported in literature [219] and nearly ~ 40 mg/mL loading could be achieved with the use of 0.2 M CMPO - 1.2 M TBP/[C_4mim][NTf_2] phase without any third phase formation while the LOC of Eu(III) in *n*-DD was ~9 mg/mL.

In the recent past, Diglycolamides (DGAs), *N*,*N*,*N'*,*N'*-alkyl- 3-oxapentane-1, 5-diamide derivatives have been receiving much attention due to their completely incinerable property [188]. They have been considered as possible alternative to CMPO due to their excellent extraction behavior towards trivalent actinide ions. Among the various DGAs, the octyl-substituted derivatives such as *N*,*N*,*N'*,*N'*-tetraoctyl diglycolamide (TODGA) and *N*,*N*,*N'*,*N'*-tetra-2-ethylhexyl diglycolamide (TEHDGA) have been studied extensively in molecular diluent (*n*-dodecane) medium [190,191,220]. However, both these reagents form third phase when 0.1 M DGA/*n*-

DD was contacted with 6 M nitric acid [181,221]. In addition, they form third phase with trivalent metal ions also when the concentration of trivalent metal ion in 3 M nitric acid exceeds 1 g/L. In contrast to this, the concentration of trivalent metal ions in nuclear waste could vary from 0.5 to 3 g/L depending upon the burn-up of the fuel [222]. The third phase formation limit goes down further with increase in the concentration of nitric acid in the feed [181]. These diglycolamides form third phase during the extraction of trivalent metal ion from nuclear waste and they require organic phase modifiers to overcome the third phase formation. However, no studies have been reported so far in literature to understand the loading behavior of trivalent metal ions in a solution of diglycolamides dissolved in RTIL diluent at high aqueous phase concentrations, even though the ionic liquids are known to stabilize the polar metalsolvate complexes.

Therefore, the objective of the present chapter is to report the results on the extraction behaviour of Eu(III) in a solution of *N*,*N*,*N'*,*N'*-tetraoctyl diglycolamide (TODGA) present in 1-octyl-3-methylimidazolium bis (trifluoromethanesulfonyl) imide ([C_8mim][NTf_2]) ionic liquid medium at higher Eu(III) loading conditions ranging from 1 to 95 g/L Eu(III).

Experimental parts of the present chapter have been discussed in the section 2.5 and 2.8.6 of the chapter 2.

Table 5.1. Structures of RTILs and molecular extractants studied in chapter 5

Name	**Structure**
Extractant	
N,N,N',N'-tetraalkyl diglycolamides i.) *N,N,N',N'*-tetraoctyl diglycolamide (TODGA) [where R= R^1 = Octyl] ii.) *N,N,N',N'*-tetra-2-ethylhexyl diglycolamide (TEHDGA) [R=R^1 = 2-ethylhexyl] iii.) *N,N,N',N'*-di-2-ethylhexyl-dioctyl diglycolamide (DEHDODGA) [R= Octyl, R^1 =2-ethylhexyl)	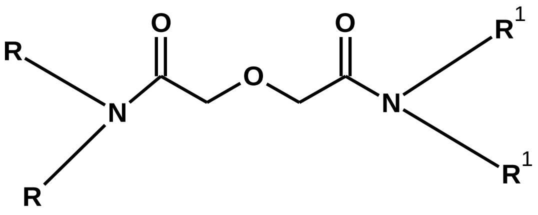
Ionic liquid	
1-Alkyl-3-methylimidazolium bis(trifluoromethanesulfonyl)imide ($[C_nmim][NTf_2]$) $[C_4mim][NTf_2]$ (R: C_4H_9) $[C_6mim][NTf_2]$ (R: C_6H_{13}) $[C_8mim][NTf_2]$ (R: C_8H_{17})	$(CF_3SO_2)_2N^-$ 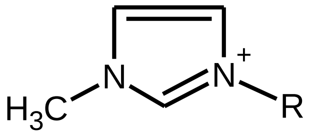

Synthesis of the ionic liquid and extractants used in this chapter have been discussed in section 2.9.1 & 2.9.9 of chapter 2.

5.2 Results and Discussion

5.2.1 Effect of nitric acid concentration

Solvent extraction of Eu(III) using a solution of TODGA dissolved in [C_8mim][NTf_2] as function of nitric acid concentration was carried out and the results are shown in figure 5.1. Concentration of Eu(III) in this case was ~10^{-4} M. The distribution data obtained in 0.01 M TODGA/ [C_8mim][NTf_2] was compared with that reported in a molecular diluent (*i.e.* 0.1 M TODGA/*n*-DD) as well as with ionic liquid alone in figure 5.1. It can be seen that the distribution ratios of Eu(III) ($D_{Eu(III)}$) in [C_8mim][NTf_2] alone are negligible (~10^{-2}) at all acidities investigated in the present study. However, remarkable increase in the $D_{Eu(III)}$ values was observed in presence of TODGA. Moreover, $D_{Eu(III)}$ in 0.01 M TODGA/[C_8mim][NTf_2] decreases with increase in concentration of nitric acid. In contrast, the distribution ratio of Eu(III) in 0.1 M TODGA/*n*-DD (molecular diluent) increases with increase in the concentration of nitric acid reaches a plateau at 2–3 M in nitric acid. The decrease in $D_{Eu(III)}$ with increase in the concentration of nitric acid observed in TODGA/[C_8mim][NTf_2] system could be attributed to the competition between the proton and Eu(III) ion for extraction by TODGA. A similar extraction trend was also reported by Shimojo *et al.* for the extraction of trivalent lanthanides (La(III), Eu(III), and Lu(III)) in a solution of TODGA present in 1-ethyl-3-methylimidazolium bis(trifluoromethylsulphonyl)imide ([C_2mim][NTf_2]) ionic liquid [126] and proposed the involvement of cation exchange mechanism for the extraction of lanthanides in TODGA/[$C_n$mim][NTf_2] (n = 2, 4, 6) and it is shown in equation 5.1. Similarly, Prathibha *et al.* studied the extraction behavior of Am(III) in TODGA/[C_4mim][NTf_2] and proposed a similar mechanism [223].

$$\mathrm{Ln}^{3+}_{aq} + 3TODGA_{IL} + 3[C_n mim]^{+}_{IL} \Leftrightarrow Ln(TODGA)^{3+}_{3\,IL} + 3[\mathrm{C_n mim}]^{+}_{\mathrm{aq}} \qquad (5.1)$$

Therefore, the extraction trend observed in the present case (*i.e.* in 0.01 M TODGA / [C_8mim][NTf_2]) also indicates the possibility of cation exchange mechanism, which is prevalent in imidazolium based ionic liquids.

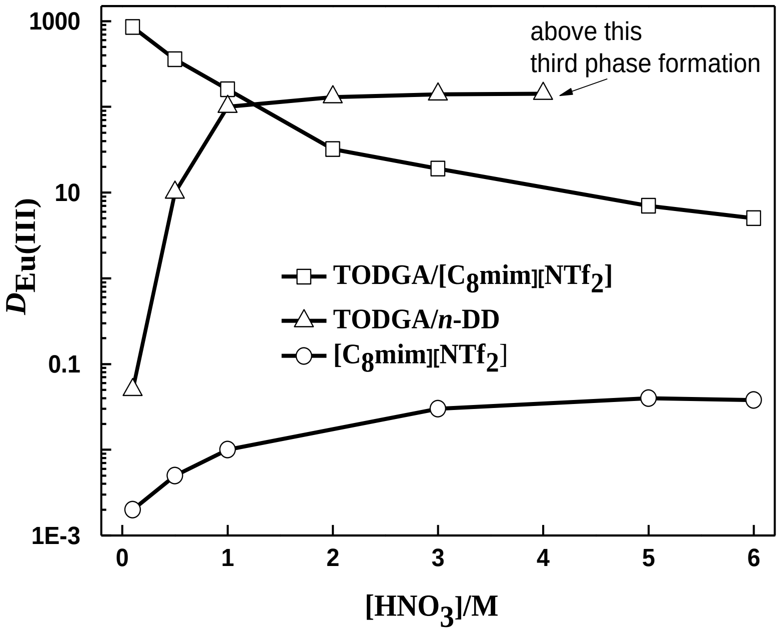

Figure 5.1.Variation in the distribution ratio of Eu(III) as a function of nitric acid concentration in aqueous phase. Ionic liquid phase: 0.01 M TODGA/ [C_8mim][NTf_2] or [C_8mim][NTf_2] alone, organic phase: 0.1 M TODGA/ n-DD and aqueous phase: 0.1 M – 6.0 M HNO_3 spiked with $^{(152+154)}$Eu(III) tracer.

It should be noted from figure 5.1 that the distribution ratio of Eu(III) obtained at lower acidities in TODGA/ionic liquid is about two to three order more than that observed in *n*-DD, even though the concentration of TODGA employed in *n*-DD is an order (0.1 M) more than that employed in ionic liquid (0.01 M) medium. Similarly, the distribution ratio of Eu(III) observed in TODGA/ionic liquid phase is quite appreciable even at higher acidities ($D_{Eu(III)}$ = 5 at 6 M HNO_3, 83% extraction), even though the distribution values in ionic liquid becomes lower than that obtained in *n*-DD, at acidities greater than 1 M. These distribution values indicate that complete extraction of Eu(III) in ionic liquid phase could be achieved in few contacts even at 6 M nitric acid.

The most important outcome of the present study is that the extraction of Eu(III) in TODGA/[C_8mim][NTf_2] phase does not result in undesirable third phase formation. In contrast to this, a solution of 0.1 M TODGA in *n*-DD, forms third phase when contacted with 6 M nitric acid as well as with a solution containing trace level concentration Eu(III) (~10^{-4} M) present in 5 M nitric acid. In view of this, the distribution ratio of Eu(III) in 0.1 M TODGA/*n*-DD could not be measured at acidities above 4 M HNO_3 (figure 5.1). Since the third phase was not observed in ionic liquid phase at trace levels of Eu(III) (~10^{-4} M), it is interesting to study the loading behavior of Eu(III) in ionic liquid phase at higher Eu(III) concentrations.

5.2.2. Loading of europium (III) as a function of [HNO_3]

The variation in the loading of Eu(III) in 0.1 M TODGA/[C_8mim][NTf_2] as a function of Eu(III) concentration in 3 M nitric acid phase is shown in figure 5.2. It can be seen that the loading of Eu(III) increases marginally with increase in the amount of Eu(III) present in aqueous phase, reaches a plateau at the loading of ~4g/L in ionic liquid phase. This can be attributed to the increased extraction of Eu(III) with increase in the amount of Eu(III) present in aqueous phase followed by saturation in extraction. Since the concentration of nitric acid in nuclear waste could vary from 3 to 4 M, the loading behavior of Eu(III) in 0.1 M TODGA/[C_8mim][NTf_2] was also studied at 4 and 5 M HNO_3. The results are also shown in figure 5.2. It can be seen that the loading of Eu(III) in ionic liquid phase increases marginally with increase in the concentration of nitric acid in aqueous phase. The Eu(III) loading of ~ 4 to 5 g/L (~0.03 M) was achieved. This observation indicates that Eu(III) could be loaded to the extent of 1:3 (Eu: TODGA) stoichiometry in ionic liquid phase. It is evident from the loading studies that third phase formation was not observed even at the initial concentration of Eu(III) reaches the value of 95 g/L, whereas the third phase formation was reported in 0.1 M TODGA/*n*-DD at the initial concentration of trivalent metal ion (Nd(III)) reaches the value of ~1.1 g/L in 3 M HNO_3 [181, 221]. This indicates that the ionic liquid, $[C_8mim][NTf_2]$, stabilizes the polar metal solvate (Eu(III)-TODGA) complex in ionic liquid phase and overcomes the undesirable third phase formation.

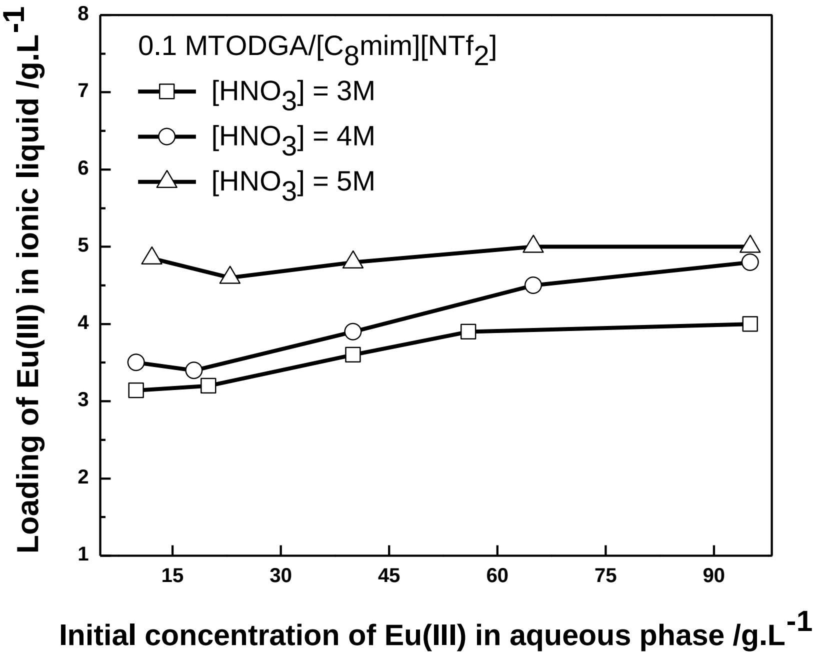

Figure 5.2 Variation in the loading of Eu(III) in the ionic liquid phase as function of europium present in aqueous phase. Ionic liquid phase: 0.1 M TODGA/$[C_8mim][NTf_2]$. Aqueous phase: 3 M - 5 M nitric acid containing 10 g/L – 95 g/L Eu(III), spiked with $^{(152+154)}$Eu(III) tracer. Equilibration time = 2 hr.

5.2.3. Loading of Eu(III) using isomeric diglycolamides

The loading behavior of Eu(III) was also studied in other isomeric diglycolamides. They differ only in the nature of alkyl group attached to the amidic nitrogen atom. The results are also shown in figure 5.3. It can be seen that the loading behavior in T2EHDGA and DEHDODGA is quite similar to TODGA. The saturation in loading is observed at ~4 g/L Eu(III) in ionic liquid phase. These findings clearly indicate that changing alkyl chain length does not affect the loading of Eu(III) in ionic liquid phase; however, a marked difference in loading has been reported when *n*-DD [221] was used as diluent in these isomeric diglycolamides.

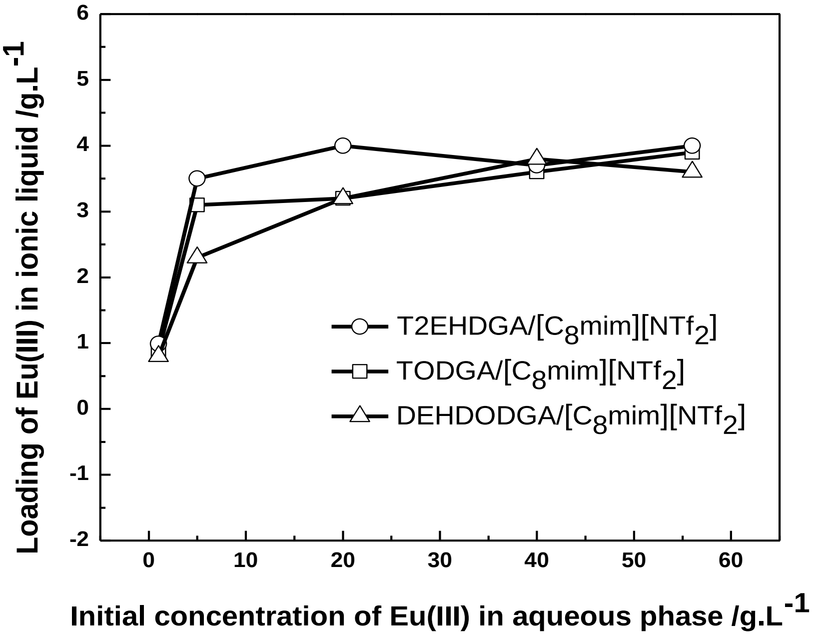

Figure 5.3. Effect of changing the extractant structure on loading of Eu(III) in ionic liquid phase. Ionic liquid phase: 0.1 M TODGA (or T2EHDGA or DEHDODGA)/[C_8mim][NTf_2]. Aqueous phase: 3 M nitric acid containing 1 g/L – 56 g/L Eu(III), spiked with $^{(152+154)}$Eu(III) tracer. Equilibration time = 2 hr.

5.2.4. Stoichiometry of europium(III) loading

The saturation of Eu(III) loading observed at 4 g/L (~0.026 M Eu(III)) in figure 5.2 indicates that the ionic liquid phase seems to reach the stoichiometric levels of Eu(III) loading. To determine the stoichiometry of metal-solvate in ionic liquid phase, the distribution ratio of Eu(III) in TODGA/[C_8mim][NTf_2] was determined as a function of TODGA concentration in ionic liquid phase at 3 M HNO_3. The results are shown in figure 5.4 The distribution ratio of Eu(III) increases with increase in the concentration of TODGA in ionic liquid. Linear regression analysis of the extraction data resulted in a slope of 3. This shows that three molecules of TODGA are involved in the extraction of Eu(III) ion.

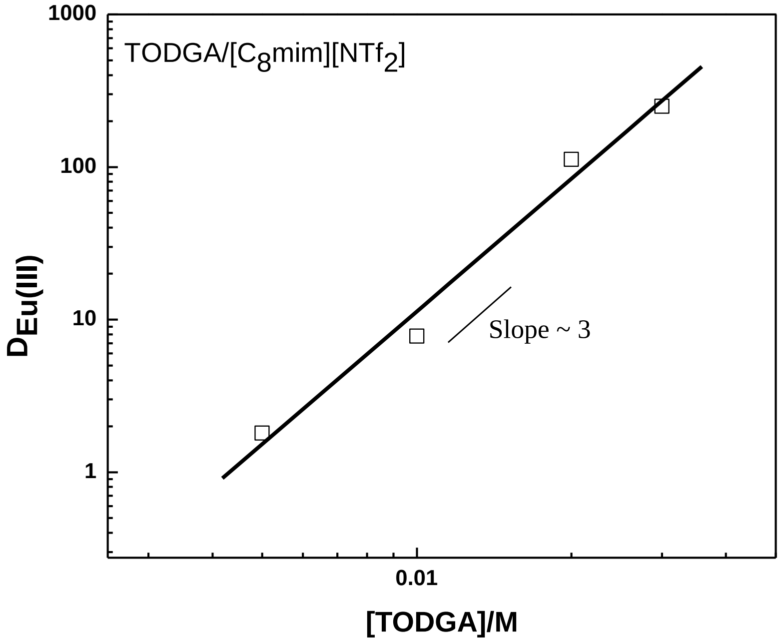

Figure.5.4: Variation of D_{Eu} (III) with concentration of TODGA. Ionic liquid phase: 0.005 M – 0.03 M TODGA/[C_8mim][NTf_2]. Aqueous phase: 3 M HNO_3 spiked with $^{(152+154)}$Eu(III) tracer.

The use of 0.1 M TODGA in ionic liquid should therefore result in a loading of about 0.033 M of Eu(III) in ionic liquid phase. The loading of Eu(III) observed (~0.03 M) in 0.1 M TODGA/[C_8mim][NTf_2] (figure 5.2) at all acidities is in good agreement with the expected loading of 0.033 M from figure 5.4.

5.2.5. Effect of alkyl group attached to imidazolium moiety of RTIL

Figure 5.5 shows the comparison in the loading behavior of Eu(III) in a solution of 0.1 M TODGA present in various ionic liquids. The ionic liquids compared are [C_4mim][NTf_2], [C_6mim][NTf_2] and [C_8mim][NTf_2]. It can be seen that the loading of Eu(III) in [C_4mim][NTf_2] phase (~1 g/L) is four to five times lower than that observed in other ionic liquids (~5 g/L). The loading behavior of Eu(III) in [C_6mim][NTf_2] and [C_8mim][NTf_2] ionic liquid phases are quite similar.

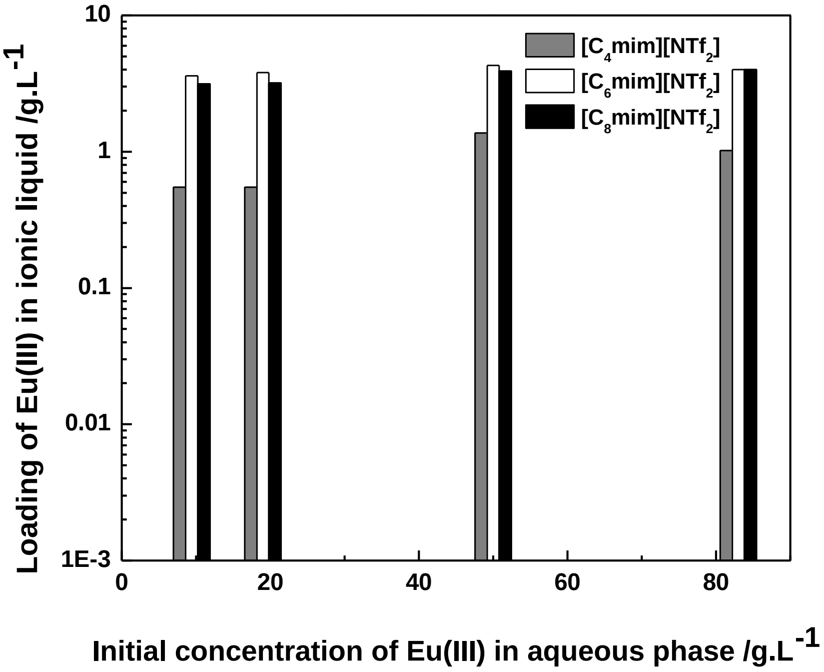

Figure 5.5. Variation in the loading of Eu (III) in ionic liquid phase as function of concentration of europium present in aqueous phase. Ionic liquid phase: 0.1 M TODGA/ [C_8mim][NTf_2] (or [C_6mim][NTf_2] or [C_4mim][NTf_2]). Aqueous phase: 3 M nitric acid containing 9.4 g/L – 83 g/L, Eu (III), spiked with $^{(152+154)}$Eu(III) tracer. Equilibration time = 2 hr.

The exact reason for the lower loading observed in [C_4mim][NTf_2] is not clear. The probable reason for such behavior could be due to the lower stability of Eu(III)-TODGA solvate in [C_4mim][NTf_2] medium, perhaps due to lower hydrophobicity, as compared to [C_8mim][NTf_2] ionic liquid. However, it was noted that in all cases the third phase formation was not observed.

5.2.6. Loading of europium (III) as a function of [TODGA]

Table 5.2 compares the loading behavior of Eu(III) observed in [C_8mim][NTf_2] phase containing different concentrations of TODGA. The loading of Eu(III) increases with increase in the concentration of TODGA from 0.1 to 0.2 M, which is obviously due to the higher availability of TODGA for extraction

Table 5.2 Comparison in the loading of Eu(III) in ionic liquid phase as function of TODGA concentration. Ionic liquid phase: 0.1 M and 0.2 M TODGA/[C_8mim][NTf_2]. Aqueous phase: 3 M nitric acid containing 9.4 g/L – 95 g/L Eu (III), spiked with $^{(152+154)}$ Eu (III) tracer. Equilibration time = 2 hr.

[Eu(III)]/gL^{-1}	**Loading of Eu(III) in gL^{-1}**	
	0.1 MTODGA /[C_8mim][NTf_2]	**0.2 M TODGA /[C_8mim][NTf_2]**
9.42	**3.14**	**5.93**
19	**3.2**	**6.4**
40	**3.7**	**7**
56	**3.9**	**7.5**
95	**4**	**9.1**

5.2.7 Effect of co-extractants

In conventional molecular diluent systems, the co-extractants (or phase modifiers) such as tri-*n*-butyl phosphate (TBP) and dihexyloctanamide (DHOA) are usually added to the *n*-DD phase, to overcome the undesirable third phase formation [188,191]. The phase modifiers in those cases do not play much role except that they overcome the limitation of third phase formation by stabilizing the polar metalsolvate complex. It can be expected that phase modifiers do have some role in the present extraction system and therefore the variation in the loading of Eu(III) from 3 M HNO_3 as a function of concentration of a phase modifiers, TBP and DHOA, was studied and the results are shown in figure 5.6. It is noted that the addition of phase modifier, TBP, in 0.1 M TODGA/[C_8mim][NTf_2] increases the loading of Eu(III). However, the same is not true for DHOA as the modifier in 0.1 M TODGA/[C_8mim] [NTf_2] and the increase in loading is marginal.

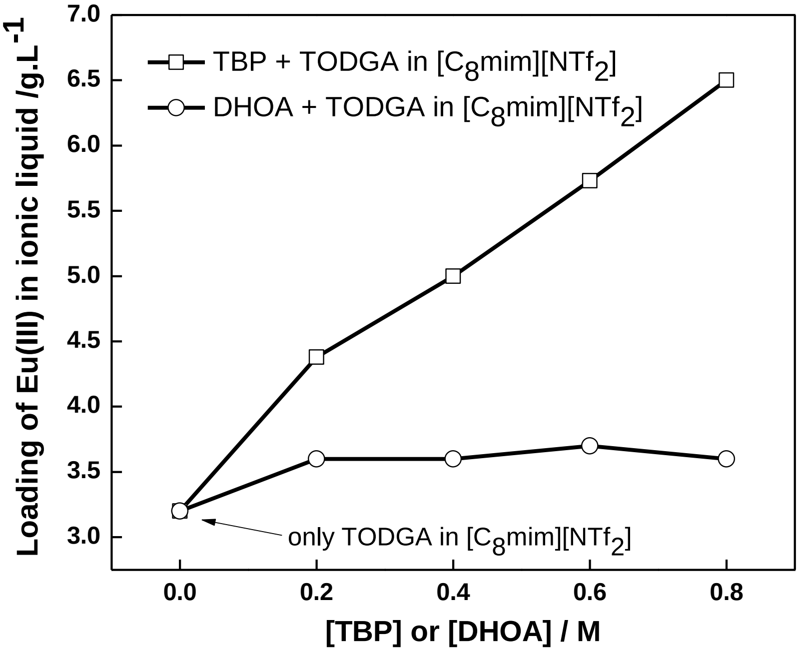

Figure 5.6: Variation in the loading of Eu(III) in the ionic liquid phase as a function of TBP and DHOA concentration. Ionic liquid phase: 0.1M TODGA + TBP (or DHOA)/ [C_8mim][NTf_2]. Aqueous phase: 3 M nitric acid containing 20g/L Eu (III), spiked with $^{(152+154)}$ Eu (III) tracer. Equilibration time = 2 hr.

The increase in loading of Eu(III) observed in the presence of TBP (Figure 5.6) could be due to the extraction by TBP itself in ionic liquid phase. Therefore, the distribution ratio of Eu(III) was determined in a solution of TBP (or DHOA) present in

$[C_8mim][NTf_2]$ (i.e. without TODGA).The results are shown in Table 5.3. It can be seen that distribution ratio of Eu(III) in these systems are of the order 10^{-2} indicating that the extraction of Eu(III) occurs only in the presence of TODGA and facilitated synergically only in a solution of TODGA containing TBP in ionic liquid phase.

Table 5.3. Variation in the distribution ratio of Eu(III) in the ionic liquid phase as a function of nitric acid concentration. Ionic liquid phase: 1M TBP (or DHOA)/$[C_8mim][NTf_2]$. Aqueous phase: 0.1 M – 5 M nitric acid spiked with $^{(152+154)}$Eu(III) tracer.

$[HNO_3]$/M	**$D_{Eu(III)}$ in**	
	1M TBP/$[C_8mim][NTf_2]$	**1M DHOA/$[C_8mim][NTf_2]$**
0.1	**0.008**	**0.002**
1	**0.01**	**0.003**
3	**0.04**	**0.007**
5	**0.06**	**0.03**

5.2.8 Dependence of TBP and TODGA

To understand the synergism and dependence of Eu(III) extraction on TBP present in ionic liquid phase, the effect of TBP concentration in 0.01 M TODGA + TBP/$[C_8mim][NTf_2]$ was studied and the results are shown in figure 5.7. It can be seen that the slope obtained is dependent on the concentration of TBP taken in ionic liquid phase. The extraction of Eu(III) is less dependent on TBP at low concentrations (0.01–0.1 M), and the dependence increases at higher concentrations of TBP. This shows that the participation of TBP in the synergic extraction of Eu(III) in TODGA + TBP/$[C_8mim][NTf_2]$ phase increases with increase in the concentration of TBP in ionic liquid.

Similarly, the variation in the distribution ratio of Eu(III) in a solution of TODGA + 0.05 M TBP/[C_8mim][NTf_2] was studied as a function of TODGA concentration in ionic liquid phase at 3 M nitric acid. The results are shown in figure 5.8. The TODGA concentration in ionic liquid was varied from 0.002 to 0.02 M. It can be seen that the distribution ratio of Eu(III) in ionic liquid phase increases with increase in the concentration of TODGA. Linear regression analysis of the extraction data resulted in a slope of 2.2, which is lower than the slope of 3.0 obtained in the absence of TBP (figure 5.4). This shows that the presence of TBP lowers the dependence of Eu(III) extraction on TODGA. This can be due to the synergic participation of TBP in the extraction of Eu(III) from aqueous phase.

A marginal increase in the loading of europium from 3.2 g/L in the absence of TBP to 6.5 g/L was observed in the presence of 0.5 M TBP in ionic liquid phase, again indicating the saturation of Eu(III) loading in ionic liquid phase due to 1: 3 stoichiometry. Therefore, the result obtained in the presence of TBP indicates that the increase in Eu(III) extraction observed in ionic liquid phase is due to the synergic participation of both TODGA and TBP.

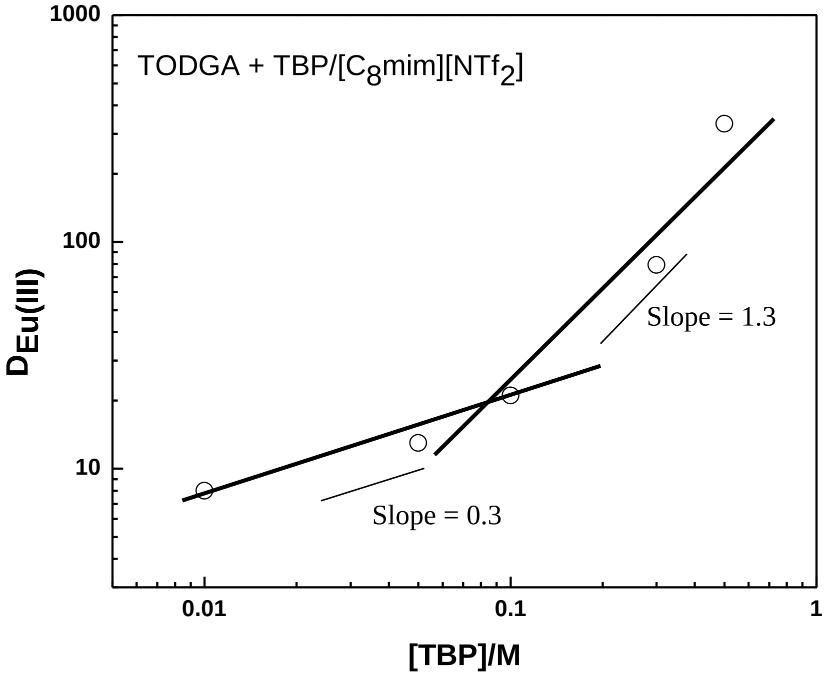

Figure 5.7: Variation of $D_{Eu(III)}$ with concentration of TBP. Ionic liquid phase: 0.01 M – 0.5 M TBP in 0.01 M TODGA/[C_8mim][NTf_2]. Aqueous phase: 3 M HNO_3 spiked with $^{(152+154)}$Eu(III) tracer.

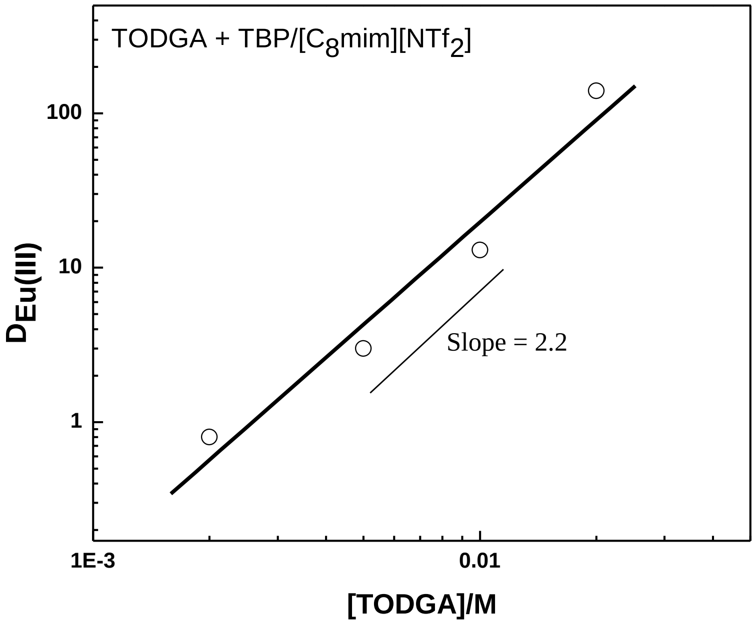

Figure 5.8. Variation of $D_{Eu(III)}$ with concentration of TODGA. Ionic liquid phase: 0.002 M – 0.02 M TODGA in 0.05 M TBP/[C_8mim][NTf_2]. Aqueous phase: 3 M HNO_3 spiked with $^{(152+154)}$Eu(III) tracer.

5.3 Conclusion

The extraction of Eu(III) from its high feed condition was studied in a solution of TODGA present in ionic liquid medium. The extraction of Eu(III) in TODGA/[C_8mim][NTf_2] decreased with increase in the concentration of nitric acid. The loading of Eu(III) in TODGA/[C_8mim][NTf_2] increased marginally with increase in the amount of Eu(III) present in nitric acid phase. Unlike molecular diluents systems the third phase formation was not observed even at 95 g/L Eu(III) present in 3–5 M nitric acid phase, perhaps due to the stabilization of polar Eu(III)-TODGA complex by ionic liquid. The study revealed that Eu(III) could be loaded to the extent of 1:3 stoichiometry in ionic liquid phase without any third phase formation. There was hardly any change in the loading values by changing the structure of TODGA into its isomeric forms. The addition of phase modifier, TBP, to TODGA/[C_8mim][NTf_2] increased the distribution ratio of Eu(III) due to synergic participation of both TODGA and TBP.

CHAPTER 6

ELECTROCHEMICAL STUDIES OF METAL IONS IN RTIL MEDIUM CONTAINING EXTRACTANTS

6.1 Introduction

The properties of room temperature ionic liquids (RTILs) such as wide electrochemical window, solubility of various extractants and unusual extraction of target metal ions from aqueous medium etc. facilitates the development of novel and environment benign procedures for the treatment of wide variety of aqueous waste using ionic liquid as medium. One such method is the extraction-electrodeposition (EX-EL) approach [115]. This approach exploits a couple of interesting properties of ionic liquid namely the hydrophobicity and wide electrochemical window [115]. It is an advanced procedure aimed at the separation and recovery of the metal ions from aqueous wastes. In EX-EL approach, the ionic liquid can be used either as extractant or as diluent in conjunction with the molecular extractant, for the liquid-liquid extraction of target metal ions from aqueous feeds. However, unlike the conventional solvent extraction procedure, the extracted metal can be recovered by electrodeposition directly from the extracted ionic liquids phase. Therefore, the process holds promise of separating the target metal ion with high separation factor (or decontamination factor), one obtained during liquid-liquid extraction and the other during electrodeposition. Moreover, the metal recovered by electrodeposition is usually in metallic or metal-oxide form such that handling of the final product is easy. In this context, the extraction– electrodeposition approach for the recovery of uranium as uranium oxide and palladium as metallic palladium, using ionic liquid as a medium have been demonstrated previously [146,147,149,158]. Sililarly, Matsumiya *et al*. investigated the extraction and electrodeposition behaviour of some lanthanides such as praseodymium, neodymium and dysprosium in a solution composed of tri-*n*-butyl phosphate (TBP) and ionic liquid [148].

In the recent past, there have been increasing studies on the electrochemical behavior of metal ions in the presence of extractants dissolved in RTIL medium [150-154]. For instance, Gupta *et al*. studied the electrochemical behavior of Eu(III) in ionic liquid medium to bring out the co-ordination behavior of Eu(III) with dihexyl *N*,*N*-diethylcarbamoylmethylphosphonate (DHDECMP) extractant [150]. Similarly, Hussey *et al*. reported the coordination behavior of *N*,*N*,*N*,*N*-tetraoctyl diglycolamide with lanthanide ions (Ln = Sm, Eu, and Yb) studied by electrochemical and spectroscopic investigations in 1-(1-butyl)trimethyl ammonium bis(trifluoromethylsulfonyl)imide ($BuMe_3NTf_2N$) and 1-butyl-3-methylpyrrolidinium bis(trifluoromethylsulfonyl)imide ($BuMePyrTf_2N$) ionic liquids [151]. Sengupta *et al*. reported the electrochemical study on Np(IV) complexes with task-specific ionic liquid containing 3-dodecylimidazolium cation appended with diphenylcarbamoylmethylphosphine oxide and bis(trifluoromethylsulfonyl)imide anion dissolved in 1-butyl-3-methylimidazolium bis(trifluoromethylsulfonyl)imide and also with task-specific ionic liquid functionalized with diglycolamide moiety (DGA-TSIL) dissolved in the room-temperature ionic liquid 1-butyl-3-methylimidazolium bis(trifluoromethylsulfonyl)imide ($[C_4mim][NTf_2]$) [153,154].

The present chapter describes the electrochemical behaviour of metal ions in the presence of extractants in RTIL electrolytic medium. Metal ions such as uranium(VI) and europium(III) have been studied. This chapter consists of two parts namely part 1 and part 2. Part 1 describes the electrochemical study of U(VI) in the presence of tri-*n*-alkylphosphate dissolved in the ionic liquid, 1-butyl-3-methylimidazolium bis(trifluoromethanesulfonyl)imide ([C_4mim][NTf_2]) and in the part 2 electrochemical behavior of Eu(III) in a solution containing acidic extractants, di(2-ethylhexyl)phosphoric acid (HDEHP) and *N,N'*-di(2-ethylhexyl) diglycolamic acid(HDGA) dissolved in 1-butyl-1-methylpyrrolidinium bis(trifluoromethanesulfonyl)imide ([C_4mpy][NTf_2]) ionic liquid have been reported.

Experimental parts of the present chapter have been discussed in the section 2.7, 2.8.7 and 2.8.8 of chapter 2.

PART 1

Electrochemical study of U(VI) in the presence of higher homologue of TBP dissolved in RTIL medium

In the recent past, higher homologs of tri-*n*-butyl phosphate such as tri-*n*-amyl phosphate, tri-*n*-octyl phosphate have been proposed for fast reactor fuel reprocessing [178,187]. In the view of this, Rama *et al*. studied the extraction behaviour of U(VI) in various trialkyl phosphates present in imidazolium ionic liquid medium and compared their extraction behavior [119]. It was shown that the distribution ratio of U(VI) in ionic liquid medium was quite similar to those observed in *n*-dodecane and the distribution ratio of U(VI) increased with the increase in the chain length of alkyl group attached to the phosphoryl group of trialkyl phosphate. This observation was attributed to the efficient complexation of U(VI) by trialkyl phosphate due to the increased basicity of trialkyl phosphate with increase of chain length [187].When higher homologs of trialkyl phosphates are proposed for the extraction of U(VI) and Pu(IV) from fast reactor fuel solution and if extraction-electrodeposition procedure is also proposed for the recovery of metal ions from the extracted phase, it is necessary to understand the electrochemical behaviour of these actinides in the presence of higher homologs of TBP present in ionic liquid medium.

The aim of part 1 in chapter 6 to investigate the electrochemical behaviour of the actinide representative, U(VI), present in 1-butyl-3-methylimidazolium bis(trifluoromethanesulfonyl)imide ([C_4mim][NTf_2]) containing higher homolog of trialkyl phosphate namely tri-*n*-octyl phosphate (TOP).

Table 6.1 Structure of RTIL and extractants studied in part 1 of chapter 6

Name	**Structure**
Extractant	
Tri-*n*-alkyl phosphates (i) Tri-*n*-butyl phosphate (R: C_4H_9) (i) Tri- *n*-octyl phosphate (R:C_8H_{17})	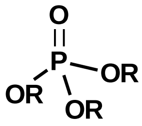
Ionic liquid	
1-Butyl-3-methylimidazolium bis(trifluoromethanesulfonyl)imide ([C_4mim][NTf_2])	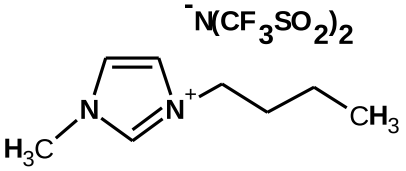

Synthesis of the ionic liquid and extractant used in part 1 have been discussed in section 2.9.1 & 2.9.6 of chapter 2. Preparation of UO_2 $(NTf_2)_2$ was mentioned in section 2.4.7 of chapter 2.

6.2 Results and discussion

6.2.1 *Cyclic voltammetric study of U(VI) in [C_4mim][NTf_2]*

The cyclic voltammogram of [C_4mim][NTf_2] recorded at glassy carbon working electrode at the scan rate of $0.1Vs^{-1}$ at 373 K is shown in figure 6.1. It can be seen that the ionic liquid [C_4mim][NTf_2] offers an electrochemical windows of 4.7 V. Figure 6.1 also shows the cyclic voltammogram of U(VI) in [C_4mim][NTf_2] recorded at the scan rate of $0.1Vs^{-1}$ at 373 K. The voltammogram shows the onset of reduction current occurring at +0.25 V (Vs. Fc/Fc^+) that results in a cathodic peak at the potential (E_p^{c1}) of -0.24 V. A couple of oxidation waves (E_p^{a1} & E_p^{a2}) are observed at +0.45 V (Vs. Fc/Fc^+) and +0.66 V (Vs. Fc/Fc^+) during scan reversal at -1.0 V. The reduction of U(VI) to U(V) could be responsible for the cathodic wave observed at -0.24 V. The reason for the occurrence of a couple of oxidation waves is not clear at present, perhaps it could be attributed to the adsorption of the reduced product U(V) on to glassy carbon working electrode. The first anodic wave (E_p^{a1}) could be due to the oxidation of U(V) to U(VI) and E_p^{a2} could be due to the oxidation of adsorbed U(V) to U(VI). Such adsorption behavior has been reported by several authors in other systems [224,225].

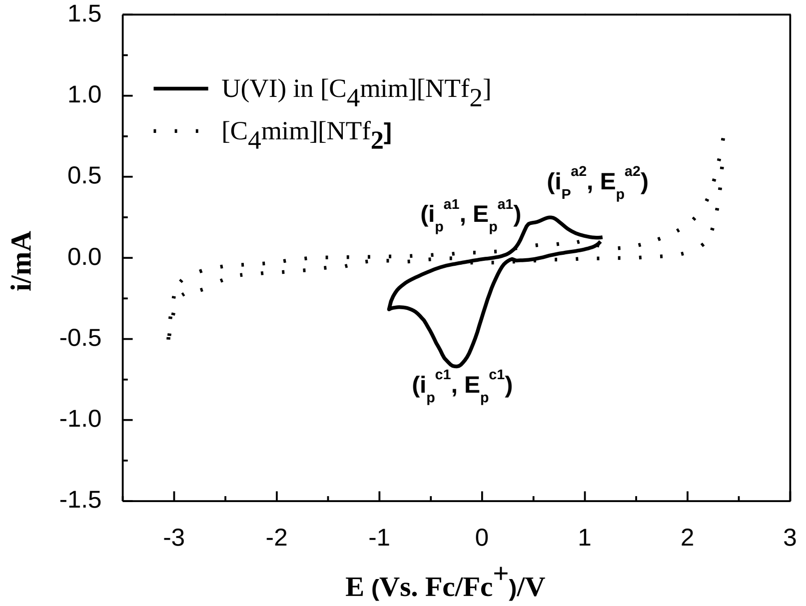

Figure 6.1. Cyclic voltamogram of [C_4mim][NTf_2] and U(VI) in [C_4mim][NTf_2] recorded at glassy carbon electrode. [U(VI)] = 0.1 M, scan rate = 0.1Vs^{-1} , temperature = 373 K.

The cyclic voltammagram of U(VI) in [C_4mim][NTf_2] recorded at glassy carbon working electrode at various scan rates is shown in figure 6.2. It is observed that the cathodic peak potential (E_p^{c1}) is shifted cathodically and the cathodic peak current (i_p^{c1}) increased with increase of scan rate. Similarly, the anodic peak potential E_p^{a1} is shifted anodically to some extent and E_p^{a2} is shifted to a larger extent. The anodic peak currents (i_p^{a1} & i_p^{a2}) increase with increase of scan rate, however, i_p^{a2} increases more than i_p^{a1}. All these observations indicate that the reduction of U(VI) to U(V) and the subsequent oxidation of U(V) during scan reversal are not completely reversible. The relation between the cathodic peak current (i_p^c) is related to the square root of scan rate (ν) is provided by Randles-Sevcik equation [164], shown in equation 6.1.

$$i_p = 0.496\, nFC_O AD_O^{1/2}\left(\frac{(\alpha\, n_\alpha)F\nu}{RT}\right)^{1/2} \tag{6.1}$$

where A is the electrode area in cm^2 (0.52 cm^2), D_o is the diffusion coefficient in cm^2/s, n is the number of electrons exchanged (=1), ν is the sweeping potential and C_o is the U(VI) concentration in mol cm^{-3} (1 x 10^{-4} mol cm^{-3}), R is the gas constant and T is absolute temperature (K).

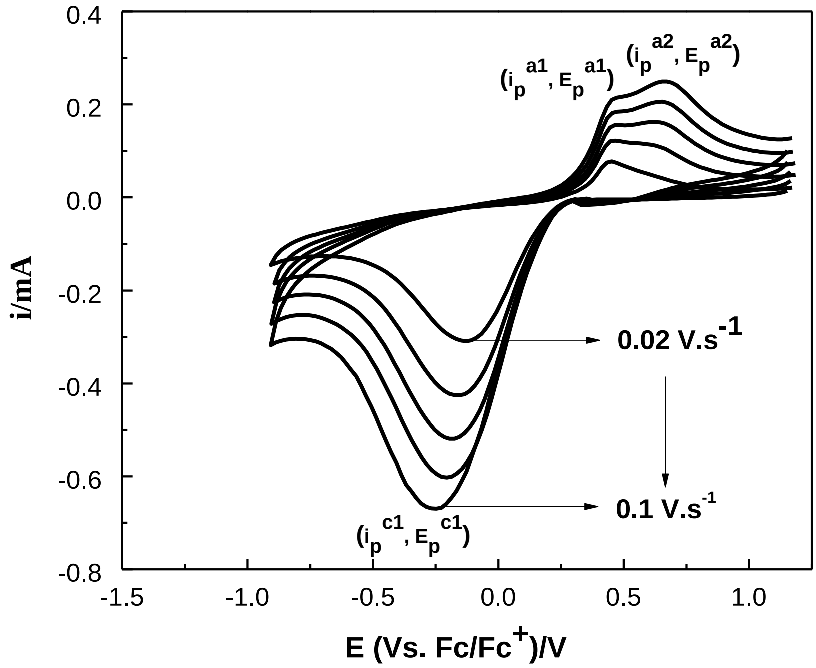

Figure 6.2. Cyclic voltamogram of U(VI) in $[C_4mim][NTf_2]$ recorded at glassy carbon electrode at various scan rates. [U(VI)] = 0.1 M , temperature = 373 K.

A plot of i_p^{c1} against $\nu^{1/2}$ for the reduction of U(VI) to U(V) obtained at 373 K is shown in figure 6.3. A linear dependence of i_p^{c1} with $\nu^{1/2}$ indicates that the electron transfer is diffusion controlled and allows the determination of diffusion coefficient of U(VI) in [C_4mim][NTf_2] medium. To determine the diffusion coefficient, the value of αn_α is required and that can be determined from equation 6.2.

$$\left|E_p^c - E_{p/2}^c\right| = \frac{1.857\ RT}{\alpha\, n_\alpha F} \tag{6.2}$$

where $E_{p/2}^{c1}$ is the cathodic half-peak potential, E_p^{c1} is cathodic peak potential, α is charge transfer coefficient and (α, $0.1 \leq \alpha \leq 0.9$) is a measure of symmetry barrier in a non-reversible (both quasi- and irreversible process) electrode reaction.

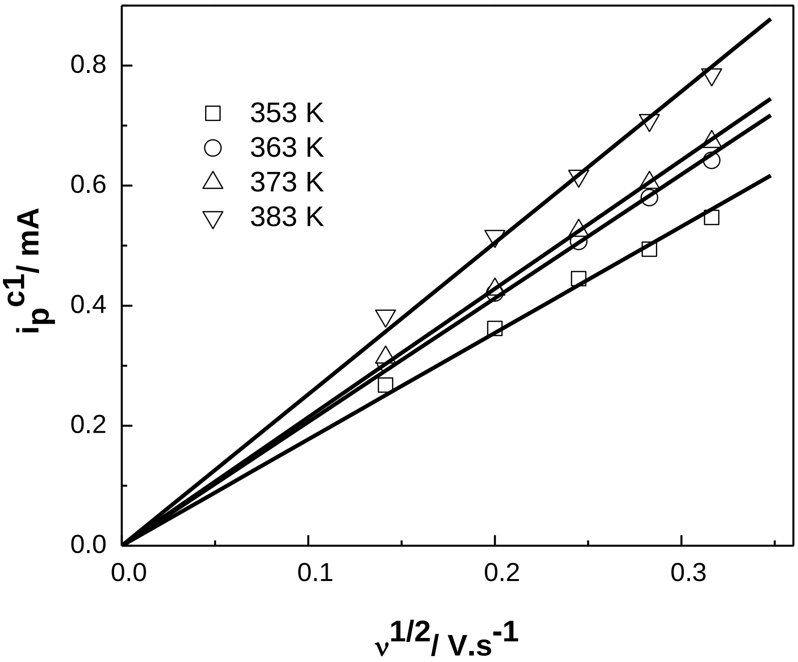

Figure 6.3. Plot of i_p^{c1} against square root of scan rate ($v^{1/2}$) for the reduction of U(VI) to U(V) in [C_4mim][NTf_2] at various temperatures. Temperature: 353 K to 383 K.

The value of αn_α was determined found to be vary from 0.22 to 0.34 at 373 K with the increase of scan rate from 0.02 to 0.1Vs^{-1}. Using equation 6.1, the diffusion coefficient of U(VI) was determined and the values are provided in table 6.2. A diffusion coefficient of 10.5 X 10^{-7} cm^2/s at 373 K and $0.1Vs^{-1}$ scan rate obtained in the present case. Previously, Giridhar *et al*. reported a diffusion coefficient of 1.7 x 10^{-8} cm^2/s at 373 K [156] and Asanuma *et al*. reported a value of $4.8x10^{-8}$ cm^2/s at 353 K for U(VI) in [C_4mim][Cl] medium [226]. Higher value of diffusion coefficient obtained in the present study could be due to the low viscosity of [C_4mim][NTf_2] (42 cP at 298 K) as compared to [C_4mim][Cl] (solid at RT).

Table 6.2. The diffusion coefficients (D) and heterogeneous rate constant (k_s) for the reduction of U(VI) to U(V) in [C_4mim][NTf_2] at glassy carbon electrode at various temperatures. [U(VI)] = 0.1 M and [TBP] or [TOP] = 0.03 M.

Temperature /K	**D x $10^7/cm^2s^{-1}$**		
	U(VI) in [C_4mim][NTf_2]	**U(VI) in TBP + [C_4mim][NTf_2]**	**U(VI) in TOP + [C_4mim][NTf_2]**
353	5.8	5.4	3
363	8.0	6.2	3.5
373	10.5	8.8	4.7
383	13.8	10.5	5.1
	k_s x $10^4/cms^{-1}$		
353	3.07	3.04	1.56
363	3.62	3.22	2.18
373	6.39	5.41	3.10
383	7.21	5.70	3.75

The cyclic voltammograms of U(VI) in [C_4mim][NTf_2] recorded at glassy carbon working electrode at the scan rate of $0.1Vs^{-1}$ at various temperatures is shown in figure 6.4. It can be seen that the cathodic peak potential (E_p^{c1}) is shifted anodically and the cathodic peak current (i_p^{c1}) is increased with increase of temperature. The cyclic voltammogram of U(VI) in [C_4mim][NTf_2] as a function of scan rate was recorded at different temperatures and from the plot of i_p^{c1} against square root of scan rate ($\nu^{1/2}$), the diffusion coefficient at various temperatures was determined. The values are tabulated in table 6.2. It can be seen that the diffusion coefficient increases with increase of temperature. This could be due to the enhanced diffusion of U(VI) in [C$_4$mim][NTf$_2$] with increase of temperature.

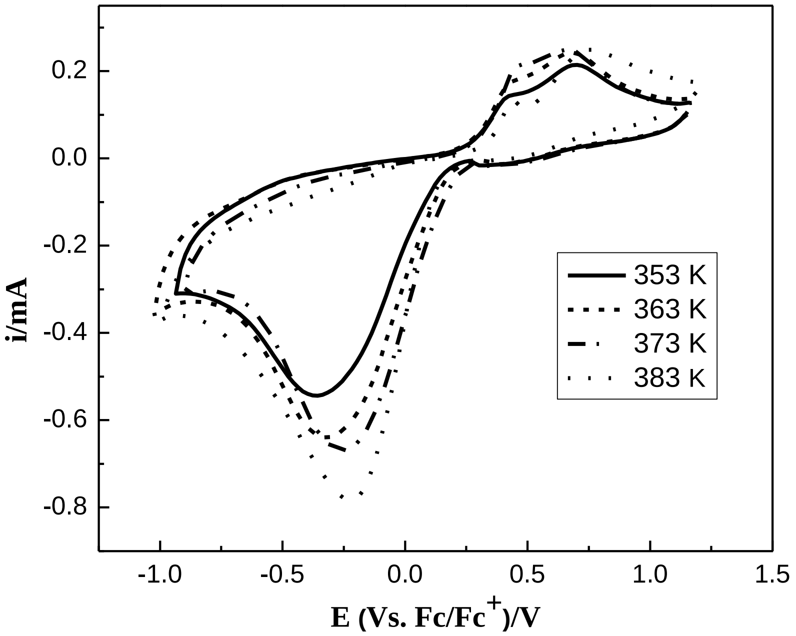

Figure 6.4. Cyclic voltamogram of U(VI) in [C$_4$mim][NTf$_2$] recorded at glassy carbon electrode at various temperatures. [U(VI)] = 0.1 M, scan rate: 0.1 M Vs^{-1}, temperature: 353 K to 383 K.

A marginal shift in the cathodic peak potential with the increase of scan rate, shown in figure 6.2 indicates that the reduction of U(VI) at glassy carbon electrode could be quasi-reversible. This indicates that the reduction of U(VI) to U(V) is not only controlled by diffusion of U(VI) ion at the working electrode, but also the rate of charge transfer reaction between the electrode electrolyte inter phase. The charge transfer rate constant, k_s (cm/s) was determined using equation 6.3 [165].

$$k_s = 2.18\left[D_0(\alpha n_\alpha)\frac{\nu F}{RT}\right]^{1/2} \exp\left[\frac{\alpha^2 nF}{RT}\left(E_P^{c1} - E_P^{a1}\right)\right] \tag{6.3}$$

Substituting the diffusion coefficient (D_0) of U(VI) in equation 6.3, the magnitude of rate constants were determined at various temperatures and the values are tabulated in table 6.2. It can be seen that the value of k_s increases with increase of temperature and the magnitude of k_s lies in the range of $0.3\nu^{1/2} \geq k_s \geq 2\text{x}10^{-5}\nu^{1/2}$, confirming that the reduction of U(VI) at glassy carbon electrode is quasi-reversible [165]. The increase in k_s with increase of temperature could be due to the facilitated electron transfer at the electrode-electrolyte inter phase at higher temperatures.

6.2.2 Cyclic voltammetric study of U(VI) in TBP/[C_4mim][NTf_2]

The cyclic voltammogram of U(VI) in a solution of tri-*n*-butyl phosphate (TBP) in [C_4mim][NTf_2] at 373 K is shown in figure 6.5. The voltammogram is compared with the voltammogram obtained in the absence of TBP under the similar condition. It can be seen that the cathodic wave occurs at the onset of -0.20 V (Vs. Fc/Fc^+), leading to a prominent cathodic wave at the peak potential of -0.35 V (Vs. Fc/Fc^+) is due to the reduction of U(VI) to U(V). The corresponding oxidation wave occurs at the peak potential of 0.36 V (Vs. Fc/Fc^+). Comparing the peak potentials observed in the presence and absence of TBP, the voltammogram shows that the presence of TBP shifts the reduction of U(VI) to more negative potentials possibly due to the co-ordination of U(VI) with TBP. Since the co-ordinated U(VI) requires higher potentials for reduction, the peak potential is shifted cathodically for U(VI) –TBP in ionic liquid system.

The cyclic voltammogram of U(VI) in 30 mM TBP/[C_4mim][NTf_2] at various scan rates at 373 K is shown in figure 6.6. It can be seen that the cathodic peak current potential (E_p^{c1}) is shifted cathodically with increase of scan rate and the magnitude $|E_p^{c1} - E_{p/2}^{c1}|$ (=0.26 V) is larger than the value needed for the reversible one electron transfer process (0.07 mV) at 373 K. This shows that the reduction of U(VI) in TBP/[C_4mim][NTf_2] is also not reversible. The value of αn_α in the present case was determined to be 0.36 at 373K at 0.02Vs^{-1}. This value is comparable to the value determined in the absence of TBP (= 0.34 at 0.02Vs^{-1}).

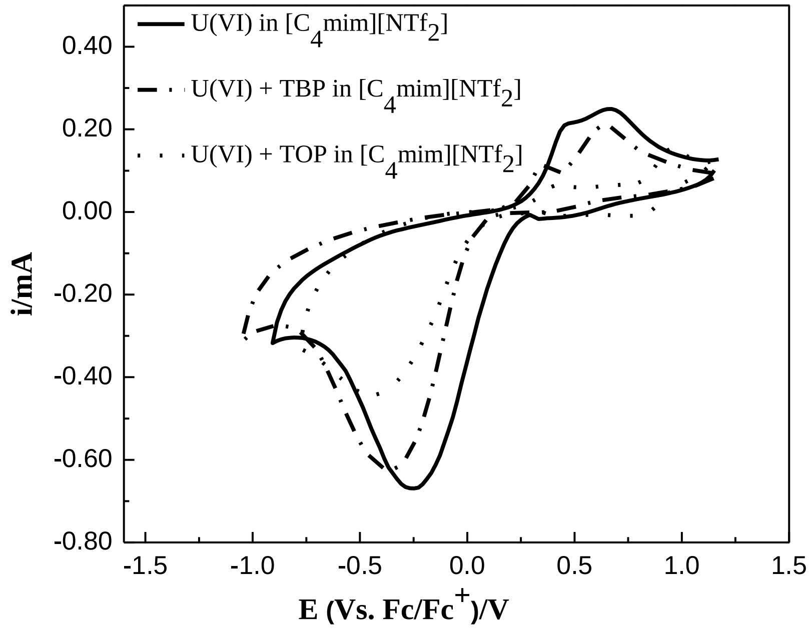

Figure 6.5. Cyclic voltammogram of U(VI) in [C_4mim][NTf_2], in TBP/[C_4mim][NTf_2] and in TOP/[C_4mim][NTf_2] recorded at glassy carbon electrode. [U(VI)] = 0.1 M, [TBP] = 0.03 M, [TOP] = 0.03 M, scan rate = 0.1Vs^{-1}, temperature = 373 K.

The plot of the cathodic current (i_p^{c1}) obtained at various temperatures against $\nu^{1/2}$ is shown in figure 6.7.Using equations 6.1 and 6.2, the diffusion coefficient of U(VI) in 0.03 M TBP /[C_4mim][NTf_2] was determined and compared with that determined in the absence of TBP in table 6.2. A marginal shift in the cathodic peak potential with increase of scan rate, shown in figure 6.6, indicates that the reduction of U(VI) in TBP/[C_4mim][NTf_2] at glassy carbon electrode is quasi-reversible. The rate constant (k_s) for the charge transfer between the electrodes – electrolyte interphase was determined using equation 6.3. The values thus obtained are tabulated in table 6.2. It can be seen that k_s values are lowered marginally in the presence of TBP, possibly due to the co-ordination of U(VI) by TBP. k_s values increased with increase of temperature and the magnitude of k_s lies in the range of $0.3\nu^{1/2} \geq k_s \geq 2x10^{-5}\nu^{1/2}$, confirming that the reduction of U(VI) at glassy carbon electrode in the presence of TBP is quasi-reversible.

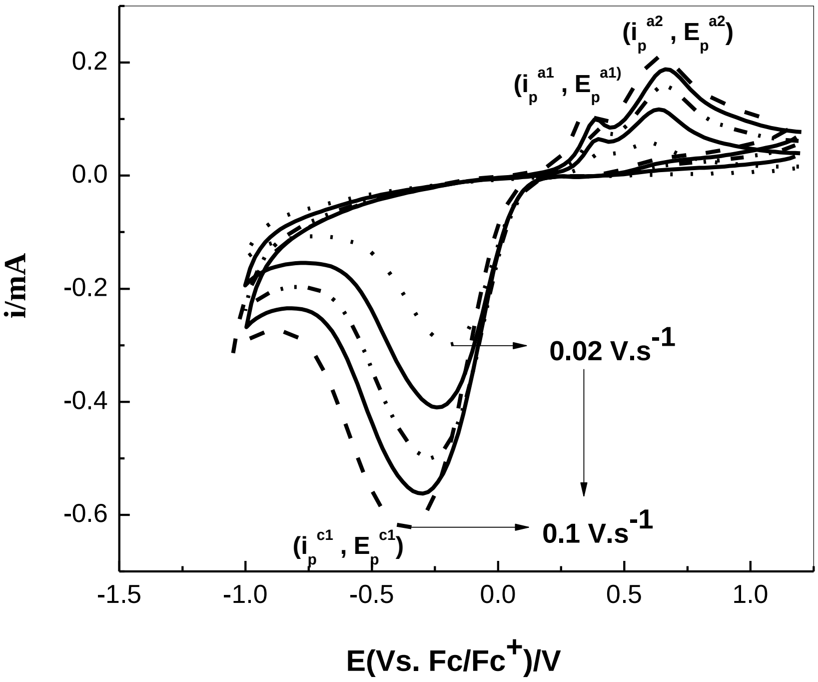

Figure 6.6. Cyclic voltammogram of U(VI) in TBP/[C_4mim][NTf_2] recorded at glassy carbon electrode at various scan rates. [U(VI)] = 0.1 M, [TBP] = 0.03 M, temperature = 373 K.

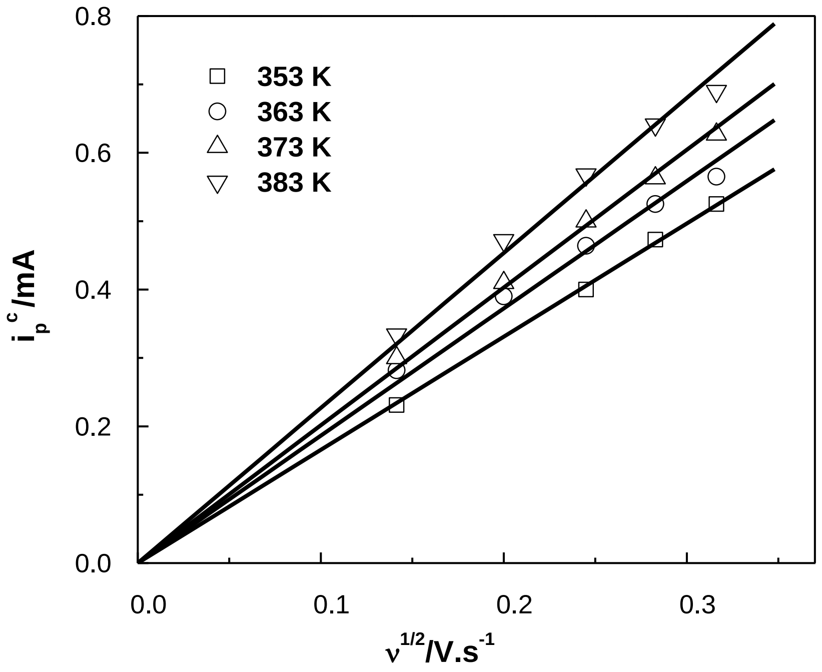

Figure 6.7. Plot of i_p^{c1} against square root of scan rate ($\nu^{1/2}$) for the reduction of U(VI) to U(V) in TBP/[C$_4$mim][NTf$_2$] at various temperatures. [U(VI)] = 0.1 M, [TBP] = 0.03 M, temperature: 353 K to 383 K.

6.2.3 Stoichiometry and stability constant of U(VI)-TBP complex

The cyclic voltammogram of U(VI) in TBP/[C$_4$mim][NTf$_2$] at various concentrations of TBP at 373 K is shown in figure 6.8. It can be seen that the cathodic peak current decreases and the peak potential is shifted cathodically with increase in the concentration of TBP, as expected. The number of molecules of TBP co-ordinated to U(VI) and the logarithmic stability constant (ln K_f) of the U(VI) - (TBP)$_m$ complex was determined from the voltammogram by using the relation shown in equation 6.4. [173,174].

$$\Delta E_{1/2} = (E_{1/2})_C - (E_{1/2})_M = -(RT/\alpha nF)(\ln K_f + m\ln[L]) \quad (6.4)$$

where $(E_{1/2})_c$ and $(E_{1/2})_M$ are the half- wave potential of complexed and free metal ion, respectively and [L] is the ligand concentration (in M), n is the number of electrons transferred, m is the co-ordination number of the complex and α is the charge transfer coefficient. The plot of $-\Delta E_{1/2}/(RT/\alpha nF)$ against the logarithmic value of TBP concentration is shown in figure 6.9.

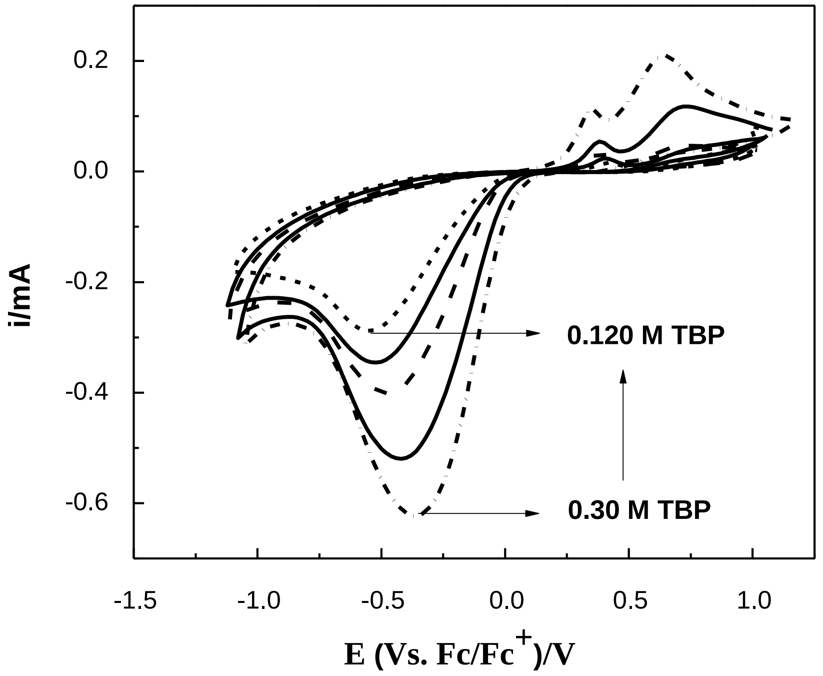

Figure 6.8. Cyclic voltammogram of U(VI) in TBP/[C$_4$mim][NTf$_2$] recorded at glassy carbon electrode for various concentrations of TBP. [U(VI)] = 0.1 M, [TBP] = 0.03 to 0.120 M, scan rate = 0.1Vs^{-1}, temperature = 373 K.

It can be seen that the magnitude of $-\Delta E_{1/2}/$ (RT/αnF) increases linearly with increase in the concentration of TBP. From the magnitude of intercept and slope, the stability constant (ln K_f) and the co-ordination number can be determined to be 2.5 and 0.55 respectively. This shows that the stoichiometry of U(VI) to TBP is 2:1 in ionic liquid phase. However, it was reported in literature [122] that about two molecules of TBP were involved during the extraction of U(VI) in a solution of 1.1 M TBP/ [C$_4$mim][NTf$_2$].

Lower value of the coordination number observed in the present case could be due to the employment of equimolar ratio of U(VI) and TBP (U(VI) = 0.1 M, TBP varied from 0.02 M to 0.120 M) during the measurement. In contrast to this, the stoichiometry obtained from solvent extraction measurement used only trace level of U(VI) for their extraction in 1.1 M TBP/[C_4mim][NTf_2].

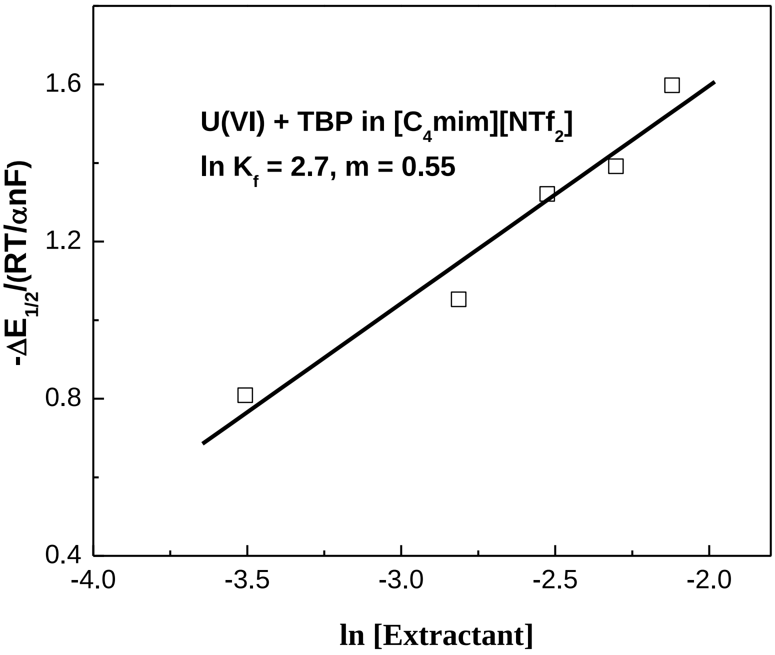

Figure 6.9. Plot of $-\Delta E_{1/2}/(RT/\alpha nF)$ against ln [TBP]. [TBP] = 0.03 M – 0.120 M, scan rate = $0.1 Vs^{-1}$, temperature = 373 K.

6.2.4. Cyclic voltammetric study of U(VI) in TOP/[C_4mim][NTf_2]

Higher homolog of TBP has been proposed for the extraction of U(VI) and Pu(IV) from fast reactor fuel reprocessing solution. In this context, tri-*n*-octyl phosphate (TOP) has been chosen as the representative for the extraction of U(VI), and the related solvent extraction studies of U(VI) in TOP/[C_4mim][NTf_2] is discussed elsewhere [119]. The cyclic voltammogram of U(VI) in 0.03 M solution of TOP in [C_4mim][NTf_2] recorded at the scan rate of $0.1 Vs^{-1}$at glassy carbon electrode at 373 K is shown in figure 6.5. The voltammogram is compared with those obtained in the absence of TOP and that obtained in the presence of TBP in $[C_4mim][NTf_2]$. A cathodic wave occurs at the peak potential of -0.45 V (Vs. Fc/Fc^+) and the anodic wave occurs at 0.42 V (Vs. Fc/Fc^+). Comparing the peak potential observed in the presence and absence of TOP, the study shows that the presence of TOP shifts the reduction potential to more cathodic values. Moreover, the presence of TOP shifts the peak potential to more negative values as compared to TBP. This shows that the stability of U(VI) - TOP complex could be more than the U(VI) - TBP complex in $[C_4mim][NTf_2]$.

The cyclic voltammogram of 0.1 M U(VI) in 0.03 M TOP/$[C_4mim][NTf_2]$ at various scan rates is shown in figure 6.10. The cathodic peak potential increases and is shifted cathodically with increase of scan rate indicating that the reduction of U(VI) present in TOP/$[C_4mim][NTf_2]$ is not reversible. The plot of cathodic peak current against $\nu^{1/2}$ obtained at various temperatures is shown in the figure 6.11. The data was fitted by a straight line. Using equations 6.1 and 6.2, the diffusion coefficient was determined and compared with those obtained in other systems in table 6.2. It can be seen that the diffusion coefficients are lowered in the presence of TOP possibly due to the bulky nature of TOP as compared to TBP.

The charge transfer rate constant (k_s) in TOP/$[C_4mim][NTf_2]$ was also determined and the values thus obtained are tabulated in table 6.2. Similar to diffusion coefficients, the k_s values also lowered in the presence of TOP. The magnitude of k_s lies in the range of $0.3\nu^{1/2} \geq k_s \geq 2x10^{-5}\nu^{1/2}$, confirming that the reduction of U(VI) at glassy carbon electrode in the presence of TOP is also quasi-reversible.

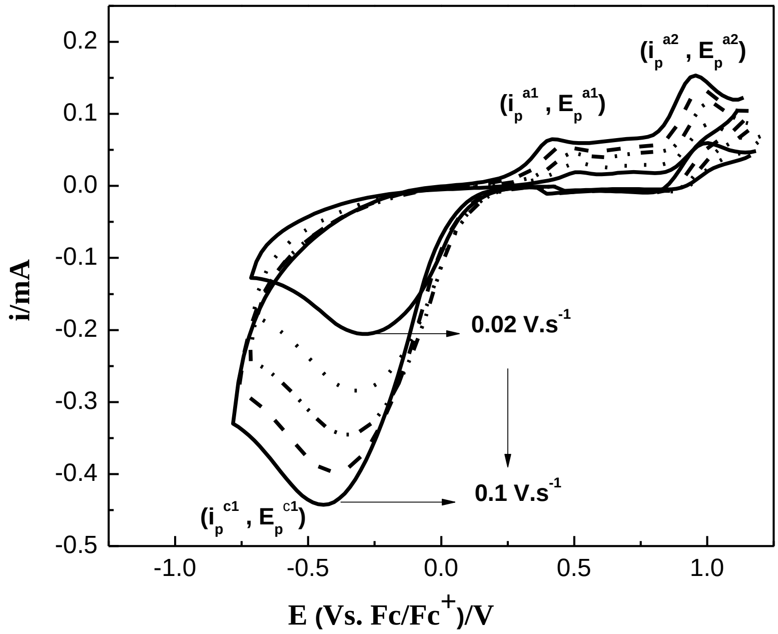

Figure 6.10. Cyclic voltammogram of U(VI) in TOP/[C$_4$mim][NTf$_2$] recorded at glassy carbon electrode at various scan rates. [U(VI)] = 0.1 M, [TOP] = 0.03 M, temperature = 373 K.

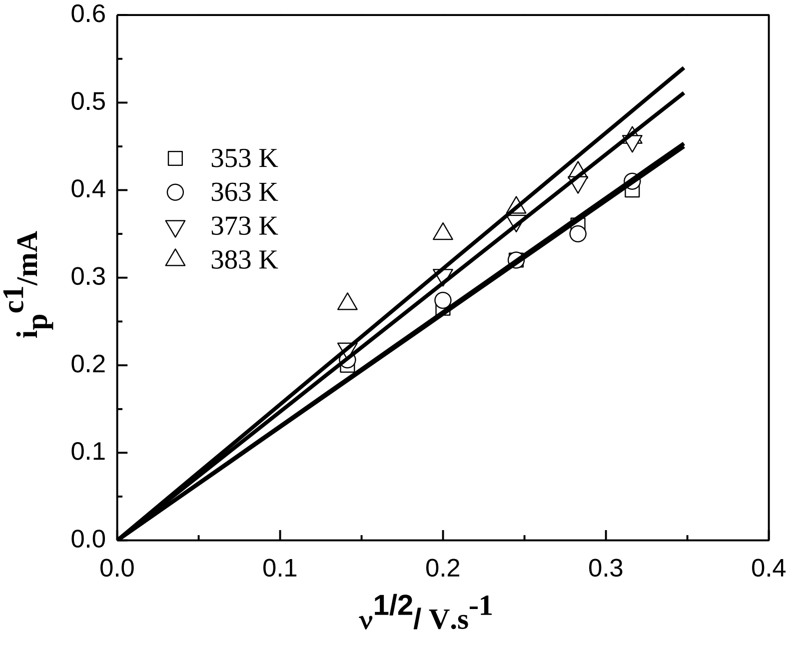

Figure 6.11. Plot of i_p^{c1} against square root of scan rate ($v^{1/2}$) for the reduction of U(VI) to U(V) in TOP/[C$_4$mim][NTf$_2$] at various temperatures.[U(VI)] = 0.1 M, [TOP] =0.03 M, temperature: 353 K to 383 K.

6.2.5 Stoichiometry and stability constant of U(VI)-TOP complex

The number of molecules of TOP co-ordinated to U(VI) and the logarithmic stability constant (ln K_f) of the U(VI) - $(TOP)_m$ complex was determined using the relation shown in equation 6.4. Figure 6.12 shows the cyclic voltammogram of U(VI) in TOP/$[C_4mim][NTf_2]$ at various concentrations of TOP at 373 K . It can be seen that the cathodic peak current decreases and the peak potential is shifted cathodically with increase in the concentration of TOP, similar to that observed for U(VI)-TBP in ionic liquid.

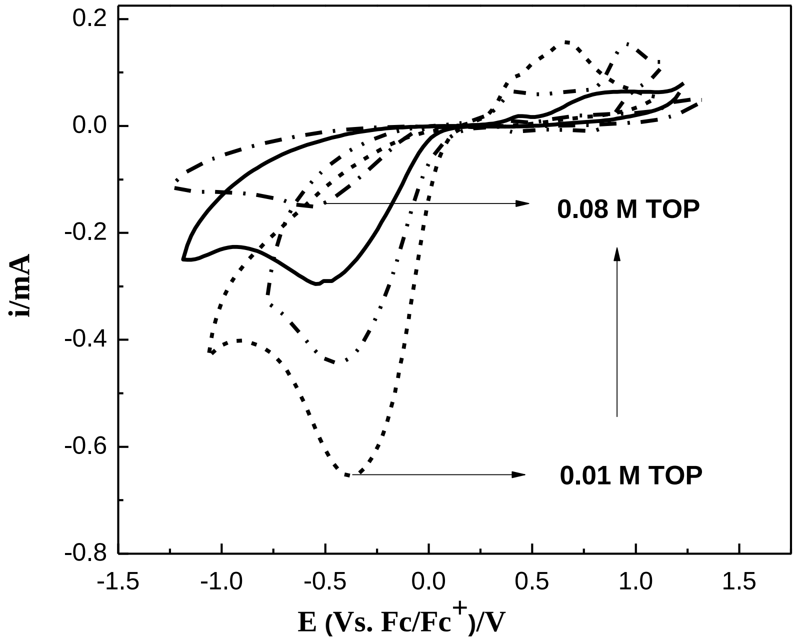

Figure 6.12. Cyclic voltammogram of U(VI) in TOP/$[C_4mim][NTf_2]$ recorded at glassy carbon electrode for various concentrations of TOP. [U(VI)] = 0.1 M, [TOP] = 0.01 to 0.08 M, scan rate = 0.1 Vs^{-1}, temperature = 373 K.

The plot of $-\Delta E_{1/2}/(RT/\alpha nF)$ against the logarithmic concentrations of TOP is shown in figure 6.13. From the intercept and slope, the stability constant (ln K_f) and the number of TOP ligands co-ordinated to U(VI) were determined to be 2.9 and 0.53

respectively. This shows that the stoichiometry of U(VI) to TOP is 2:1 in ionic liquid phase. It was also noted that the stability constant for U(VI) - TOP complex is slightly higher than that for obtained for U(VI) - TBP. This behavior is in line with extraction studies reported for U(VI) in TBP/[$C_n$mim][NTf_2] and TOP/[$C_n$mim][NTf_2][119]. It was reported that the extraction of U(VI) was higher in TOP as compared to TBP in both ionic liquid and molecular diluents (*n*-dodecane) medium. This was attributed to the increased basicity of TOP, due to the presence of longer chain length of alkyl group (+I effect) attached to phosphoryl group, as compared to TBP. Therefore, the extraction and stability constant of U(VI) – TOP complex is higher than U(VI) - TBP.

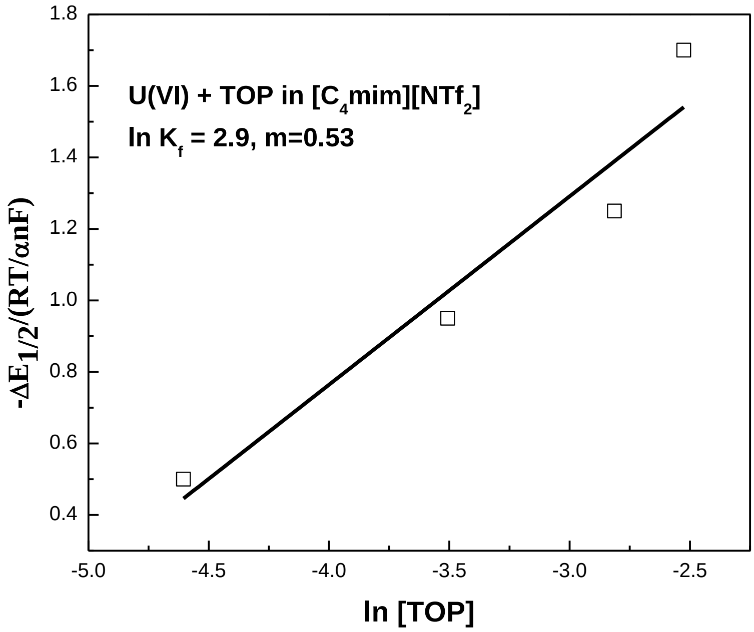

Figure 6.13. Plot of -$\Delta E_{1/2}$/ (RT/αnF) against ln [TOP]. [TOP] = 0.01 to 0.08 M, scan rate = 0.1 Vs^{-1}, temperature = 373 K.

6.3. Conclusion

The electrochemical behaviour of U(VI) in [C_4mim][NTf_2] was studied in the presence of TBP and TOP. The cathodic wave responsible for the reduction of U(VI) to U(V) shifted cathodically and the peak current lowered in the presence of these ligands. Since the octyl moiety attached to TOP was bulkier and offered more basicity to the phosphoryl moiety as compared to TBP, the stability constant of U(VI)-TOP determined from the voltammogram was slightly higher than that observed for U(VI)-TBP complex. The diffusion coefficient of U(VI) and the heterogeneous electron transfer rate constant in [C_4mim][NTf_2] decreased in the order U(VI) > U(VI) – TBP > U(VI) –TOP. All these observations indicate that the electrochemical behaviour of U(VI) in [C_4mim][NTf_2] medium would show a strong dependence on the nature of ligand employed for extraction.

PART 2

Electrochemical study of Eu(III) in the presence of acidic extractants dissolved in RTIL medium

In the recent past, several authors have reported the separation of lanthanides and actinides using various acidic extractants by solvent extraction procedures [120,227-232]. Among the series of acidic extractants, di(2-ethylhexyl)phosphoric acid (HDEHP) is a well-established extractant for the mutual separation of trivalent lanthanides and actinides. As the pKa of HDEHP is 3.21, it is strongly acidic in nature and complexes with trivalent metal ions through –POO− moiety [120, 227,228]. Similarly, diglycolamic acids (HDGA) are receiving increased attention in the recent past for the separation of lanthanides and actinides from dilute acid medium [120, 229-232]. Essentially, HDGA coordinates through carboxyl group (-COO−) as well by the etheric oxygen present in it. In view of this, HDGA is regarded as a strongly coordinating ligand as compared to HDEHP though the pKa of HDGA is 4.11 (more than that of HDEHP). Recently, Alok *et al*. [120] has reported the mutual separation of europium(III) from americium(III) using a solution of HDEHP/HDGA in imidazolium based ionic liquid. However, there is no report available in literature on the electrochemical of behavior of lanthanide(III) or actinide(III) ions present in the solution of HDEHP or HDGA in ionic liquid medium. Since these acidic extractants play a dominant role at the back end of fuel cycle, it is essential to investigate the electrochemical behavior of trivalent lanthanides and actinides in the presence of these acidic extractants dissolved in RTIL medium. Therefore, the objective of part 2 in chapter 6 is to report electrochemical behavior of Eu(III) in RTIL medium containing acidic extractants, HDEHP and HDGA.

Table 6.3 Structure of RTIL and extractants studied in part 2 of chapter 6

Name	Structure
Extractant	
Di(2-ethylhexyl)phosphoric acid (HDEHP)	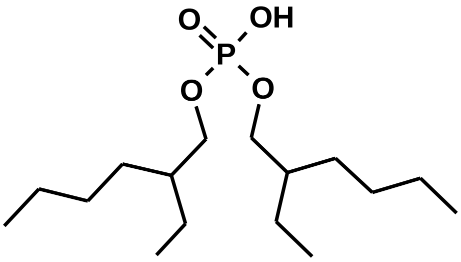
N,N'-di(2-ethylhexyl) diglycolamic acid (HDGA)	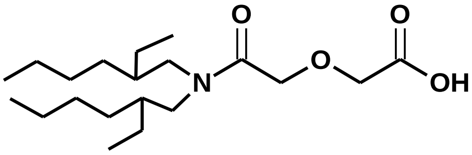
Ionic liquid	
1-Butyl-1-methylpyrrolidinium bis(trifluoromethanesulfonyl)imide ([C4mpy][NTf2])	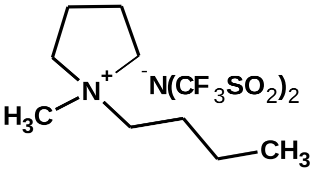

Synthesis of the ionic liquid and extractant used in part 2 have been discussed in section 2.9.2 & 2.9.10 of chapter 2. Preparation of Eu(NTf₂)₃ was discussed in section 2.4.6 of chapter 2.

6.4 Results and Discussion

6.4.1 Cyclic voltammetric study of Eu(III) in [C_4mpy][NTf_2]

Cyclic voltammogram of [C_4mpy][NTf_2] and Eu(III) in [C_4mpy][NTf_2] was recorded at glassy carbon electrode at 373K at the scan rate of 0.1Vs^{-1}. The ionic liquid, [C_4mpy][NTf_2] exhibits an electrochemical window of 5.5 V. Eu(III) in [C_4mpy][NTf_2] shows a prominent reduction wave occurring at the onset of -0.01 V (vs. Fc/Fc$^+$) that results in a peak at the cathodic potential (E_p^c) of -0.40 V (vs. Fc/Fc$^+$) due to the reduction of Eu(III) to Eu(II). The corresponding oxidation wave occurs at the peak potential of -0.05 V (vs. Fc/Fc$^+$). These results are shown in figure 6.14.

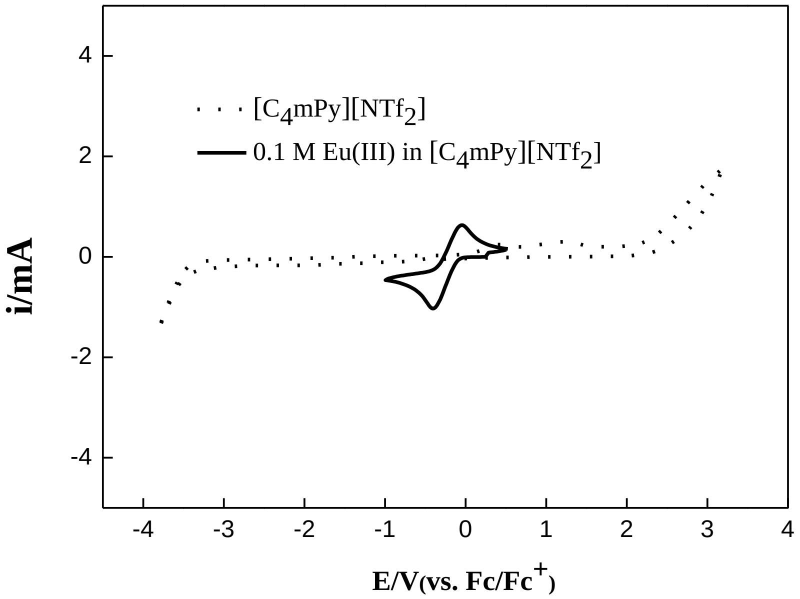

Figure 6.14. Cyclic voltamogram of [C_4mpy][NTf_2] and recorded Eu(III) in [C_4mpy][NTf_2] at glassy carbon electrode. [Eu(III)] = 0.1 M, temperature = 373 K, scan rate = 0.1 V/s.

The cyclic voltammogram of Eu(III) in [C$_4$mpy][NTf$_2$] recorded at various scan rates at glassy carbon electrode at 373 K is shown in figure 6.15. It can be seen that the cathodic current (i_p^c) increases and the cathodic peak potential (E_p^c) is shifted cathodically with increase of scan rate. This indicates that the reduction of Eu(III) to Eu(II) at glassy carbon electrode is not reversible. The difference in the value of $|E_p^c - E_{p/2}^c|$ is quite significant (0.13 V at 373 K) than the value needed for a reversible (0.07 mV at 373 K) one electron transfer process. This shows that the reduction of Eu(III) to Eu(II) is not reversible.The charge transfer coefficient was determined from the magnitude of $|E_p^c$-$E_{p/2}^c|$ using equation 6.2. The value of αn_α was determined to be ~0.5 at 373 K in a range of scan rates from 0.01 Vs^{-1}/s to 0.1Vs^{-1}.

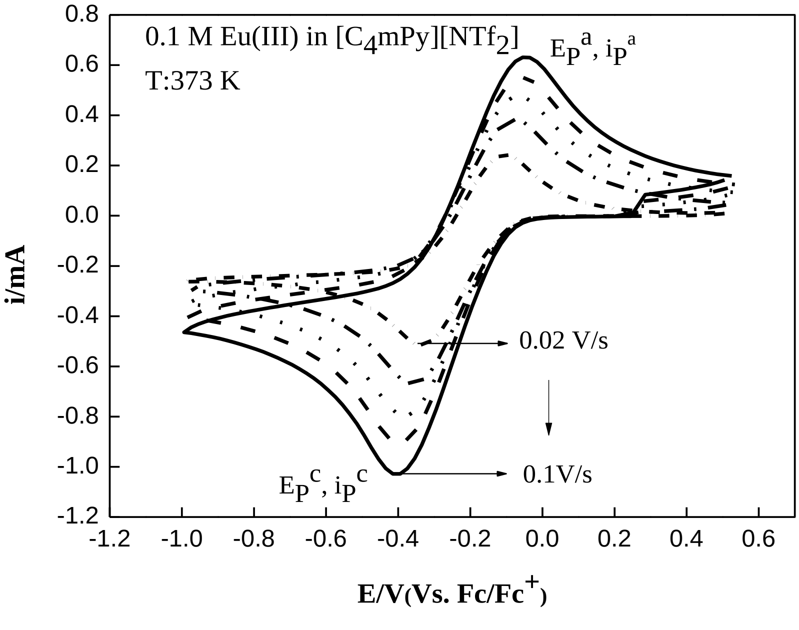

Figure 6.15. Cyclic voltamogram of Eu(III) in [C$_4$mpy][NTf$_2$] recorded at glassy carbon electrode at various scan rates. [Eu(III)] = 0.1 M, temperature = 373 K.

A plot of i_p^c against the square root of the scan rate ($\nu^{1/2}$) at 373 K for the reduction of Eu(III) to Eu(II) in [C$_4$mpy][NTf$_2$] is shown in figure 6.16. The linear dependence of the cathodic peak current with zero-intercept indicates the validity of equation 6.1 and allows the determination of the diffusion coefficient of Eu(III) in [C$_4$mpy][NTf$_2$] medium. From the slope of the straight line, the diffusion coefficients of Eu(III) was determined and provided in table 6.4. A diffusion coefficient of 3.84 x10^{-11} m^2/s at 373 K was obtained in the present study in [C$_4$mpy][NTf$_2$] at 373 K and it compares well with the diffusion coefficients reported, 2.7 x10^{-11} m^2/s, for Eu(III) in [C$_4$mpy][NTf$_2$] at 373 K by Jagadeeswara Rao *et al.* [160] and with the value 1.2 x10^{-11} m^2/s in the same ionic liquid but at lower temperature of 323 K reported by Pan *et al* [151].

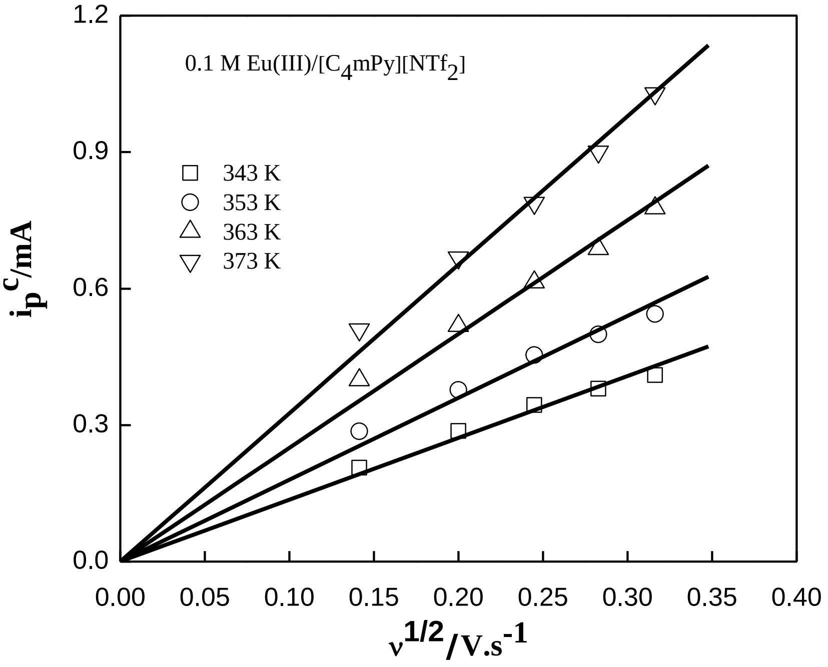

Figure 6.16. Plot of i_p^c against square root of scan rate ($\nu^{1/2}$) for the reduction of Eu(III) to Eu (II) in [C$_4$mpy][NTf$_2$] at various temperatures. Temperature: 343 K to 373 K.

Table 6.4. The diffusion coefficients (D) and heterogeneous rate constant (k_s) for the reduction of Eu(III) to Eu (II) in [C_4mpy][NTf_2] at glassy carbon electrode at various temperature [Eu(III)] = 0.1 M and [HDGA] or [HDEHP] = 0.02 M.

Temperature /K	**D x 10^{11}/m^2s^{-1}**		
	Eu(III) in [C_4mpy][NTf_2]	**Eu(III) in HDEHP / [C_4mpy][NTf_2]**	**Eu(III) in HDGA/ [C_4mpy][NTf_2]**
343	0.73	0.72	0.39
353	1.30	1.13	0.57
363	2.30	1.63	0.87
373	3.84	2.22	1.12
	k_s x 10^7/ms^{-1}		
343	12.00	7.20	2.50
353	12.90	9.00	4.50
343	14.50	9.40	6.90
373	15.60	10.50	9.50

The cyclic voltammograms of Eu(III) in [C_4mpy][NTf_2] recorded at glassy carbon working electrode at various temperatures are shown in figure 6.17. The peak potential (E_p^c) is shifted anodically and the cathodic peak current (i_p^c) increased with increase of temperature. The cyclic voltammogram of Eu(III) in [C_4mpy][NTf_2] as a function of scan rate was obtained at different temperatures and from the plot of i_p^c against the square root of the scan rate ($\nu^{1/2}$) (figure 6.16), the diffusion coefficient at various temperatures was determined. The values are tabulated in table 6.4. It can be seen that the diffusion coefficients increase with increase of temperature. This could be attributed to the decrease in viscosity of the medium with increase of temperature and enhances the diffusion coefficients.

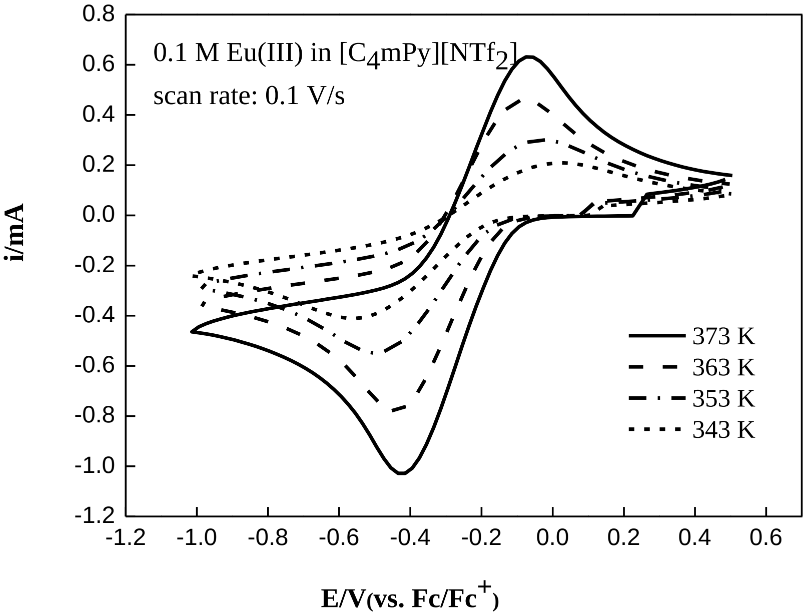

Figure 6.17. Cyclic voltamogram of Eu(III) in [C_4mpy][NTf_2] recorded at glassy carbon electrode at various temperatures. [Eu(III)] = 0.1 M, scan rate: 0.1 Vs^{-1} , temperature: 343 K to 373 K.

A marginal shift in the cathodic peak potential with the increase of scan rate, shown in figure 6.15 indicates that the reduction of Eu(III) at glassy carbon electrode could be quasi-reversible. It is observed that E_p^c is shifted cathodically and E_p^a is shifted anodically with increasing scan rate. This indicates that the reduction of Eu(III) to Eu(II) is not only controlled by diffusion of Eu(III) ion at the working electrode, but also the rate of charge transfer reaction between the electrode electrolyte inter phase. Substituting the diffusion coefficient of Eu(III) in equation 6.4, the magnitude of charge transfer rate constants were determined at various temperatures and the values are tabulated in table 6.4.

It can be seen that the value of k_s increases with increasing temperature and the magnitude of the k_s lies in the range of $0.3\ \nu^{1/2} \geq k_s \geq 2 \times 10^{-5}\ \nu^{1/2}$ cm/s, confirming that the reduction of Eu(III) at glassy carbon electrode is quasi-reversible. The increase of k_s with increasing temperature could be attributed to the decrease in viscosity of the ionic liquid medium with increase in temperature, resulting in the increase in the abundance of Eu(III) ions at the working electrode surface. Therefore, the heterogeneous charge transfer rate (k_s) occurring between the electrode-electrolyte interphase (to Eu(III) ion) increases with increase of temperature.

6.4.2 Cyclic voltammetric study of Eu(III) in HDGA/[C$_4$mpy][NTf$_2$]

The cyclic voltammogram of Eu(III) in a solution of 0.02 M bis(2-ethylhexyl)diglycolamic acid (HDGA) in [C$_4$mpy][NTf$_2$] at the scan rate of 0.1Vs^{-1} at 373 K is shown in figure 6.18. The voltammogram is compared with the voltammogram obtained in the absence of HDGA. It can be seen that the cathodic wave occurs at the onset of -0.2 V (Vs. Fc/Fc$^+$), leading to a prominent cathodic wave at the peak potential of -0.47 V is due to the reduction of Eu(III) to Eu(II). The corresponding oxidation wave occurs at the peak potential of -0.27 V (Vs. Fc/Fc$^+$). Comparing the peak potentials observed in the presence and absence of HDGA, the voltammogram shows that the presence of HDGA shifts the reduction of Eu(III) to more negative potentials possibly due to the co-ordination of Eu(III) with HDGA. Since the co-ordinated Eu(III) requires higher potentials for reduction, the peak potential is shifted cathodically for Eu(III) – HDGA in ionic liquid system. The shift of the peak potential of the HDGA complex against the non-complexed Eu(III) gives information about the strength of the co-ordindation.

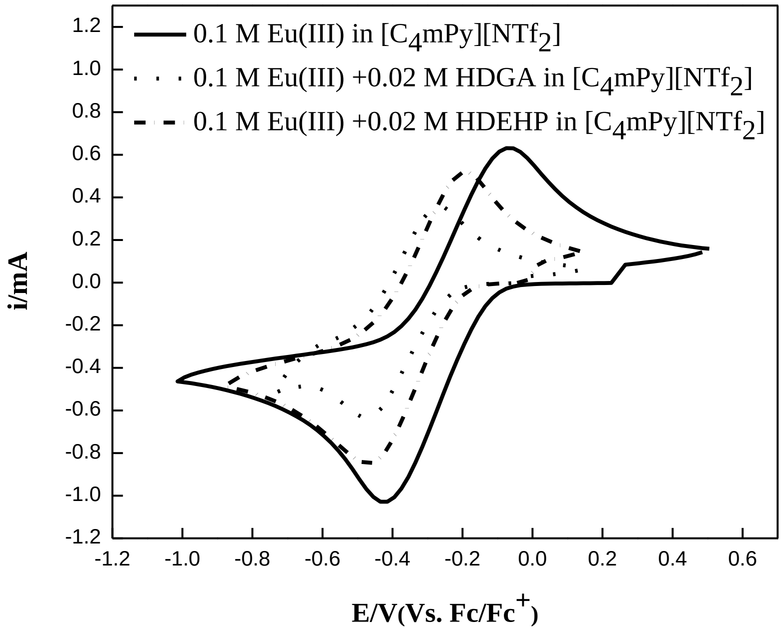

Figure 6.18. Cyclic voltammogram of Eu(III) in [C_4mpy][NTf_2], in HDGA/[C_4mpy][NTf_2] and in HDEHP/[C_4mpy][NTf_2] recorded at glassy carbon electrode. [Eu(III)] = 0.1 M, [HDGA] = 0.02 M, [HDEHP] = 0.02 M, scan rate = 0.1 Vs^{-1}, temperature = 373 K.

The cyclic voltammogram of Eu(III) in 0.02 M HDGA/[C_4mpy][NTf_2] at various scan rates at 373 K is shown in figure 6.19. It can be seen that the cathodic peak current potential (E_p^c) is shifted cathodically with increasing scan rate and the magnitude $|E_p^c - E_{p/2}^c|$ (= 0.1 V) is larger than the value needed for the reversible one electron transfer process at 373 K. This shows that the reduction of Eu(III) in HDGA/[C_4mpy][NTf_2] is also not reversible. The value of αn_α in the present case was determined to be ~0.6 at 373 K in a range of scan rates from 0.01Vs^{-1} to 0.1Vs^{-1}.

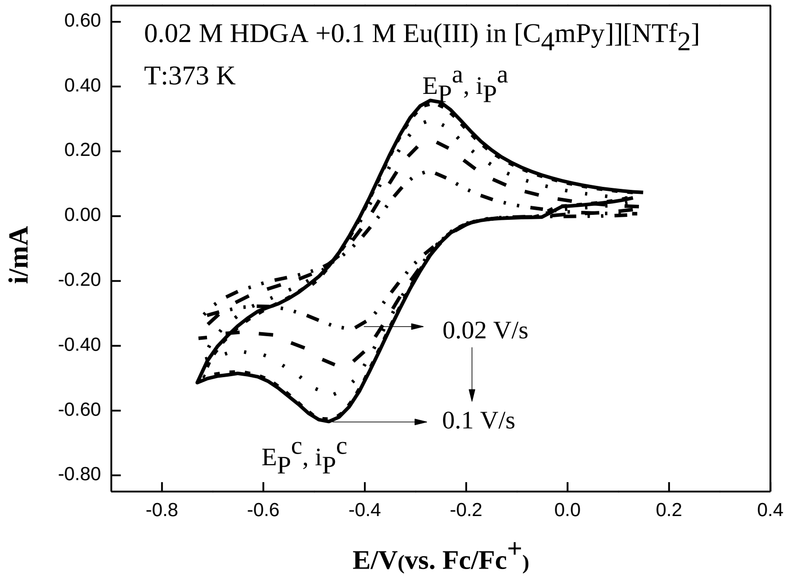

Figure 6.19. Cyclic voltammogram of Eu(III) in HDGA/[C_4mpy][NTf_2] recorded at glassy carbon electrode at various scan rates. [Eu(III)] = 0.1 M, [HDGA] = 0.02 M, temperature = 373 K.

The plot of the cathodic current (i_p^c) obtained at various temperatures against $\nu^{1/2}$ is shown in figure 6.20. From the slope of the straight line, equations 6.1 and 6.2, the diffusion coefficient of Eu(III) in 0.02 M HDGA /[C_4mpy][NTf_2] was determined and compared with that determined in the absence of HDGA in table 6.4. The rate constant (k_s) for the charge transfer between the electrode – electrolyte interphase was determined using equation 6.3. The values thus obtained are tabulated in table 6.2. It can be seen that k_s values indicated that reductionof U(VI) in the presence of HDGA is quasireversible and k_s values are lowered marginally in the presence of HDGA, due to the co-ordination of Eu(III) by HDGA.

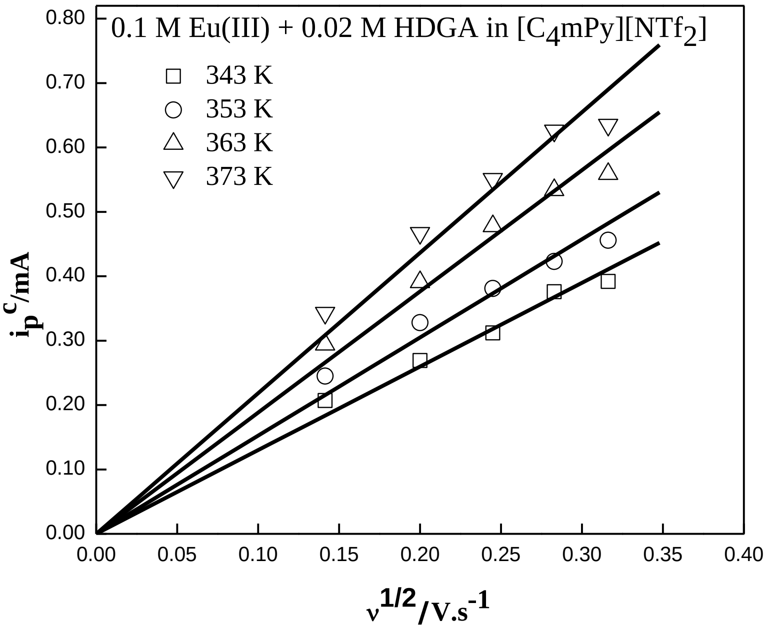

Figure 6.20. Plot of i_p^c against square root of scan rate ($v^{1/2}$) for the reduction of Eu(III) to Eu (II) in HDGA/[C_4mpy][NTf_2] at various temperatures.[Eu(III)] =0.1 M, [HDGA] = 0.02 M, temperature: 343 K to 373 K.

6.4.3 Stoichiometry stability constant of Eu(III)-HDGA complex

The cyclic voltammogram of Eu(III) in HDGA/[C_4mpy][NTf_2] at various concentrations of HDGA at 373K is shown in figure 6.21. It can be seen that the cathodic peak current decreases and the peak potential is shifted cathodically with increase in the concentration of HDGA, as expected. The number of molecules of HDGA co-ordinated to Eu(III), and the logarithmic stability constant (ln K_f) for the Eu(III) - $(HDGA)_m$ complex was determined from the voltammogram by using the relation shown in equation 6.4. The plot of $-\Delta E_{1/2}/(RT/\alpha nF)$ against the logarithmic value of HDGA concentration is shown in figure 6.22. It can be seen that the magnitude of $-\Delta E_{1/2}/(RT/\alpha nF)$ increases linearly with increase in the concentration of HDGA. From the magnitude of the intercept and slope, the stability constant (ln K_f) and the co-ordination number can be determined to be 5.65 and 0.97 respectively.

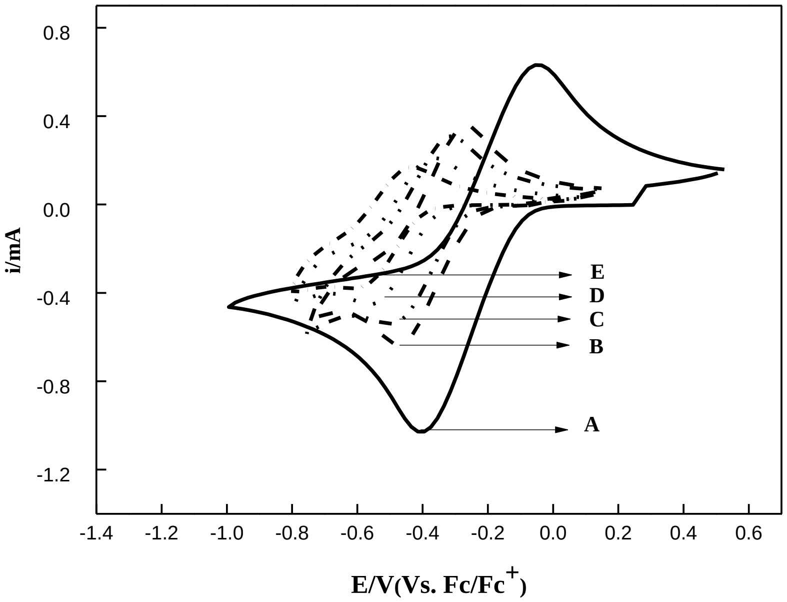

Figure 6.21. Cyclic voltammogram of Eu(III) in HDGA/[C_4mpy][NTf_2] recorded at glassy carbon electrode for various concentrations of HDGA. Eu alone (A), Eu(III) + 0.02 M HDGA (B), Eu(III) + 0.04 M HDGA (C), Eu(III) + 0.06 M HDGA (D) and Eu(III) + 0.08 M HDGA (E),[Eu(III)] = 0.1 M, scan rate = 0.1 Vs^{-1} , temperature = 373 K.

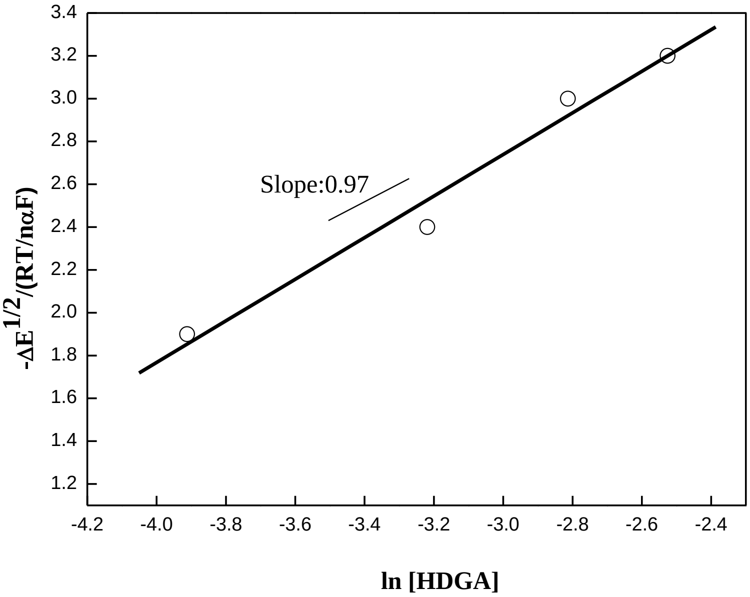

Figure 6.22. Plot of -$\Delta E_{1/2}$/ (RT/αnF) against the ln [HDGA]. [HDGA] = 0.02 M – 0.08 M, scan rate = 0.1 Vs^{-1} , temperature = 373 K.

6.4.4. Cyclic voltammetric study of Eu(III) in HDEHP/[C_4mpy][NTf_2]

The cyclic voltammogram of Eu(III) in 0.02 M solution of HDEHP in [C_4mpy][NTf_2] recorded at the scan rate of 0.1Vs^{-1} on the glassy carbon electrode at 373 K is shown in figure 6.18. The voltammogram is compared with those obtained in the absence of HDEHP and that obtained in the presence of HDGA in [C_4mpy][NTf_2]. A cathodic wave occurs at the peak potential of -0.46 V and the anodic wave occurs at -0.19 V (vs. Fc/Fc^+). Comparing the peak potential observed in the presence and absence of HDEHP, HDEHP shifts the reduction potential to more cathodic values. The shift in the reduction potential of Eu(III) to Eu(II) in the presence of HDEHP is comparable with that obtained in the presence of HDGA. This shows that the stability of Eu-HDEHP complex in [C_4mpy][NTf_2] is comparable with the Eu- HDGA complex in [C_4mpy][NTf_2]. The cyclic voltammogram of 0.1M Eu(III) in 0.02 M HDEHP/[C_4mpy][NTf_2] at various scan rates is shown in figure 6.23. The cathodic peak potential increases and shifted cathodically with increasing scan rate indicating that the reduction of Eu(III) present in HDEHP/[C_4mpy][NTf_2] is not reversible. The cathodic peak current i_P^c against $\nu^{1/2}$ obtained at various temperatures is shown in figure 6.24. The data was fitted by a straight line. From the slope of the straight line and using equations 1 and 2, the diffusion coefficient was determined and compared with those obtained in other systems in table 6.4. The diffusion coefficients decreased in the order Eu(III) in [C_4mPy][NTf_2] > Eu(III) in HDEHP in [C_4mPy][NTf_2] > Eu(III) in HDGA in [C_4mPy][NTf_2]. These results are in good agreement with the stability constants obtained for HDEHP and HDGA complexes with Eu(III). The charge transfer rate constant (k_s) in HDEHP/[C_4mpy][NTf_2] was also determined and the values are tabulated in table 6.4. It can be seen that the k_s values are marginally lower than that obtained in the absence of ligands.

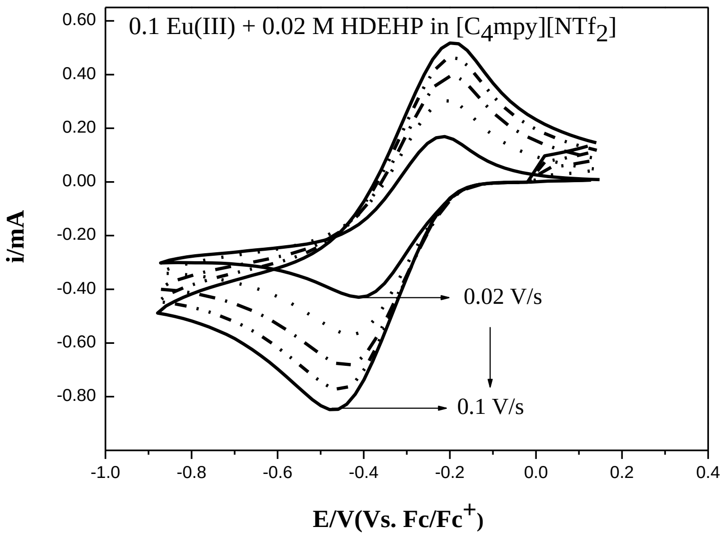

Figure 6.23. Cyclic voltammogram of Eu(III) in HDEHP/[C_4mpy][NTf_2] recorded at glassy carbon electrode at various scan rates. [Eu(III)] = 0.1 M, [HDEHP] = 0.02 M, temperature = 373 K.

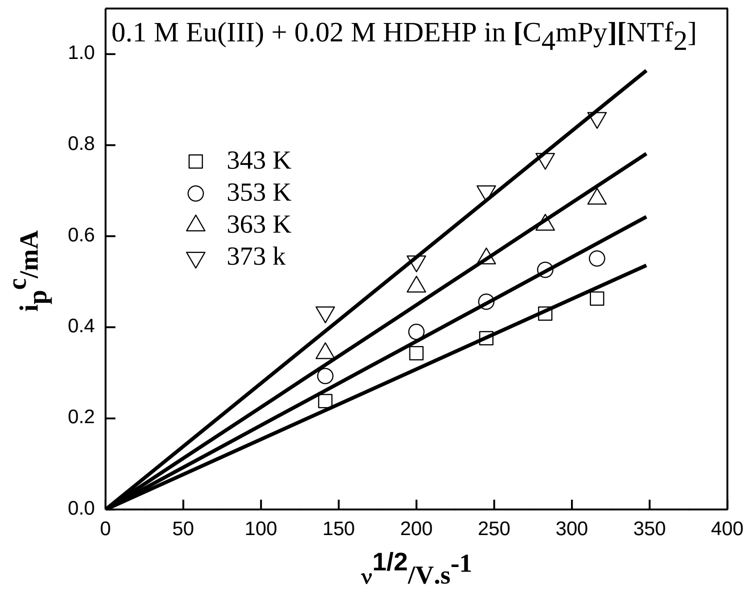

Figure 6.24. Plot of i_p^c against square root of scan rate ($v^{1/2}$) for the reduction of Eu(III) to Eu (II) in HDEHP/[C_4mpy][NTf_2] at various temperatures. [Eu(III)] = 0.1 M, [HDEHP] = 0.02 M, temperature: 343 K to 373 K.

6.4.5 Stoichiometry and stability constant of Eu(III)- HDEHP complex

The Eu-HDEHP stoichiometry and the stability constant (ln K_f) were determined using the relation shown in equation 6.4. Figure 6.25 shows the cyclic voltammogram of Eu(III) in HDEHP/[C_4mpy][NTf_2] at various concentrations of HDEHP at 373 K . It can be seen that the cathodic peak current decreases and the peak potential is shifted cathodically with increasing concentration of HDEHP similar to that observed for Eu(III)-HDGA.

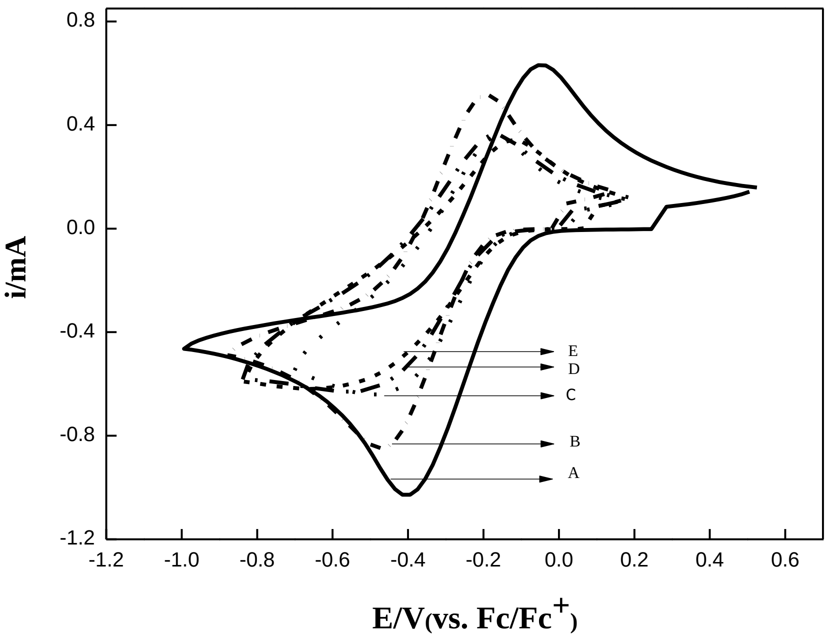

Figure 6.25. Cyclic voltammogram of Eu(III) in HDEHP/[C_4mpy][NTf_2] recorded at glassy carbon electrode for various concentrations of HDEHP. Eu alone (A), Eu(III) + 0.02 M HDEHP (B), Eu(III) + 0.04 M HDEHP (C), Eu(III) + 0.06 M HDEHP (D) and Eu(III) + 0.08 M HDEHP (E), [Eu(III)] = 0.1 M, scan rate = 0.1 Vs^{-1} , temperature = 373 K.

The plot of -$\Delta E_{1/2}$/ (RT/αnF) against the logarithmic concentrations of HDEHP is shown in figure 6.26. From the intercept and slope, the stability constant (ln K_f) and the number of HDEHP ligands co-ordinated to Eu(III) are determined to be 5 and 0.92 respectively. This shows that about 1 molecule of HDEHP is co-ordinated to Eu(III) in ionic liquid phase.

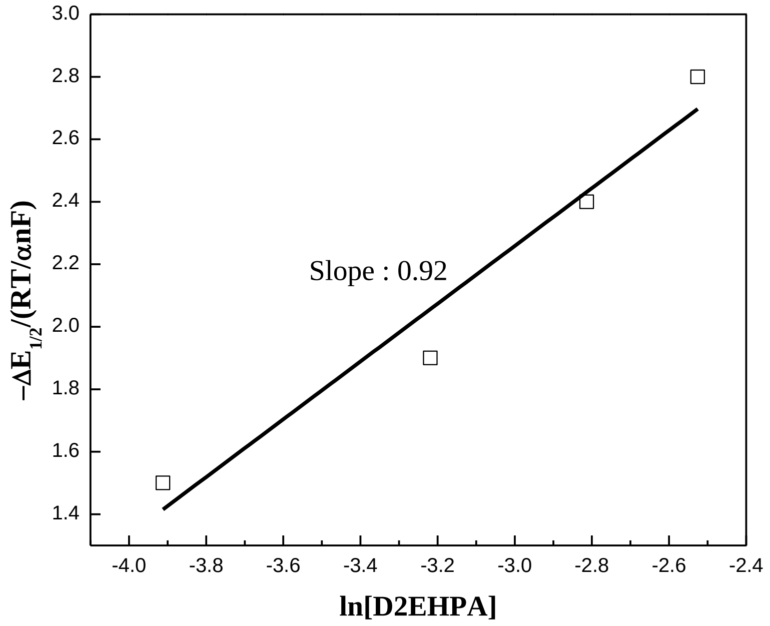

Figure 6.26. Plot of -$\Delta E_{1/2}$/ (RT/αnF) against the ln [HDEHP]. [HDEHP] = 0.02 M – 0.08 M, scan rate = 0.1 Vs^{-1}, temperature = 373 K.

A marginally lower value of stability constant was obtained for HDEHP as compared to HDGA, shows that the stability of Eu(III) - HDEHP and Eu(III) – HDGA complexes are comparable. Previously, Alok *et al*. studied the solvent extraction behavior of radioactive $^{(152+154)}$Eu(III) in HDGA or HDEHP present in ionic liquid medium [120]. In those studies, the Eu(III) (concentration of radioactive tracer = 10^{-5} M) distribution ratios were measured in 0.05 M solution of HDGA or HDEHP present in ionic liquid medium. From these measurements, the Eu(III) – ligand stoichiometry of 1:3 was reported. However, to carry out the electrochemical measurements in the present study, significant concentration of Eu(III) ion in ionic liquid medium was required to obtain good current response in the voltammogram. Therefore, the concentration of Eu(III) in ionic liquid was fixed at 0.1 M and the ligand concentration was varied from 0.02 M to 0.08 M to determine the stoichiometry. From these measurements, the stoichiometry of Eu(III): ligand was determined to be 1:1, which can be attributed to the high concentration of metal ion employed in electrochemical measurements.

6.4.6 Chronopotentiometric study (CP)

The electrochemical behavior of Eu (III) in $[C_4mpy][NTf_2]$ was studied using chronopotentiometry also. The chronopotentiogram was recorded at various applied current densities at glassy carbon electrode and the traces are shown in figure 6.27. The relation between the applied current and transition time is given by Sand’s relation [164, 165] shown in equation 6.5.

$$i\tau^{1/2} = nFAD_o^{1/2}\pi^{1/2}C/2 \qquad (6.5)$$

The transient time (τ) shown in figure 6.27 is a measure of the time elapsed between the commencement of constant potential regime and the time at which the concentration of electroactive species resulting from diffusion reaches zero at the electrode. Transient time can be obtained by the linear extrapolation of the sections on the chronopotentiometry transients before and after the inflection. The τ observed is due to the reduction of Eu(III) to Eu(II). The product $i\tau^{1/2}$ determined from various transients is tabulated in table 6.5. It can be seen that $i\tau^{1/2}$ is nearly constant. The plot of i against $\tau^{-1/2}$, shown in figure 6.28 is linear and thus enables the determination of the diffusion coefficient.

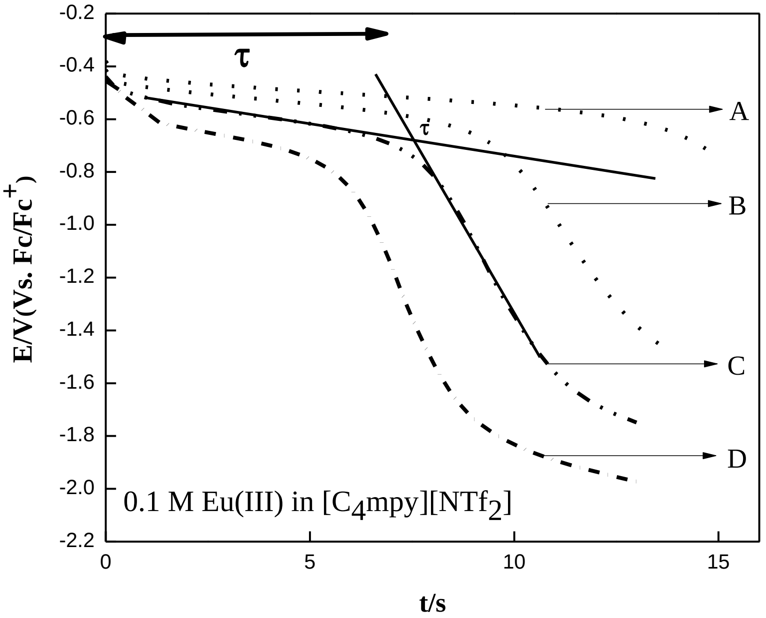

Figure 6.27. Comparison of chronopotentiograms for the reduction of Eu(III) to Eu(II) in [C_4mpy][NTf_2] at 373 K at the applied current of −0.2 mA (A), −0.25 mA (B), −0.3 mA (C) and −0.35 mA (D). Working and counter electrode: glassy carbon.

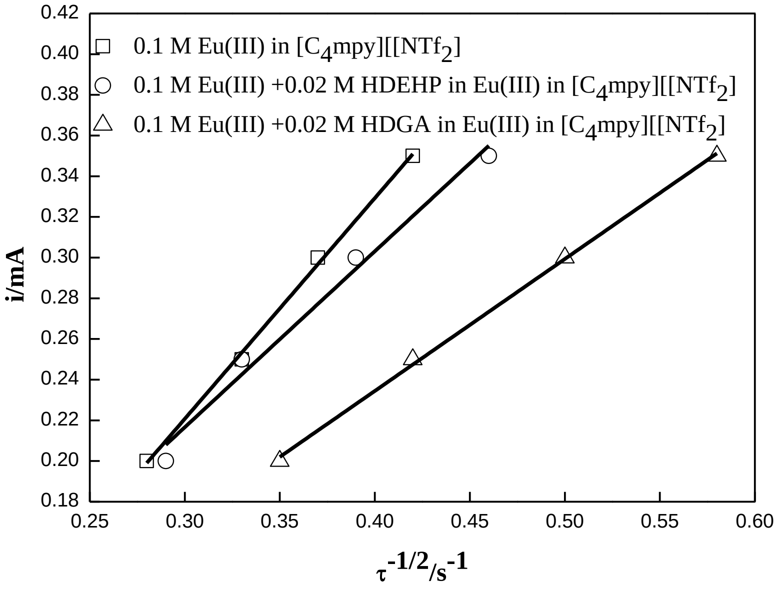

Figure 6.28. Plot of i vs $\tau^{-1/2}$ for the reduction of Eu(III) to Eu (II) in [C_4mpy][NTf_2] or HDEHP + [C_4mpy][NTf_2] or HDGA + [C_4mpy][NTf_2] at 373 K.

The chronopotentiograms of Eu(III) to Eu(II) is recorded in the presence of ligands (HDEHP and HDGA) and they are compared in figure 6.29. The product $i\tau^{1/2}$ is constant (Table 6.5) and the plot of i against $\tau^{-1/2}$ is linear as shown in figure 6.28. The diffusion coefficient values for the reduction of Eu(III) to Eu(II) determined from chronopotentiometry are shown in table 6.5. It can be seen the diffusion coefficients are lower in the presence of ligands. The diffusion coefficients obtained by chronopotentiometry are in good agreement with result obtained by cyclic voltammetry.

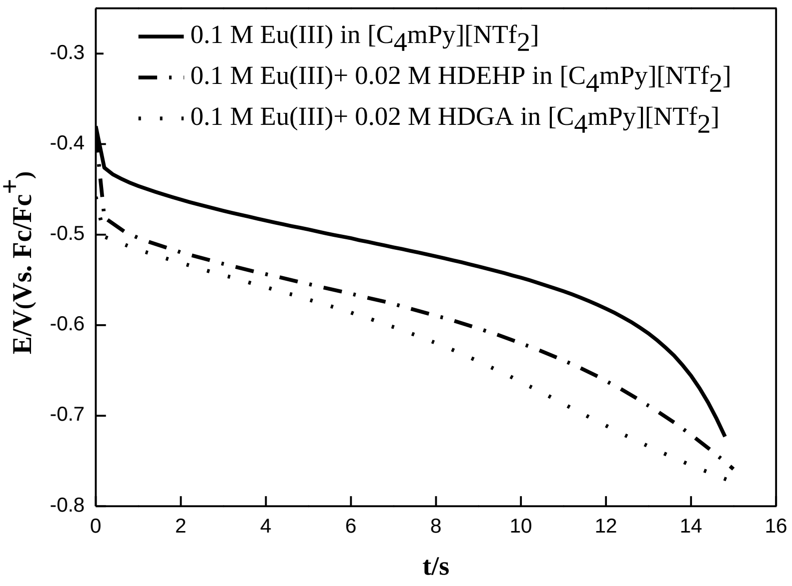

Figure 6.29. Comparison of chronopotentiograms for the reduction of Eu(III) to Eu(II) in [C_4mPy][NTf_2] or HDEHP + [C_4mPy][NTf_2] or HDGA + [C_4mPy][NTf_2] at 373 K at the applied current of −0.2 mA. Working and counter electrode: glassy carbon.

6.4.7 Chronoamperometric study (CA)

The chronoamperograms for the cathodic reduction of Eu(III) to Eu(II) in [C_4mPy][NTf_2] at 373 K was recorded in the presence and absence of ligands (HDEHP and HDGA) and they are shown in figure 6.30.The linearity with zero-intercept obtained from the plot of i against $t^{-1/2}$ (Cottrell plot, Figure 18 inset) gives the validity of simple diffusion controlled reduction and the diffusion coefficient of Eu(III) was determined using equation 6.7 [164,165]. The diffusion coefficient of Eu(III) is determined to be 1.6 x 10^{11}/m^2s^{-1} at 373 K.

$$i = \frac{nFAD_o^{1/2}C}{(\pi t)^{1/2}} \qquad (6.7)$$

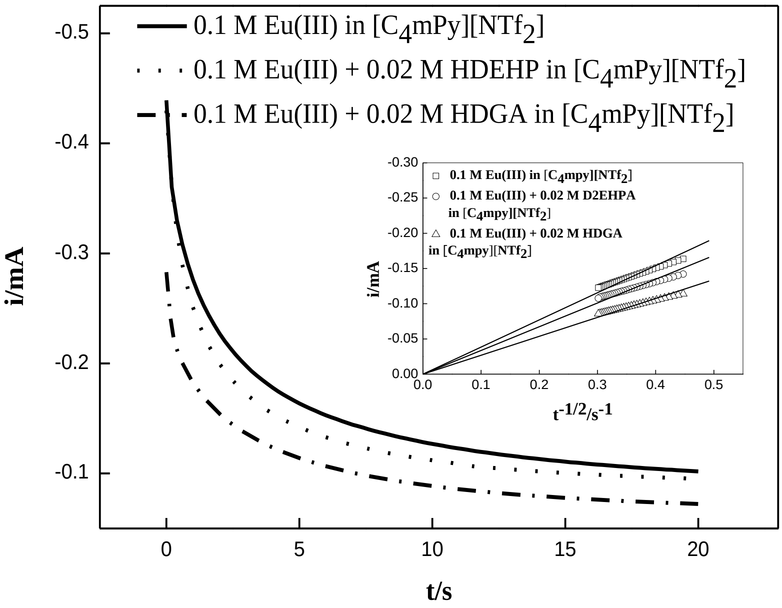

Figure 6.30. Comparison of chronoamperograms for the reduction of Eu(III) to Eu(II) in [C_4MPy][NTf_2] or HDEHP + [C_4MPy][NTf_2] or HDGA + [C_4MPy][NTf_2] at 373 K at the applied potential(-0.2 V). Inset: Cottrell plot for the reduction of Eu(III) to Eu(II).

The diffusion coefficient of Eu(III) was determined from chronoamperograms in the presence of ligands also using equation 6.7. The diffusion coefficients are tabulated in table 6.6 that compares the values obtained with other techniques. The values indicate that the diffusion coefficient of Eu(III) decreases in the presence of ligand in the order HDEHP > HDGA, and the diffusion coefficient obtained by various techniques are comparable.

Table 6.5. Chronopotentiometric constant (i$\tau^{1/2}$) and diffusion coefficient of Eu(III) obtained from chronopotentiograms at 373 K for the reduction of Eu(III) (0.1 M) at glassy carbon electrode at constant current in the presense and absent of ligands.

System	**i/mA**	**τ/s**	**i$\tau^{1/2}$/mA s**	**Diffusion coefficient, D x 10^{11}/m^2s^{-1}**
Eu(III) in [C_4mpy][NTf_2]	0.20	13.1	0.72	4.2
	0.25	9.2	0.76	
	0.30	7.4	0.82	
	0.35	5.8	0.84	
Eu(III) + HDEHP in [C_4mpy][NTf_2]	0.20	11.3	0.67	2.7
	0.25	9.0	0.75	
	0.30	6.5	0.76	
	0.35	4.7	0.76	
Eu(III) + HDGA in [C_4mpy][NTf_2]	0.20	8.0	0.57	1.5
	0.25	5.7	0.60	
	0.30	4.0	0.60	
	0.35	3.0	0.60	

Table 6.6. Comparison of diffusion coefficient of Eu(III) obtained in various techniques for the reduction of Eu(III) in [C_4mpy][NTf_2] at 373 K.

System	**D x 10^{11}/m^2s^{-1}**		
	CV	**CP**	**CA**
0.1 M Eu(III) in [C_4mpy][NTf_2]	3.8	4.2	1.6
0.1 M Eu(III) + 0.02 M HDEHP in [C_4mpy][NTf_2]	2.2	2.7	1.4
0.1 M Eu(III) + 0.02 M HDGA in [C_4mpy][NTf_2]	1.1	1.5	0.8

6.5 Conclusion

The electrochemical behavior of Eu(III) in [C_4mpy][NTf_2] was studied on glassy carbon as working electrode in the presence and absence HDEHP and HDGA by cyclic voltammetry, chronopotentiometry and chronoamperometry . The cyclic voltammogram of Eu(III) exhibited a prominent quasi-reversible redox couple in the potential range -1 V to +0.5 V. The addition of HDEHP and HDGA to the Eu(III)/[C_4mpy][NTf_2] solution lowered the cathodic peak current and shifted the cathodic peak potential cathodically due to the co-ordination of Eu(III) with ligands in the ionic liquid medium. The magnitude of the diffusion coefficients obtained by different electrochemical methods was comparable. In the presence of ligands, the diffusion coefficients and heterogeneous rate constants decreased in the order Eu(III) > (Eu(III) + HDEHP) > (Eu(III) + HDGA) in the ionic liquid. Both diffusion coefficient and heterogeneous charge transfer rate constant increased with increase of temperature. The stability constant (ln K_f) of Eu(III)-ligand complex was determined to be 5 and 5.65 for (Eu(III)-HDEHP) and (Eu(III)- HDGA) complexes respectively, which was in accordance with diffusion coefficients.

CHAPTER 7

SUMMARY AND SCOPE OF FUTURE STUDIES

In this chapter, the summary of the work discussed in various chapters and the scope of the future work are discussed.

7.1 ROOM TEMPERATURE IONIC LIQUID AS A DILUENT FOR SOLVENT EXTRACTION OF ACTINIDES

Room temperature ionic liquids such as 1-alkyl-3-methylimidazolium bis(trifluoromethanesulfonyl)imide ($[C_nmim][NTf_2]$) and 1-butyl-1-methylpyrrolidinium bis(trifluoromethane-sulfonyl)imide ($[C_4mpy][NTf_2]$) have been explored as diluents in solvent extraction applications. Extractants such as tri-*n*-alkyl phosphates, *N*, *N*-dialkyl 2-hydroxyacetamide and benzoyl pyrazalone have been dissolved in RTIL diluents and used for extraction of actinides.

7.1.1 Extraction behavior of U(VI) in some tri n-alkyl phosphates (TAlP) present in imidazolium based room temperature ionic liquid

The extraction behavior of U(VI) in some tri-*n*-alkylphosphates dissolved in 1-octyl-3-methylimidazolium bis(trifluoromethanesulfonyl)imide ($[C_8mim][NTf_2]$) was studied to compare the interaction of U(VI) in ionic liquid vis-à-vis *n*-DD medium for fast reactor fuel reprocessing application. The distribution ratio of U(VI) increased with increase in the concentration of nitric acid, reached maximum at value 5 M nitric acid followed by a plateau with further increase in the nitric acid concentration. The extraction of U(VI) in TAlP present in $[C_8mim][NTf_2]$ was very similar to those observed in a molecular diluent, *n*-dodecane. The distribution ratio of U(VI) increased in the order TPP < TBP < TAP < TOP, which was attributed to the increase in the basicity of TAlP upon increasing in the chain length of alkyl group attached to the phosphoryl moiety. Stoichiometry of U(VI)-TAlP solvate was found to be 1:2 for all TAlPs. Change in the nature of ionic liquid hardly altered the distribution ratio of U(VI) at 3 M nitric acid. The extraction of U(VI) in all the extractants was found to be exothermic. The extraction mechanism in ionic liquid medium was strongly dependent on the chain length of alkyl group attached to the imidozolium moiety and neutral solvation mechanism was applicable for the extraction of U(VI) when the octyl derivative of imidazolium ionic liquid was employed as diluent. Complete stripping of U(VI) from the loaded ionic liquid phase was achieved using dilute nitric acid in 2–3 contacts. The results showed that TAlP present in ionic liquid medium was a promising candidate for fast reactor fuel reprocessing applications.

7.1.2 *Mutual separation of Pu(IV) from other actinides using 2-hydroxy acetamide extractant in room temperature ionic liquid*

N,*N*-dioctyl-2-hydroxyacetamide (DOHyA) in 1-butyl-3-methylimidazolium bis(trifluoromethanesulfonyl)amide ($[C_4mim][NTf_2]$) was employed for the extraction of actinides from nitric acid medium. The extraction of Pu(IV) was studied as a function of various parameters such as concentration of nitric acid, extractant concentration, temperature, alkyl chain length attached to amidic nitrogen of the extractant etc. The distribution ratio of plutonium (IV) ($D_{Pu(IV)}$) obtained in DOHyA/$[C_4mim][NTf_2]$ was compared with that obtained in DOHyA/ *n*-dodecane. Extradinary extraction of Pu(IV) was achieved when ionic liquid was employed as a diluent. The Distribution ratio of Pu(IV) decreased marginally with increase in the concentration of nitric acid up to 3 M and thereafter it attained a plateau. The distribution ratio of uranium(VI) and amrecium(III) were much lower than that obtained for Pu(IV) in DOHyA/$[C_4mim][NTf_2]$. Unlike the traditional molecular extractant, the separation factor of Pu(IV) over U(VI) was in the order of 10^3 and Pu(IV) over Am(III) was of the order of 10^2. These results indicated the possibility of separating Pu(IV) from other hexavalent (e.g. U(VI)) and trivalent actinides (e.g. Am(III)) using DOHyA/[C_4mim][NTf_2]. The $D_{Pu(IV)}$ obtained by DOHyA/[C_4mim][NTf_2] was compared with that obtained for *N*, *N*-di-alkyl-2-methoxyacetamides (DOMeOA) and *N*,*N*-Dihexyloctanamide (DHOA) in [C_4mim][NTf_2]. Extradinary extraction of Pu(IV) in DOHyA/[C_4mim][NTf_2] compared to DOMeOA/[C_4mim][NTf_2] and DHOA/[C_4mim][NTf_2] revealed that –OH group at the 2-position is mandatory for the extraction of Pu(IV) in acetamide. The effect of temperature on the extraction of Pu(IV) was studied and it was found to be endothermic. Quantitative stripping of Pu(IV) from the loaded ionic liquid phase was achieved using complexing agents.

7.1.3 Solvent extraction study of americium(III) using benzoylpyrazolone extractant dissolved in pyrrolidinium based room temperature ionic liquid

The extraction behavior of americium (III) from the nitric acid medium was studied in a solution of 1-phenyl-3-methyl-4-benzoylpyrazol-5-one (HPMBP) dissolved in 1-butyl-1-methylpyrrolidinium bis(trifluoromethanesulfonyl)imide ([C_4mpy][NTf_2]). The extraction behavior of Am(III) in ionic liquid phase was investigated as a function of various parameters, such as pH of aqueous phase, duration of equilibration, concentration of ionic liquid and nitrate in aqueous phase. The distribution ratio of Am (III) increased with increase of aqueous phase pH. Appreciable extraction of Am(III) was obtained at low pH medium (< pH 2) unlike other diketone based extractant. Stoichiometry of metal – solvate was found to be 1:3. Cation exchange mechanism seems to be most plausible mode for the extraction of Am (III) in ionic liquid phase. The extraction of Am(III) in ionic liquid was remarkably higher than that observed in conventional solvent (*n*-DD). Stripping of Am (III) from loaded ionic liquid phase increases from 54% to 80% using the stripping phase of 0.5M to 3 M nitric acid in one contact. Quantitative recovery of Am (III) can be achieved in few contacts with dilute nitric acid.

7.2 ROOM TEMPERATURE IONIC LIQUID AS AN EXTRACTANT FOR SOLVENT EXTRACTION OF ACTINIDES

Phosphoramide functionalized ionic liquid, diethyl-3-(-3-butylimidazolium) propylphosphoramide bis(trifluoromethanesulfonyl)imide ([BuImPA][NTf_2]) and RTIL containing strongly coordinating anion, tri-*n*-octylmethylammonium bis-(2-ethylhexyl)phosphate ($[A336]^+[DEHP]^-$) have been explored as extractants for the extraction of actinides from nitric acid medium. [BuImPA][NTf_2] was synthesized and studied for the selective separation of Pu(IV) from the other actinides such as Am(III) and U(VI). The extraction mechanism of U(VI) using PUREX solvent in the presence of small concentration of the RTIL, $[A336]^+[DEHP]^-$ have been investigated.

7.2.1 Mutual separation of Pu(IV) from other actinides using TSIL

A novel phosphoramide task specific ionic liquid, diethyl-3-(-3-butylimidazolium)propylphosphoramide bis(trifluoromethanesulfonyl)imide ([BuImPA][NTf_2]), was synthesized and characterized by NMR, mass and FTIR spectroscopy for the first time. The extraction behaviour of Pu(IV), U(VI) and Am(III) from nitric acid medium was studied using [BuImPA][NTf_2] dissolved in [C_4mim][NTf_2]. The extraction of Pu(IV) was studied as a function of various parameters such as concentration of nitric acid, extractant concentration, temperature, alkyl chain length attached to imidazolium moiety etc. The extraction of Pu(IV) increased with increase in the concentration of nitric acid reached a plateau at nitric acid concentration more than 4 M. In contrast to this, the extraction of U(VI) and Am(III) showed a decreasing trend and the $D_{U(VI)}$ and $D_{Am(III)}$ were much lower than that obtained for Pu(IV). Unlike traditional extractants, the separation factor of Pu(IV) over U(VI) was about 10 and that over Am(III) was of the order 10^3, suggesting the possibility of separating the fissile element plutonium from other actinides. Below 4 M nitric acid, the primary mode of Pu(IV) extraction in ionic liquid phase seems to be through the ($Pu(NO_3)_4$–([BuImPA][NTf_2])$_2$) neutral species extraction. However, above 4 M nitric acid, anion exchange mode also participates in the extraction of Pu(IV). The -NH- moiety in phosphormide-TSIL was protonated predominantly over >P=O and that seems to facilitate the extraction of Pu(IV) in ionic liquid phase**.**

7.2.2 Insights into the solvent extraction behavior of U(VI) in PUREX solvent containing RTIL with strongly coordinating anion

The extraction behavior of U(VI) in the PUREX solvent namely 1.1 M tri-*n*-butyl phosphate (TBP) in *n*-dodecane (*n*-DD) was studied in the presence and absence of the ionic liquid, tri-*n*-octylmethylammonium bis-(2-ethylhexyl)phosphate ($[A336]^+[DEHP]^-$). Remarkable enhancement in the distribution ratio of U(VI) was observed in the presence of ionic liquid. The extraction of U(VI) in $[A336]^+[DEHP]^-$/*n*-DD alone was studied to understand the role of ionic liquid in the PUREX solvent during extraction. The distribution ratio of U(VI) in $[A336]^+[DEHP]^-$/*n*-DD decreased with increase in the concentration of nitric acid. The extraction of U(VI) in $[A336]^+[DEHP]^-$ medium was accompanied by the extraction of nitric acid leading to the formation of ionic liquid components namely $[A336]^+[NO_3]^-$ and HDEHP in organic phase. The presence of these constituents facilitated the extraction of U(VI) in organic phase. Synergic extraction of U(VI) was observed when HDEHP was employed in conjunction with $[A336]^+[NO_3]^-$ and TBP. The study revealed that the distribution ratio of U(VI) in the presence of $[A336]^+[DEHP]^-$) was due to the synergic contributions of ionic liquid components and TBP.

7.3 LOADING BEHAVIOUR OF Eu(III) IN DIGLYCOLAMIDE/ROOM TEMPERATURE IONIC LIQUID SYSTEM

Extraction of europium(III) from nitric acid medium was studied in a solution of *N*,*N*,*N*’,*N*’-tetra-*n*-octyldiglycolamide (TODGA) dissolved in 1-methyl-3-octylimidazolium bis(trifluormethanesulfonyl)imide ([C_8mim][NTf_2]) at higher Eu(III) loading conditions in aqueous phase. The extraction of Eu(III) in TODGA/[C_8mim][NTf_2] decreased with increase in the concentration of nitric acid. The loading of Eu(III) in TODGA/[C_8mim][NTf_2] increased marginally with increase in the amount of Eu(III) present in nitric acid phase. Unlike molecular diluents systems the third phase formation was not observed even at ~100 g/L Eu(III) present in 3–5 M nitric acid phase, perhaps due to the stabilization of polar Eu(III)-TODGA complex by ionic liquid. The study revealed that Eu(III) could be loaded to the extent of 1:3 stoichiometry in ionic liquid phase without any third phase formation. There was hardly any change in the loading values by changing the structure of TODGA into its isomeric forms. The addition of phase modifier, TBP, to TODGA/[C_8mim][NTf_2] increased the distribution ratio of Eu(III) due to synergic participation of both TODGA and TBP.

7.4 ELECTROCHEMICAL STUDIES OF METAL IONS IN RTIL MEDIUM CONTAINING EXTRACTANTS

The electrochemical study of U(VI) in the presence of tri-*n*-alkyl phosphates (tri-*n*-butyl phosphates (TBP) and tri-*n*-octyl phosphate (TOP)) and Eu(III) in the presence of acidic extractants such as di(2-ethylhexyl)phosphoric acid (HDEHP) and diglycolamic acids (HDGA) have been carried out using RTIL as electrolytic medium.

7.4.1 Electrochemical study of U(VI) in the presence of higher homologue of TBP dissolved in RTIL medium

The electrochemical behaviour of U(VI) in tri-*n*-octyl phosphate (TOP) in the ionic liquid, 1-butyl-3-methylimidazolium bis(trifluoromethanesulfonyl)imide

($[C_4mim][NTf_2]$) was studied by cyclic voltammetry. The results were compared with those obtained with reference extractant, tri-*n*-butyl phosphate in $[C_4mim][NTf_2]$. The cyclic voltammogram of U(VI) in $[C_4mim][NTf_2]$ exhibited a prominent quasi-reversible reduction wave at -0.24 V(Vs. Fc/Fc^+) was due to the reduction of U(VI) to U(V) and a couple of oxidation waves at +0.45 V(Vs. Fc/Fc^+) and +0.66 V (Vs. Fc/Fc^+). The cathodic wave responsible for the reduction of U(VI) to U(V) shifted cathodically and the peak current lowered in the presence of these ligands. Since the octyl moiety attached to TOP was bulkier and offered more basicity to the phosphoryl moiety as compared to TBP, the stability constant (ln K_f) of U(VI)-TOP (2.9) determined from the voltammogram was slightly higher than that observed for U(VI)-TBP (2.7) complex. The diffusion coefficient of U(VI) and the heterogeneous electron transfer rate constant in $[C_4mim][NTf_2]$ decreased in the order U(VI) > U(VI) – TBP > U(VI) –TOP. All these observations indicate that the electrochemical behaviour of U(VI) in $[C_4mim][NTf_2]$ medium would show a strong dependence on the nature of ligand employed for extraction.

7.4.2 Electrochemical study of Eu(III) in the presence of acidic extractants dissolved in RTIL medium

The electrochemical behavior of Eu(III) in the room temperature ionic liquid, 1-butyl-1-methylpyrrolidinium bis(trifluoromethanesulfonyl)imide ($[C_4mpy][NTf_2]$) was studied in the presence and absence of HDEHP and HDGA by various transient electrochemical techniques such as cyclic voltammetry, chronopotentiometry and chronoamperometry. The cyclic voltammogram of Eu(III) exhibited a prominent quasi-reversible redox couple in the potential range -1 V to +0.5 V. The addition of HDEHP and HDGA to the Eu(III)/$[C_4mpy][NTf_2]$ solution lowered the cathodic peak current and shifted the cathodic peak potential cathodically due to the co-ordination of Eu(III) with ligands in the ionic liquid medium. The magnitude of the diffusion coefficients obtained by different electrochemical methods was comparable. In the presence of ligands, the diffusion coefficients and heterogeneous rate constants decreased in the order Eu(III) > (Eu(III) + HDEHP) > (Eu(III) + HDGA) in the ionic liquid. The stability constant (ln K_f) of Eu(III)-ligand complex was determined to be 5 and 5.65 for (Eu(III)-HDEHP) and (Eu(III)- HDGA) complexes respectively, which was in accordance with diffusion coefficients.

7.5 SCOPE OF THE FUTURE STUDY

In this thesis, RTILs have been studied for various applications and the results indicate that RTILs are promising candidates for the nuclear fuel cycle applications. Though these results hold great promise, there are some of the studies yet to be done to bring a robust technology based on RTIL medium. They are,

1. Since the solvent extraction & electrochemical studies in RTIL medium have been reported only for a limited number of metal ions (U(VI), Am(III), Eu(III) & Pu(IV)) in the present work, the other metal ions which are likely to be present in HLLW also need to be studied using RTIL medium.
2. Phosphoramide based TSIL have been reported for the selective separation of Pu(IV) from U(IV) and Am(III). Similarly, various novel functionalized ionic liquids need to be identified for the mutual separation of lanthanide (III) and actinide (III) from HLLW.
3. The coordination environment of metal ions with the extractant in the ionic liquid phase need to be investigated carefully to bring out the correct mechanism associated with the solvent extraction of metal ions in RTIL medium.
4. Interesting results have been obtained in the present study using imidazolium or pyrrolidinium based RTIL diluents as compared to the molecular diluent (*n*-DD)

but there is a loss of ionic liquid cation or anion into the aqueous phase during the solvent extraction of metal ions. Hence, it is required to synthesize ionic liquid with lower aqueous solubility and study for solvent extraction of actinides and fission products.

5. In the present thesis, quantitave stripping of actinides from the loaded ionic liquid phase was achieved using dilute HNO_3 or in some cases using complexing agents. Since ionic liquids have wide electrochemical window, the extracted metal ion can also be recovered by electrodeposition directly from the extracted ionic liquid phase (EX-EL process) which holds promise of separating the target metal ion with high separation factor. In this aspect, only a limited number of studies are available in literature and more studies need to be done for the EX-EL process of actinides and fission products.

6. Loading behavior of Eu(III) in DGA/[C_8mim][NTf_2] system have been investigated and unlike molecular diluent (*n*-DD) system, the third phase formation was not observed even at ~100 g/L Eu(III) present in 3–5 M nitric acid phase. Loading behavior of actindes and other fission products also need to be investigated in RTIL medium.

7. A systematic understanding of aggregation behavior of metal – ligand complex in RTIL medium was not reported and it can be studied in various types of RTILs and compared with molecular diluent to have clear understanding on ionic liquid based system**.**

8. Different thermophysical and physicochemical properties of ionic liquid based extractant systems such as molecular extractants or functionalized ionic liquids dissolved in RTIL diluents need to be investigated.

REFERENCES

1. Infrastructure, Indian economic development, Text book for class XI, National Council of educational research and training, 2006.editors: shveta uppal, page: 146.
2. S. David, Future Scenarios of fission based reactors, Nucl. Phys. A, 751 (2005) 429–441.
3. S.A. Bhardwaj, Indian nuclear power programmed–Past, present and future. Sadhana 38 (2013) 775-794.
4. R.B. Grover, S. Chandra, Scenario for growth of electricity in India. Energy Policy 34 (2006) 2834-2847.
5. R.G. Cochran, E.E. Lewis, N. Tsoulfanidis, W.F. Miller, The nuclear fuel cycle: analysis and management. American Nuclear Society (1990).
6. H.J. Bhabha, The role of atomic power in India and its immediate possibilities, Proc. of the international conference on the peaceful uses of atomic energy held in Geneva, 1 (1955) 103.
7. http://www.npcil.nic.in/main/AllProjectOperationDisplay.aspx
8. IGC news letter, volume 86, October 2010, page 3.
9. http://www.dae.gov.in/ni/nisep02/xx/kamini.htm
10. http://www.neuton.kth.se/publications/library/kamlPh.D.pdf.
11. J. L. Swanson, “PUREX Process Flow sheets”, In: Science and Technology of Tributyl phosphate, Eds. W.W. Schulz, L.L. Burger, J.D. Navratil, K.P. Bender, CRC Press Inc. Boca Raton, p 55, 1984.
12. Ramanujam, A. (1998). An introduction to the PUREX process. IANCAS, 14 (1998) 11-20.

13. P.K. Dey, N.K. Bansal, Spent fuel reprocessing: A vital link in Indian nuclear power program. Nuclear Engineering and Design, 236 (2006) 723.

14. I.W. Donald, B.L. Metcalfe, R.J. Taylor, The immobilization of high level radioactive wastes using ceramics and glasses. J. Mater. Sci. 32 (1997) 5851-5887.

15. M. Salvatores, G. Palmiotti, Radioactive waste partitioning and transmutationwithin advanced fuel cycles: Achievements and challenges. Prog. Part. Nucl. Phy.66 (2011) 144-166.

16. T. Inoue, M. Sakata, H. Miyashiro, T. Matsumura, A. Sasahara, N. Yoshiki, Development of partitioning and transmutation technology for long-lived nuclides.Nucl. Technol. 93 (1991) 206-220.

17. E.P. Horwitz, D.G. Kalina, L. Kaplan, G.W. Mason, H. Diamond, Selected alkyl(phenyl)-N,N-dialkylcarbomylmethylphophine oxides as extractants for Am(III) from nitric acid media. Sep. Sci. Technol. 17 (1982) 1261-1279.

18. E.P. Horwitz, D.G. Kalina, The extraction of Am (III) from nitric acid by octyl(phenyl)-N,N-diisobutylcarbomylmethylphosphine oxide- tri-n-butylphosphate mixtures. Solvent Extr. Ion Exch. 2 (1984) 179–200.

19. M. Ozawa, S. Nemoto, A. Togashi, T. Kawata, K. Onishi, Partitioning of actinides and fission products in highly-active raffinate from PUREX process by mixer-settlers. Solvent Extr. Ion Exch.10 (1992) 829-846.

20. M.P Antony, R. Kumaresan, A.S. Suneesh, S. Rajeswari, B. Robertselvan, V. Sukumaran, R. Manivannan, K.V. Syamala, K.A. Venkatesan, T.G. Srinivasan, P.R.Vasudeva Rao, Development of a CMPO based extraction process for partitioning of minor actinides and demonstration with genuine fast reactor fuel solution (155 GWd/Te). Radiochim. Acta 99 (2011) 207–215.

21. W. Jianchen, S. Chongli, Hot test of trialkyl phosphine oxide (TRPO) for removing actinides from highly saline high-level liquid waste (HLLW). Solvent Extr. Ion Exch. 19 (2001) 231-242.

22. X. Liu, J. Liang, J. Xu, Simplified Chinese TRPO process to extract and recover trasuranium elements from high-level liquid waste. Solvent Extr. Ion Exch. 22 (2004) 163-173.

23. Y. Zhu, R. Jiao, Chinese experience in the removal of actinides from highly active waste by tri alkyl phosphine oxide extraction. Nucl. Technol. 108 (1994) 361.

24. Y. Morita, J.P. Glatz, M. Kubota, L. Koch, G. Pagliosa, K. Roemer, A. Nicholl, Actinide Partitioning from HLW in a continuous DIDPA extraction process by means of centrifugal extractors. Solvent Extr. Ion Exch. 14 (1996) 385–400.

25. Y. Morita, M. Kubota, Extraction of neptunium with di-isodecyl phosphoric acid from nitric acid solution containing hydrogen peroxide. Solvent Extr. Ion Exch. 6 (1988) 233.

26. O. Courson, M. Lebrun, R. Malmbeck, G. Pagliosa, K. Romer, B. Satmark, J.P. Glatz, Partitioning of minor actinides from HLLW using the DIAMEX process. Part 1 - Demonstration of extraction performances and hydraulic behaviour of the solvent in a continuous process. Radiochim. Acta 88 (2000) 857–863.

27. R. Malmbeck, O. Courson, G. Pagliosa, K. Römer, B. Sätmark, J.P. Glatz, P.R. Baron, Partitioning of minor actinides from HLLW using the DIAMEX process. Part 2-“Hot” continuous counter-current experiment. Radiochim. Acta, 88 (2000) 865–871.

28. D. Serrano-Purroy, B. Christiansen, J.P. Glatz, R. Malmbeck, G. Modolo, Towards a DIAMEX process using high active concentrate. Production of genuine solutions. Radiochim. Acta 93 (2005) 357–361.

29. S.A. Ansari, P.N. Pathak, P.K. Mohapatra, V.K. Manchanda, Aqueous Partitioning of Minor Actinides by Different Processes. Sep & Purif.Rev.40 (2011) 43-76.

30. Y. Sasaki, Y. Sugo, S. Suzuki, S. Tachimori, The novel extractants diglycolamides for extraction of lanthanides and actinides in HNO_3-n-dodecane system. Solvent Extr. Ion Exch. 19 (2001) 91-103.

31. E.A. Mowafy, H.F. Aly, Synthesis of some N,N,N'N'-tetraalkyl-3-oxa-pentane-1, 5-diamide and their applications in solvent extraction. Solvent Extr. Ion Exch. 25 (2007) 205-224.

32. S.A. Ansari, P.N. Pathak, V.K. Manchanda, M. Hussain, A.K. Prasad, V.S.Parmar, N,N,N'N'-Tetraoctyldiglycolamide (TODGA): A promising extractant for actinide –partitioning from high-level waste (HLW). Solvent Extr. Ion Exch. 23 (2005) 463-479.

33. E.P. Horwitza, D.R. McAlistera, A.H. Bonda, R.E. Barrans, Novel Extraction of Chromatographic Resins Based on Tetraalkyldiglycolamides: Characterization and Potential Applications. Solvent Extr. Ion Exch. 23 (2005) 319-344.

34. H. Narita, T. Yaita, S. Tachimori, Extraction of lanthanides with N, N'-dimethyl-N, N'-diphenyl-malonamide and-3,6-dioxaoctanediamide. Solvent Extr. Ion Exch. 22 (2004) 135–145.

35. A.V. Gelis, G.F. Vandegrift, A. Bakel, D.L. Bowers, A.S. Hebden, C. Pereira, M.Regalbuto, Extraction behaviour of actinides and lanthanides in TALSPEAK.,TRUEX and NPEX processes of UREX+. Radiochim. Acta 97 (2008) 231-245.

36. A.V. Bychkov, O.V. Skiba, Review of non-aqueous nuclear fuel reprocessing and separation methods, Chemical Separation Technologies and Related Methods of Nuclear Waste Management (1999) 71-98.

37. C.C. Mcpheeters, R.D. Pierce, T.P. Mulcahey, Application of the pyrochemical process to recycle of actinides from LWR spentfuel. Prog. Nucl. Energy, 31 (1997) 175.

38. S. Vavilov, T. Kobayashi, M. Myochin, Principle and test experience of the RIAR's oxide pyro-process. J. Nucl. Sci. Technol. 41 (2004) 1018-1025.

39. J.J. Laidler, J.E. Battles, W.E. Miller, A.P. Ackerman, E.L. Carls, Development of pyroprocessing technology. Prog.Nucl.Ener 31 (1997) 131-140.

40. H J.D. Holbrey, K.R. Seddon, Ionic Liquids. Clean Products and Processes 1 (1999) 223- 236.

41. United Nations Environment Programme. Ozone Secretariat (2006) Handbook for the Montreal protocol on substances that deplete the ozone layer. UNEP/Earthprint.

42. J. Sherman, B. Chin, P.D. Huibers, R. Garcia-Valls, T.A. Hatton, Solvent replacement for green processing, Environmental health perspectives, 10 (1998) 253-236.

43. T. Welton, Room-temperature ionic liquids. Solvents for synthesis and catalysis, Chem. Rev., 99 (1999) 2071–2084.

44. P.V. Natalia, K.R. Seddon, Applications of ionic liquids in the chemical industry, Chem. Soc. Rev. 37 (2008) 123–150.

45. M. Freemantle, An Introduction to Ionic liquids, RSC Publishing (2010).

46. K.R. Seddon, Ionic liquids: A taste of the future. Nat. Mater 2 (2003) 363–365.

47. J.S. Wilkes, A short history of ionic liquids—from molten salts to neoteric solvents. Green Chem 4 (2002) 73–80.

48. M.J. Earle, K.R. Seddon, Ionic liquids. Green solvents for the future. Pure Appl. Chem 72 (2000) 1391-1398.

49. S. Gabriel, J. Weiner, Ueber einige Abkommlinge des Propulamins, Eur. J. Inorg. Chem 21 (1888) 2669-2679.

50. P. Walden, Bull. Acad.Imper.Sci. (St. Petersberg), (1914) 1800.

51. M. Smiglak, A. Metlen, R. D. Rogers, The Second Evolution of Ionic Liquids: From Solvents and Separations to Advanced Materials—Energetic Examples from the Ionic Liquid Cookbook. Acc. Chem. Res. 40 (2007) 1182 – 1192.

52. W.L. Hough, M. Smiglak, H. Rodríguez, R.P. Swatloski, S.K. Spear, D.T. Daly, J. Pernak, J.E. Grisel, R.D. Carliss, M.D. Soutullo, J.H. Davis, The third evolution of ionic liquids: active pharmaceutical ingredients. New J. Chem 31 (2007) 1429-1436.

53. J.S. Wilkes, J.A. Levisky, R.A. Wilkes, C.L. Hussey, Dialkylimidazolium chloroaluminate melts: a new class of room temperature ionic liquids for electrochemistry, spectroscopy andsynthesis. Inorg Chem 21 (1982) 1263-1264.

54. J.S. Wilkes, M.J. Zaworotko, Air and water stable 1-ethyl-3-methylimidazolium based ionic liquids. J. Chem. Soc., Chem. Commun. (1992) 965 - 967.

55. J.H. Davis Jr, Task-specific ionic liquids. Chem. Lett, 33 (2004) 1072.

56. C.C. Brasse, U. Englert, A. Salzer, H. Waffenschmidt, P. Wasserscheid, Ionic Phosphine Ligands with Cobaltocenium Backbone: Novel Ligands for the Highly Selective, Biphasic, Rhodium-Catalyzed Hydroformylation of 1-Octene in Ionic Liquids. Organometallics 19 (2000) 3818 - 3823.

57. P. Wasserscheid, H. Waffenschmidt, P. Machnitzki, K. Kottsieper, O. Selzer, Cationic phosphine ligands with phenylguanidinium modified xanthene moieties—a successful concept for highly regioselective, biphasic hydroformylation of oct-1-ene in hexafluorophosphate ionic liquids. Chem. Commun. (2001) 451 - 452.

58. R. Giernoth, Task-Specific Ionic Liquids. Angew. Chem. Int. Ed. 49 (2010) 2834–2839.

59. A.E. Visser, R.P. Swatloski, W.M. Reichert, R. Mayton, S. Sheff, A. Wierzbicki, J.H. Davis, R. D. Rogers, Task specific ionic liquids incorporating novel cations for the coordination and extraction of Hg^{2+} and Cd^{2+} : Synthesis, characterization and extraction studies. Envir. Sci. Technol. 36 (11) (2002) 2523-2529.

60. A.E. Visser, R.P. Swatloski, W.M. Reichert, R. Mayton, S. Sheff, A. Wierzbicki, J.H. Davis Jr, R.D. Rogers, Task specific ionic liquids for the extraction of metal ions from aqueous solutions. Chem. Commun. (2001)135-136.

61. I.L. Odinets, E.V. Sharova, O.I. Artyshin, K.A. Lyssenko, Y. Nelyubina, V. Myasoedova, V. Galina, N.P. Molochnikova, E.A. Zakharchenro, Novel class of functionalized ionic liquids with grafted CMPO-moieties for actinides and rareearth elements recovery. Dalton Trans. 39 (2010) 4170-4178.

62. A. Ouadi, B. Gadenne, P. Hesemann, J.E. Moreau, I. Billard, C. Gaillard, S. Mekki, G. Moutiers, Task-Specific Ionic Liquids Bearing 2-Hydroxybenzylamine Units: Synthesis and Americium-Extraction Studies. Chem. Eur. J. 12 (2006) 3074 – 3081.

63. A. Ouadi, O. Klimchuk, C. Gaillard, I. Billard, Solvent extraction of U(VI) by task specific ionic liquids bearing phosphoryl groups. Green Chem. 9 (2007) 1160–1162.

64. H. Luo, S. Dai, P. V. Bonnesen, A.C. Buchanan, Separation of fission products based on ionic liquids: Task-specific ionic liquids containing an aza-crown ether fragment. J alloys and Compds. 418 (2006) 195–199.

65. P. Nockemann, B. Thijs, S. Pittois, J. Thoen, C. Glorieux, K.V. Hecke, L. Van Meervelt, B. Kirchner, K. Binemanns, Task specific ionic liquid for solubilizing metal oxides. J. Phys.Chem.B, 110 (2006) 20978-20992.

66. J.H. Olivier, F. Camerel, R. Ziessel, Lanthanide Ion Extraction by Trifluoromethyl-1,3-diketonate-Functionalised Ionic Liquids Adsorbed on Silica. Chem. Eur. J. 17 (2011) 9113 - 9122.

67. X. Sun, Y. Ji, L. Zhang, J. Chen, D. Li, Separation of cobalt and nickel using inner synergic extraction from bifunctional ionic liquid extractant (Bif-ILE). J.Hazard. Matter. 182 (2010) 447-452.

68. H. Mehdi, K. Binnemans, V. Hecke, L.V. Meervelt, P. Nockemann, Hydrophobic ionic liquids with strongly corodinating anions. Chem. Commun. (2010) 234-236.

69. X. Sun, Y. Ji, F. Hu, Bo. He, Ji. Chen, D. Li, The inner synergic effect of bifunctional ionic liquid extractant for solvent extraction. Talanta 81 (2010) 1877–1883.

70. Y. Hua-Ling, W. Wei, C. Hong-Min, C. Ji, Extraction Mechanism of Rare Earths with Bifuncional Ionic Liquids (Bif-ILs) [A336][CA-12]/[A336][CA-100] in Nitrate Medium. Chin J Anal Chem. 39 (2011) 1561–1566.

71. Stark, K.R. Seddon, Ionic liquids, In: Kirk-Othmer Encyclopedia of Chemical Technology. Vol. 26, John Wiley, New York, 2007.

72. J.G. Huddleston, A.E. Visser, W.M. Reichert, H.D. Willauer, G.A. Broker, R.D. Rogers, Characterization and comparison of hydrophilic and hydrophobic room temperature ionic liquids incorporating the imidazolium cation. Green Chem. 3 (2001) 156–164.

73. T. Welton, Electrodeposition from Ionic Liquids. Edited by F. Endres, A.P. Abbott, D.R. MacFarlane (2008) 4468-4468.

74. P. Wasserscheid, E.T. Welton, Ionic Liquids in Synthesis. Wiley-VCH verlag GmbH & Co. KGaA, 2008.

75. H.L. Ngo,K. LeCompte, L. Hargens, A.B. McEwen, Thermal properties of imidazolium ionic liquids. Thermochim. Acta 357 (2000) 97 – 102.

76. Y. Song, L. Liu, X. Zhu, X. Wang, H. Jia, X. Xiao, H. Yu, X. Yang, Physicochemical properties of ionic liquids based on imidazolium/pyrrolidinium cations and maleate/phthalate anions. Solid State Ionics, 179 (2008) 516-521.

77. H. okuda, K. Hayamizu, K. Ishii, M.A.B.H. Susan, M. Watanabe, Physicochemical properties and structures of room temperature ionic liquids. 2. Variation of alkyl chain length in imidazolium cation. J. Phys. Chem. B, 109 (2005) 6103-6110.

78. P. Bonhote, A.P. Duasm, B. Papageorgiou, K. Kalyanasundaram, M. Graetzel, Hydrophobic, highly conductive ambient-temperature molten salts. Inorg. Chem, 35 (1996) 1168-1178.

79. K.N. Marsh, J.A. Boxall, R. Lichtenthaler, Room temperature ionic liquids and their mixtures—a review. Fluid Phase Equilibria, 219 (2004) 93-98.

80. K.R. Seddon, A. Stark and M.J. Torres, Influence of chloride, water, and organic solvents on the physical properties of ionic liquids. Pure Appl. Chem. 72 (2001) 2275-2287.

81. D.R. MacFarlane, J. Golding, S. Forsyth, M. Forsyth, G.B. Deacon, Low viscosity ionic liquids based on organic salts of the dicyanamide anion.Chem. Commun. 16 (2001) 1430-1431.

82. K.R. Seddon, A.Stark, M.J. Torres, Viscosity and Density of 1-Alkyl-3-ethylimidazolium Ionic Liquids (2002).

83. J.P. Mikkola, P. Virtanen, R. Sjöholm, Aliquat 336 - A versatile and affordable cation source for an entirely new family of hydrophobic ionic liquids. Green Chem. 8 (2006) 250-255.

84. J. Jacquemin, P. Husson, A. Padua, V. Majer, Density and viscosity of several pure and water-saturated ionic liquids. Green Chem. 8 (2006) 172-180.

85. M. Galinski, A. Lewandowski, I. Stepniak, Ionic liquids as electrolytes. Electrochim. Acta 51 (2006) 5567-5580.

86. G. Law, P.R. Watson, Surface tension measurements of N-alkylimidazolium ionic liquids. Langmuir 17 (2001) 6138-6141.

87. M.G. Freire, P.J. Carvalho, A.M. Fernandes, I.M. Marrucho, A.J. Queimada, J.A. Coutinho, Surface tensions of imidazolium based ionic liquids: anion, cation, temperature and water effect. J. Colloid Interface Sci, 314 (2007) 621-630.

88. S.P. Ong, O. Andreussi, Y. Wu, N. Marzari, G. Ceder, Electrochemical windows of room-temperature ionic liquids from molecular dynamics and density functional theory calculations. Chem. Mater., 23 (2011) 2979-2986.

89. N.V. Plechkova, K.R. Seddon, Applications of ionic liquids in the chemical industry. Chem. Soc. Rev. 37 (208) 123-150.

90. S. Kazemiabnavi, Z. Zhang, K. Thornton, S. Banerjee, Electrochemical Stability Window of Imidazolium-Based Ionic Liquids as Electrolytes for Lithium Batteries. J. Phys. Chem. B, 120 (2016) 5691-5702.

91. P.A. Suarez, V.M. Selbach, J.E. Dullius, S, Einloft, C.M. Piatnicki, D.S. Azambuja, J. Dupont, Enlarged electrochemical window in dialkyl-imidazolium cation based room-temperature air and water-stable molten salts. Electrochim. Acta 42 (1997) 2533-2535.

92. M. Hayyan, F.S. Mjalli, M.A. Hashim, I.M. AlNashef, T.X. Mei, Investigating the electrochemical windows of ionic liquids.Ind. Eng. Chem. Res. 19 (2013) 106-112.

93. Ch. Jagadeeswara Rao, K.A. Venkatesan, B. V. R. Tata, K. Nagarajan, T. G. Srinivasan, P.R Vasudeva Rao, Radiation stability of some room temperature ionic liquids. Radiat. Phys. Chem. 80 (2011) 643-649.

94. D. Allen, G. Baston, A. E. Bradley, T. Gorman, A. Haile, I. Hamblett, J. E. Hatter, M. J. F. Healey, B. Hodgson, R. Lewin, K. V. Lovell, B. Newton, W. R. Pitner, D. W. Rooney, D. Sanders, K. R. Seddon, H. E. Sims, R. C. Thied, An investigation of the radiochemical stability of ionic liquids. Green Chem. 4 (2002) 152-158.

95. L. Berthon, S. I. Nikitenko, I. Bisel, C. Berthon, M. Faucon, B. Saucerotte, N. Zorza, Ph. Moisy, Influence of gamma irradiation on hydrophobic room-temperature ionic liquids [BuMeIm]PF_6 and [BuMeIm]$(CF_3SO_2)_2N$. Dalton Trans. (2006) 2526–2534.

96. S.I. Lall-Ramnarine, A. Castano, G. Subramaniam, M.F. Thomas, J.F. Wishart, Synthesis, characterization and radiolytic properties of bis (oxalato) borate containing ionic liquids. Radiat. Phys. Chem., 78 (2009) 1120-1125.

97. G. Le Rouzo, C. Lamouroux, V. Dauvois, A. Dannoux, S. Legand, D. Durand, P. Moisy, G. Moutiers, Anion effect on radiochemical stability of room-temperature ionic liquids under gamma irradiation. Dalton Trans. 31 (2009) 6175-6184.

98. J.D. Holbrey, K.R. Seddon, The phase behaviour of 1-alkyl-3-methylimidazolium tetrafluoroborates: Ionic liquids and ionic liquid crystals. J.Chem. Soc. Dalton Trans. 13 (1999) 2133 - 2139.

99. H.L. Ngo, K. LeCompte, L. Hargens, A. B. McEwen, Thermal properties of imidazolium ionic liquids. Thermochim. Acta 357 (2000) 97 – 102.

100. M. Kosmulski, J. Gustafsson, J.B. Rosenholm, Thermal stability of low temperature ionic liquids revisited. Thermochim. Acta 412 (2004) 47-53.

101. Y.U. Paulechka, D.H. Zaitsau, G.J. Kabo, A.A. Strechan, Vapor pressure and thermal stability of ionic liquid 1-butyl-3-methylimidazolium Bis (trifluoromethylsulfonyl) amide. Thermochim. Acta 439 (2005)158-160.

102. M. Shukla, S. Saha, A comparative study of piperidinium and imidazolium based ionic liquids: thermal, spectroscopic and theoretical studies. INTECH Open Access Publisher (2013).

103. S.E. Fry, N.J. Pienta, Effects of molten salts on reactions. Nucleophilic aromatic substitution by halide ions in molten dodecyltributylphosphonium salts. J. Am. Chem. Soc 107 (1985) 6399-6400.

104. A.R. Sethi, P. Smith, N. Srinivasan, T. Welton, Ionic liquids as solvents for organic synthesis, In: Green industrial applications of ionic liquids, Eds. R.D. Rogers, K.R. Seddon, S. Volkov, NATO science series, Kluwer Academic publishers, Netherlands, 2002.

105. S.V. Malhotra, ed., Ionic liquids in organic synthesis. American Chemical Society (2007).

106. M. Koel, Ionic liquids in chemical analysis. Crit. Rev. Anal. Chem. 35 (2005) 177-192.

107. W. Simka, D. Puszczyk, G. Nawrat, Electrodeposition of metals from non-aqueous solutions. Electrochim. Acta 54 (2009) 5307-5319.

108. D. Wei, A. Ivaska, Applications of ionic liquids in electrochemical sensors. Anal. Chim. Acta, 607 (2008) 126-135.

109. D. Han, K.H. Row, Recent applications of ionic liquids in separation technology, Molecules 15 (2010) 2405-2426.

110. B. Weyershausen, K. Lehmann, Industrial application of ionic liquids as performance additives. Green Chem. 7(2005)15-19.

111. X. Sun, H. Luo, S. Dai, Ionic liquids-based extraction: a promising strategy for the advanced nuclear fuel cycle. Chem. Rev. 112 (2011) 2100-2128.

112. I. Billard, A. Ouadi, C. Gaillard, Liquid–liquid extraction of actinides, lanthanides, and fission products by use of ionic liquids: from discovery to understanding. Anal.Bioanal.Chem. 400 (2011) 1555-1566.

113. A.E. Visser, R.D. Rogers, Room-temperature ionic liquids: new solvents for f-element separations and associated solution chemistry. J. Solid State Chem 171 (2003) 109-113.

114. P.R. Vasudeva Rao, K.A. Venkatesan, Alok Rout, T.G. Srinivasan, K. Nagarajan, Potential applications of room temperature ionic liquids for fission products and actinide separation. Sep. Sci. Technol. 47 (2012) 204-222.

115. K.A. Venkatesan, T.G. Srinivasan, P.R. Vasudeva Rao, A review on the electrochemical applications of room temperature ionic liquids in nuclear fuel cycle. Sep. Sci.Technol.10 (2009) 1_R1-1_R6.

116. X. Sun, D. Wu, Ji. Chen, D. Li, Separation of scandium(III) from lanthanides(III) with room temperature ionic liquid based extraction containing Cyanex 925. J Chem. Technol. Biotechnol. 82 (2007) 267–272.

117. A.E. Visser, R.P. Swatloski, W.M. Reichert, S.T. Griffin, R.D. Rogers, Traditional extractants in non-traditional solvents: Group 1 and 2 extractions by crown ethers in room temperature ionic liquids. Ind. Eng. Chem. Res. 39 (2000) 3596 - 3604.

118. Z.B. Xie, H.T. Kang, Z.S. Chen, S.H. Zhang, Z.G. Le, Liquid–liquid extraction of U (VI) using malonamide in room temperature ionic liquid. J. Radioanal. Nucl. Chem. 308 (2016) 573-578.

119. R. Rama, Alok Rout, K.A. Venkatesan, M.P. Antony, A. Suresh, Comparison in the solvent extraction behavior of uranium (VI) in some trialkyl phosphates in ionic liquid. Radiochim. Acta. 104 (2016) 865-872.

120. A. Rout, S. Karmakar, K.A. Venkatesan, T.G. Srinivasan, P.R. Vasudeva Rao, Room temperature ionic liquid diluent for the mutual separation of europium (III) from americium (III). Sep. Purif. Technol. 81 (2011) 109-115.

121. S. Dai, Y.H. Ju, C.E. Barnes, Solvent extraction of strontium nitrate by a crown ether using room-temperature ionic liquids. J. Chem. Soc. Dalton Trans. 1 (1999) 1201-1202.

122. M.L. Dietz, D.C. Stepinski, Anion concentration-dependent partitioning mechanism in the extraction of uranium into room-temperature ionic liquids. Talanta. 75 (2008) 598-603.

123. Billard, A. Ouadi, E. Jobin, J. Champion, C. Gaillard, S. Georg, Understanding the Extraction Mechanism in Ionic Liquids: UO_2^{2+}/HNO_3/TBP/C_4mimTf_2N as a Case Study. Sol. Extr. Ion. Exch. 29 (2011) 577-601.

124. D.C. Gaillard, M. Boltoeva, I. Billard, S. Georg, V. Mazan, A. Ouadi, D. Ternova, C. Hennig, Insights into the Mechanism of Extraction of Uranium (VI) from Nitric Acid solution into an Ionic Liquid by using Tri-n- butyl phosphate. ChemPhysChem. 6 (2015) 2653-2662.

125. S. Panja, P.K. Mohapatra, S.C. Tripathi, P.M. Gandhi, P. Janardan, A highly efficient solvent system containing TODGA in room temperature ionic liquids for actinide extraction. Sep. Purif. Technol. 96 (2012) 289-295.

126. K. Shimojo, K. Kurahashi, H. Naganawa, Extraction behavior of lanthanides using a diglycolamide derivative TODGA in ionic liquids. Dalton Transactions, 37 (2008) 5083-5088.

127. A.N. Turanov, V.K. Karandashev, V.E. Baulin, Extraction of lanthanides (III) with N, N′-bis (diphenylphosphinyl-methylcarbonyl) diaza-18-crown-6 in the presence of ionic liquids. Solvent Extr. Ion Exch. 30 (2012) 244-261.

128. P. Giridhar, K.A. Venkatesan, T.G. Srinivasan, P.R. Vasudeva Rao, Extraction of uranium(VI) from nitric acid medium by 1.1M tri-n-butylphosphate in ionic liquid diluent. J. Radio anal.Nucl.Chem, 265 (2005) 31-38.

129. P. Giridhar, K.A. Venkatesan, T.G. Srinivasan, P.R. Vasudeva Rao, Effect of Alkyl Group in 1-Alkyl-3-methylimidazolium Hexafluorophosphate Ionic Liquids on the Extraction of Uranium by Tri-*n*-butylphosphate Diluted with Ionic Liquids. J. Nucl. Radiochem. Sci. 5 (2004) 21-26.

130. K. Nakashima, F. Kubota, T. Maruyama, M. GOTO, Ionic liquids as a novel solvent for lanthanide extraction. Anal. Sci. 19 (2003) 1097-1098.

131. Alok Rout, K.A. Venkatesan, T.G. Srinivasan, P.R. Vasudeva Rao, Liquid–liquid extraction of Pu(IV), U(VI) and Am(III) using malonamide in room temperature ionic liquid as diluents. J. Hazard. Mater. 221 (2012) 62-67.

132. A. Rout, K.A. Venkatesan, T.G. Srinivasan, P.R. Vasudeva Rao, Ionic liquid extractants in molecular diluents: Extraction behavior of europium (III) in quarternary ammonium-based ionic liquids. Sep. Purif. Technol. 95 (2012) 26-31.

133. Alok Rout, K.A. Venkatesan, T.G. Srinivasan, P.R. Vasudeva Rao, Extraction behavior of actinides and fission products in amide functionalized ionic liquid. Sep. Purif. Technol. 97 (2012) 164-171.

134. Alok Rout, K.A. Venkatesan, T.G. Srinivasan, P.R. Vasudeva Rao, Unusual extraction of plutonium (IV) from uranium (VI) and americium (III) using phosphonate based task specific ionic liquid. Radiochim. Acta. 98 (2010) 459-466.

135. R. Rama, Alok Rout, K.A. Venkatesan, M.P. Antony, A novel phosphoramide task specific ionic liquid for the selective separation of plutonium (IV) from other actinides. Sep. Purif. Technol. 172 (2017) 7-15.

136. A. Sengupta, P.K. Mohapatra. M. Iqbal, J. Huskens, W.A. Verboom, Diglycolamide-functionalized task specific ionic liquid (TSIL) for actinide extraction: solvent extraction, thermodynamics and radiolytic stability studies. Sep. Purif. Technol. 118 (2013) 264-270.

137. P.K. Mohapatra, P. Kandwal, M. Iqbal, J. Huskens, M.S. Murali, W.A. Verboom, novel CMPO-functionalized task specific ionic liquid: synthesis, extraction and spectroscopic investigations of actinide and lanthanide complexes. Dalton Trans. 42 (2013) 4343-4347.

138. M. Paramanik, D.R. Raut, A. Sengupta, S.K. Ghosh, P.K. Mohapatra, A trialkyl phosphine oxide functionalized task specific ionic liquid for actinide ion complexation: extraction and spectroscopic studies. RSC Adv.6 (2016) 19763-19767.

139. J.A. Vicente, A. Mlonka, H.N. Gunaratne, M. Swadzba Kwasny, P. Nockemann, Phosphine oxide functionalised imidazolium ionic liquids as tuneable ligands for lanthanide complexation. Chem. Commun. 48 (2012) 6115-6117.

140. A. Rout, K.A. Venkatesan, T.G. Srinivasan, P.R. Vasudeva Rao, Tuning the extractive properties of Purex solvent using room temperature ionic liquid. Sep. Sci. Technol. 8 (2013) 2576-2581.

141. J. Wang, J. Zhao, D. Feng, X. Kang, Y. Sun, L. Zhao, H. Liang, Enhancing extraction ability by rational design of phosphoryl functionalized ionic liquids and mechanistic investigation on neodymium (III) extraction. J. Rare Ear. 34 (2016) 83-90.

142. H.Li.B. Wang, L. Zhang, L. Shen, Task-specific ionic liquids incorporating alkyl phosphate cations for extraction of U(VI) from nitric acid medium: synthesis, characterization, and extraction performance. J. Radioanal. Nucl. Chem. 303 (2015) 433-440.

143. De Waele, L. Heerman, W. D.'Olieslager, Potentiometric and spectroscopic study of uranium (IV)-uranium (III) in acidic AlCl3-N-(n-BUTYL) pyridinium chloride melts. J. Less-Common Metals. 122 (1983) 319-327.

144. J.P. Schoebrechts, B. Gilbert, Electrochemical and spectroscopic studies of neptunium in the aluminum chloride-1-n-butylpyridinium chloride melt at 40. degree. C. Inorg Chem., 24 (1985) 2105-2110.

145. S.I. Nikitenko, C. Cannes, C. Le Naour, P. Moisy, D. Trubert, Spectroscopic and Electrochemical Studies of U (IV)− Hexachloro Complexes in Hydrophobic Room-Temperature Ionic Liquids [BuMeIm][Tf2N] and [MeBu3N][Tf2N]. Inorg Chem. 44 (2005) 9497-9505.

146. P. Giridhar, K.A. Venkatesan, T.G. Srinivasan, PR Vasudeva Rao, Extraction of fission palladium by Aliquat 336 and electrochemical studies on direct recovery from ionic liquid phase. Hydrometallurgy 81 (2006) 30-39.

147. R. Kumaresan, Rakesh Jain, K.A. Venkatesan, M.P. Antony, B.M. Bhanage, Extraction and electrochemical behavior of fission palladium in room-temperature ionic liquid. J Radioanal Nucl Chem. 303 (2015) 1047-1052.

148. M. Matsumiya, Y. Kikuchi, T. Yamada, S. Kawakami, Extraction of rare earth ions by tri-n-butylphosphate/phosphonium ionic liquids and the feasibility of recovery by direct electrodeposition. Sep. Purif. Technol.130 (2014) 91-101.

149. M. Jayakumar, K.A. Venkatesan, T.G. Srinivasan, Electrochemical behavior of fission palladium in 1-butyl-3-methylimidazolium chloride, Electrochim. Acta 52 (2007) 7121-7127.

150. R. Gupta, S.K. Gupta, J.S. Gamre, K.V. Lohithakshan, V. Natarajan, S.K. Aggarwal, Understanding the Dynamics of Eu^{3+} Ions in Room Temperature Ionic Liquids–Electrochemical and Time Resolved Fluorescence Spectroscopy Studies. J. Inorg. Chem. 1 (2015) 104-111.

151. Y. Pan, C. L. Hussey, Electrochemical and Spectroscopic Investigation of Ln^{3+} (Ln= Sm, Eu, and Yb) Solvation in Bis (trifluoromethylsulfonyl) imide-Based Ionic Liquids and Coordination by *N, N, N′, N′*-Tetraoctyl-3-oxa-pentane Diamide (TODGA) and Chloride. Inorg Chem, 52 (2013) 3241-3252.

152. R. Rama, Alok Rout, K.A. Venkatesan, M.P. Antony, P.R. Vasudeva Rao, Electrochemical behavior of Eu (III) in imidazolium ionic liquid containing tri-n-butyl phosphate and N, N-dihexyloctanamide ligands. J. Electroanal.Chem. 757 (2015) 36-43.

153. A. Sengupta, M.S. Murali, P.K. Mohapatra, M Iqbal, J Huskens, W. Verboom, Np (IV) complex with task-specific ionic liquid based on CMPO: first cyclic voltammetric study. Monatsh. Chem. 146 (2015) 1815-1821.

154. A. Sengupta,M.S. Murali, P.K. Mohapatra, M. Iqbal, J. Huskens, W. Verboom, Extracted species of Np (IV) complex with diglycolamide functionalized task specific ionic liquid: diffusion, kinetics and thermodynamics by cyclic voltammetry. J. Radioanal. Nucl. Chem. 304 (2015) 563-570.

155. G.M. Krishna, A.S. Suneesh, K.A. Venkatesan, M.P. Antony, Electrochemical behavior of zirconium (IV) in 1-butyl-3-methylimidazolium bis (trifluoromethylsulfonyl) imide ionic liquid. J. Electroanal. Chem. 776 (2016) 120-126.

156. P. Giridhar, K.A. Venkatesan, T.G. Srinivasan, P.R. Vasudeva Rao, Electrochemical behavior of uranium (VI) in 1-butyl-3-methylimidazolium chloride and thermal characterization of uranium oxide deposit. Electrochim. Acta 52 (2007) 3006-3012.

157. Ch Jagadeeswara Rao, K.A. Venkatesan, K. Nagarajan, T.G. Srinivasan, P.R Vasudeva Rao, Treatment of tissue paper containing radioactive waste and electrochemical recovery of valuables using ionic liquids. Electrochim. Acta 53 (2007) 1911-1919.

158. P. Giridhar, K.A. Venkatesan, T.G. Srinivasan, P.R. Vasudeva Rao, Extraction of Uranium (VI) by 1.1 M Tri-n-butylphosphate/onic liquid and the feasibility of recovery by direct electrodeposition from organic phase. J Alloys and Compds. 448 (2008) 104–108.

159. P. R. Vasudeva Rao: PhD Thesis, Bombay university, (1978) 62.

160. Ch. Jagadeeswara Rao, K. A. Venkatesan, K. Nagarajan, T.G. Srinivasan, P. R. Vasudeva Rao. Electrochemical behavior of europium (III) in N-butyl-N-methylpyrrolidinium bis (trifluoromethylsulfonyl) imide. Electrochem. Acta, 54 (2009) 4718 – 4725.

161. J.W. Freiderich, E. Wanigasekara, X.G. Sun, R.A. Meisner, H.M. Meyer, H. Luo, L.H. Delmau, S. Dai, B.A. Moyer. Direct Electrodeposition of UO $_2$ from Uranyl Bis (trifluoromethanesulfonyl) imide Dissolved in 1-Ethyl-3-methylimidazolium Bis (trifluoromethanesulfonyl) imide Room Temperature Ionic Liquid System. Electrochim.Acta 115 (2014) 630-638.

162. B. Joseph, K.A.Venkatesan, K. Nagarajan, P.R. Vasudeva Rao, Electrowinning of UO_2 from Ionic Liquid Medium. Sep. Sci.Technol. 48 (2013) 2506–2511.

163. M .Donald, Transient techniques in electrochemistry, Plenum Press, New York (1977).

164. A.J. Bard and L.R. Faulkner, Electrochemical Methods—Fundamentals and Applications, Wiley, N.ew York, 1980.

165. E.R. Brown, J.R. Sandifer, Cyclic voltammetry AC polorography and related techniques, in: B.W. Rossiter, J.F. Hamilton (Eds.), Physical Methods of Chemistry—Volume II, Electrochemical Methods, Wiley, New York, 1986.

166. F. Scholz, Electroanalytical methods: Guide to experiments and applications,1st Edition,Springer, Berlin, 2005.

167. P.T. Kissinger, W.R. Heineman, Cyclic voltammetry, J.Chem.Ed. 60 (1983) 702-706.

168. R.S. Nicholson, Semiempirical Procedure for Measuring with Stationary Electrode Polarography Rates of Chemical Reactions Involving the Product of Electron Transfer. Anal. Chem. 38 (1966) 1406-1406.

169. C.H. Bamford, C.F.H. Tipper, R.G. Compton (Eds.), Electrode kinetics: Principles and methodology (Vol. 26). Elsevier (1986).

170. R.J. Klingler, J.K. Kochi, Electron-transfer kinetics from cyclic voltammetry. Quantitative description of electrochemical reversibility, J. Phys. Chem. 85, no. 12 (1981) 1731-1741.

171. M. Paunovic, Chronopotentiometry, J. electroanal. chem. interfacial electrochem. 14 (1967) 447-447.

172. P. Delahay, New instrumental methods in electrochemistry: Theory, instrumentation and application to analytical and physical chemistry, Interscience, New York (1954).

173. R. Tamamushi, N. Tanaka, Fundamental Studies on the Current-Voltage Curve in Polarography. II: Derivation of the Activation-Controlled Polarographic Waves of Simple Metal Ions from the Standpoint of Chemical Kinetic. Bull. Chem. Soc. Jpn. 22 (1949) 227-236.

174. R. Ernst, H.E. Allen, K.H. Mancy, Characterization of trace metal species and measurement of trace metal stability constants by electrochemical techniques. Water Research 9 (1975) 969-979.

175. D.R. MacFarlane, P. Meakin, J. Sun, N. Amini, M. Forsyth, Pyrrolidinium imides: a new family of molten salts and conductive plastic crystal phases, J. Phys. Chem. B 103 (1999) 4164-4170.

176. B.S. Jensen, The synthesis of 1-phenyl-3-methyl-4-acyl-pyrazolones-5, Acta chem. scand, 13 (1959) 1668-1670.

177. X. Sun, Y. Ji, Y. Liu, J. Chen, D. Li, An engineering-purpose preparation strategy for ammonium-type ionic liquid with high purity, AlChE J. 56 (2010) 989-996.

178. A. Suresh, T.G. Srinivasan, P.R. Vasudeva Rao, Extraction of U(VI), Pu(IV) and Th(IV) by some trialkyl phosphates, Sol. Extr. Ion Exch. 12 (1994) 727-744.

179. R. Kumaresan, T. Prathibha, B. Robert Selvan. K.A. Venkatesan, M.P. Antony, Synthesis and Evaluation of *N,N*-di-alkyl-2-methoxyacetamides for the separation of U(VI) and Pu(IV) from nitric acid medium, Radiochim. Acta. DOI 10.1515/ract-2016-2671.

180. T. Prathibha, R. Kumaresan, B. Robert Selvan, K.A. Venkatesan, M.P. Antony, P.R. Vasudeva Rao, N, N-dialkyl-2-hydroxyacetamides for modifier-free separation of trivalent actinides from nitric acid medium, Radiochim. Acta. 104 (2016) 73-181.

181. J. Ravi, A.S. Suneesh, T. Prathibha, K.A. Venkatesan, M.P. Antony, T.G. Srinivasan, P.R. Vasudeva Rao, Extraction behavior of some actinides and fission products from nitric acid medium by a new unsymmetrical diglycolamide. Solvent Extr. Ion Exch. 29 (2011) 86-105.

182. R.K. Sinha, Advanced Nuclear Reactor Systems – An Indian Perspective. Energy Procedia, 7 (2011) 34-50.

183. R. Natarajan, V. Vijayakumar, R.S. Rao, N.K. Pandey, Experiences of reprocessing of plutonium-rich mixed carbide fuels. J. Radioanal. Nucl. Chem 304 (2015) 401-407.

184. R. Natarajan, Baldev Raj, Fast Reactor Fuel Reprocessing Technology: Successes and Challenges. Energy Procedia, 7 (2011) 414-420.

185. P.R. Vasudev Rao, Z. Kolarik, A review of third phase formation in extraction of actinides by neutral organophosphorus extractants. Solvent Extr. Ion Exch. 14 (1996) 955-993.

186. T.H. Siddall III, The effects of altering alkyl substituents in trialkyl phosphates on the extraction of actinides. J. Inorg. Nucl. Chem. 13 (1960) 151.

187. A. Suresh, T.G. Srinivasan, P.R.Vasudeva Rao, The effect of the structure of trialkyl phosphates on their physicochemical properties and extraction behavior. Sol. Extr. Ion. Exch. 27 (2009) 258-294.

188. S.A. Ansari, P.Pathak. P.K. Mohapatra, V.K. Manchanda, Chemistry of diglycolamides: promising extractants for actinide partitioning, Chem. Rev. 112 (2012) 1751–1772.

189. A.N. Turanov, V.K. Karandashev, M. Boltoeva, C. Gaillard, V. Mazan, Synergic extraction of uranium (VI) with TODGA and hydrophobic ionic liquid mixtures into molecular diluent. Sep. Purif. Technol. 164 (2016) 97-106.

190. G. Modolo, H. Asp, C. Schreinemachers, H.Vijgen, Development of TODGA based process for partitioning of actinides from purex raffinate part-I: batch extraction optimization studies and stability test. Solvent Extr. Ion Exch. 25 (2007) 703–721.

191. Magnusson, B. Christiansen, J.P. Glatz, R. Malmeck , G. Modolo, D.S. Purroy, C.Sorel, Demonstration of a TODGA based extraction process for the partitioning of minor actinides from a PUREX raffinate. Solvent Extr. Ion Exch. 27 (2009) 26–35.

192. P. Deepika, K.N. Sabharwal, T.G. Srinivasan, P.R.Vasudeva Rao, Studies on the use of N, N, N, N-tetra (2-ethylhexyl) diglycolamide (TEHDGA) for actinide partitioning. I: Investigation on third-phase formation and extraction behavior. Solvent Extr. Ion Exch. 28 (2010) 184-201.

193. S. Kannan, B.G. Vats, I.C. Pius, D.M. Noronha, P.S. Dhami, P.W. Naik, M. Kumar, Extraction and structural studies of an unexplored monoamide, N, N′-

dioctyl, α-hydroxy acetamide with lanthanide (III) and actinide (III) ions. Dalton Trans. 43 (2014) 5252-5255.

194. T. Prathibha, B. Robert Selvan, K.A. Venkatesan, S. Rajeswari, and M.P. Antony, Radiolytic stability of N, N-di-alkyl-2-hydroxyacetamides, J. Radioanal. Nucl. Chem. 311 (2017) 1929-1935.

195. H. Takeishi, Y. Kitatsuji, T. Kimura, Y. Meguro, Z. Yoshida, S. Kihara, Solvent extraction of uranium, neptunium, plutonium, americium, curium and californium ions by bis(1-phenyl-3-methyl-4-acylpyrazol-5-one) derivatives. Anal. Chim. Acta, 431 (2001) 69–80.

196. Y. Akama, K. Sato, M. Ukaji, T Kawata, Studies on the extraction of Copper(II) with 1-phenyl-3-methyl-4-acyl-5-pyrazolone. Polyhedron (1985) 59-63.

197. Czakis-Sulikowska, B. Kuznik, A. Anna Malinowska, Solvent extraction of Yttrium(III), Lantyhanum(III) and some lanthanides(III) by 1-phenyl-3-methyl-4-benzoyl-5- pyrazolone from water –methanol solutions. Chim. Analityczna, 37 (1992) 537-543.

198. B.A. Uzoukwu, K. Gloe, Extraction studies and synthesis of Molybdenum(VI) complexs of 4-adipoyl and 4-sebacoyl derivatives of bis (1-phenyl-3-methylpyrrazolone-5). Ind.J.Chem. 42 (2003) 2727-2734.

199. J, Zhao, Y. Bai, D. Li, W. Li, Extraction of rare earths (III) from nitrate medium with Di-(2-ethylhexyl) 2-ethylhexyl phosphonate and synergic extraction combined with 1-Phenyl-3-Methyl-4-Benzoy l-Pyrazolone-5. Sep. Sci. Technol. 41 (2006) 3047-3063.

200. J. Zhao, S. Meng, D. Li, Synergic extraction of rare earths (III) from chloride medium with mixtures of 1-phenyl-3-methyl-4-benzoyl-pyrazalone-5 and di-(2-ethylhexyl)-2-ethylhexylphosphonate. J. Chem. Technol. Biotechnol. 81 (2006) 1384-1390.

201. M. Atanassova, V. Lachkova, N. Vassilev, S. Varbanov, I. Dukov, Effect of p-tert-butylcalix [4] arene fitted with phosphinoyl pendant arms as synergic agent in the solvent extraction and separation of some trivalent lanthanoids with 4-benzoyl-3-methyl-1-phenyl-5-pyrazolone. J. Inclusion Phenom.Macrocyclic Chem 58 (2007) 173-179.

202. V.K. Manchanda, P.K. Mohapatra, 1-Phenyl-3-methyl-4-benzoyl-pyrazolone-5: A Promising Extractant for Plutonium, Sep. Sci. Technol.29 (1994) 1073-1086.

203. Z.W. Pan, J.H. Lin, W.J. Li, T.C. Wu, J.D. Pan, Studies on extraction equilibrium of rare earths in ion liquid extraction system using 1-butyl-3-methyl-imidazolium hexafluorophosphate and 1-phenyl-3-methyl-4-benzoyl-pyrazolone-5. Adv. Mat. Res., 602 (2013) 887-891.

204. Gujar, S.A. Ansari, A. Sengupta, M.S. Murali, P.K. Mohapatra, Extractive complexation of lanthanides and Am (III) by 1-phenyl-3-methyl-4-benzoyl-5-pyrazolone in ionic liquid: Solvent extraction and spectroscopic studies. Inorg. Chem. Commun.73 (2016)72-76.

205. Alok Rout, J. Kotlarska, W. Dehaen, K. Binnemans, Liquid–liquid extraction of neodymium (III) by dialkylphosphate ionic liquids from acidic medium: the importance of the ionic liquid cation. Phys. Chem. Chem. Phys. 15 (2013) 16533-16541.

206. T. Mori, K. Takao, K. Sasaki, T. Suzuki, T. Arai, Y. Ikeda, Homogeneous liquid–liquid extraction of U(VI) from HNO_3 aqueous solution to betainium bis (trifluoromethylsulfonyl) imide ionic liquid and recovery of extracted U (VI).

Sep. Purif. Technol. 15 (2015) 133-138.

207. P.S. Barber, S.P. Kelley, R.D. Rogers, Highly selective extraction of the uranyl ion with hydrophobic amidoxime-functionalized ionic liquids via η 2 coordination. RSC Adv. 2 (2012) 8526-8530.

208. M.B. Moity, A. Ouadi, V. Mazan, S. Miroshnichenko, D. Ternova, S. Georg, M. Sypula, C. Gaillard, I. Billard, Comparison of uranyl extraction mechanisms in an ionic liquid by use of malonamide or malonamide-functionalized ionic liquid. Dalton Trans. 41 (2012) 7526-7536.

209. P.K. Mohapatra, A. Sengupta, M. Iqbal, J. Huskens, W. Verboom, Efficient Diglycolamide-Based Task-Specific Ionic Liquids: Synthesis, Unusual Extraction Behaviour, Irradiation, and Fluorescence Studies. Chem. Eur. J. 19 (2013) 3230-3238.

210. X. Sun, Y. Ji, L. Guo, J. Chen, D. Li, A novel ammonium ionic liquid based extraction strategy for separating scandium from yttrium and lanthanides. Sep. Purif. Technol. 81 (2011) 25-30.

211. P.N. Pathak, N,N-Dialkyl amides as extractants for spent fuel reprocessing: an overview, J. Radio. Anal. Nucl. Chem. 300 (2014) 7–15.

212. V.K. Manchanda, P.N. Pathak, Amides and diamides as promising extractants in the back end of the nuclear fuel cycle: an overview. Sep. Purif. Technol. 35 (2004) 85–103.

213. M.L. Dietz, J.A. Dzielawa, I.L. Blake, A. Young, M.P. Jensen, Influence of solvent structural variation on the mechanism of facilitated ion transfer into room-temperature ionic liquids, Green Chem. 5 (2003) 682–685.

214. C.T. Huanga, T.C. Huang, The equilibrium reaction of the extraction of uranium(VI) with di-(2-ethylhexyl) phosphoric acid from nitric acid solutions, Solvent Extr. Ion Exch. 5 (1987) 611-631.

215. V. Ramakrishna, S.K. Patil, Synergic extraction of actinides, In: B.Dobias, I.R. Epstein, K. Kustin, S.K. Patil, V.V. Ramakrishna (Eds.) Structure and Bonding – New Developments Springer-Verlag, Berlin 56 (1984) 35−90.

216. Suresh, T.G. Srinivasan, P.R. Vasudeva Rao, Parameters Influencing third phase formation in the extraction of Th(NO3)4 by some trialkyl phosphates. Solvent Extr.Ion Exch. 27 (2009) 132-158.

217. R.B.Gujar RB, S.R. Ansari, P.K. Mohapatra, V.K. Manchanda, Development of T2EHDGA based process for actinide partitioning. Part I: batch studies for process optimization. Solvent Extr. Ion Exch. 28 (2010) 350-366.

218. S. Tachimori, Y. Sasaki, S. Suzuki, Modification of TODGA in n -dodecane solvent with a monoamide for high loading of lanthanides(III) and actinides(III). Solvent Extr. Ion Exch. 20 (2002) 687-699.

219. Alok Rout, K.A. Venkatesan, T.G. Srinivasan, P.R. Vasudeva Rao, Extraction and third phase formation behavior of Eu (III) in CMPO–TBP extractants present in room temperature ionic liquid. Sep. Purif. Technol. 76 (2011) 238-243.

220. E.A. Mowafy, D. Mohamed , Extraction behavior of trivalent lanthanides from nitric acid medium by selected structurally related diglycolamides as novel extractants. Sep. Purif. Technol. 128 (2014) 18-24.

221. J.Ravi, K.A.Venkatesan, M.P. Antony, T.G. Srinivasan, P.R.Vasudeva Rao, Feasibility of using Di-Dodecyl-Di-Octyl Diglycolamide for Partitioning of Minor Actinides from Fast Reactor High-Level Liquid Waste. Solvent Extr. Ion Exch. 32 (2014) 424-436.

222. P.K. Nayak , R. Kumaresan , K.A. Venkatesan, S. Rajeswari , C.G.S. Subramanian , M.P. Antony, P.R. Vasudeva Rao, Single-cycle separation of americium (III) from simulated high-level liquid waste using tetra-bis(2-ethylhexyl)diglycolamide and bis(2-ethylhexyl)phosphoric acid solution. Journal of Environmental Chemical Engineering, 19 (2013) 559-565.

223. T. Prathibha , K.A. Venkatesan , B. Robert Selvan , M.P. Antony, P.R. Vasudeva Rao, Anomalous extraction behavior of americium (III) in some diglycolamide isomers present in ionic liquid medium. Radiochim. Acta, 100 (2012) 907-913.

224. S. Legeai, S. Diliberto, N. Stein, C. Boulanger, J. Estager, N. Papaiconomou, M. Draye, Room-temperature ionic liquid for lanthanum electrodeposition, Electrochem. Commun. 10 (2008) 1661-1664.

225. Ch. Jagadeeswara Rao, K.A. Venkatesan, K. Nagarajan, T.G. Srinivasan, P.R Vasudeva Rao, Electrochemical and thermodynamic properties of europium (III), samarium (III) and cerium (III) in 1-butyl-3-methylimidazolium chloride ionic liquid,

J. Nucl. Mater. 399 (2010) 81-86.

226. N. Asanuma, M. Harada, Y. Yasuike, M. Nogami, K. Suzuki, Y. Ikeda, Electrochemical properties of uranyl ion in ionic liquids as media for pyrochemical reprocessing. J. Nucl. Sci. Technol. 44 (2007) 368-372.

227. S. Suneesh, Jammu Ravi, K.A. Venkatesan, M.P. Antony, T.G. Srinivasan, P.R.Vasudeva Rao, Lanthanide–actinide separation by bis-2-ethylhexylphosphoric acid from citric acid–nitric acid medium, J. Radioanal. Nucl. Chem. 285 (2010) 653-658.

228. S.J. Yoon, J.G. Lee, H. Tajima, A. Yamasaki, F. Kiyono, T. Nakazato, H. Tao, Extraction of lanthanide ions from aqueous solution by bis (2-ethylhexyl) phosphoric acid with room-temperature ionic liquids. J. Ind. Eng. Chem.16 (2011) 350-354.

229. A.S. Suneesh, K.A. Venkatesan, K.V. Syamala, M.P. Antony, P.R. Vasudeva Rao, Mutual separation of americium (III) and europium (III) using glycolamic acid and thioglycolamic acid, Radiochimica Acta. 100 (2012) 425-430.

230. A.S. Suneesh, R. Kumaresan, S. Rajeswari, Prasant Kumar Nayak, K.V. Syamala, K.A. Venkatesan, M.P. Antony, P.R. Vasudeva Rao, Development and demonstration of americium (III)-europium (III) separation using diglycolamic acid. Sep. Sci.Technol. 48 (2013) 1998-2006.

231. K. Shimojo, N. Aoyagi, T. Saito, H. Okamura, F. Kubota, M. Goto, H. Naganawa, Highly efficient extraction separation of lanthanides using a diglycolamic acid extractant, Anal. Sci. 30 (2014) 263-269.

232. T. Ogata, H. Narita, T. Mikiya, Immobilization of diglycol amic acid on silica gel for selective recovery of rare earth elements, Chem. Lett. 43 (2014) 1414-1416.

Glossary

Abbreviations	Full Name
ADS	Accelerator driven system
AHA	Acetohydroxamic acid
AHWR	Advance heavy water reactor
Aliquat336	Tri-*n*-octylmethylammonium chloride
$[A336]^+[DEHP]^-$	Tri-*n*-octylmethylammonium di (2-ethylhexyl)phosphate
$[A336]^+[DGA]^-$	Tri-*n*-octylmethylammonium bis(ethylhexyl)diglycolamate
$[A336]^+[NO_3]^-$	Tri-*n*-octyl-methylammonium nitrate
An	Actinide
BF_4^-	Tetrafluoroborate
$[BuImPA][NTf_2]$	Diethyl-3-(3-alkylimidazolium)propylphosphoramide bis(trifluoromethanesulfonyl)imide
BWR	Boiling Water Reactor
CAC	Critical aqueous concentration
CMPO	*n*-Octyl(phenyl)-N,N-diisobutylcarbamoylmethyphosphine oxide
$[C_nmim][NTf_2]$	1-Alkyl-3-methylimidazolium bis(trifluoromethanesulfonyl)imide
$[C_4mpy][NTf_2]$	1-Butyl-1-methylpyrrolidinium bis(trifluoromethanesulfonyl)imide
$[C_3mim][NTf_2]$	1-Propyl-1-methylpiperidinium bis(trifluoromethanesulfonyl)imide
$[C_2mim][NTf_2]$	1-Ethyl-1-methylpiperidinium trifluoroacetate
CA	Chronoamperometry
CP	Chronopotentiometry
CV	Cyclic voltammetry
D_M	Distribution ratio of metal ion
DAlkHyA	*N, N*-Dialkyl-2-hydroxy acetamide
DCH18C6	Di-cyclohexano- 18 –crown 6
DCM	Dichloromethane
DGA	Diglycolamide
DHOA	*N,N*-Dihexyloctanamide
DIAMEX	Diamide extraction
DIDPA	Diisodecylphosphoric acid

$\mathrm{DOAImNTf_2}$	*N*,*N*–dioctyl-2-(3-methyl imidazolium) bis(trifluoromethanesulfonyl)imide
DOBA	Dioctylbutyramide
DOMeOA	*N*, *N*-Dioctyl-2-methoxyacetamide
EDTA	Bis(ethylenediamine)tetraacetic acid
EX-EL	Extraction-Electrodeposition
FBTR	Fast breeder test reactor
FILs	Functionalized ionic liquids
FP	Fission product
HbetNTf2	Betaine bis (trifluoromethylsulfonyl imide)
HDGA	Bis(2-ethylhexyl)diglycolamic acid
HDEHP	Di(2-ethylhexyl)phosphate
HLLW	High level liquid waste
HMTA	Hexamethylenetetramine
HPMBP	1-Phenyl -3-methyl- 4-benzoyl pyrazalone-5
IL	Ionic liquid
$\mathrm{ImPNTf_2}$	Diethyl-2-(3-methylimidazolium)ethylphosphonate bis(trifluoromethansulfonyl)imide
KAMINI	KAlpakkam MINI reactor
$\mathrm{LiNTf_2}$	Lithium bis(trifluoromethansulfonyl)imide
Ln	Lanthanide
LOC	Limiting organic concentration
MA	Minor actinide
$\mathrm{MeBu_3NTf_2}$	Tri-*n*-butylmethylammonium bis(trifluoromethansulfonyl)imide
MPP	3-Methyl -1-phenyl-2- pyrazolin-5-one
n-DD	*n*-Dodecane
NFC	Nuclear fuel cycle
$\mathrm{NTf_2^-}$	Bis(trifluoromethansulfonyl)imide
OA	Oxalic acid
$\mathrm{Otf^-}$	Trifluoromethanesulfonate
$\mathrm{PF_6^-}$	Hexafluorophosphate
PFBR	Prototype fast breeder reactor
PHWR	Pressurized heavy water reactor

POPOP	1,4-Bis (5-phenyloxazol-2-yl) benzene
PPO	2,5-Diphenyl Oxazole
P&T	Partitioning & Transmutation
PUREX	Plutonium Uranium Reduction Extraction or Plutonium Uranium Recovery by Extraction
PWR	Pressurized water reactor
RTIL	Room temperature ionic liquid
SETFICS	Solvent Extraction for Trivalent f-elements Intragroup Separation in CMPO-complexant solvent
SF	Separation factor
TALSPEAK	Trivalent actinides and lanthanide Separation by Phosphorus Extractants from Aqueous Komplexes
TAlP	Tri alkylphosphate
TEA	Triethylamine
THF	Tetrahydrofuran
TODGA	*N,N,N’N’*-Tetraoctyldiglycolamide
TEHDGA	*N,N,N′,N′*-tetra-2-ethylhexyldiglycolamide
DEHDODGA	*N,N,N’,N*’-di-2-ethylhexyl-dioctyl diglycolamide
TOPO	Tri-*n*-octyl phosphinoxide
TRPO	Trans Uranium Extraction
TSIL	Task specific ionic liquid
TRUEX	Transuranic extraction
TTA	Theonyltrifluoroacetonate
VOCs	Volatile organic compounds
VVER	Water - Water Energetic Reactor